Ministério da Saúde

FIOCRUZ
Fundação Oswaldo Cruz

ESCOLA NACIONAL DE SAÚDE PÚBLICA
SERGIO AROUCA
ENSP

"Efeito do dióxido de titânio na decomposição fotocatalítica de substâncias persistentes no ambiente: corantes têxteis e interferentes endócrinos"

por

Enrico Mendes Saggioro

Tese apresentada com vistas à obtenção do título de Doutor em Ciências na área de Saúde Pública e Meio Ambiente.

Orientador principal: Prof. Dr. Josino Costa Moreira
Segunda orientadora: Prof.ª Dr.ª Anabela Sousa de Oliveira

Rio de Janeiro, fevereiro de 2014.

Ministério da Saúde

FIOCRUZ
Fundação Oswaldo Cruz

ESCOLA NACIONAL DE SAÚDE PÚBLICA
SERGIO AROUCA
ENSP

Esta tese, intitulada

"Efeito do dióxido de titânio na decomposição fotocatalítica de substâncias persistentes no ambiente: corantes têxteis e interferentes endócrinos"

apresentada por

Enrico Mendes Saggioro

foi avaliada pela Banca Examinadora composta pelos seguintes membros:

Prof. Dr. Daniel Vidal Pérez

Prof.ª Dr.ª Roberta Lourenço Ziolli

Prof.ª Dr.ª Lisia Maria Gobbo dos Santos

Prof. Dr. Fabio Veríssimo Correia

Prof. Dr. Josino Costa Moreira – Orientador principal

Tese defendida e aprovada em 26 de fevereiro de 2014.

S129 Saggioro, Enrico Mendes.
Efeito do dióxido de titânio na decomposição fotocatalítica de substâncias persistentes no ambiente: corantes têxteis e interferentes endócrinos. / Enrico Mendes Saggioro. -- 2014.
268 f. : ilus.; tab. ; graf.

Orientador: Moreira, Josino Costa
Oliveira, Anabela Sousa de

Tese (Doutorado) – Escola Nacional de Saúde Pública Sergio Arouca, Rio de Janeiro, 2014.

1. Corantes – toxicidade. 2. Titânio – antagonistas & inibidores. 3. Sistema Endócrino – metabolismo. 4. Indústria Têxtil. 5. Tratamento de Águas Residuárias. I. Meio Ambiente. I. Título

CDD - 22.ed. – 363.728

Partes dos experimentos desta tese foram realizadas na Plataforma Solar de Almería (PSA), Espanha (http://www.psa.es), do Centro de Investigaciones Energéticas, Medioambientales y Tecnológica (http://www.ciemat.es) e no Centro Interdisciplinar de Investigação e Inovação, na Escola Superior de Tecnologia e Gestão, Portalegre, Portugal (http://www.estgp.pt).

Esta tese é dedicada
Aos meus pais, Adalberto Gerkem Saggioro e Flávia Mendes Saggioro, por tornarem sonhos realidade e a liberdade que tive para tomar minhas decisões com total apoio desses anjos;
à minha irmã querida, Giovanna, por ser esse orgulho de irmã companheira e fiel que tenho a sorte de ter em minha vida.

Agradecimentos

A Deus por me dar saúde, força e fé para poder realizar esta tese.

As diversas agências financiadoras, CNPq, CAPES e Fiocruz.

Um agradecimento particular ao meu orientador Dr. Josino Costa Moreira, na graduação me aceitou como seu aluno de iniciação científica sem mesmo antes sem ter me conhecido pessoalmente. Este grande homem, um incentivador incansável da pesquisa, sempre me orientando, como ele mesmo disse: "ensino o caminho das pedras". O meu muito obrigado e eterna admiração.

Não menos importante, mas uma grande pessoa e amiga nesta jornada foi minha também segunda orientadora Dra. Anabela Sousa Oliveira, esta apresentada pelo meu orientador, conhecia-la há seis anos atrás. Uma pessoa de alto astral e companheira, foi fundamental para meu crescimento pessoal e científico. Muito obrigado e espero ser sempre um amigo e companheiro de trabalho.

Esta pessoa não foi minha orientadora, mas tenham certeza que se não fosse por sua amizade, persistência, companheirismo e força de vontade de trabalhar esta tese não teria um desfecho. Muito obrigada Thelma Pavesi, pelas risadas, pelo trabalho, pelos conselhos e pela nossa eterna amizade.

Aos meus dois grandes guardiões mãe e pai, para vocês não existem palavras, um simples, porém enorme EU AMO vocês!!! Obrigado pelo carinho e amor que vocês me proporcionam.

A minha irmã Giovanna, muito obrigada pelas conversas e apoio durante todo esse tempo. Você é especial para mim, amo muito você!!! Obrigado ao Zequinha também.

A minha linda namorada, Aline Paiva. Você é uma grande mulher que me fez ser de mim um homem melhor. Muito obrigada pela paciência e tolerância durante meu estágio sanduíche, e por me proporcionar todo o equilíbrio emocional que precisei. Amo você!!!

A minhas avós Célia e Geralda que já se foram, e minha amável Vó Leda, que foram e são fontes de inspiração. A minha madrinha, Tia Rosinha, sempre fiel aos meus desejos. A minha Tia Bel, a minhas primas Amanda e Aline pela torcida. Ao meu Tio/professor Roberto e ao meu primo Fabiano pelo incentivo e apoio.

Aos amigos de CESTEH, um obrigado em particular ao Leandro (companheiro de corrida e copos) e Vinicio (copos), dois grandes amigos. A Eline, pela amizade, incentivo e ajuda científica na tese, a Cris Barata pelas conversas e auxílio na reta final do trabalho. Ao grande Mário, mineiríssimo, motivos de risadas e descontração. A Lucineide, Ione, Simone Mitri, Fernanda, Renato, Sayonara, Juliana, Regina e todos os outros que fazem os dias do laboratório mais agitados, por vezes mais barulhentos, mas certamente mais vivos.

Obrigado ao Dr. Frederico Peres da Costa pela ajuda no final da tese.

A Fiocruz, por ser esta instituição grandiosa e por ter me proporcionado toda estrutura necessária. Obrigado aos amigos Fiocruz, da academia e grupo de corrida.

Ao Dr. Sixto Malato por ter me aceitado na Plataforma Solar de Almería (PSA), Espanha, para meu estágio de doutorado sanduíche, e ao Dr. Manuel Ignácio Maldonado, pela orientação na qual dispensou toda a atenção que podia. Um agradecimento mais que especial à amiga e doutoranda Margarida Jimenez-Tototzintle, que me acompanhou com maestria em todos os experimentos na PSA e pela amizade

fora do laboratório. Outro grande amigo de PSA, Stefanos Papoutsakis, grandes conversas filosóficas com esse grego, Fuerza. John...!!!! Muito obrigado a Agostín (Cabaña del Tío Tin) e Elisa pelos ensinamentos. Muito obrigada a Dra. Pilar e Dr. Isa Oller pela abertura e aprendizado. A todos do laboratório de tecnologías del agua; Isa Fernandes, Sara Mirales, Maria, Estefanía De Torres, Irene e Ima. A todos que passaram pelo laboratório.

Aos meus amigos de infância que fazem a vida ser mais alegre e divertida. Muito obrigado, ao Fabim, Cuia, Cléo, Dieguim, Lucão, Barretos, Bellei, Rodolfo, Junecão, Dudinha, Danilim, Wilder, Guilherme e Sam. Aos amigos de mestrado e doutorado, em particular a Poliany e Róber.

Ao Dr. Fábio Verissimo Correia, por realizar e participar dos experimentos desta tese, e ceder suas minhoquetes para realização do trabalho. Obrigado a minhoquete Patricia Pereira.

Ao Dr. Daniel Buss, também por realizar e participar dos experimentos desta tese e por engrandecer o trabalho com seus debates. Obrigado a Danielly Magalhães e Louise Godoy.

A Dr. Andrea Machado Costa e Dr. Elena Mavropoulos pela abertura e compreensão no CBPF, para realização de experimentos desta tese.

Ao Dr. Luis Filipe Vieira Ferreira, por ajudar na publicação e desenvolvimento dos artigos.

Ao Instituto Politécnico de Portalegre, Portugal, pela estrutura e acolhimento para realização de parte dos experimentos. Aos amigos ali formados, Cátia Maia e Luís Calado.

A todos os espíritos que me guiam e me acompanham para o bem.

A todos o muito obrigado, que passaram na minha vida nesses quatro anos de tese, que me ajudaram direta ou indiretamente e fizeram o sonho se tornar realidade.

ÍNDICE

LISTA DE FIGURAS

LISTA DE TABELAS

LISTA DE ABREVIATURAS E SIGLAS

Al_2O_3 – Óxido de Alumínio

BV – Banda de valência

BC – Banda de condução

BTFA - *N,O*-bis(trimetilsilil)trifluoracetamida

-C=O – Carbonila

-C-OH – Carboxila

CO_2 – Dióxido de carbono

Cl_2 – Cloro

CH_4 – Metano

CeO_3 – Óxido de Cério

$CaCO_3$ – Carbonato de Cálcio

DL_{50} – Dose Letal

eV – elétron volt

ETAD – *The Ecological and Toxicological Association of Dyes and Organic Pigments Manufacturers*

Fe^{2+} – íon ferroso

Fe^{3+} – íon férrico

H_2O – Água

H_2O_2 – Peróxido de Hidrogênio

HCl – Ácido Clorídrico

H_2SO_4 – Ácido Sulfúrico

IOC – Instituto Oswaldo Cruz

$KMnO_2$ – Permanganato de Potássio

LAPS – Laborátorio de Avaliação e Promoção da Saúde Ambiental

NaCl – Cloreto de Sódio

Na_2SO_4 – Sulfato de Sódio

NO_3^- - íon nitrato

NaOH – Hidróxido de Sódio

$-NH_2$ – Radical amina

=NH – Radical amida

NaOCl - Hipoclorito de Sódio

O.D – Oxigênio Dissolvido

O_3 – Ozônio

$O_2^{\bullet}$ - Radical Superóxido

PIB – Produto Interno Bruto

POAs – Processos Oxidativos Avançados

$OH^{\bullet}$ - Radical Hidroxila

rpm – rotações por minuto

SO_4^{2-} – íon sulfato

TiO_2 – Dióxido de Titânio

UV – Radiação Ultravioleta

ZnO – Óxido de zinco

λ - Comprimento de onda

$Ti(OC_4H_9)_4$ – Tetrabutil de titânio

HNO_3 – Ácido nítrico

RESUMO

O objetivo do presente trabalho foi estudar a degradação fotocatalítica de três corantes e um interferente endócrino mediado pelo dióxido de titânio (TiO_2). Foi estudada a degradação fotocatalítica de dois azo corantes comerciais, respectivamente o C.I Reactive Black 5 e o C.I Reactive Red 239. Para esse estudo foi utilizado o TiO_2 P25 Evonik como catalisador e os experimentos foram realizados em solução aquosa com reator artificial equipado com lâmpada de vapor de mercúrio 125W. Nesse estudo, foram avaliados os seguintes parâmetros: concentração de TiO_2, tempo de irradiação, pH, concentração inicial de corante, presença de diferentes concentrações de peróxido de hidrogênio e degradação em sistema bi-compartimental para os dois azo corantes. O outro corante estudado foi o Índigo Carmine (IC). Primeiramente foi investigada a descoloração do corante em efluente modelo usando processo físico e químico para sua remoção. Os experimentos de descoloração do efluente contendo o corante IC foram realizados usando carvão ativado no escuro e com irradiação. Além disso, o efeito do carvão ativado/TiO_2/UV foi avaliado pelo mesmo sistema. Os parâmetros da degradação do IC foram realizados, seguindo: concentração de TiO_2, pH, concentração inicial de corante, presença de ânions inorgânicos, temperatura, concentração de peróxido de hidrogênio. A eficiência de três diferentes reatores (Reator 1 – reator do tipo batch com lâmpada vapor de mercúrio 125W; Reator 2 – reator do tipo batch equipado com 4 lâmpadas daylight 20W; Reator 3 – reator tubular de fluxo contínuo equipado com uma lâmpada daylight 20W) e reator batch com luz solar foram avaliados para degradação do IC. Além disso, otimizados experimentos foram realizados em planta piloto com compound parabolic collector reatores (CPC) na Plataforma Solar de

Almería, Espanha, com TiO_2 em suspensão e suportado. O IC foi estudado em diferentes tipos de águas, sendo elas: água destilada, água sintética moderadamente dura, água sintética e real de estação de tratamento de água residuária (ETAR). Testes ecotoxicológicos para o IC foram realizados em dois diferentes níveis tróficos de cadeia alimentar (*Daphnia similis* e *Pseudokirchneriella subcapitata*) e testes com minhocas *Eisenia andrei*. A degradação fotocatalítica do Bisfenol A (BPA) em diferentes tipos de águas na presença de TiO_2 foi feita sob diferentes condições. O TiO_2 em suspensão foi utilizado para comparar a eficiência da degradação do BPA (20 mgL^{-1}) em batch e CPC reatores. O TiO_2 foi suportado em esferas de vidro pelo método sol-gel e usado em reatores solares CPC em escala piloto para degradação do BPA (100 μgL^{-1}). A influência das espécies reativas ($OH^{\bullet}$, $O_2^{\bullet-}$, h^+) foi avaliada. Testes ecotoxicológicos com minhocas *Eisenia andrei* também foram realizados para o BPA e seus produtos de degradação.

Palavras-chave: Corantes, Interferentes endócrinos, TiO_2, Tratamento de águas residuais, Ecotoxicologia

ABSTRACT

The aim this study was evaluated the photocatalytic degradation mediated titanium dioxide (TiO_2) for three dyes and one endocrine disruptor. The photocatalytic degradation of two commercial textile azo dyes, respectively C.I Reactive Black 5 and C.I Reactive Red 239 has been studied. TiO_2 P25 Evonik was used as catalyst and photodegradation was carried out in aqueous solution under artificial irradiation with a 125W mercury vapor lamp. The effects of the amount of TiO_2 used, UV-light irradiation time, pH of the solution under treatment, initial concentration of the azo dye and addition of different concentrations of hydrogen peroxide were investigated. The effect of the simultaneous photodegradation of the two azo dyes was also investigated. The other dye studied was Indigo Carmine (IC). First was investigated the decolorization of a model water effluent containing indigo carmine dye under physical and chemical different treatments. Experiments on decolorization of the effluent containing indigo dye were performed using activated carbon in the dark and under irradiation. Furthermore the effect of activated carbon/TiO_2/UV was tested for the same system. The effects of parameters in the IC degradation were evaluated under artificial irradiation with a 125 W mercury vapor lamp. The effects of the amount of TiO_2, pH of the solution, initial concentration of the dye, presence of inorganic anions, temperature and addition of different concentrations of hydrogen peroxide were investigated. The efficiency of three different artificial photoreactors (Reactor 1 – batch magnetically stirred reactor with 125 watts mercury vapor lamp; Reactor 2 - batch magnetically stirred reactor with 4 lamps daylight 20 watts; Reactor 3 - glass tubular continuous-flow reactor, illuminated inside by one daylight 20W lamp) were evaluated. Also, the same

parameters were evaluated for batch solar experiments. Furthemore, the optimized experiments was performed in a solar compound parabolic collector (CPC) pilot plant in Plataforma Solar de Almería, Espanha, under suspended and supported TiO_2. IC was spiked in several types of water such as distilled water, synthetic moderately hard freshwater, synthetic and real secondary municipal wastewater treatment plant (MWWTP). The ecotoxicological effects of IC were evaluated for two different food chain levels (*Daphnia similis and Pseudokirchneriella subcapitata*) and *Eisenia andrei* earthworms. Photocatalytic degradation of Bisphenol A (BPA) in waters and wastewaters in the presence of titanium dioxide (TiO_2) was performed under different conditions. Suspensions of the TiO_2 were used to compare the degradation efficiency of BPA (20 mgL^{-1}) in batch and CPC reactors. A TiO_2 catalyst supported on glass spheres beads was prepared (sol-gel method) and used in a CPC solar pilot plant for the photodegradation of BPA (100 μgL^{-1}). The influence of $OH^{\bullet}$, $O_2^{\bullet-}$, h^+ on the BPA degradation were evaluated. Some toxicological effects of BPA and its photoproducts on *Eisenia andrei* earthworms were evaluated.

Keywords: Dyes, endocrine disruptors, TiO_2, wastewater treatment, Ecotoxicology

1 INTRODUÇÃO

Desde os primórdios da história, nossos ancestrais usavam corantes como formas de expressão. Escritos utilizando corantes, datados de 2500 a.C., foram encontrados na China. Posteriormente, os romanos já dominavam o processo para o tingimento dos fios de lã com corantes naturais (Zanoni and Carneiro 2001).

Relatos históricos revelam a grande importância econômica dos corantes, mostrando que estes influenciavam nas atividades comerciais, tornando-se bastante valiosos, como quando em 1501, para atender aos pedidos da corte Portuguesa, cerca de 2 milhões de árvores foram devastadas para obtenção de um corante natural advindo do pau-brasil (Zanoni and Carneiro 2001).

Em 1856, foi produzido o primeiro corante sintético por William Henry Perkin, a Mauveína, podendo-se afirmar ser esta data um divisor de águas no mercado destes produtos. Sendo assim, desde o início do século XX, os corantes naturais foram sendo substituídos pelos sintéticos, representando estes, hoje, mais de 10 mil compostos orgânicos sintéticos ligados a indústria têxtil (Karkmaz et al. 2004).

Devido à crescente demanda que o mercado exerce sobre as indústrias, buscando novas combinações que atendam os clientes, as empresas, diante deste mundo diversificado de corantes sintéticos, vem cada vez mais usando estes produtos. A grande questão atual é: usar os corantes de maneira sustentável, sem causar danos a saúde ambiental e humana, ocasionada principalmente pelos resíduos gerados pelas indústrias têxteis.

Diante deste cenário, a preservação do meio ambiente e da saúde pública ganha forte importância, pois os problemas ambientais tem se tornado cada vez mais críticos e freqüentes (Zanoni and Carneiro 2001; Karkmaz et al. 2004). Os efluentes industriais, quando não tratados corretamente, tornam-se potencialmente nocivos ao ambiente, devido às diversas substâncias utilizadas no processo. Dentre essas substâncias, encontram-se os corantes, largamente utilizados na indústria têxtil (Daneshvar et al. 2004).

As indústrias têxteis produzem, como efluentes, quantidades significativas de água fortemente contaminada por corantes e outros produtos químicos. Isso as torna uma fonte potencialmente poluidora do meio ambiente, devido ao fato de 5 a 20% do corante ser perdido no processo de tingimento, causado pela incompleta fixação deste nas fibras têxteis durante a lavagem do tecido (Paschoal and Tremiliosi-Filho 2005). Grande parte do efluente contendo corante não sofre qualquer tipo de tratamento, gerando grandes volumes de efluentes com altas cargas de compostos orgânicos fortemente coloridos, alterando os processos fotossintéticos naturais dos meios aquosos onde são descarregados (Kunz et al. 2002).

Estima-se que o consumo anual de corantes sintéticos possa atingir cerca de 7 x 10^5 toneladas no mundo, e no Brasil esses números giram em torno de 26.500 toneladas (Kunz et al. 2002; Daneshvar et al. 2004). O Brasil exerce uma grande importância no cenário mundial, estando entre os principais produtores da indústria têxtil-vestuário. As principais indústrias localizam-se na região sul (Santa Catarina), sudeste (São Paulo e Minas Gerais) e nordeste (Pernambuco, Bahia e Ceará) (Guaratini and Zanoni 2000).

Os corantes quando descartados no ambiente, sem nenhum tipo de tratamento, não são facilmente biodegradados pelas bactérias presentes nos sistemas, devido a sua estrutura química complexa, ficando assim por um longo período nos ecossistemas. Dados do The Ecological and Toxicological Association of Dyes and Organic Pigments Manufacturers (ETAD), indicam que cerca de 90% dos 4000 corantes testados possuíam valores de dose letal em humanos (DL_{50}) maiores do que 2×10^3 mg/kg. Devido o valor de dose letal da grande maioria dos corantes ser bastante elevado para os seres humanos, as empresas do setor têxtil fundamentam seu argumento neste aspecto, afirmando que os corantes provavelmente não apresentam efeitos na saúde humana. Porém, é de se lembrar de que os resíduos provindos das indústrias causam primeiramente seus efeitos na biota aquática, acumulando-se em altas concentrações nos níveis mais elevados da cadeia alimentar (Robinson et al. 2000).

Para além dos corantes, um novo grupo de contaminantes vem despontando como potencial risco à saúde pública por abranger substâncias amplamente utilizadas pela população em seu dia-a-dia, presente na composição de alimentos, medicamentos, produtos de uso pessoal (como por exemplo, protetores solares), revestimento de panelas, etc. A esse grupo de contaminantes é dado o nome de contaminantes emergentes, cuja pesquisa é ainda incipiente e não constam em normativas vinculadas à saúde e ao meio ambiente (Billa and Dezotti 2007; USEPA, 2014). Inseridos neste grupo, encontram-se compostos cuja pesquisa já indicou serem capazes de causar ação tóxica e/ou poderem interferir no normal funcionamento do sistema endócrino humano e animal, substâncias essas conhecidas como interferentes endócrinos (USEPA, 2014).

Esta classe de substâncias é bem conhecida no meio científico, desde 1900 pesquisadores já reconheciam os efeitos causados nos sistema endócrino em animais de laboratório (Allen and Doisy 1923). Porém, atualmente essas moléculas têm ganhando visibilidade com reconhecimento como contaminante, já que o desenvolvimento das técnicas analíticas vem possibilitando a determinação de compostos em concentrações cada vez mais reduzidas (ngL^{-1}).

Diferentes pesquisas têm indicado que mesmo presentes em reduzidas quantidades, alguns desses compostos são capazes de interferir no sistema endócrino, causando alterações celulares (como crescimento desordenado, e aumento da incidência de diferentes formas de câncer), alterações no sistema reprodutor masculino (como baixa contagem de células reprodutivas e infertilidade) e feminino, e outros efeitos adversos (Caliman and Gavrilescu 2009; Burkhardt-Holm 2010)

Esses compostos entram continuamente no ambiente aquático oriundos dos efluentes das estações de esgoto, cujo tratamento aplicado não é capaz de removê-los por completo, e também pela entrada de esgoto *in natura*, despejado nos corpos hídricos mediante a ausência de adequada rede coletora e de tratamento (Mboula et al. 2013).

Os interferentes endócrinos abrangem uma ampla faixa de classes de substâncias, que incluem o Bisfenol A (BPA) um plastificante orgânico muito comumente incorporado a outros materiais, muito utilizado como intermediário na produção de policarbonatos, resinas epóxi, retardantes de chama, entre outros produtos (Rubin 2011). Os produtos finais advindos do BPA incluem: adesivos, garrafas de água,

tintas em pó, brinquedos, revestimentos de partes elétricas, lentes ópticas, materiais de construção, proteção de vidros de janela e discos compactos (Staples et al. 1998).

Alguns estudos realizados no Brasil quantificaram o BPA em água de rios e lagos. Montagner and Jardim (2011) encontraram concentrações de BPA entre 0,5 e 141 ngL^{-1} nas águas dos rios de Atibaia e Capivari em Campinas, São Paulo. Outro estudo desenvolvido por Simões et al. (2012) avaliou a presença de 35 fármacos de diferentes classes terapêuticas no Estado do Rio de Janeiro. Os resultados obtidos mostraram que nenhuma das 47 amostras analisadas estava livre da contaminação por esses compostos, sendo que o interferente endócrino BPA foi detectado em 96% das amostras analisadas em concentrações que variaram entre <9,7 a 31.700 ng L^{-1}.

Na tentativa de tratar as águas residuais contaminadas por diversas substâncias persistentes, diversos processos oxidativos avançados (POAs) têm se destacado pela sua elevada capacidade destrutiva de moléculas orgânicas. Estes se baseiam na formação de espécies reativas altamente oxidantes, que possuem capacidade de reagir com os mais variados tipos de componentes orgânicos e inorgânicos, levando à formação de produtos intermediários de menor toxicidade ou a completa mineralização, com formação de dióxido de carbono (CO_2) e água (Moreira et al. 2005; Oliveira et al. 2012).

Os (POAs) são processos limpos e não seletivos, podendo degradar inúmeras substâncias, independentes da presença de outras. Além disso, podem ser usados para tratamento de todo o tipo de poluentes orgânicos em meio líquido, gasoso ou sólido. As reações ocorrem em temperatura e pressão normais, e existem diversos caminhos para formação do radical hidroxila, diferenciando e classificando os diversos processos que

podem ser heterogêneos ou homogêneos, conforme a ausência ou presença de catalisadores, além de estarem ou não sob irradiação (Legrini et al. 1993; Teixeira and Jardim 2004; Oliveira et al. 2012).

Desta forma, a presente tese objetivou avaliar comparativamente a eficiência do TiO_2 na fotodegradação de substâncias persistentes no ambiente, como corantes e Bisfenol A. Além disso, alguns objetivos específicos contemplaram a tese, sendo eles: testar comparativamente metodologias de fotodegradação de corantes e Bisfenol A com TiO_2 utilizando a luz solar e diferentes reatores com luz artificial, testar um método de tratamento convencional de efluentes com carvão ativado isoladamente e a mistura de carvão ativado com dióxido de titânio, avaliar diversos parâmetros que podem influenciar o processo fotocatalítico (ex: pH, H_2O_2, solvente, temperatura, conc. corante e TiO_2, íons inorgânicos), suportar o TiO_2 e verificar a eficiência do processo fotocatalítico, testar a eficiência do processo fotocatalítico em diferentes matrizes de água, avaliar as principais espécies fotoativas envolvidas na fotodegradação do Bisfenol A, promover a fotodegradação dos compostos utilizando reatores em escala piloto e realizar testes ecotoxicológicos com diferente organismos, antes e após o tratamento.

2 REFERENCIAL TEÓRICO

2.1 A indústria têxtil no Brasil

O processo de industrialização no Brasil teve início com a indústria têxtil, tendo íncio das atividades com a ocupação Portuguesa. As primeiras fábricas foram implantadas em 1816, em Minas Gerais, e em 1826 em Pernambuco, constituídas de parques rudimentares (Zanoni and Carneiro 2001). As características do país nesta época eram voltadas para a cultura algodoeira, sendo a matéria-prima básica em grande quantidade e mão-de-obra abundante, o que juntamente com um mercado em expansão, ajudaram a impulsionar o setor. Entretando, com a explosão da 1ª Guerra Mundial, aconteceu à consolidação deste empreendimento no país, principalmente devido a uma redução significativa das importações, estimulando assim a produção interna (IEMI 2002).

Com o passar das décadas, o segmento das indústrias têxteis adquiriram forte tradição, ocupando lugar de destaque na economia dos países desenvolvidos, e sendo de vital importância nos países hoje conhecidos como emergentes, incluindo o Brasil. Dados estatísticos revelam que o Brasil possui 70% da indústria têxtil voltada para o algodão, demandando 4% da produção mundial de corantes (IEMI 2002).

Os dados do Instituto de Estudos e Marketing Industrial (IEMI) com apoio institucional do Programa de Exportação da Indústria da Moda Brasileira (Texbrasil), da Associação Brasileira de Indústria Têxtil e de Confecção (ABIT) e da Agência

Brasileira de Promoção de Exportações e Investimentos (Apex-Brasil) revelaram que o Brasil é o quinto maior produtor mundial de têxteis básicos, ficando atrás somente da China, Índia, EUA e Paquistão. O volume de produção em 2010 para têxteis básicos foi de 2,25 milhões de toneladas e o setor investiu US$ 4,3 bilhões de dólares em modernização, promovendo uma capacidade anual de produção de US$ 1,5 bilhão em 2010, Brasil.

2.2 A indústria têxtil e o meio ambiente

Com o crescimento populacional acentuado, aliado a um modelo capitalista de consumo, tem acontecido uma explosão pela busca de produtos de primeira linha. Neste conjunto, destaca-se a indústria têxtil, na produção de tecidos e roupas, gerando quantidades significativas de poluentes altamente tóxicos ao homem e ao meio ambiente (Zamora et al. 2002).

O fenômeno de contaminação nas últimas décadas passou a ser preocupação de ambientalistas e cientistas, determinando tomadas de decisões no âmbito de consciência ambiental (Zamora et al. 2002). A adaptação da legislação nacional e comunitária proibiu a descarga de efluentes industriais não tratados no ambiente, restringindo fortemente os limites em que diversas classes de substâncias neles presentes que podem ser libertadas (Davis and Cornwell 1998; Eckenfelder Jr 2000).

Genericamente, designa-se por efluente (do latim *effluente,* que significa derramar-se) qualquer fluido residual lançado para o ambiente e que constitui um agente

poluidor (Zamora et al. 2002). Os efluentes mais comuns encontram-se os esgotos domésticos e os diversos tipos de efluentes industriais.

As descargas de águas residuais com tratamento deficiente ou incompleto podem provocar a contaminação das águas superficiais e subterrâneas. Entre as principais causas de contaminação de águas superficiais e subterrâneas estão ainda o uso excessivo de pesticidas e fertilizantes, além da deposição de resíduos sólidos urbanos no solo (Tochobanoglous et al. 1993). Como as águas superficiais e subterrâneas são a fonte das águas para abastecimento público, estas sofrem tratamentos de modo a conferir-lhes qualidade adequada.

O tratamento de águas residuais (domésticas e industriais) baseia-se numa sequência de tratamentos mecânicos, físicos, químicos e biológicos (Metcalf and Eddy 2003). Tanto em efluentes líquidos como em gasosos, no entanto, existem substâncias orgânicas passíveis de não serem tradadas por processos tradicionais resistindo à degradação biológica, tornando-se persistentes no ambiente (Davis and Cornwell 1998).

Os poluentes orgânicos persistentes são aquelas substâncias de origem natural ou antropogênica, que se acumulam no ambiente devido à sua complexa natureza química. Estruturalmente, são compostos policíclicos conjugados (hidrocarbonetos policíclicos aromáticos) ou de elevado teor de átomos de halogêneo, em especial cloro (pesticidas, dibenzodioxinas, dibenzofuranos e bifenilos policlorados, entre outros) (Albers 2006). Muitos são voláteis, sofrendo transportes a longas distâncias podendo chegar a praticamente todas as regiões do globo, mesmo a zonas onde nunca foram produzidos ou derramados (Baird 1999). Pelo fato de, muitas vezes, apresentarem

caráter hidrofóbico e lipofílico, sofrem bioacumulação nos tecidos gordos dos seres vivos e biomagnificação nas cadeias alimentares, atingindo concentrações mais elevadas nas espécies da cadeia alimentar (Albers 2006; Stokstad 2007).

Embora as suas fontes naturais se mantenham aproximadamente constantes, o rápido desenvolvimento industrial desde o final do século XIX tem conduzido a um enorme aumento da quantidade e da diversidade de poluentes orgânicos persistentes de origem humana no ambiente (Nevers 2000). A conjugação destas características faz com que os poluentes orgânicos representem um elevado risco para a saúde pública e para o ambiente (Stokstad 2007).

Como exemplo de compostos deste tipo existem os corantes, tendo como principal fonte produtora as indústrias têxteis. Como a descarga deste tipo de substâncias nos diversos segmentos ambientais parece ser difícil de controlar e impossível de evitar, torna-se indispensável encontrar novas tecnologias de descontaminação ambiental para os compostos orgânicos recalcitrantes, que sejam simultaneamente poderosas, limpas e seguras (Eckenfelder Jr. 2000; Metcalf and Eddy 2003).

Dentro do setor industrial brasileiro, as atividades têxteis estão em destaque, embora ocupem lugar de importância na economia, possuem peculiaridades que fazem questionar seu potencial, principalmente por necessitarem de elevadas quantidades de água (consumindo aproximadamente 15% de toda água da indústria), de corantes e de diversos compostos químicos ao longo da complexa cadeia produtiva (Paschoal and Tremiliosi-Filho 2005). Além disso, estima-se que 90% aproximadamente das espécies

químicas, incluindo os corantes, são eliminadas nos efluentes após o processamento, tornando-se uma fonte potencialmente poluidora. Fato este decorrente da dificuldade de se tratar essas águas residuárias, ricas em compostos de baixa biodegrabilidade, e principalmente devido aos custos do tratamento ocasionado pela geração de grande volume de efluente (Cisneros et al. 2002).

Podemos citar como exemplo de paradoxo ocasionado pela indústria têxtil, os fatos que acontecem no estado de Pernambuco. Neste estado concentra-se um pólo de confecção localizado na meso região do agreste pernambucano, microrregião do alto do Capibaribe, contando com cerca de 12 mil microempresas, situadas nos municípios de Santa Cruz do Capibaribe, Toritama e do Vale do Ipojuca – município de Caruaru. A cidade de Toritama destaca-se pela sua elevada capacidade produtiva de jeans, sendo conhecida como a capital do jeans, contando com cerca de 900 pequenas indústrias de confecção. Toritama é responsável por 14% da produção nacional de jeans no País, com cerca de 2 milhões/peças ano, perfazendo um montante de 6 milhões de reais/ano (Santos 2006).

Estas indústrias têxteis situadas nesta região de clima semiárido constituem um grave problema ambiental, pois de acordo com o diagnóstico ambiental feito pela agência estadual de meio ambiente e recursos hídricos (CPRH) de Pernambuco, constatou que das 56 lavanderias visitadas em Toritama, 67% não constavam de alvará para funcionamento, 100% não apresentavam licenciamento ambiental, 70% do destino final dos efluentes industriais e sanitários eram descartados na rede pluvial e 85% das lavanderias não possuíam sistema de controle de poluição atmosférica.

Os corantes, mesmo em baixas concentrações, são de fácil percepção, e quando presentes em altas concentrações podem impedir a penetração de luz, prejudicando o ciclo dos gases e os processos biológicos, assim como diminuem a quantidade de oxigénio dissolvido, modificando as propriedades dos cursos d`água (Cisneros et al. 2002).

Observam-se na Figura 1, as etapas gerais de um processamento têxtil, onde se destaca os elevados gastos com água, que podem girar em torno de 100 a 300 litros por kg de tecido e os diversos produtos químicos envolvidos nas etapas de manufaturamento da matéria-prima até o produto final acabado (Balan 1999; Hassemer 2001; Zamora 2002).

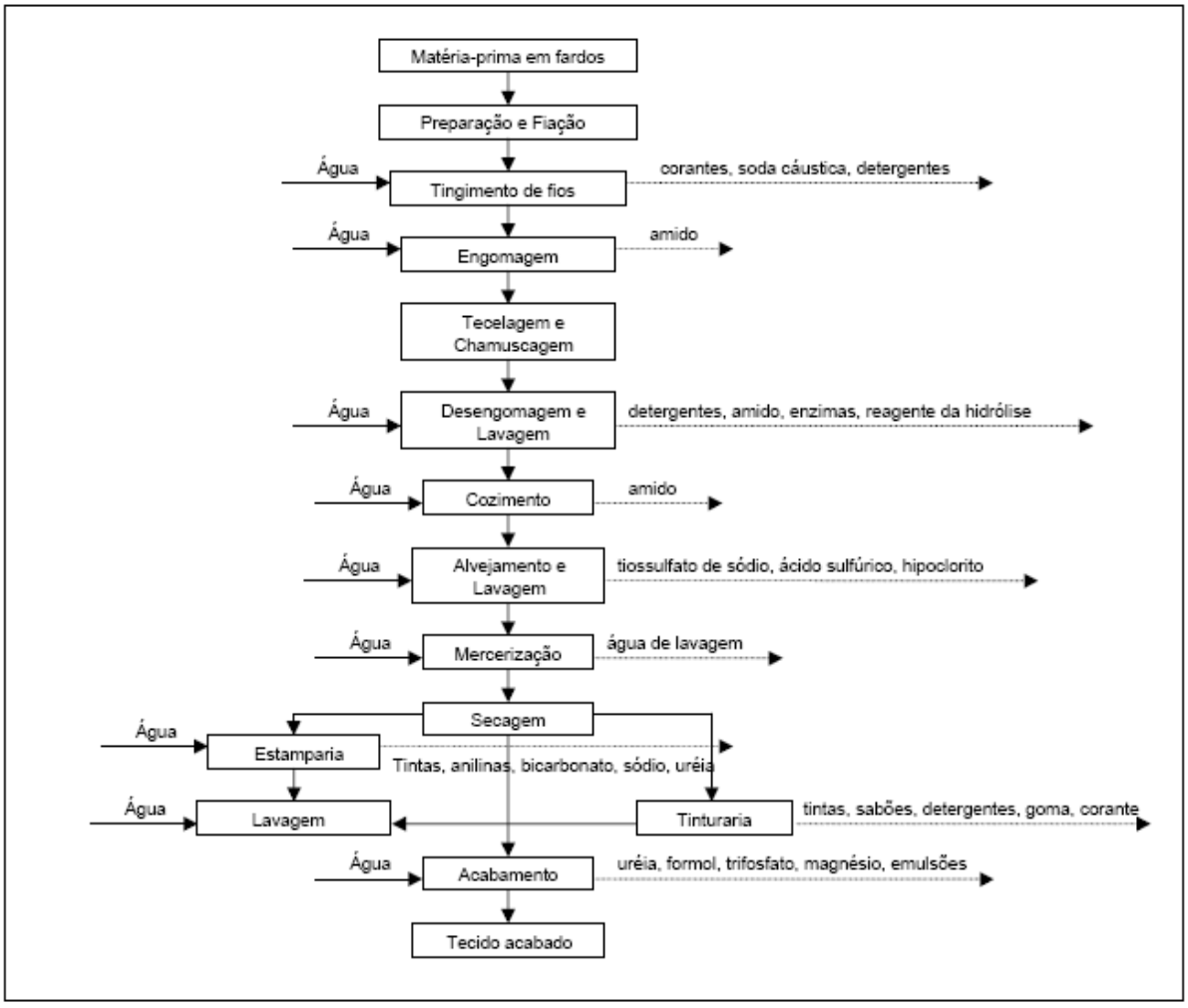

Figura 1. Processamento dos tecidos de algodão.
Fonte: Adaptado de Santos (2006).

Frente a estes inconvenientes, alternativas são trabalhadas para degradar estes compostos, ou seja, provocar a total mineralização de tais substâncias de forma sustentável. Deste modo, métodos de tratamentos convencionais como floculação, adsorção em carbono ativado, coagulação e osmose reversa são utilizadas como ferramentas para este tipo de problema, porém possuem somente a capacidade de promoverem a separação das fases, produzindo um resíduo secundário contaminado

com elevada carga orgânica. (Ferreira and Daniel 2004). Metodologias que visam à produção de espécies altamente reativas, denominadas por processos oxidativos avançados, se enquadram como uma possível alternativa para o tratamento destes efluentes não tratados e até mesmo os efluentes tratados que ainda possuem carga orgânica persistente (Robinson et al. 2000).

2.2.1 Problemas toxicológicos associados aos corantes

Apesar de sabermos que toneladas de resíduos são geradas pelas indústrias ao redor do mundo, poucas informações são difundidas em relação ao impacto desses rejeitos nos ecossistemas. Em virtude disso, The Ecological and Toxicological Association of Dyes and Organic Pigments Manufacturers (ETAD), tem realizado um grande esforço na tentativa de minimizar os impactos causados ao homem e ao meio ambiente, através da fiscalização durante o processo de produção e aplicação dos corantes. Esta entidade trabalha com a divulgação de artigos, identificando os riscos potenciais dos corantes.

Os riscos de intoxicação são decorrentes principalmente pelo contado dérmico ou ocular prolongado (Barka et al. 2007). Outro mecanismo desencadeador de efeito tóxico dos corantes pode ser ocasionado por bioativação molecular, ocorrendo principalmente via metabolismo enzimático. Reações hepáticas de 1ª fase podem transformar as moléculas dos corantes em subprodutos mais tóxicos, com propriedades carcinogênicas e mutagênicas, como por exemplo, radicais livres, que levam a

peroxidação lipídica com consequente dano celular e genético (Kudlich et al. 1999; Muthukumar et al. 2005).

Quando se trata de saúde humana, os riscos dos corantes sintéticos estão fortemente ligados ao tempo de exposição e pelas diversas vias de intoxicação (ingestão oral, contato com a pele e vias respiratórias) (Pinheiro et al. 2004). O contato com a pele parece ocorrer por certos corantes não incorporados à fibra, mantendo proximidade entre o tecido tinto e as zonas de pele sujeita a transpiração, propiciando a ocorrência de dermatites (Barka et al. 2007).

Para entender melhor os danos causados pelas intoxicações por via oral, é importante lembrar que os corantes são produzidos com o intuito de reagirem se ligando eficientemente com substâncias portadoras do grupamento amina e hidroxila, presentes na fibra natural, grupamentos estes também presentes em todos os organismos vivos (Kudlich et al. 1999; Pinheiro et al. 2004).

2.3 Os corantes

O primeiro corante conhecido pela humanidade foi o Negro-de-Fumo (*carbon black*), utilizado pelos homens primitivos nas paredes das cavernas reservadas ao culto. Outro corante, muito utilizado na antiguidade foi o azul egípcio, encontrado em amostras de tecido em tumbas egípcias, datados de 2.500 a.C (Guaratini and Zanoni 2000; Zanoni and Carneiro 2001).

Até meados do século XIX, somente eram usados corantes oriundos de matrizes naturais, como vegetais, insetos e moluscos. Como exemplo, é o caso do tradicional corante índigo blue, um pigmento azul, extraído da *Indigofera tinctoria L*, sendo largamente utilizado industrialmente nos dias atuais (Guaratini and Zanoni 2000).

Atualmente, a maior parte (90%) dos corantes utilizados na indústria têxtil é sintética. O *Colour Index*, catálogo utilizado para classificação internacional dos corantes, criado em 1924, registra cerca de 10.000 mil corantes orgânicos sintéticos empregados pela indústria têxtil (Zanoni and Carneiro 2001).

Os corantes são substâncias químicas extremamente diversificadas. Podem ser classificados de diversas formas: de acordo com sua constituição molecular, método de aplicação e tipo de excitação eletrônica (Balan 1999; Guaratini and Zanoni 2000).

2.3.1 Tipos de corantes

Os corantes podem ser classificados, de acordo com a constituição do grupo cromóforo, em três classes principais: corantes azóicos, corantes antraquinônicos e corantes indigóides (Guaratini and Zanoni 2000).

Os corantes azóicos representam o principal grupo de corantes comercializados. São compostos insolúveis em água e sintetizados sobre a fibra durante o processo de tingimento. São caracterizados por possuírem dois nitrogênios ligados por dupla ligação (–N=N–), quando ligados às moléculas distinguem-se pelo número de

grupamentos (mono-azo, di-azo ou poli-azo). A fabricação destes compostos oferece uma gama de possibilidades para realizar diversas ligações (Behnajady et al. 2007).

Os corantes antraquinônicos possuem o grupamento cromóforo carbonila >C=O sobre o grupo quinônico. Esta classe é extremamente resistente à degradação devido as suas estruturas aromáticas fundidas (Kim and Choi 2013).

Posteriormente, se encontram os corantes indigóides, com a dupla ligação entre dois carbonos (–C=C–). Derivam de duas reações, a primeira consiste na reação da anilina com o ácido monocloacético, resultando na fenilglicina, e por final a segunda reação de condensação. O resultado destas etapas culmina na oxidação final que é o índigo blue, principal produto utilizado na fabricação do *blue jeans* (Vautier et al. 2001).

2.3.2 Modo de fixação dos principais corantes

Esta forma de classificação dos corantes baseia-se de acordo com a forma de fixação têxtil. Podem ser principalmente classificados em: corantes reativos, direto, pré-metalizados, ácidos, básicos e corantes à cuba.

Os corantes reativos são aqueles compostos que possuem um grupo eletrofílico (reativo), com capacidade de reagir formando uma ligação covalente com grupos hidroxila e amino das fibras celulósicas, cuja ligação confere maior estabilidade na cor do tecido tingido (Lee et al. 1999). São os corantes mais utilizados na manufatura têxtil devido à rapidez de tingimento, facilidade de manejo e baixo consumo de energia. Na

tentativa de aumentar a fixação, uréia e sais são adicionados em grandes quantidades durante o processo de fixação. Este grupo possui alta solubilidade em água e baixa biodegradabilidade. (Guaratini and Zanoni 2000).

Os corantes diretos são solúveis em água, e tingem os tecidos (algodão, viscose) através das interações de *van der Waals*. Estes corantes são preparados de forma simples em salmoras de cloreto de sódio (NaCl) ou sulfato de sódio (Na_2SO_4). Esta classe possui uma vantagem, em consequência da necessidade de se lavar várias vezes o tecido, com a finalidade de esgotar o corante a fibra, diminui-se a concentração da corante nas águas residuárias (Guaratini and Zanoni 2000).

A próxima classe de corante é denominada como pré-metalizados, utilizados normalmente para tintura de fibras protéicas e poliamida. Esta classe caracteriza-se pela presença de um grupo hidroxila ou carbonila na posição orto em relação ao cromóforo azo, favorecendo a formação de complexos com íons metálicos (Chirila et al. 2011). Nesta classe, explora-se a capacidade de interação entre o metal e os grupamentos funcionais portadores de elétrons livres. Possui uma desvantagem ecológica pela elevada concentração de íons nas águas de rejeito (Santos 2006).

Os corantes ácidos são corantes aniônicos portadores de um a três grupamentos sulfônicos ($–SO_3Na$) ou carboxilados (–COONa). Estes grupos, quando associados tornam a molécula solúvel em água. Em contrapartida, os corantes básicos são moléculas catiônicas compostas de sais dos diversos compostos orgânicos do grupamento amino ($–NH_2$) e (=NH). Estes corantes apresentam cores vivas e variadas, mas pouco duráveis (Grcic et al. 2014).

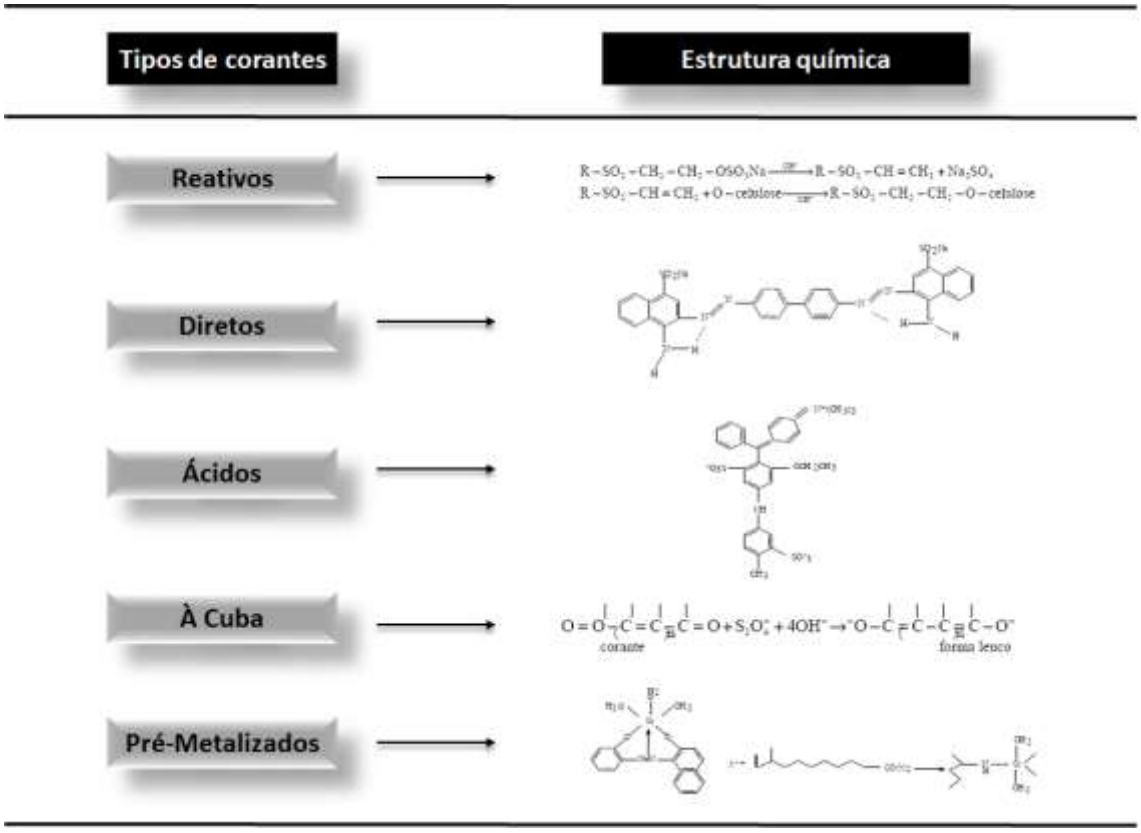

Figura 2. Principais grupos de corantes e suas especificações.
Fonte: adaptado de Guaratini and Zanoni (2000).

Por fim, temos os corantes à cuba, sendo uma importante classe de corantes baseadas nos índigos, tioindigóides e antraquinóides. Eles são praticamente insolúveis em água, porém, durante o processo de tingimento são reduzidos com ditionito, em solução alcalina, transformando-se em um composto solúvel (forma leuco). A maior aplicação deste tipo de corante está no tingimento dos fios de algodão (Paschoal and Tremiliosi-Filho 2005).

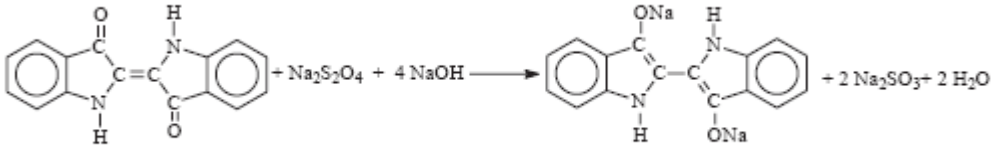

Figura 3. Reação de redução química do índigo a leucoíndigo pelo ditionito.
Fonte: Paschoal and Tremiliosi-Filho (2005).

2.3.3 O corante índigo

O índigo é conhecido desde a antiguidade, tendo sua origem na Índia, nas antigas civilizações do Egito, Grécia e Roma, sendo considerado um corante nobre devido as suas excelentes qualidades em tingir. A origem do índigo não foi diferente, tendo suas origens na natureza na forma da Indigotina, a qual era extraída diretamente das plantas em países tropicais da *Indigosfera tictória* e nos países temperados da *Polygoniun tintoctorun*. Sua extração era realizada com água, resultando em uma solução de glicósido de indoxilo, e em virtude da sua oxidação com o ar originava o índigo (Guaratini and Zanoni 2000).

Com o advento da industrialização, em 1897, a BASF iniciou a produção do índigo sintético a preços mais baixos do que o produto fabricado naturalmente. Fruto da industrialização é que nos dias de hoje, cerca de 20.000 toneladas/ano de índigo sintético são produzidos, principalmente como agente corante dos “blue jeans” (Santos 2006).

Existem duas formas de apresentação do índigo, primeiramente temos o índigo blue tradicional, possuindo como característica química a presença do grupo cetônico (C=O), insolúvel em água, porém quando se encontra na forma reduzida (C-OH), torna-se solúvel e o corante passa a ter afinidade química pela fibra celulósica. Este processo é feito na indústria têxtil reduzindo-se o índigo blue com ditionito de sódio, para se tornar solúvel em meio aquoso, processo mostrado anteriormente na Figura 3 (Paschoal and Tremiliosi-Filho 2005).

A segunda forma de apresentação é o corante índigo carmim, solúvel em água. Os corantes à cuba são insolúveis em água, porém quando se adicionam grupamentos sulfônicos ($–SO_3Na$), estes corantes tornam-se hidrofílicos (Liao et al. 2009). É de fato, o que acontece com esta molécula, quando na estrutura do índigo blue são adicionados dois grupamentos sulfônicos, originando-se o índigo carmim.

O corante índigo carmim é considerado um indigóide altamente tóxico, podendo causar irritações na pele e na córnea. O corante possui propriedades cancerígenas e que interferem no desenvolvimento neural; e o seu consumo pode ser fatal (Secula et al. 2011). Othman et al. (2007) demonstraram que o corante induz a ocorrência de tumores nos locais de aplicação e, quando administrado por via intravenosa, pode causar hipertensão grave, doenças cardiovasculares e problemas respiratórios.

Na Figura 4, observamos as duas estruturas dos corantes, atentando para os grupamentos $NaSO_3$ do índigo carmim, os quais lhe confere solubilidade em meio aquoso. Também na figura abaixo, é evidenciando o grupo cromóforo, responsável pela

cor do corante, este consiste de um sistema conjugado de uma ligação (–C=C–) substituído por dois grupos doadores de eletróns (NH) e dois grupos aceitadores de eletróns (C=O) (Vautier et al. 2001).

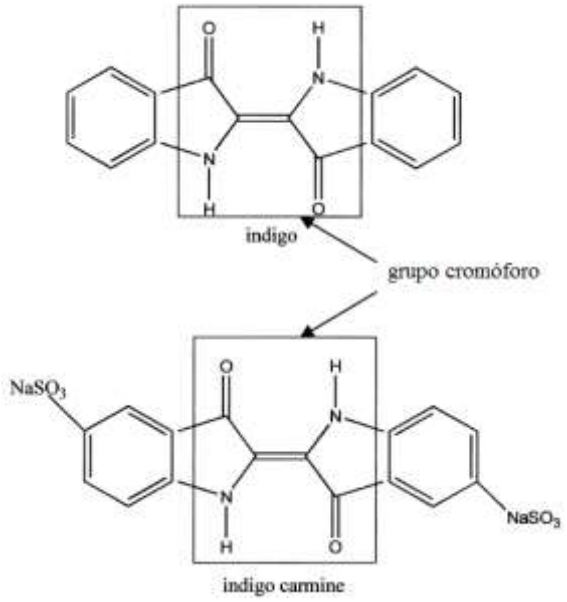

Figura 4. Estrutura química do índigo blue e índigo carmim.
Fonte: adaptado de Vautier et al. (2001).

2.3.4 Corantes Azo

Os corantes azos fazem parte de uma importante classe de corantes utilizadas na indústria têxtil. Possuem em sua estrutura o grupamento cromóforo -N=N- comum para todos os corantes azo, e representam de 60-70% de todos os corantes produzidos (Robinson et al. 2000; Behnajady et al. 2007).

Esta classe de corante possui alta estabilidade e baixa biodegradabilidade em condições aeróbicas, devido principalmente a sua complexidade estrutural (Habibi et al. 2005). Em condições anaérobicas esses corantes podem ser degradados, porém originam substâncias potencialmente danosas como aminas aromáticas carcinogênicas. Aminas estas quando em contato com o corpo interagem com enzimas hepáticas e células intestinais, sendo potencialmente causadores de câncer em humanos (Bizani et al. 2006).

Devido a sua estrutua química, esses corantes são produzidos para serem resistentes a exposição à luz, a lavagem e a produtos químicos, consequentemente os tratamentos tradicionais aplicados para esta classe especifica de efluentes são usualmente ineficazes (Zainal et al. 2005).

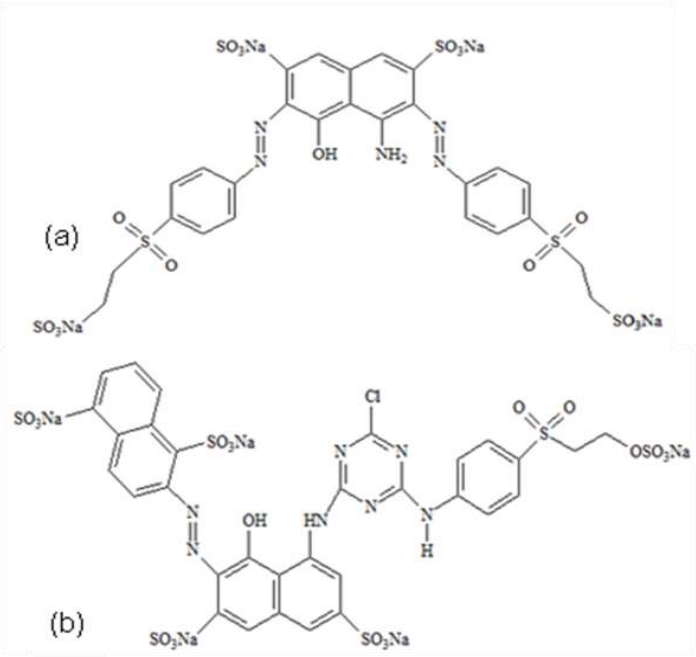

Figura 5. Estruturas químicas de dois azos corantes: (a) Remazol Marinho RGB 150% gran (C.I Reactive Black 5. (b) Remazol Vermelho Ultra gran (C.I Reactive Red 239).

2.4 Interferentes endócrinos

Esta classe de substâncias é bem conhecida no meio científico, desde 1900 pesquisadores já reconheciam os efeitos causados nos sistema endócrino em animais de laboratório (Allen and Doisy 1923). Porém, atualmente essas moléculas têm ganhando visibilidade, devido ao desenvolvimento das técnicas analíticas mais sensíveis que possibilitaram a detecção destas substâncias em água potável, além dos efeitos detectados na saúde humana e ambiental (Billa and Dezotti 2007).

Um grande debate acontece em torno da definição sobre os interferentes endócrinos, por diversos pesquisadores do meio científico. Do termo em inglês, "Endocrine Disrupting Chemicals", alguns autores somente consideram as substâncias que interagem com sítios receptores de hormônios, enquanto outros entendem como qualquer substância que cause desequilíbrio, interferência ou alteração no sistema endócrino, independentemente se atua diretamente no sítio receptor ou não (Billa and Dezotti 2007).

Por outro a lado a Environmental Protection Agency (EPA), define como interferente endócrino um "agente exógeno que interfere com síntese, secreção, transporte, ligação, ação ou eliminação de hormônio natural no corpo que são responsáveis pela manutenção, reprodução, desenvolvimento e/ou comportamento dos organismos" (EPA 1997). Em linhas gerais, usaremos o termo Interferente Endócrino (IE) no referido trabalho.

Os casos mais emblemáticos em relação à exposição aos IE foram às anomalias encontradas no sistema reprodutivo em jacarés nos diversos lagos da Flórida contaminados com DDT e seus produtos, pesticida hoje banido em diversos países do mundo, pois apresenta elevada persistência no ambiente e possui reconhecida atividade estrogênica (Guillette et al. 1996). Fato este registrado em 1962 por Rachel Carson, na qual publicou o conhecido livro "Silent Spring", notoriamente um dos primeiros relatos sobre a relação entre o DDT no ambiente e a redução de diversas espécies de pássaros e mamíferos.

Outro problema estudado e registrado em virtude da atividade estrogênica decorrente dos interferentes endócrinos foi registrado entre os anos de 1948 e 1970. Uma classe de médicos habituou-se a prescrever o fármaco dietilestilbestrol (DES), um potente estrogênico sintético (Birkett and Lester 2003). A administração de tal substância vinha com o intuito de prevenir abortos e promover o desenvolvimento fetal. Porém, com o passar dos anos descobriu-se que filhas de mães que fizeram o uso do DES, quando atingiam a puberdade apresentaram disfunção no sistema reprodutivo, gravidez anormal, redução na fertilidade, desordem no sistema imunológico e muitas desenvolveram câncer vaginal (Colborn et al. 1993).

Um importante estudo realizado por Carlsen et al. (1992) mostrou o declínio da qualidade do sêmen de homens entre os anos de 1938 e 1990, e um outro estudo realizado por Jobling et al. (1998) em rios da Inglaterra durante a década de 1990, revelou a ocorrência de pseudo-hermafroditismo em peixes machos (*Rutilus rutilus*).

Podemos dizer que tais casos foram um marco de interesse e preocupação relevante no meio científico frente a esta classe de substâncias, promovendo um desenvolvimento das pesquisas para este tema, e consequentemente a publicação de diversos livros e artigos referentes ao tema.

2.4.1 Classificação das substâncias e meios de exposição aos IE

Ainda são inconclusivos os dados para identificar os critérios de seleção utilizados para agrupar as substâncias, porém podemos classificar a substâncias ditas como interferentes endócrinos em duas classes. A primeira é a classe dos IE sintéticos, empregados na agricultura e seus subprodutos, como pesticidas, herbicidas, fungicidas e moluscicidas; utilizadas nas indústrias e seus subprodutos, como dioxinas, PCB, alquilfenóis, hidrocarbonetos policíclicos aromáticos, ftalatos, bisfenol A, metais pesados; compostos farmacêuticos, como os estrogênios sintéticos. E a outra classe são os IE de origem natural, como os fitoestrogênios (genisteína e metaresinol) e os estrogênios naturais (estradiol, estrona e estriol) (Billa and Dezotti 2007).

As diferentes classes dos interferentes endócrinos estão presentes nos diversos compartimentos ambientais, possuindo elevada persistência no ambiente, lipossolubilidade e baixa pressão de vapor, o que facilita sua dispersão e difusão no meio ambiente (Billa and Dezotti 2007).

Consideráveis quantidades de substâncias sintéticas são liberadas no ambiente ao redor do globo, e uma grande parcela destas é considerada como interferentes

endócrinos. As vias de exposição ao homem frente aos IE podem ser por via direta, tanto no local de trabalho como em casa, ou por via indireta através de água, ar ou alimentos, sendo a principal via de contaminação por via oral através de alimentos contaminados (Vandenberg et al. 2007).

A ingestão de carne, peixes, ovos, leite e seus derivados é uma importante fonte de contaminação por IE, principalmente devido ao uso de hormônios na criação dos animais, que se bioacumulam nos tecidos com composição adiposa. Os resíduos de agrotóxicos em frutas e vegetais são também outra fonte significativa de exposição aos interferentes endócrinos (Peterson et al. 2000).

2.4.2 Bisfenol A

O Bisfenol A (BPA) é um plastificante orgânico muito comumente incorporado a outros materiais, com a finalidade de ganho de flexibilidade e maleabilidade (Staples et al. 1998). BPA é o nome comumente usado para o 4,4’-diidroxi-2,2-difenilpropano e sua obtenção é originada pela combinação de duas moles de fenol com uma mole de acetona. A grande maioria (99,9%) de BPA produzido é usado como intermediário na produção de policarbonatos, resinas epóxi, retardantes de chama e entre outros produtos (Rubin 2011). Os produtos finais advindos do BPA incluem: adesivos, garrafas de água, tintas em pó, brinquedos, revestimentos de partes elétricas, lentes ópticas, materiais de construção, proteção de vidros de janela e discos compactos (Staples et al. 1998).

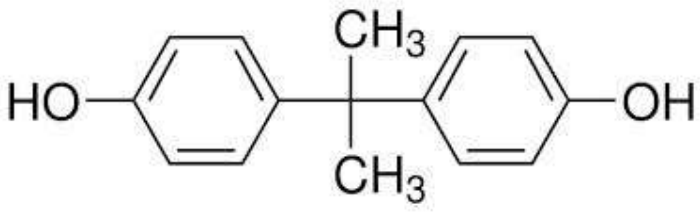

Figura 6. Estrutura química do Bisfenol A

A principalmente fonte de contaminação ambiental pelo BPA é a industrial, durante a manufatura do produto nas fases de manipulação, descarregamento e aquecimento, assim como possíveis derramamentos acidentais, sendo o compartimento aquático o principal local onde se encontra o composto (Mercea 2009). Estima-se que a produção global anual de BPA gira em torno de 5,2 milhões de toneladas (European Union 2010).

A exposição humana pelo BPA acontece primariamente através da dieta (comidas enlatadas, garrafas de água, etc) (Vandenberg et al. 2007). Os produtos manufaturados com resinas e plásticos policarbonatos podem conter quantidades vestigiais de BPA, que podem estar presentes, quer como resultado de hidrólise, ou como um monómero que não reagiu a partir processo de produção, desta forma o BPA é transferido através do contato de alimentos e bebidas embalados por materiais plásticos (Mercea 2009; European Union 2010).

Nos últimos anos, têm se consolidado e avançado a hipótese de que a exposição a doses extremamente baixas a substâncias com atividade endócrina (hormonal) poderia causar efeitos adversos na saúde de seres humanos, incluindo interrupção do

desenvolvimento normal do feto ou de funções reprodutoras (PlasticsEurope 2012). O BPA se enquadra em tal hipótese, podendo até mesmo provocar efeitos adversos em doses muito mais baixas do que os níveis de segurança pré-estabelecidos (vom Saal and Welshons 2006). A norma de segurança estabelecida pela Environmental Protection Agency (EPA) em 1988 e adaptada pela Food and Drug Administration (FDA) como uma dose referência para o BPA foi calculada como sendo de 50µg/kg (peso corporal) /dia, esta dose referência continua a ser o padrão de segurança atual hoje, apesar de novos conhecimentos sobre os perigos da exposição ao BPA (Vandenberg et al. 2009).

Com base na DL_{50} observada em animais, a União Europeia (2003) concluiu que o bisfenol A possui baixa toxicidade aguda através de todas as vias de exposição relevantes para os seres humanos. Entretando foram observados sinais de dano hepático e hemorragia gastrointestinal em ratos agudamente expostos ao BPA por via oral. Paralelamente efeitos agudos da exposição por inalação em ratos incluíram leve inflamação transitória do epitélio nasal e ulceração do ducto oronasal (União Europeia 2003).

Efeitos estrogênicos ao BPA são relatados, estudos compararam a potência estrogênica do BPA ao do 17β-estradiol, etinilestradiol, dietilestilbestrol, revelando variabilidade considerável nas ordens de magnitude entre os compostos estudados (Chapin et al. 2008). Outro estudo *in vivo*, avaliou o efeito estrogênico, examinando o peso do útero de ratos ou comundongos adultos ovariectomizadas, podendo o BPA

aumentar ou diminuir o peso uterino dependendo da concentração e tempo de exposição (Chapin et al. 2008).

Efeitos genotóxicos ao BPA foram somente observados em *estudos in vitro* de acordo com Haighton et al. (2002), sendo evidênciado potencial aneugênicos, aberração cromossómica, formação de micronúcleos e aductos de DNA. Heimeier and Shi (2010) sugeriram que o BPA pode afetar a embriogênese humana e desenvolvimento neonatal através da ruptura ou inibição de vias de hormônio da tireóide. Provavelmente o BPA se liga ao receptor do hormônio da tireóide agindo como um antagonista da atividade da transcrição da triiodotironina-T3 (Moriyama et al. 2002).

Diversos outros efeitos do BPA foram descritos por Rubin (2011), e podem ser visualizados na Figura 7.

Figura 7. Alguns dos efeitos relacionados à exposição ao BPA.
Fonte: adaptado Rubin (2011).

2.5 Métodos convencionais para tratamento de efluentes

Diversos processos de tratamento estão sendo aplicados para a remediação de efluentes contendo poluentes orgânicos persistentes. Entre os variados tipos de tratamentos encontram-se a classe dos processos convencionais, que podem se dividir em: físicos, químicos e biológicos (Baird 1999; Teixeira and Jardim 2004).

Os métodos físicos baseiam-se somente na transferência de fase do contaminante, sem que ele seja realmente destruído. Quando o efluente sofre este tipo de tratamento, são formadas duas fases, uma composta pela água limpa e outra pelo resíduo do contaminante concentrado (Figueiredo et al. 2005). As técnicas que se enquadram neste tipo de tratamento podem ser: precipitação, coagulação, floculação, sedimentação, filtração, ultrafiltração, osmose reversa e destilação (Teixeira and Jardim 2004).

Embora de grande aplicabilidade, essas tecnologias apresentam algumas desvantagens. Por exemplo, a coagulação com posterior floculação, vem sendo utilizada no tratamento de efluentes têxteis. São usados sais de ferro, alumínio e polímeros como agentes coagulantes, com a finalidade de formar flocos com as substâncias dispersas em água, sendo então separados por filtração. É um método eficiente para tratar corantes dispersos, porém não são capazes de remover corantes solúveis em meio aquoso. (Vandevivere et al. 1998).

Métodos de adsorção também possuem aplicabilidade no tratamento de efluentes industriais, no qual o carvão ativado entra como o adsorvente mais utilizado,

entretanto o produto apresenta um custo elevado, tornando o método desfavorável economicamente (Figueiredo et al. 2005).

Outro processo físico que se baseia na mineralização dos compostos orgânicos é a incineração. Esta metodologia possui excelentes resultados no tratamento de poluentes altamente tóxicos e recalcitrantes, no entanto, as elevadas temperaturas (850ºC) aplicadas, elevam o seu custo e dificultam as operações. Além disso, o método gera um passivo desfavorável, devido à formação de gases altamente tóxicos, como as doxinas e furanos, caso não haja um controle rigoroso das temperaturas, ou se por razões econômicas energéticas o processo for conduzido a baixas temperaturas (Baird 1999; Teixeira and Jardim 2004).

Os tratamentos químicos mais empregados visam à oxidação da matéria orgânica. Os agentes mais comumente utilizados no tratamento das águas residuárias são cloro (Cl_2), hipoclorito de sódio (OCl^-), permanganato de potássio ($KMnO_4$), ozônio (O_3) e peróxido de hidrogênio (H_2O_2) (Teixeira and Canela 2007).

Dentre estes, a ozonização é um método bem difundido, pois oferece resultados satisfatórios no tratamento de corantes e resíduos com alta carga orgânica. Os grupamentos cromóforos dos corantes em sua maioria possuem dupla ligação; a ozonização possui alto poder oxidante promovendo rapidamente a quebra das duplas ligações e consequentemente formando compostos menores e favorecendo a redução da coloração (Umar et al. 2013). Normalmente a ozonização é aplicada como um pré-tratamento para de resíduos com alta carga orgânica e inorgânica.

O tratamento biológico, por sua vez, é a técnica mais utilizada devido ao seu baixo custo e a sua versatilidade para depurar diferentes tipos de efluentes, sendo comumente aplicado no tratamento de efluentes com baixa toxicidade e grande volume (Haimi et al. 2013). Este tipo de tratamento pode se dividir nos processos aeróbicos, que utilizam bactérias e fungos, os quais requerem oxigênio molecular, depurando a matéria orgânica, e os processos anaeróbicos, que utilizam bactérias específicas na formação de CO_2 e metano (CH_4) (Kunz et al. 2002). Os tratamentos biológicos são atrativos, principalmente pelo seu baixo custo e versatilidade, porém, na presença de poluentes com alta toxicidade e em elevadas concentrações, os micro-organismos podem ser inativados e consequentemente interromper o tratamento pelo qual estão sendo empregados (Manahan et al. 2001).

Os tratamentos biológicos utilizam lodo ativado para promover a depuração de águas contaminadas, que vem a ser um adjuvante após o efluente sofrer processos de tratamento físicos e/ou químicos (Haimi et al. 2013). Este tipo de sistema apresenta alta eficiência, permitindo remover 80% da carga orgânica. Infelizmente, o problema do acúmulo de lodo torna-se um problema crítico, uma vez que se encontram alto teor de substâncias orgânicas não biodegradadas adsorvidas ao lodo (Clarke and Smith 2011). Além do mais, muito do lodo produzido, pode ser aproveitados como adubo na agricultura como biosólidos após processo de compostagem (Gibson et al. 2010).

2.6 Sistema biológico convencional utilizado no tratamento de águas residuárias

O tratamento biológico pelo processo de lodo ativado é o método mais difundido nos dias de hoje para o tratamento de águas residuais com o objetivo de remover grandes quantidades de matéria orgânica e nutrientes (Olsson 1977). O sistema de lodo ativado utiliza diversos micro-organismos específicos (bactérias, fungos e protozoários) que vivem suspensas nas águas residuais. Para que toda essa biota tenha a capacidade de decompor toda a massa de compostos orgânicos e inorgânicos, torna-se necessário um tempo de adaptação dos micro-organismos as água residuais para que os processos biológicos ocorram (Cirja et al. 2010).

Uma importante fase do tratamento biológico é a aeração, o ar é introduzido no tanque através de bombas de recirculação fornecendo oxigênio necessário para a oxidação dos contaminantes via micro-organismos (Haimi et al. 2013). Além disso, a recirculação limita a formação de zonas mortas e evita que os flocos de bactérias se decantem, mantendo sempre misturado a água residuária a ser tratada com a biomassa (Sipma et al. 2010).

Durante o processo do tratamento biológico, acontece o aumento da massa de lodo em consequência da reprodução bacteriana, que se nutre dos compostos orgânicos presentes na água a ser tratada (Cirja et al. 2010; Haimi et al. 2013). O lodo pode ser reutilizado, introduzindo-se novamente no tanque de aeração ou a parte do lodo considerada como excesso deve ser descartada, após tratamento adequado (Sipma et al.

2010). Surge então a segunda etapa do tratamento, podendo ser denominada como clarificação secundária.

O processo de clarificação nada mais é que a separação do lodo/conteúdo líquido tratado. O lodo é ligeiramente mais pesado do que a água, então a biomassa é direcionada a um decantandor para que os flocos de lodo assentem por meio da gravidade, a separação é facilitada pelo design do clarificador o qual deve garantir baixa turbulência e velocidade (Jefferson et al. 2001). Parte do lodo sedimentando regressa ao tanque e o efluente tratado é descartado nos corpos d´água receptores.

A qualidade de um tratamento biológico em sistemas de lodo ativado está diretamente relacionada tanto com a composição da comunidade dos micro-organismos no reator, quanto com a eficiência da separação sólido-líqudo (Olsson 1977; Jefferson et al. 2001; Haimi et al. 2013).

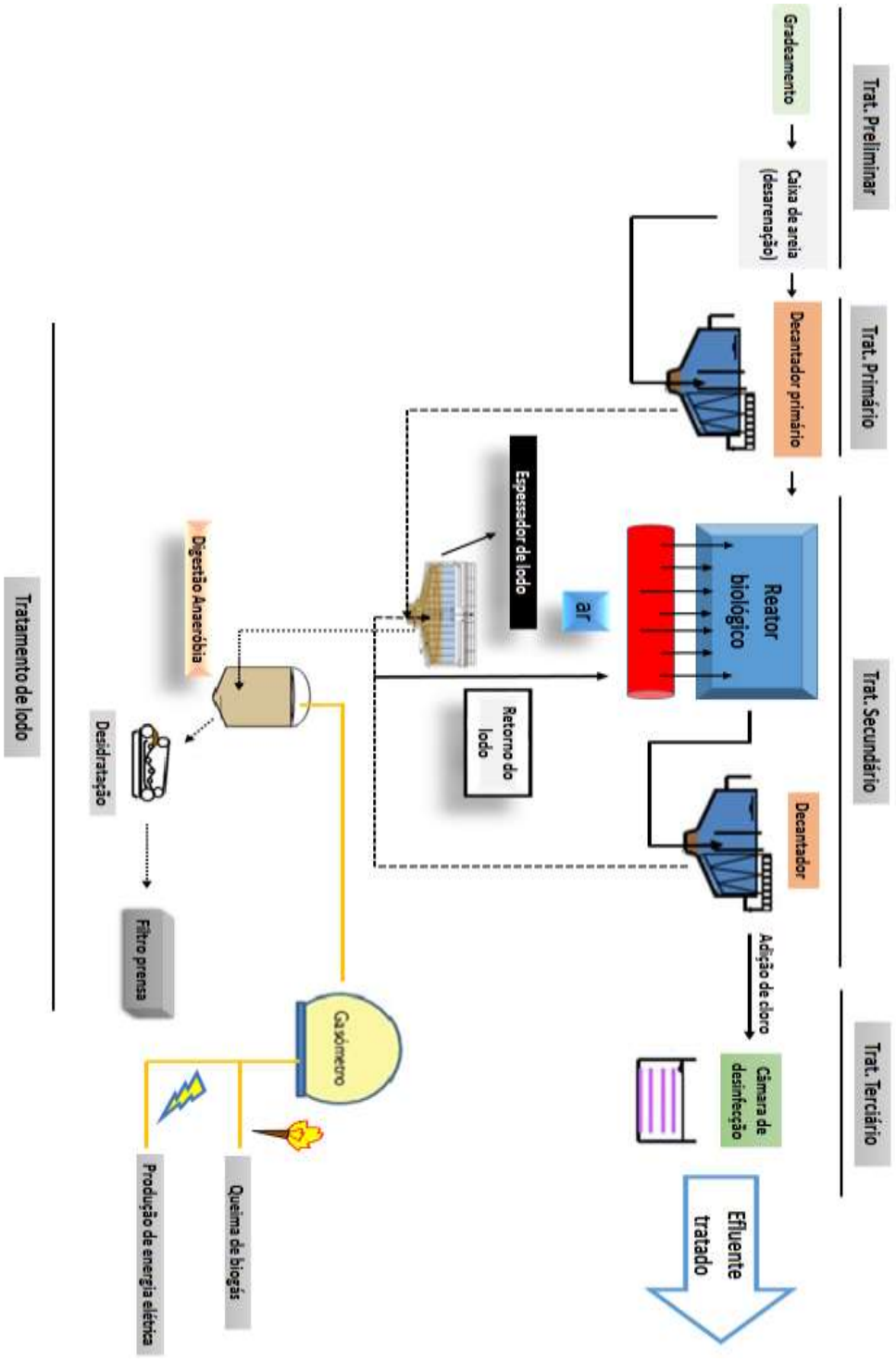

Figura 8. Esquema simplificado de uma estação de tratamento de água residual (ETAR) por tratamento biológico pelo processo de lodo ativado.

2.7 Processos oxidativos avançados (POAs) no tratamento de efluentes

É antiga a utilização de agentes oxidantes no tratamento (degradação, depuração e desinfecção) de água. O primeiro trabalho que reportou o uso de ozônio como desinfetante foi feito por De Meritens em 1886. Entretanto, somente em 1975, em um trabalho que combinava ozônio e radiação ultravioleta para oxidar complexos de cianeto, usou-se a terminologia "Tecnologias de Oxidação Avançada" (Matsuda et al. 1975). Além disso, nesta mesma década, Fujishima e Honda (1972) descreveram a oxidação da água em suspensão de dióxido de titânio (TiO_2) gerando oxigênio e hidrogênio. E na segunda metade da década, em 1976, foi publicado o primeiro trabalho utilizando fotocatálise heterogênea na degradação de contaminantes. Talvez, estes trabalhos tenham sido o ponto de partida para difundir o conhecimento destes processos (Teixeira and Jardim 2004; Oliveira et al. 2012 2,

Os processos oxidativos avançados (POAs) são um conjunto de métodos de oxidação química usados para degradar matéria orgânica biorecalcitrante. A oxidação pode não ser completa; frequentemente uma oxidação parcial é suficiente para diminuir a toxicidade dos compostos persistentes ou permitir a adequação do efluente para ser tratado por processos biológicos (Eckenfelder Jr. 2000). O quadro 1 sumariza os principais tratamento não biológicos para o tratamento de efluentes.

Quadro1. Principais métodos não biológicos para tratamento de efluentes.

Métodos não biológicos	**Vantagem**	**Desvantagem**
Reagente *Fenton*	Efetiva descoloração de corantes solúveis e insolúveis	Geração de lodo
Ozonização	Aplicado no estado gasoso, sem alterar o volume do efluente	Baixo tempo de vida (20minutos)
Fotoquímico (Reação de oxidação com NaOCl)	Não produção de lodo e aceleração de quebra da ligação azo	Formação de aminas aromáticas
Destruição eletroquímica (Reação de oxidação usando eletricidade)	Compostos formados não são perigosos	Alto custo de eletricidade
Carvão ativado	Boa remoção de todos os tipos de corante	Muito caro
Filtração por membrana	Remoção de todos os tipos de corantes	Concentrada produção de iodo
Resina de troca iônica	Não há perda de resina	Não efetivo para todos os corantes
Coagulação eletrocinética	Viável economicamente	Alta produção de lodo

Fonte: adaptado de Braúna (2007).

O tratamento ideal consiste na completa oxidação dos compostos orgânicos (mineralização), ou seja, conversão em dióxido de carbono (CO_2), água (H_2O) e íons inorgânicos. Porém, é importante verificar se a degradação parcial não resulta na formação de produtos de degradação mais tóxicos que o composto original (Legrini et al. 1993).

2.7.1 Teoria da oxidação avançada

Embora os diversos processos oxidativos avançados façam usos de vários sistemas reacionais, todos eles têm uma mesma característica química: a produção e utilização de radicais hidroxila ($OH^{\bullet}$), que tanto em solução aquosa, como no ar, é um agente oxidante efetivo (E_v=2,8Ev) (Fujishima and Honda 1972). Estes radicais são espécies altamente reativas, capazes de atacar e destruir moléculas orgânicas que normalmente não são oxidadas por oxidantes comuns como oxigênio, ozônio ou cloro (Metcalf and Eddy 2003)

Os radicais podem ser gerados através de reações envolvendo fortes oxidantes, como ozónio (O_3) e peróxido de hidrogênio (H_2O_2), semicondutores, como dióxido de titânio (TiO_2), óxido de zinco (ZnO) e radiação ultravioleta (UV) (Fujishima et al. 2010). No Quadro 2 compara-se o poder oxidante do radical hidroxila com o de outros oxidantes mais comuns também comumente empregados em oxidação química.

Quadro 2. Potenciais de oxidação de vários agentes oxidantes.

Agente oxidante	Potencial de oxidação (Volts)
Flúor	3,06
Radical hidroxila	2,80
Oxigênio atómico	2,42
Ozônio	2,08
Peróxido de hidrogênio	1,78
Permanganato	1,68
Hipoclorito	1,49
Cloro	1,36
Oxigênio molecular	1,23

Fonte: Adaptado a partir de Teixeira and Jardim (2004).

O radical hidroxila é o oxidante mais poderoso a seguir ao flúor e consegue dar início a uma série de reações de oxidação que podem conduzir a mineralização completa do composto de partida e dos seus produtos de degradação (Oliveira et al. 2012). O radical hidroxila reage com todas as classes e grupos de compostos, principalmente por reações de abstração de hidrogênio (1), adição eletrofílica (2), transferência de elétrons (3) e reações entre radicais hidroxila (4) (Will et al. 2004).

$$HO^{\bullet} + RH \longrightarrow R^{\bullet} + H_2O \quad (1)$$

$$HO^{\bullet} + PhX \longrightarrow HOPhX^{\bullet} \quad (2)$$

$$HO^{\bullet} + RX \longrightarrow RX^{\cdot +} + HO^{-} \quad (3)$$

$$2\ HO^{\bullet} \longrightarrow H_2O_2 \quad (4)$$

O radical hidroxila caracteriza-se pelo seu ataque pouco seletivo, o que constitui um atributo muito útil para um oxidante usado em descontaminação ambiental (Moreira et al. 2005).

Os POAs podem ser classificados como processos heterogêneos ou homogêneos. Os primeiros são processos que utilizam semicondutores como catalisadores na fase sólida, a reação química ocorre na interface entre as duas fases e a velocidade é proporcional à área de contato. E os últimos são aqueles em que o catalisador e o sistema constituem apenas uma fase (Oliveira et al. 2012). A Figura 9 apresenta típicos sistemas de POAs.

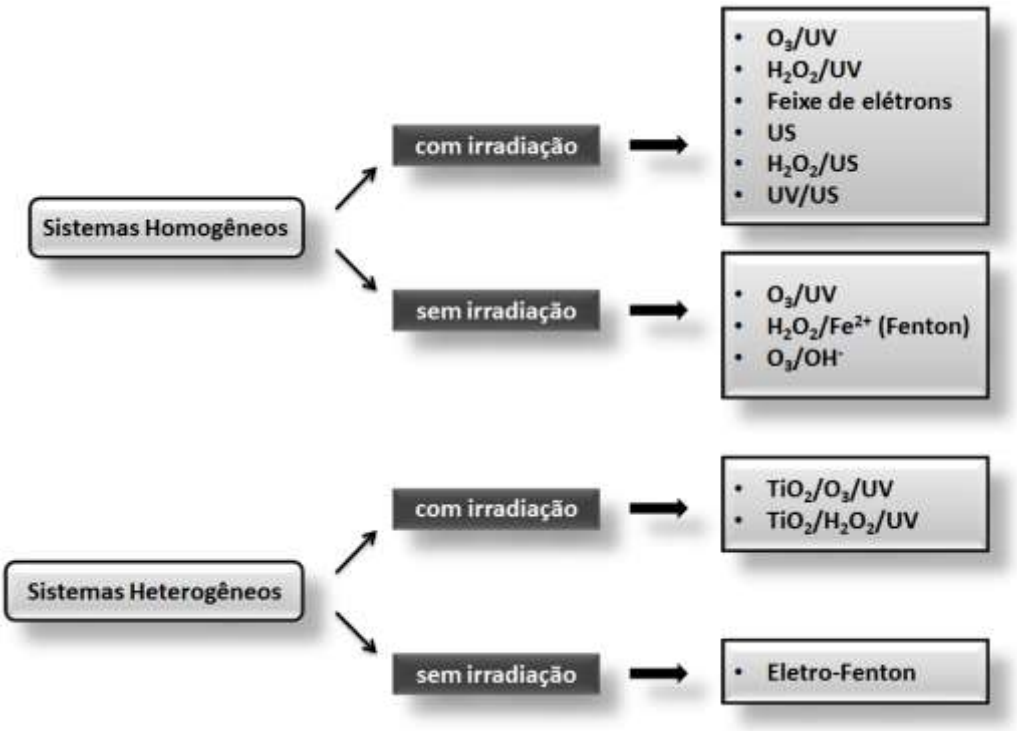

Figura 9. Sistemas típicos de processos oxidativos avançados.
Fonte: adaptado de Silva (2007).

Este grupo de tratamentos difere dos tratamentos clássicos por promover a degradação dos poluentes, ao invés de simplesmente garantir a sua concentração ou transferência para outra fase. Deste modo, resíduos secundários podem ser suprimidos.

2.7.2 Principais sistemas de POAs utilizando radiação ultravioleta (UV)

2.7.2.1 Fotólise direta com radiação ultravioleta

Neste tipo de tratamento a luz é a única fonte capaz de destruir o poluente (Wols and Hofman-Caris 2012). É um processo com baixa eficiência quando comparado com outros processos oxidativos. Assim, a maioria dos estudos são realizados em acoplamento com outros recursos, como por exemplo: H_2O_2/UV, O_3/UV, H_2O_2/O_3/UV, apresentando nesses casos, resultados mais satisfatórios que o uso desses agentes isolados (Morais et al. 2006).

2.7.2.2 Ozônio/UV

O ozônio é a forma triatômica do oxigênio, sendo um gás incolor de odor pungente e com alto poder oxidante (E_0=2,08V). Devido a sua instabilidade, em meio aquoso se decompõe rapidamente a oxigênio e espécies radicalares. Em função disso, o uso do ozônio costuma ser muito eficiente na remoção da coloração dos efluentes (Kunz et al. 2002).

A produção de radicais hidroxila por irradiação do ozônio (O_3) com radiação ultravioleta (UV) ocorre seguindo a reação:

$$O_3 + h\gamma_{uv} \longrightarrow O_2 + \text{oxigênio singleto} \quad (5)$$

$$\text{Oxigênio singleto} + H_2O \longrightarrow OH^{\bullet} + OH^{\bullet} \text{ (em ar húmido)} \quad (6)$$

$$\text{Oxigênio singleto} + H_2O \longrightarrow OH^{\bullet} + OH^{\bullet} \rightarrow H_2O_2 \text{ (em água)} \quad (7)$$

Em ar húmido, a fotólise do ozônio conduz à formação de radicais hidroxila, enquanto que, em água os radicais hidroxila recombinam e dão rapidamente origem a peróxido de hidrogênio (Ramstedt et al. 2010). Devido a esta reação o uso deste processo em água se torna economicamente inviável, pois gasta-se muito com energia para manter uma elevada concentração de radicais hidroxila em solução. Porém em sistemas reativos complexos, a geração dos radicais ocorre em meio aquoso pela decomposição do peróxido de hidrogênio (8), formado através da fotólise do ozônio (Sillanpää et al. 2011).

$$H_2O_2 + h\gamma_{uv} \longrightarrow 2\ HO^{\bullet} \quad (8)$$

Em termos operacionais, o efluente é saturado com ozônio e submetido à radiação ultravioleta. O ozônio absorve radiação UV a comprimentos de onda a 310 nm, desta forma utiliza-se uma faixa de comprimento de onda menor ou até 254 nm, correspondente ao máximo de adsorção (Ramstedt et al. 2010; Sillanpää et al. 2011).

No entanto o processo ozônio/UV possui uma maior eficiente na degradação de compostos em correntes gasosas. Sendo muito bem aplicados no tratamento de grandes volumes de efluente, na degradação de poluentes orgânicos tóxicos e nocivos em pequenas concentrações (Wu 2007).

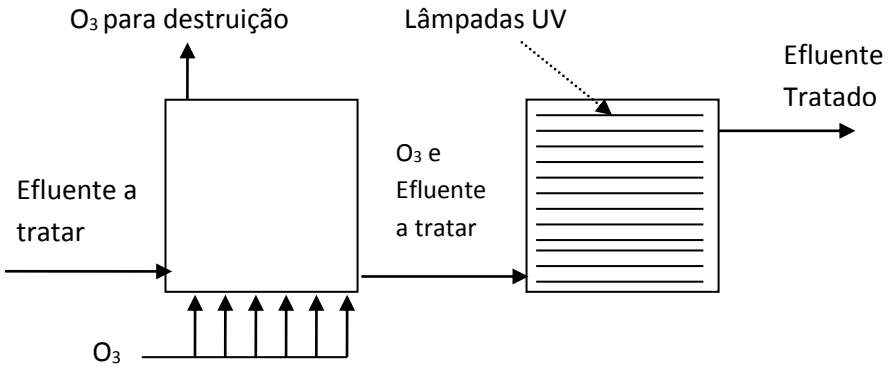

Figura 10. Representação esquemática de um processo oxidativo avançado utilizando ozônio e radiação UV.
Fonte: Metcalf and Eddy (2003).

2.7.2.3 Ozônio/peróxido de hidrogênio

Para compostos que não absorvam eficientemente radiação ultravioleta, o rendimento do processo de degradação pode ser aumentada adicionando peróxido de hidrogênio, uma vez que este em contato com o ozônio permite a ocorrência de uma reação adicional, também ela geradora de radicais hidroxila (Aguinaco et al. 2014). A reação inicia-se com uma transferência eletrônica do peróxido de hidrogênio, produzindo o íon hidroperóxido. Posteriormente, este íon reage com o ozônio para

produzir O_3^- e o radical hidroperóxido, conseqüentemente estes produtos podem formar radicais hidroxilas; uma forma simplificada de expressar a reação envolvida segue logo abaixo (Hassemer 2006):

$$H_2O_2 + 2\ O_3 \longrightarrow OH^{\bullet} + OH^{\bullet} + 3\ O_2 \qquad (9)$$

Na Figura 11, apresenta-se um esquema de uma unidade de oxidação avançada utilizando ozônio e peróxido de hidrogênio.

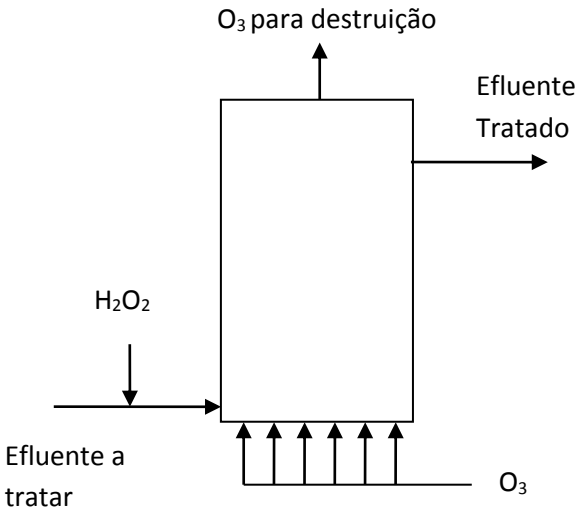

Figura 11. Representação esquemática de um processo oxidativo avançado utilizando ozônio e peróxido de hidrogênio.
Fonte: Metcalf and Eddy (2003).

2.7.2.4 Peróxido de hidrogênio/UV

O peróxido de hidrogênio é um agente oxidante, com potencial de oxidação de 1,8 eV. Ele é muito usado no branqueamento do papel, na indústria têxtil, na manufatura de alimentos, na indústria petroquímica, eletrônica e metalúrgica (Kwon et al. 2014). Além disso, tem sido utilizado nos tratamentos de solos contaminados e no tratamento de efluentes perigosos, quando associados à radiação UV sua eficiência torna-se mais evidente (Teixeira and Jardim 2004).

Foi proposto por Sillanpää et al. (2011), o mecanismo de produção do radical hidroxila a partir de H_2O_2 e radiação UV, produzindo dois radicais hidroxila para cada molécula de H_2O_2. A irradiação a comprimentos de onda inferiores a 365 nm e com intensidade adequada provoca a cisão O–O do peróxido, sendo então iniciada a reação a seguir.

$$H_2O_2 + h\gamma \longrightarrow 2\ OH^{\bullet} \qquad (10)$$

Por outro lado, o peróxido de hidrogênio pode reagir com o radical hidroxila gerado, produzindo o radical hidroxiperoxila (11), que por sua vez reage com o peróxido de hidrogênio, gerando novamente o radical hidroxila, água e oxigênio (12), como mostrado nas reações.

$H_2O_2 + OH^{\bullet} \longrightarrow HO_2^{\bullet} + H_2O$ (11)

$H_2O_2 + HO_2^{\bullet} \longrightarrow OH^{\bullet} + H_2O + O_2$ (12)

A utilização de peróxido de hidrogênio (H_2O_2) em altas concentrações, poderá gerar uma recombinação dos radicais $OH^{\bullet}$, formando H_2O_2 (13).

$2\ OH^{\bullet} \longrightarrow H_2O_2$ (13)

Freqüentemente este processo não é economicamente viável porque o baixo coeficiente de extinção molar do peróxido de hidrogênio obriga ao uso de elevadas concentrações deste composto para que a absorção de radiação UV produza a quantidade de radical hidroxila necessária (Glaze et al. 1987). Por outro lado, estudos (Alshamsi et al. 2006; Yonar et al. 2006) usam tais processos com sucesso na remoção rápida e eficiente de contaminantes ambientais.

2.7.2.5 Ozônio/UV/peróxido de hidrogênio

Este processo é uma co-oxidação, em que se combinam o ozônio e peróxido de hidrogênio com radiação UV. Em solução aquosa, acontece uma cascata de reações que se seguem de acordo (Gogate and Pandit 2004):

$H_2O_2 + H_2O \Leftrightarrow H_3O^+ + HO_2^-$ (14)

$O_3 + H_2O_2 \xrightarrow{\text{lento}} O_2 + HO^\bullet + HO_2^\bullet$ (15)

$O_3 + HO_2^- \xrightarrow{\text{rápido}} {}^\bullet O_3^- + HO_2^\bullet$ (16)

${}^\bullet O_2^- + H^+_{(aq)} \Leftrightarrow HO_2^\bullet$ (17)

$O_3 + {}^\bullet O_2^- \longrightarrow {}^\bullet O_3^- + O_2$ (18)

${}^\bullet O_3^- + H^+_{(aq)} \Leftrightarrow HO_3^\bullet$ (19)

$HO_3^\bullet \longrightarrow O_2 + HO^\bullet$ (20)

Neste sistema o radical hidroxila é a espécie mais reativa, e com a adição do peróxido de hidrogênio o resultado é um aumento na velocidade de oxidação devido a predominância do radical $OH^\bullet$. A combinação de radiação UV, favorece a ativação fotônica do ozônio e do peróxido presente (Robinson et al. 2000). Abaixo se apresenta um esquema de uma unidade de oxidação avançada utilizando ozônio, peróxido de hidrogênio e radiação UV.

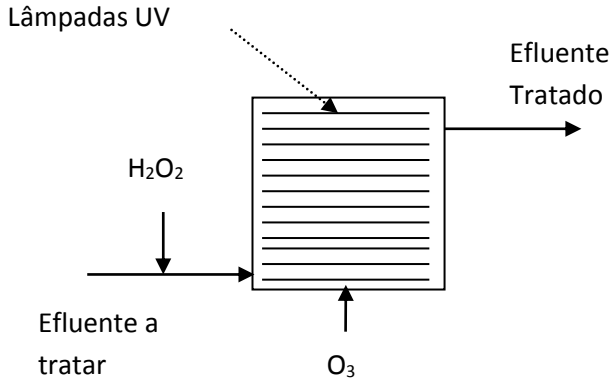

Figura 12. Representação esquemática de um processo oxidativo avançado utilizando ozônio, peróxido de hidrogênio e radiação UV.
Fonte: Metcalf and Eddy (2003).

Os métodos descritos atingem aplicação comercial, especialmente no tratamento de águas residuais de diversas indústrias e na desinfecção de águas de abastecimento, porém possuem a grande desvantagem de utilizarem reagentes com alto valor no mercado (como o peróxido de hidrogênio e o ozônio) e o alto consumo de energia para a geração de radiação UV (Medellin-Castillo et al. 2013). Por outro lado, como os processos oxidativos avançados são fundamentais para o tratamento de substâncias recalcitrantes, as investigações mais recentes têm visado o desenvolvimento de processos mais econômicos, fundamentalmente em termos energéticos. São aqueles que não necessitam de radiação ultravioleta para ativar o processo e que alternativamente possam ser promovidos pela luz solar (luz de comprimento de onda superior a 300 nm) (Gogate and Pandit 2004; Zahraa et al. 2006).

2.7.3 Sistemas de POAs que utilizam a luz solar

Existem dois processos oxidativos avançados que utilizam luz solar como fonte energética. Estes são a fotocatálise heterogênea usando semicondutores, tipicamente dióxido de titânio, e a fotocatálise homogênea utilizando o processo de foto-*Fenton*. Os processos de descontaminação por fotocatálise heterogênea ativada por luz solar utilizam a parte do ultravioleta próximo do espectro solar, isto é, comprimentos de onda inferiores a 380 nm (Gogate and Pandit 2004). No processo de fotocatálise homogênea por foto-*Fenton* é aproveitada uma maior porção do espectro solar, já que é usada toda a radiação solar com comprimentos de onda inferiores a 580 nm. Na Figura 13, compara-

se o espectro solar com os espectros de absorção de fotocatalisadores usados nestes dois processos (Malato et al. 2002).

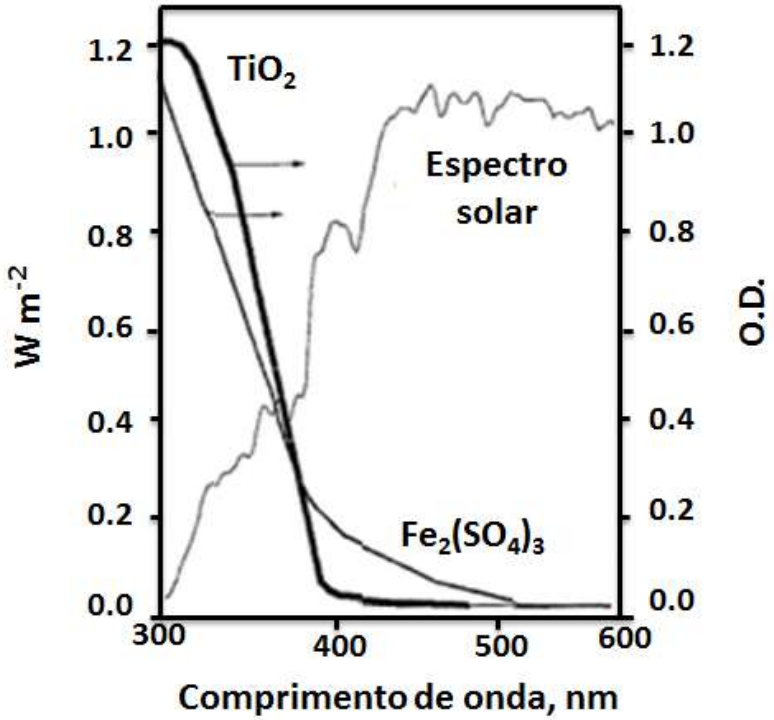

Figura 13. Comparação do espectro de emissão solar com os espectros de absorção de uma amostra de TiO_2 em pó e de uma solução de reagente de Fenton.
Fonte: Malato et al. (2002).

2.7.3.1 Fotocatálise heterogênea usando semicondutores – TiO_2/UV

Este sistema baseia-se na utilização de semicondutores que atuam como fotocatalisadores possuindo duas regiões energéticas: a região de energia mais baixa denominada banda de valência (BV), onde os elétrons não possuem movimento livre, e uma outra região de energia mais alta conhecida como banda de condução (BC), onde

os elétrons são capazes de se movimentar. Entre as duas regiões existe uma zona denominada de "band gap". A energia de "band gap" é a energia mínima necessária para promover a excitação de um elétron para que ele salte da camada de valência para a camada de condução (Ziolli 1998).

Os semicondutores possuem uma descontinuidade de energia entre as bandas, e em algumas condições, podem superá-las, sendo promovidas da banda de menor energia para de maior energia, gerando um par elétron/lacuna. Essa descontinuidade de energia dos semicondutores determina a diferença entre os condutores, nos quais os níveis de energia são contínuos, não havendo separação entre as BV e BC, e para os não condutores, que possuem uma descontinuidade de energia tão grande que impedem a promoção eletrônica (Teixeira and Jardim 2004). A Figura 14 ilustra as diferenças entre os níves de energia dos diferentes materiais.

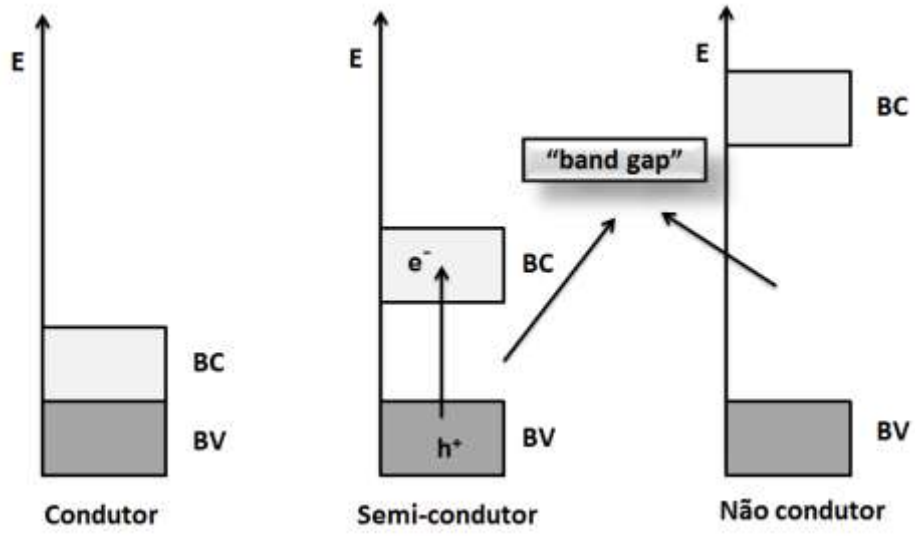

Figura 14. Diferença esquemática entre os materiais condutores, semicondutores e não condutores.
Fonte: adaptado de Teixeira and Jardim (2004).

Existem diversos semicondutores que podem ser utilizados em processos oxidativos, como: TiO_2, ZnO, Al_2O_3, CeO_2. Entretanto, de todos eles, o dióxido de titânio é o fotocatalisador mais ativo e o mais utilizado na degradação de compostos orgânicos presentes em águas e efluentes (Nogueira and Jardim 1997). O dióxido de titânio (TiO_2) apresenta como característica o baixo custo, baixa toxicidade, a insolubilidade em água, a estabilidade química em ampla faixa de pH, a possibilidade de utilizar luz solar e por fim possibilidade de imobilização sobre sólidos. Esta última vantagem facilita o processo de fotodegradação, eliminando as etapas de filtração quando o mesmo é utilizado em suspensão (Ferreira and Daniel 2004).

O TiO_2 pode apresentar-se sob três formas cristalinas: anatase, rutilo e brokite, sendo as formas mais comuns a anatase e rutilo, ambas tetragonais. A anatase é considerada a forma fotoativa, e possui um "band gap" de 3,2 eV, já a fase rutilo é atribuída um baixo poder catalítico (Mitsionis and Vaimakis 2012). Existem diversas preparações de TiO_2 que possuem ambas as fases em diferentes proporções variando de fabricante para fabricante. Deste modo chegou-se a um consenso internacional sobre o uso do TiO_2 Evonik P25 (anteriormente Degussa P25), como padrão de atividade fotocatalítica (Fujishima et al. 2010).

O TiO_2 P25 é um pó comercialmente disponível com uma pureza de 99.5% e aproximadamente 70% de anatase e 30% de rutilo. Com uma área superficial de cerca de 50 ± 15 m^2/g, sem porosidade, possuindo partículas cúbicas de arestas arredondadas e um diâmetro médio de partícula de 21 nm (Ziolli 1998).

A Figura 15 exibe as duas principais estruturas cristalinas do TiO_2, onde cada átomo de dióxido de titânio esta cercado por seis átomos de oxigênio. As duas estruturas se diferenciam pelo comprimento de ligação e uma considerável distorção no ângulo de 90º da ligação observada na forma anatase (Fujishima et al. 2010).

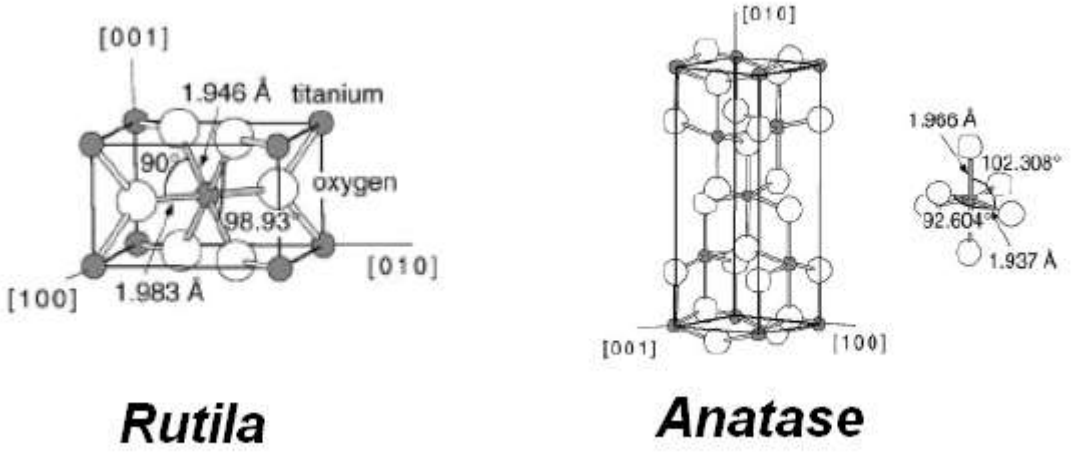

Figura 15. Estrutura das duas principais formas do TiO_2.
Fonte: adaptado de Bonancêa (2005).

O TiO_2 em seu estado normal, possui níveis de energia não contínuos e, com isso, não conduz eletricidade. Em contrapartida, quando irradiados com fótons de energia igual ou superior ao seu "band gap", ocorre uma excitação eletrônica, promovendo a migração do elétron da banda de valência para banda de condução, gerando um par elétron/lacuna (21) (Moreira et al. 2005).

$$TiO_2 \longrightarrow TiO_2\,(e^- + h^+) \qquad (21)$$

Caso esse processo ocorra em meio aquoso, o buraco produzido na superfície do TiO_2 reage com água (22) ou íons hidroxila (23) produzindo o radical hidroxila, altamente reativo.

$$TiO_2(h^+) + H_2O \longrightarrow OH^\bullet + H^+ \quad (22)$$

$$TiO_2(h^+) + OH^- \longrightarrow OH^\bullet \quad (23)$$

O elétron promovido para banda de condução por sua vez, pode reagir com o oxigênio molecular dissolvido na água (24), produzindo o radical superóxido $O_2\bullet$.

$$TiO_2(e^-) + O_2 \longrightarrow O_2^\bullet \quad (24)$$

Esse radical possui a capacidade de reagir com água e íons hidroxila para formação de radical hidroxila, peróxido de hidrogênio e outras espécies reativas. O radical hidroxila e as outras substâncias formadas apresentam alto poder oxidante, e em contanto com moléculas orgânicas podem levar a sua oxidação e, idealmente sua mineralização (Moreira et al. 2005; Fujishima et al. 2010). A figura 16 mostra esquematicamente todo processo de ativação do TiO_2.

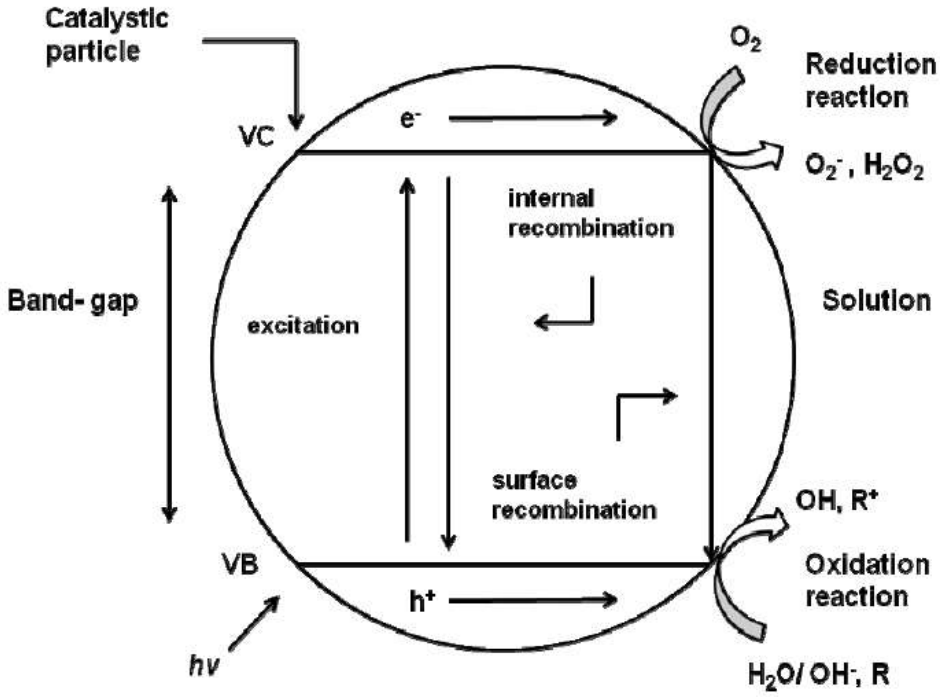

Figura 16. Mecanismo de ativação de uma partícula de dióxido de titânio.
Fonte: adaptado de Teixeira and Jardim (2004).

2.7.3.2 Fotocatálise homogênea – Processo de Fenton

O reagente de Fenton foi descoberto em 1894 por H.J.H Fenton, este oxidou ácido tartárico a partir da reação entre peróxido de hidrogênio e íons ferro Huang et al. (1993). A partir dessa mistura, foram formados radicais hidroxila, capazes de reagir com as substâncias orgânicas.

Em geral, propõe-se que o mecanismo de ação do H_2O_2 com Fe^{2+} geram íons hidroxila (OH^-), radical hidroxila ($OH^\bullet$) e Fe^{3+} (25).

$$H_2O_2 + Fe^{+2} \longrightarrow OH^\bullet + OH^- + Fe^{+3} \quad (25)$$

O radical hidroxila pode reagir com o Fe^{+2}.

$$Fe^{+2} + OH^{\bullet} \longrightarrow Fe^{+3} + OH^{-} \quad (26)$$

Os íons férricos formados podem reagir com o peróxido de hidrogênio (27) e o produto formado degrada-se, formando os íons ferrosos e radicais livres (28). A reação do radical $HO_2^{\bullet}$ com o Fe^{+3} leva a formação de Fe^{+2} e O_2 (29), enquanto que a decomposição do peróxido de hidrogênio pelo radical $OH^{\bullet}$ resulta na formação de água e radical peroxil (30) (Péres et al. 2002; Bautista et al. 2008).

$$Fe^{+3} + H_2O_2 \longrightarrow Fe - OOH^{+2} + H^{+} \quad (27)$$

$$Fe - OOH^{+2} \longrightarrow HO_2^{\bullet} + Fe^{+2} \quad (28)$$

$$Fe^{+3} + HO_2^{\bullet} \longrightarrow Fe^{+2} + H^{+} + O_2 \quad (29)$$

$$OH^{\bullet} + H_2O_2 \longrightarrow H_2O + HO_2^{\bullet} \quad (30)$$

Nas reações de foton-*Fenton* (31) combina-se a aplicação da radiação a uma reação de *Fenton*, na qual produz uma maior eficiência na degradação, pois a fotólise do peróxido de hidrogênio contribui para a aceleração na produção de radical hidroxila ($OH^{\bullet}$) (Bautista et al. 2008). A utilização da radiação, que pode ser solar, nesse processo provoca a foto-redução do Fe^{+3} a Fe^{+2}, recuperando o íon ferroso e possibilitando a geração de mais radical hidroxila (Al-Hayek and Doré 1985).

$$Fe^{2+} + H_2O + h\gamma_{UV\text{-}Vis} \longrightarrow Fe^{3+} + H^+ + OH^{\bullet} \quad (31)$$

Neste tipo de processo observa-se a presença do íon H^+ na reação, o que indica a necessidade de um pH ácido (pH= 2 – 4) para que a reação ocorra com melhor eficiência (Al-Hayek and Doré 1985). Este processo é sensível à luz até comprimentos de onda de 580 nm. O contato entre o poluente e o agente oxidante é efetivo, pelo fato do processo ocorrer em fase homogênea (Al-Hayek and Doré 1985; Bautista et al. 2008; Oliveira et al. 2012). Porém o processo de foto-*Fenton* é possui alguns pontos negativos, como a necessidade de se utilizar baixos valores de pH para que a reação ocorra, o elevado consumo de peróxido de hidrogênio e a necessidade de remover o ferro no final do tratamento (Silva 2007).

2.8 Reatores solares para processos fotoquímicos

A utilização de processos oxidativos avançados ativados pela luz obriga ao desenvolvimento de uma tecnologia fotoquímica solar que pode ser definida como uma tecnologia de aproveitamento eficiente de fótons solares e a sua posterior condução para o reactor adequado, com o objetivo de promover a fotodegradação de poluentes orgânicos persistentes (Bahnemamm 1999). Para os processos de fotoquímica solar interessa principalmente o aproveitamento de fótons de alta energia e baixo comprimento de onda, já que tipicamente a grande maioria dos processos de fotocatálise

utiliza radiação solar na zona do ultravioleta (300 - 400 nm). Uma exceção é o processo de foto-Fenton, que utiliza toda a luz solar abaixo de 580 nm (Malato et al. 2002).

O equipamento que promove o aproveitamento eficiente de fótons é o coletor solar. Este representa a maior fonte de custos de operação de uma unidade de fotocatálise para tratamento de efluentes (Malato et al. 2002). Os reatores solares podem ser classificados em três tipos, de acordo com o nível de concentração solar atingido, o qual está em geral diretamente relacionado com a temperatura atingida pelo sistema. Assim temos reatores solares não concentradores, mediamente concentradores ou altamente concentradores. Podem também chamar-se concentradores de baixa (< 150ºC), média (150 – 400 ºC) e alta (>400 ºC) temperatura (Oliveira et al. 2012).

Os reatores não concentradores ou de baixa temperatura são estáticos e usualmente constituídos por pratos planos dirigidos para o sol com certa inclinação, dependente da sua localização geográfica. A sua principal vantagem é a grande simplicidade e baixo custo (Malato et al. 2002). Os reatores mediamente concentradores ou de média temperatura concentram o sol de 5 a 50 vezes, porém têm que ter a capacidade de acompanhar o sol continuamente (Blanco et al. 1993). Estes reatores fazem o uso eficiente da radiação solar direta, e adicionalmente a energia térmica concentrada poderia ser usada simultaneamente para outras aplicações. Por outro lado, são reatores caros e somente utlizam a radiação direta (Alfano et al. 2000).

Os reatores altamente concentradores ou de alta temperatura possuem um foco pontual e baseiam-se em uma parabolóide com acompanhamento do movimento solar.

Asseguram concentrações solares de 100 a 10000 vezes, para o que requerem elementos ópticos de alta precisão (Oliveira et al. 2012).

Normalmente as aplicações tecnológicas usam reatores de baixa e média temperatura, de construção mais econômica. Uma diferença importante entre estes dois reatores é que o primeiro usa radiação direta e difusa, enquanto que os reatores concentradores usam apenas radiação direta (Malato et al. 2002).

2.8.1 Reator de filme fino em leito fixo (Thin Film Fixed Bed Reactor)

Este reator, cujo esquema simplificado se apresenta na Figura 17, é um dos primeiros reatores solares não concentradores que utilizam a radiação total (direta e difusa) para o processo fotocatalítico, apresentando simplicidade e baixo custo em sua construção (Khan et al. 2012).

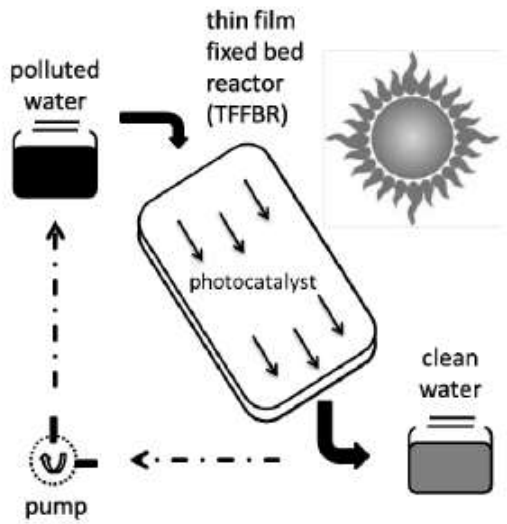

Figura 17. Diagrama simplificado de um reator de filme fino em leito fixo.
Fonte: Oliveira et al. (2012).

A parte mais importante do reator é um prato fixo inclinado (0,6 m x 1,2 m) revestido com um filme fino do fotocatalisador, tipicamente de TiO_2 P25, ao qual é lavada com um filme de cerca de 100 µm do efluente líquido a tratar a uma velocidade de 1 a 6,5 litros por hora (Bahnemamm 1999; Malato et al. 2002).

2.8.2 Reator parabólico aberto (Parabolic Trough Reactor)

Este reator concentra raios solares diretos por um fator de 5 a 50. O acompanhamento da radiação solar é feito por um sistema simples ou duplo de motores que permitem o contínuo alinhamento com a radiação solar, com a possibilidade de acoplamento com vários reatores ligados em sério ou em paralelo (Braham and Harris 2009). Este reator possui um refletor com um perfil parabólico, onde o tubo onde ocorre a reação está no seu foco; deste modo, apenas a luz que entre paralela no refletor pode ser focada no tubo da reação (Braham and Harris 2009). Este tipo de reatores são utilizados em circuitos de descontaminação solar instalados nos Estados Unidos (em Albuquerque, Sandia National Laboratories, e na Califórnia, Lawrence Livermoore Laboratories) e na Espanha (Plataforma Solar de Almería, Figura 18).

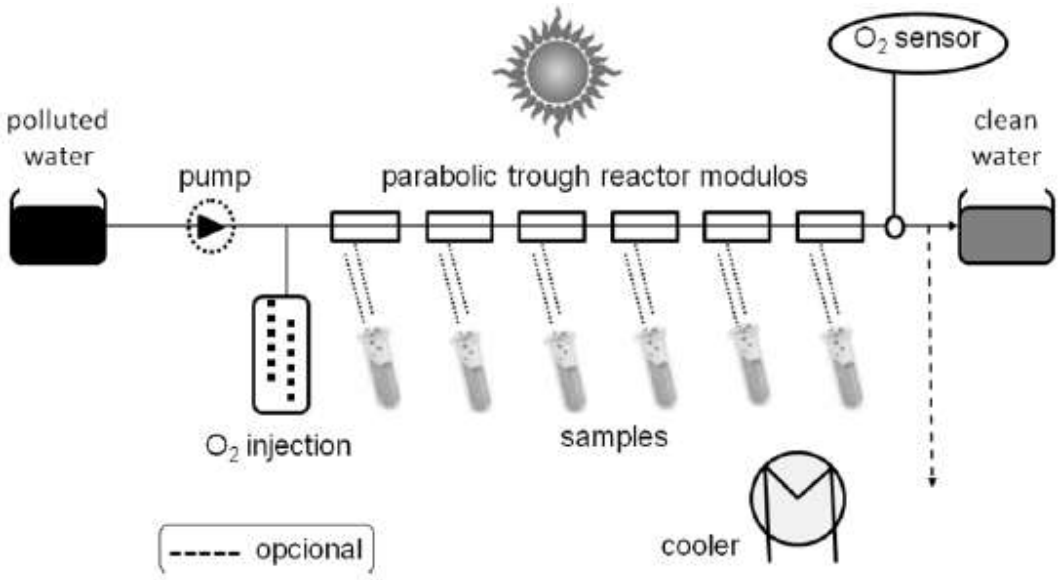

Figura 18. Diagrama simplificado de uma instalação com reatores parabólicos abertos. Fonte: Oliveira et al. (2012).

2.8.3 Reator parabólico composto de recolha (Compound Parabolic Collecting Reactor)

Basicamente difere do reator parabólico aberto convencional na forma dos refletores. Estes reatores são coletores estáticos com uma superfície refletora que envolve um reator circular, como se mostra na Figura 19. Este reator representa uma síntese eficaz dos dois tipos de reatores anteriormente descritos e pode capturar tando a radiação direta como a difusa (Curcó et al. 1996; Malato et al. 1997).

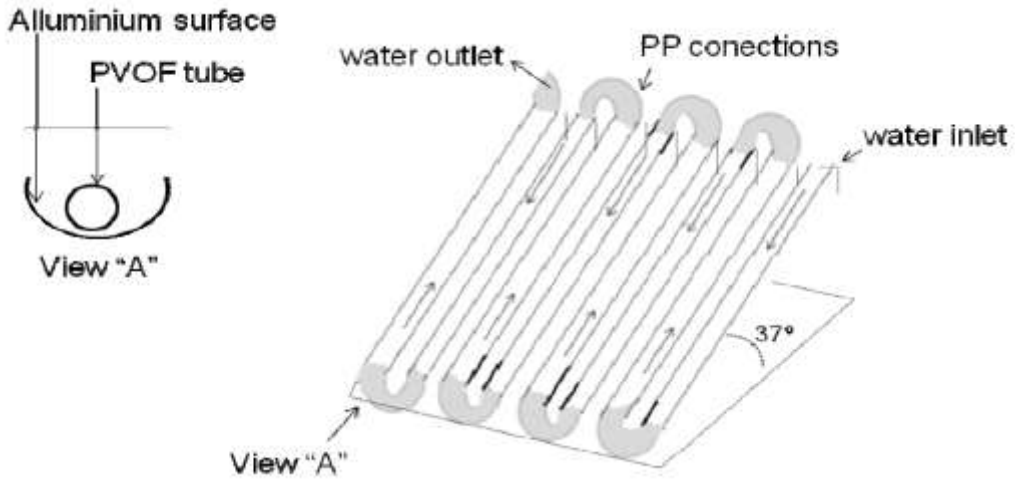

Figura 19. Diagrama simplificado de um reator parabólico composto de recolha. Fonte: adaptado de Malato et al. 2002.

2.8.4 Reator de dupla folha (Double Skin Sheet Reactor)

Este é um novo tipo reator, sem concentração de raios solares, ainda em fase de teste. É constituído por uma caixa transparente com uma estrutura interna idêntica à apresentada na Figura 20, através da qual é bombeada a suspensão contendo poluente e o fotocatalisador. Possui a vantagem de usar a radiação total e de ser bastante simples de operar (Braham and Harris 2009).

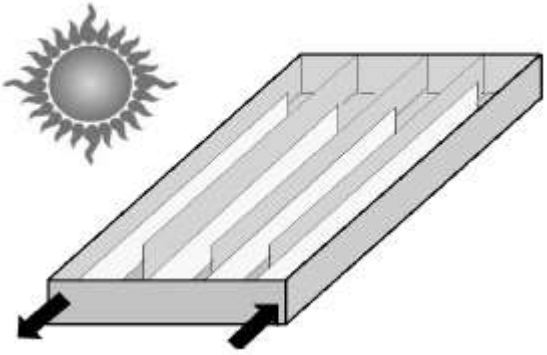

Figura 20. Diagrama simplificado de um reator de dupla folha.
Fonte: Oliveira et al. (2012).

O projeto inicial do DSS é de van Well et al. (1997), o qual era constituído por uma área de superfície de 1,37 m^2, volume de 14,4 L e poderia suportar um fluxo máximo de 11,8 L min^{-1}. Estimou que para uma área de recolha de fótons de cerca de 100 m^2 seria capaz de tratar completamente (10 m^3h^{-1}) de efluentes contaminatos.

2.9 Unidades industriais

A figura 21 mostra o diagrama de uma instalação fotocatalítica que pode ser usada quer para o processo de fotocatálise heterogênea mediada por TiO_2, quer para o processo de fotocatálise homogênea por foto-Fenton. Em ambos os casos o catalisador (TiO_2 ou Ferro) deve ser separado para ser reciclado e/ou reutilizado.

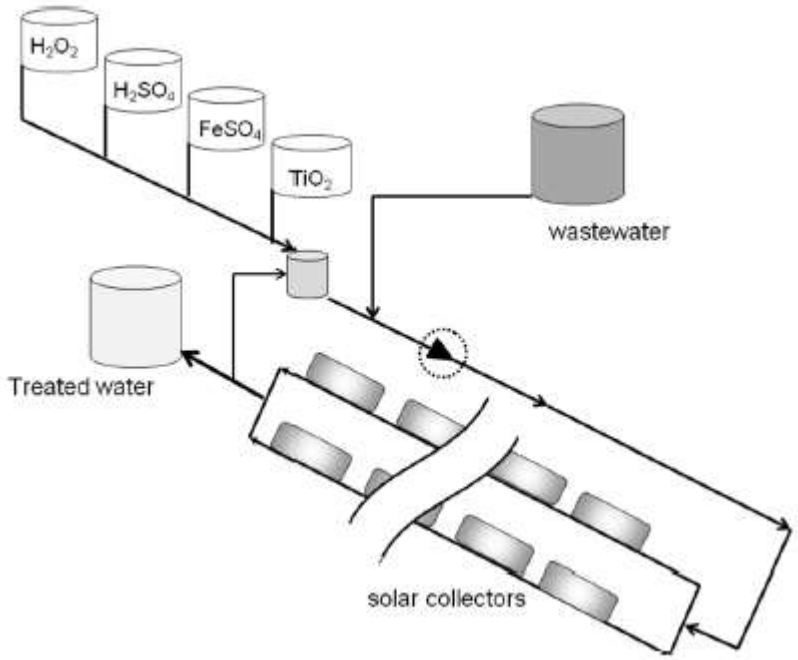

Figura 21. Diagrama simplificado de uma unidade industrial de tratamento fotocatalítico de efluentes.
Fonte: Oliveira et al. (2012).

A área superficial do coletor solar depende essencialmente do efluente a ser tratado, como por exemplo: a classe de contaminante, a concentração e as condições solares do local de instalação (Oliveira et al. 2012). O tempo de vida dos catalisadores usados depende basicamente do tipo de efluente a tratar e da qualidade do tratamento final que se pretende obter (Oliveira et al. 2012; Malato et al. 2002). No final do processo, é importante avaliar a toxicidade do efluente tratado (Oliveira et al. 2012).

O projeto de uma unidade industrial de descontaminação de efluentes por fotocatálise obriga a uma cuidadosa seleção do tipo de reator a usar, da disposição dos reatores na instalação (série ou paralelo), do modo de operação do fotocatalisador (fixo

ou em suspensão), do sistema de reciclagem dos catalisadores e da velocidade de fluxo, entre outros (Wilkins et al 1994; Goswami et al. 1997). A concentração de fotocatalisador é também um parâmetro chave e deve ser ajustada de acordo com o volume de efluente a ser tratado, assim como o tamanho do percurso óptico (Fernández-Ibáñez et al. 1999).

Os resultados desta tese foram organizados em cinco artigos científicos, sendo que um se encontra publicado, um aceito para publicação, um submetido aguardando revisão e dois a submeter, até o presente momento da redação desta tese. Embora cada artigo apresente sua própria introdução e discussão, o texto introdutório acima se faz necessário, uma vez que busca harmonizar os objetivos e experimentos de cada estudo/artigo, mas também permitiu abordar uma série de conceitos básicos necessários ao completo entendimento desta tese e que a seção de introdução de um artigo, por limitações editoriais, não permite.

3. ARTIGO 1

molecules
Research
Article
ISSN 1420-3049

doi: 10.3390/molecules161210370

Use of Titanium Dioxide Photocatalysis on the Remediation of model textile wastewaters containing azo dyes

Enrico Mendes Saggioro[1,*], Anabela Sousa Oliveira[2,3], Thelma Pavesi[1], Cátia Gil Maia[3], Luis Filipe Vieira Ferreira[2], Josino Costa Moreira[1]

[1] Centro de Estudos da Saúde do Trabalhador e Ecologia Humana Escola Nacional de Saúde Pública - Fundação Oswaldo Cruz, Av. Leopoldo Bulhões, 1480, Rio de Janeiro, 21041-210 RJ, Brasil;
[2] CQFM - Centro de Química-Física Molecular and IN – Instituto de Nanociencias e Nanotecnologia, Complexo Interdisciplinar, Instituto Superior Técnico, Universidade Técnica de Lisboa, Av. Rovisco Pais 1049-001, Lisboa, Portugal;
[3] C3i - Centro Interdisciplinar de Investigação e Inovação, Escola Superior de Tecnologia e Gestão, Instituto Politécnico de Portalegre, Lugar da Abadessa Apartado 148 - 7301901 Portalegre, Portugal;

Abstract

The photocatalytic degradation of two commercial textile azo dyes, respectively C.I Reactive Black 5 and C.I Reactive Red 239 has been studied. TiO_2 P25 Degussa was used as catalyst and photodegradation was carried out in aqueous solution under artificial irradiation with a 125W mercury vapor lamp. The effects of the amount of TiO_2 used, UV-light irradiation time, pH of the solution under treatment, initial concentration of the azo dye and addition of different concentrations of hydrogen peroxide were investigated. The effect of the simultaneous photodegradation of the two azo dyes was also investigated and we observed that the degradation rates achieved in mono and bi-component system were identical. The repeatability of photocatalytic activity of the photocatalyst was also tested. After five cycles of TiO_2 reuse the rate of colour lost was still 77% of initial rate. The degradation was followed monitoring the change of azo dye concentration by UV-Vis spectroscopy. Results show that the use of an efficient photocatalyst and the adequate selection of optimal operational parameters may easily lead to a complete decolorization of the aqueous solutions of both azo dyes.

Keywords: Photocatalytic Degradation, Semiconductor, Photocatalysis, Azo dyes, TiO_2, TiO_2 Reuse

3.1 Introduction

Dyes are an important source of environmental contamination. Textile wastewaters contain usually a considerable amount of unfixed dyes, many of which are azo dyes [1]. Fifteen percent of the total world dye production is lost during dyeing process and it is released in textile effluents [2]. The colours produced by minute amounts of dyes accidentally released in water during dying processes are considered to pose serious problems, because they have considerable environmental effects on the water and make hem visually unpleasant [3]. Moreover, environmental pollution by organic dyes also sets a severe ecological problem, which is increased by the fact that most of them are often toxic to microorganisms and a have long degradation times in the environment [4].

The number of dyes currently used in textile industry is about 100.000 with over 7×10^5 ton of dye-stuff produced annually. Among these dyes, the azo dyes constitute the largest and the most important class of commercial dyes [5, 6]. Those dyes, which typically have the chromophoric -N=N- group unit in their molecular structure [7] makes up to 60-70% of all textile dyestuffs produced.

Azo dyes are known to be largely non-biodegradable in aerobic conditions and their stability is proportional to the structural complexity of their molecular structure [7, 8]. In order to overcome this problem, azo dyes can be degraded under anaerobic conditions originating in this case potentially hazardous and carcinogenic aromatic amines [8, 9]. It is well known that azo dye structure when incorporated into the body is split by liver enzymes and intestinal flora into the corresponding aromatic amines, which can cause cancer in humans [7]. Dyes are synthesized to be resistant to fading

upon exposure to light, washing and many chemicals [5]. Consequently, traditional wastewater treatment methods such as flocculation, adsorption and biological degradation are usually ineffective [4].

In recent years Advanced Oxidation Processes (AOPs) using titanium dioxide (TiO_2) are being effectively used to detoxify recalcitrant pollutants present in industrial wastewater [9-12]. TiO_2 have singular characteristics that made him an extremely attractive photocatalyst: high photochemical reactive, high photocatalytic activity, low cost, stability on aquatic systems and low environmental toxicity [13, 14]. When a semiconductor such as TiO_2 absorbs a photon with energy equal to or greater than its band gap width (3.2 eV), an electron may be promoted from the valence band to the conduction band (e^-_{cb}) leaving behind an electron vacancy in the valence band (h^+_{vb}) [15]. The holes at the TiO_2 valence band, having an oxidation potential of +2.6V can oxidize water or hydroxide to produce hydroxyl radicals. The hydroxyl radical is a powerful oxidizing agent and enables a non specific attack to organic compounds; under favorable conditions the final photoproducts are H_2O, CO_2 and inorganic anions. The general detailed mechanism of dye degradation upon irradiation is described by Eqs. 1-6 [4, 15]:

$$\text{Dye} + h\nu \rightarrow \text{Dye}^* \quad (1)$$

$$\text{Dye}^* + TiO_2 \rightarrow \text{Dye}^{\bullet+} + TiO_2(e) \quad (2)$$

$$TiO_2\,(e) + O_2 \rightarrow TiO_2 + O_2^{\bullet-} \quad (3)$$

$$O_2^{\bullet-} + TiO_2\,(e) + 2H^+ \rightarrow H_2O_2 \quad (4)$$

$$H_2O_2 + TiO_2\,(e) \rightarrow {}^{\bullet}OH + OH^- \quad (5)$$

$$\text{Dye}^{\bullet+} + O_2 \text{ (or } O_2^{\bullet-} \text{ or } {}^{\bullet}OH) \quad (6)$$

→ peroxylated or hydroxylated intermediates

→ degraded or mineralized products

Nowadays it is well known that TiO_2 is one of the most suitable semiconductors for photocatalysis and has been applied into various photocatalytic reactions [16-26].

The aim of the present work is to investigate the influence of various parameters on the photocatalytic degradation of two textile azo dyes respectively C.I Reactive Black 5 and C.I Reactive Red 239 in the presence of TiO_2 irradiated by UV-light. In this paper, we will also examine the effects of the amount of TiO_2 used, pH, initial concentration of the dyes, the use of an electron acceptor such as hydrogen peroxide and tested the efficiency of TiO_2 recycling and reuse.

3.2 Experimental

3.2.1 Reagents and Materials

Marine Remazol RGB 150% gran (C.I Reactive Black 5, M.W. = 981.82 g/mol), Ultra Red Remazol gran (C.I. Reactive Red 239, M.W. =1085.84 g/mol) textile dyes were obtained from DyStar (Brazil). The chemical structure of the dyes is shown in Figure 1. These compounds were used as received from the supplier without any further purification.

The photocatalyst used was titanium dioxide, Degussa P25, which consists of 75% anatase and 25% rutile with a specific BET - surface area of 50 m^2g^{-1} and a primary particle size of 20 nm. The other chemicals used in this study such NaOH, HCl

and H_2O_2 were obtained from Merck. Water used to prepare dye solutions was MiliQwater.

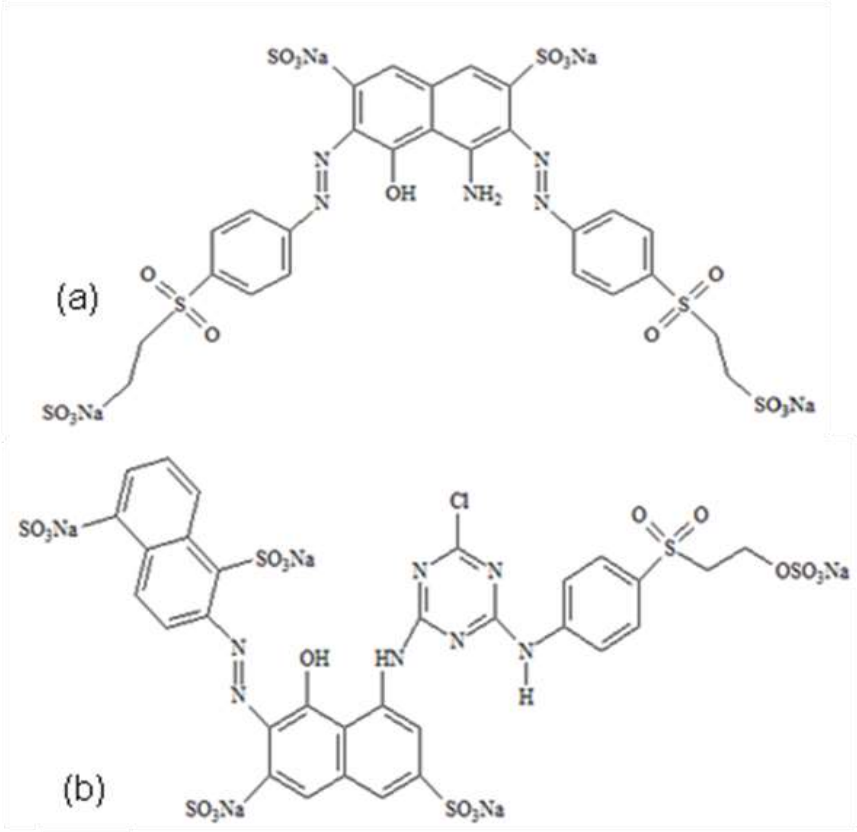

Figure 1. Chemical structure of commercial azo dyes: (a) Marine Remazol RGB 150% gran (C.I Reactive Black 5). (b) Ultra Red Remazol gran (C.I. Reactive Red 239).

3.2.2 Experiments procedure

Fresh solutions of the dyes were prepared always just before use and diluted according to the requirements of the experiments. The photodegradation cell was feed with 100 ml of the solution with stirring. Before irradiation, each sample was kept in the dark for 40 min. During irradiation, continuous stirring was maintained to keep the suspension homogenous. Samples (ca. 3mL) were withdrawn at specific times (0, 15,

30, 45, 60, 90 and 120 min) for UV–Visible analysis and centrifuged for 10 min at 1000 rpm. The concentration of the azo dyes in each sample was evaluated spectrophotometrically measuring the UV-Visible absorption at the maximum absorption wavelength of each dye (C.I Reactive Black 5; λmax = 615 nm; C.I. Reactive Red 239; λmax = 540 nm) and comparing it with the dye concentration calibration curve of each of the azo dyes used.

The samples were irradiated with a 125 Watts mercury vapour lamp (HQL 125 watts, from Osram). In this type of commercial lamps, the filament is protected by a glass bulb that cuts all UV-A and UV-B radiation. The glass bulb presents a white colour due to the internal phosphor coating that improves the radiation of the lamp on the visible region. This type of lamps with glass bulb is appropriated to selectively illuminate and exclusively excite TiO_2 band gap, avoiding direct photolysis of the dye molecules that could be simultaneously promoted if all the lamp emission profile was available. The photoreactor is composed of an elliptical cover that supports the irradiation source described above and of a base containing a magnetic stirrer, where the samples to be irradiated are placed in 100 mL beackers. The light arising from the mercury lamp was measured at 366 nm (the wavelength of TiO_2 bandgap [47]) with the help of a Cole Parmer radiometer (series 9811-50) placed above the beaker with the sample to be irradiated. All samples were illuminated with an irradiation power of 2.6±0.2 mW/cm^2.

3.2.3 Effect of TiO_2 photocatalyst concentration

100 ml of a 30 mgL^{-1} dye solution of each azo dye containing different concentrations of TiO_2 (0, $1x10^{-3}$, $5x10^{-3}$, $1x10^{-2}$, $1x10^{-1}$ and $1gL^{-1}$) were irradiated in the photoreactor described above for 120 min.

3.2.4 Effect of pH

100 ml of a 30 mgL^{-1} C.I Reactive Black 5 solution and $0.1gL^{-1}$ of TiO_2 was used to degrade the azo dye solution at different pH values, which were adjusted by addition of HCl and NaOH. Irradiation in the photoreactor described above was carried out for 60 min.

3.2.5 Recycling of TiO_2

The recycling of the photocatalyst was performed as follows: after a first photodegradation cycle of 100 ml of a 30 mgL^{-1} solution of C.I. Reactive Red 239 using 0.1 gL^{-1} of TiO_2 and 60 min irradiation, the treated solution of the dye was centrifuged with a rotation of 4000 rpm for 15 min to remove TiO_2. The liquid phase was filtered by a vacuum system with a Millipore membrane (0,45μm) and the solid phase containing the photocatalyst was carefully separated for reuse. After allowing it to dry in a desiccator with silica gel, the separated catalyst was added again to a new identical batch of C.I. Reactive Red 239 to be remediated. The process was repeated 5 times.

3.2.6 Effect of dye concentration

100 ml of different concentrations of each azo dye solutions (30, 50, 80, 100, 120 and 150 mgL^{-1}) containing $0.1gL^{-1}$ of TiO_2 were illuminated in the photoreactor for 120 min.

3.2.7 Effect of H_2O_2

100 ml of $30mgL^{-1}$ dye solution of each azo dye containing $0.1gL^{-1}$ of TiO_2 and different concentrations of hydrogen peroxide (0, $3x10^{-3}$, $6x10^{-3}$, $9x10^{-3}$, $1.2x10^{-2}$, $3x10^{-2}$ and $6x10^{-2}$ $molL^{-1}$) was illuminated in the photoreactor for 60 min.

3.2.8 Effect of the mixture of the two azo dyes

50 ml of $30mgL^{-1}$ dye solution of each azo dye under study were added in a beaker in order to have a 100 ml mixed solution of the two azo dyes. The photodegradation of the mixture of the two azo dyes was tested with two different concentrations of TiO_2 ($1gL^{-1}$ and $0.1gL^{-1}$) and were irradiated in the photoreactor described above for 120 min.

3.2.9 Equipment

A double beam UV-Visible spectrophotometer (Shimadzu UV-1601PC) was used for the spectrophotometric determination of azo dyes absorption spectra from 200-900 nm. Spectra of the dye in water were recorded with the help of 1 cm quartz cuvettes.

3.3 Results and Discussion

3.3.1 Effect of TiO_2 photocatalyst concentration

The photocatalytic degradation of the two azo dyes (30 mgL^{-1}) with different TiO_2 amounts was studied according to the described below at section 3.3 and the obtained results are show in Figure 2. The efficiency of photocatalytic degradation of both dyes was clearly grow with the increase of the amount of photocatalyst. The concentration of 1 gL^{-1} of TiO_2 degraded around 90% of both dyes in about 45 min and 99% of degradation was attained after 120 min. However, the concentration of 0.1 gL^{-1} of TiO_2 in the end of 120 min of irradiation yielded a similar degradation to that of the highest concentration of TiO_2 used. This can be rationalized in terms of availability of active sites on the TiO_2 surface and of the light penetration of photoactivating light into the dye – TiO_2 suspension; in fact in the solutions of both azo dyes, containing 1 gL^{-1} of TiO_2 in suspension the light penetration depth is considerably smaller than in those containing only 0.1 gL^{-1} of TiO_2 and so the effect of the increase on the amount of

photocatalyst becomes reduced. For the two azo dyes studied in this work the treatment with TiO_2 under artificial irradiation of a 125 W mercury vapor lamp was an extremely efficient photodegradation method, since after 2 hours all dyes showed substantial colour losses .

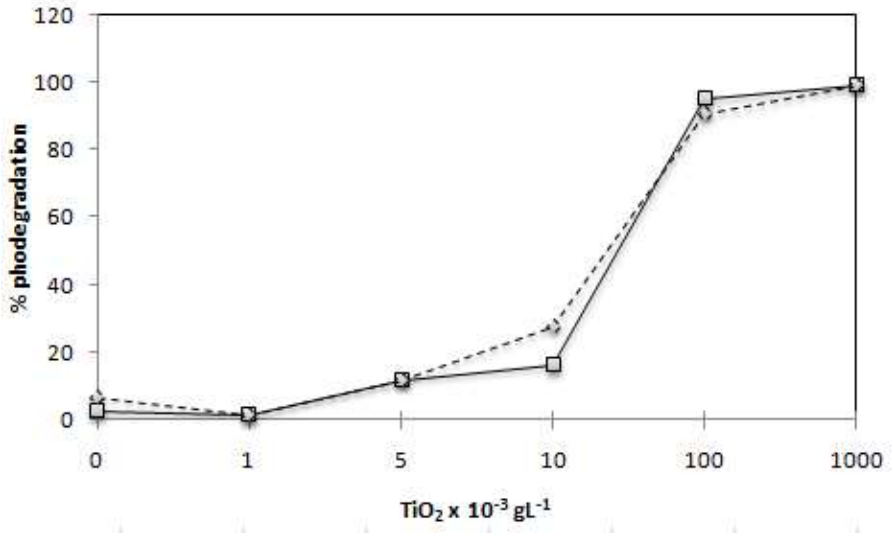

Figure 2. Effect of TiO_2 amount on the complete degradation of 30 mgL^{-1}. C.I. Reactive Red 239(———) and C.I Reactive Black 5 (------) dyes in 120 minutes of irradiation with 2,60 mW/cm^2 of irradiation power by a 125W mercury lamp.

The photodegradation is mostly promoted by titanium dioxide since we observed that direct photolysis, in the two hours irradiation period, is only responsible for the degradation of 0 to 6% of both of these azo dyes. Therefore, under irradiation, only the molecules adsorbed on the surface of TiO_2 can be degraded. When the amount of catalyst used on the photocatalytic degradation is very high the turbidity of the suspension strongly inhibits further light penetration in the photoreactor [26, 27]. This limit on TiO_2 amount to be used depends on the geometry and working conditions of the photoreactor which should enable that all the photocatalyst particles present on the

entire exposed surface are fully illuminated [28]. In this way, for each system to be remediated thought this method, the optimum amount of TiO_2 has to be determined in order to avoid the use of unnecessary catalyst in excess and also to ensure the total absorption of the irradiating photons in order to achieve an efficient photoremediation.

3.3.2 Effect of UV-Irradiation time

Figure 3 and 4 show de effect of UV-light irradiation time on the photocatalytic degradation of C.I. Reactive Black 5 and C.I. Reactive Red 239 with the two most efficient added amounts of TiO_2, respectively $0.1gL^{-1}$ and $1gL^{-1}$. In the presence of $1gL^{-1}$ of TiO_2 and UV-light, respectively 75 and 79% of the two azo dyes were degraded at an irradiation time of 30 min. It is also evident that for both of them the percentage of decolorization and photodegradation increases with increasing irradiation time. As expected the concentration of 1 gL^{-1} of TiO_2 promoted the highest percentage of degradation for the two dyes. This concentration degraded 90 to 93% in 45 minutes of both azo dyes. The rate of degradation became slower after 45 minutes. By the end of two hours up to 90 to 95% of the azo dyes were degraded by 0.1 gL^{-1} of catalyst. However, 1 gL^{-1} degraded up to 93 to 99% of dyes for the longest irradiation times.

The slow kinetics of azo dyes degradation after a long time of irradiation arises from the difficulty in converting the N atoms of the dyes into oxidized nitrogen compounds, since aliphatic chain interaction with hydroxyl radicals is small and these radicals are short lived [29]. The quick lost of colour of both azo dyes solutions was associated with cleavage of the azo linkage in dyes molecules. The nitrogen to nitrogen

double bonds (-N=N-) are characteristic of azo dyes molecules and theirs colours are determined by azo bonds. Azo bonds are the most active bonds in azo dyes molecules and can be easily oxidize either by positive hole or hydroxyl radical [30, 31].

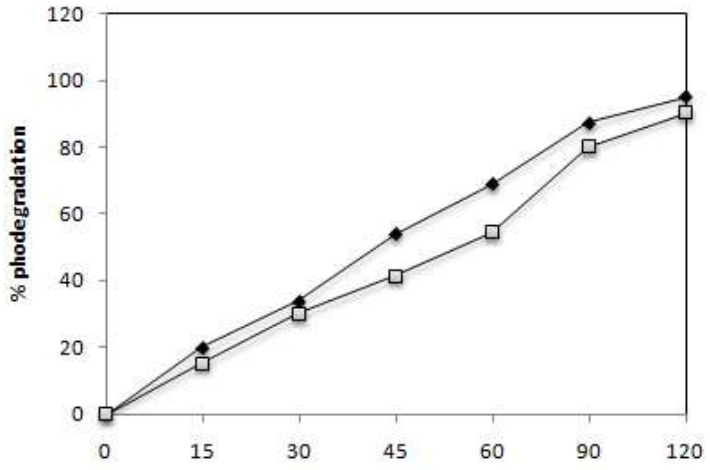

Figure 3. Effect of UV-Irradiation time on the degradation of 30 mgL^{-1} of the azo dyes C.I. Reactive Red 239 (—◆—) and C.I Reactive Black 5 (—□—) with 0.1 gL^{-1} of TiO_2 and 2.60 mW/cm^2 of irradiation power by a 125W mercury lamp.

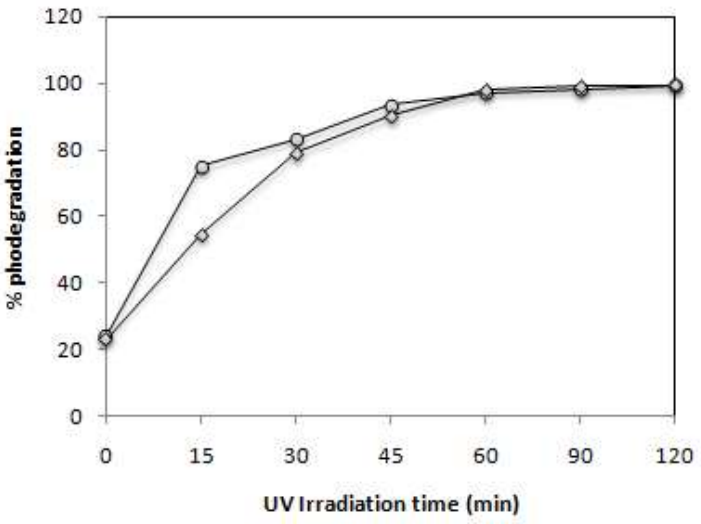

Figure 4. Effect of UV-Irradiation time on the degradation of 30 mgL^{-1} of the azo dyes C.I. Reactive Red 239 (—○—) and C.I Reactive Black 5 (—◇—) with 1 gL^{-1} of TiO_2 and 2.60 mW/cm^2 of irradiation power by a 125W mercury lamp.

The cleavage of double bands leads to the decolorization of the dye. The UV-Vis spectra measured during photodegradation of the two commercial azo dyes are showed in Figure 5. Before irradiation, C.I Reactive Black 5 exhibits peaks at 615, 397, 312 and 231 nm and C.I. Reactive Red 239 exhibits peaks at 540, 328, 289 and 215 nm. The visible spectrum peaks are due to chromophoric groups absorption, whereas the bands observed in the UV region can be assigned to the aromatic rings present in both azo dyes structure, as can be observe in Figure 10 [32, 33]. Figure 5 shows for both dyes the fast decolorization observed and also a significant degradation of theirs aromatic structures.

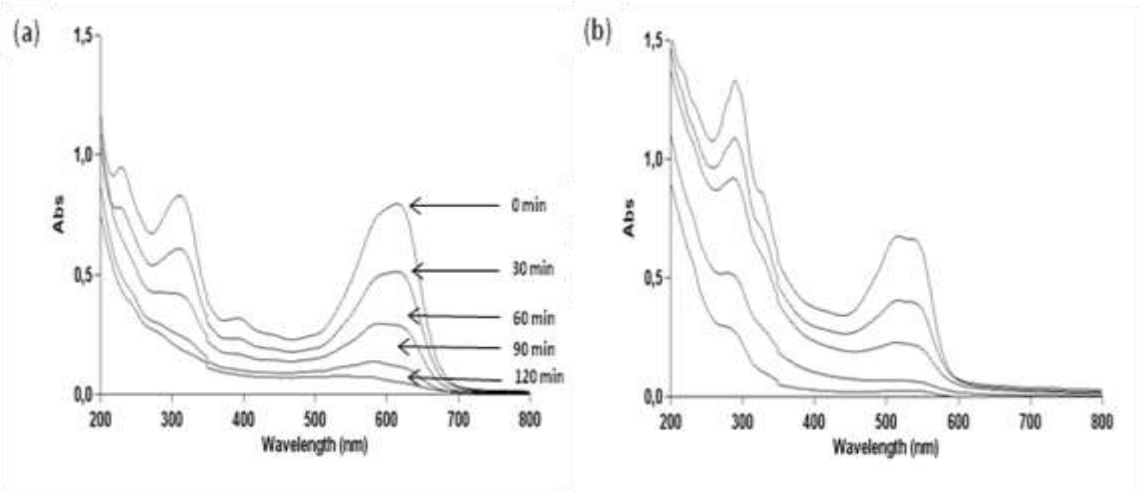

Figure 5. Photocatalytic degradation under 125W mercury-vapor lamp irradiation with 0.1gL^{-1} of TiO_2 followed by UV-Vis spectrophotometry from 200 to 900 nm for 30 mgL^{-1} of (a) C.I Reactive Black 5 and (b) C.I Reactive Red 239.

3.3.3 Effect of pH

pH is an important parameter for reactions taking place on the surface of a particulate, as is the case of TiO_2 photocatalysis. pH variation can in fact influence the

adsorption of dye molecules onto the TiO_2 surfaces [34]. The effect of solution pH was studied in the range of 2 to 10 for the optimized catalyst amounts (i.e. 0.1 gL^{-1}) and UV-irradiation times (up to 120 min) for the azo dyes under study. Figure 6 shows the variation on the efficiency photocatalytic degradation of C.I Reactive Black 5 at different pH values. Photodegradation was higher in acid medium (pH 2 to 4) with rates of degradation of 95 and 93%, respectively. Up to a pH value of 7, the dye degradation efficiency decreased to 77%. Above pH 7, the degradation continued to decrease until about 70% to pH 10.

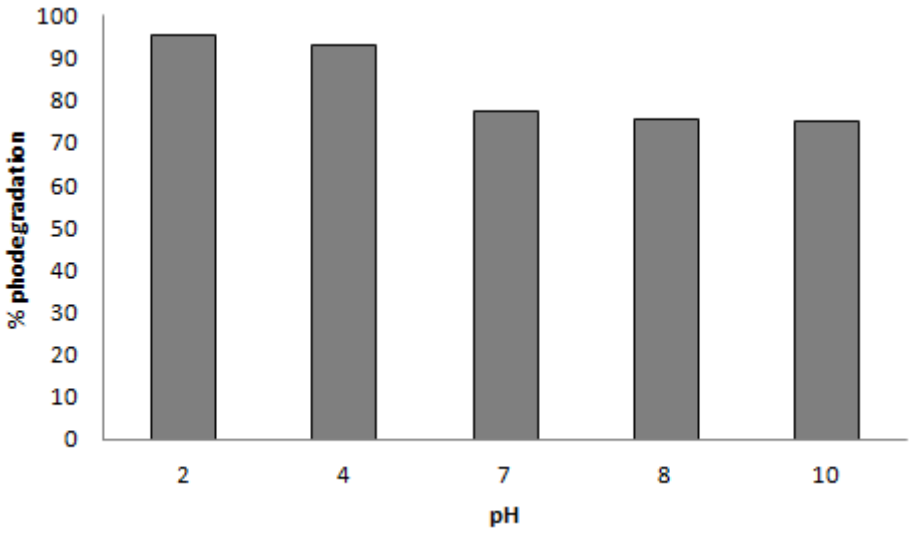

Figure 6. TiO_2 (0.1 gL^{-1}) photodegradation efficiency of 30 mgL^{-1} C.I Reactive Black 5 at different pH values.

This catalyst behavior can be explained by TiO_2 surface charge density. The point of zero charge (pzc) of the TiO_2 (Degussa P25) is at pH 6.8. In acid media ($pH \leq 6.8$) the TiO_2 surface is positively charged; whereas under alkaline conditions ($pH \geq 6.8$) it is negatively charged [25, 35]. Considering the structure of C.I Reactive

Black 5 (Figure 10a), a positive charge excess in the TiO_2 surface promotes a strong interaction with SO_3^- groups of the dye (Figure 7a). A negative charge excess promotes the repulsion of the dye by the titanium surface, diminishing the catalytic activity of this semiconductor (Figure 7b). These results suggest that the influence of the initial pH of the solution on photocatalysis kinetics is due to the amount of the dye adsorbed on TiO_2 [23, 34]. This hypothesis agrees with a reaction occurring at TiO_2 surface and not in the solution, close to the surface.

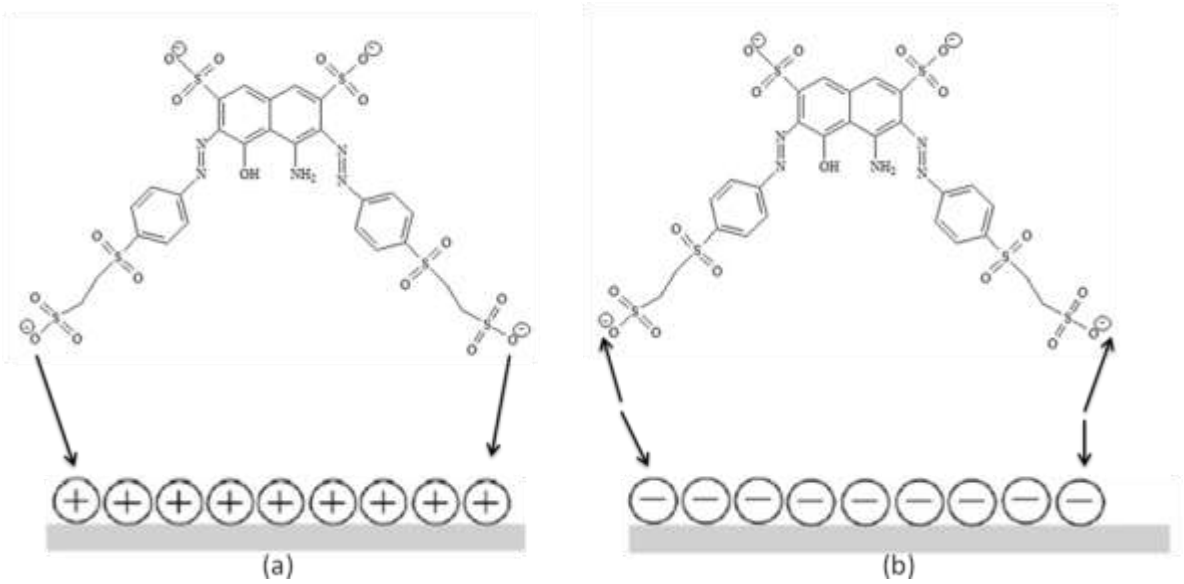

Figure 7. Schematic interaction model of C.I Reactive Black 5 and TiO_2: (a) acid sites and (b) basic sites.

3.3.4 Recycling of TiO_2

One of today`s main industrial wastewater treatment strategies is focused on the development of green technologies and management practices for environmental benefit. Then, TiO_2 recycling can be foreseen as a good practice for sustainable

wastewater treatment. Consequently, it is necessary to demonstrate whether, after a photocatalytic treatment the catalyst can be reused. The TiO_2 catalyst was used and recycled for consecutive reuse on the C.I. Reactive Red 239 degradation; the process was repeated up to 5 times. The TiO_2 recycling studies were performed with 0.1 gL^{-1} of the catalyst and the efficiency of the photodegradation process was evaluated and compared between the reuse cycles, as shown in Figure 8.

These studies reveled that TiO_2 demonstrated a good stability after recovery and that catalyst reuse is effective. The first cycle degraded 99% of the dye after 60 min of irradiation. Subsequently, the second and third cycle degraded 96 and 94% the dye, respectively. After these cycles, the efficiency markedly decreased as demonstrated on fourth and fifth cycles where the rates of degradation felt to 63 and 62% respectively. However, the rate of degradation is still significant after five times of TiO_2 reuse. Agglomeration and sedimentation of the dye around TiO_2 particles after each cycle of photocatalytic degradation is a possible cause of the observed decrease on the degradation rate, because each time the photocatalyst is reused new parts of the catalyst surface become unavailable for dye adsorption and thus photon absorption, reducing the efficiency of the catalytic reaction.

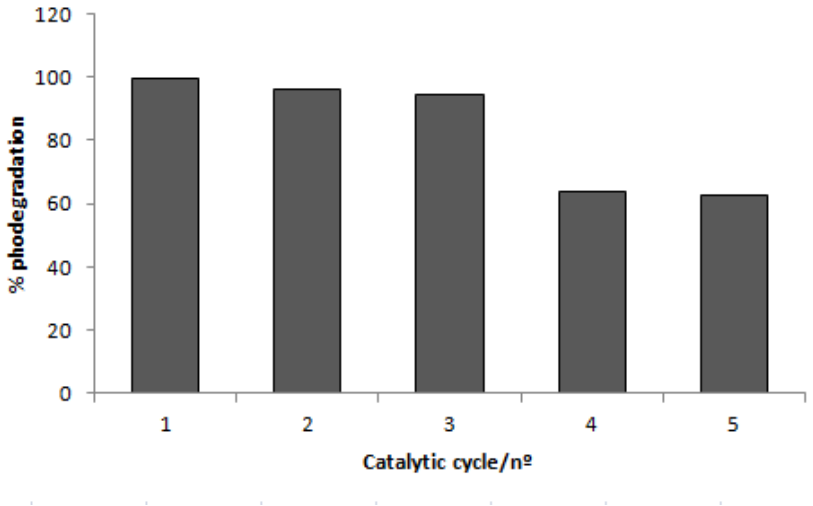

Figure 8. Catalytic yields of 0.1 gL^{-1} of TiO_2 as a function of its reuse of 30 mgL^{-1} of C.I. Reactive Red 239 photodegradation.

An alternative to regenerate TiO_2 after each usage is to apply H_2O_2 under UV irradiation [36]. Wang et al. [37] used TiO_2 modified by photocatalytic degradation through six successive batches and obtained successively similar rates of degradation, demonstrating that the H_2O_2 coated TiO_2 have an enhanced photochemical stability for reuse. Xie and Yuan [38] utilized a pure recycled TiO_2 in the degradation of an organic dye and observed that the removal ratio kept above 90% after three times or reuse, and above 77% after five times of reuse. This ability of titanium dioxide to be reused goes towards green chemistry key principles.

3.3.5 Effect of dye concentration

The effect of the initial concentration of C.I Reactive Black 5 and C.I. Reactive Red 239 on the decomposition of the dye under the 125 W mercury lamp reactor was

determined. The obtained results are presented in Figure 9. The results indicate that the decomposition rate of both dyes strongly depends on the initial dye concentration. The efficiency of photodegradation of both dyes decreased with increase of the initial dye concentration.

C.I Reactive Black 5 and C.I. Reactive Red 239 with 30 mgL^{-1} of photocatalyst show rates of degradation of 95 and 97%, respectively. On increasing the concentration of the dye until 150 mgL^{-1} the photodegradation became very slow, presenting a degradation of only 9% for C.I. Reactive Red 239 and 10% for C.I Reactive Black 5. As the initial concentration of the dye increased, more dye molecules were adsorbed on the surface on the catalyst, consequently the generation of hydroxyl radicals was reduced since the active sites were occupied by dyes [24, 39, 40]. An increase of the initial dye concentration results in an increase of the amount of dye adsorbed on the catalyst surface, affecting the catalytic activity of the photocatalyst [41, 42]. Moreover the reduction of the light path length as the concentration and deepness of the colour of the solution rises also can not be neglected.

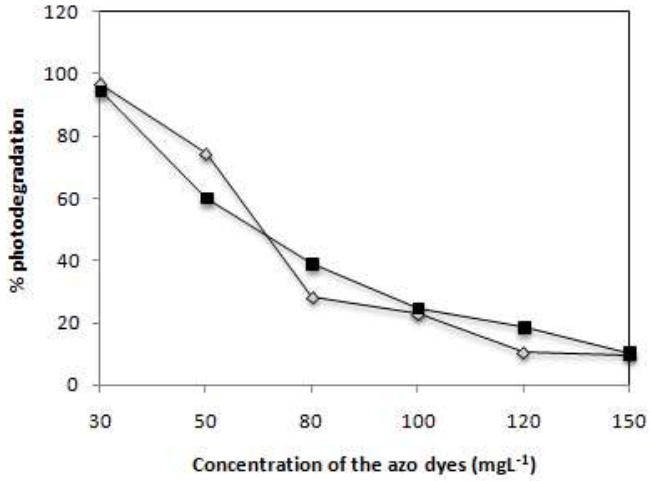

Figure 9. Effect of the initial concentration of C.I. Reactive Red 239 (—◇—) and C.I Reactive Black 5 (—■—) dyes on the efficiency attained after 2 hours of irradiation with 0.1 gL^{-1} of TiO_2 and 2,60 mW/cm^2 of irradiation power by a 125W mercury lamp.

3.3.6 Effect of H_2O_2

Since hydroxyl radicals appear to play an important role in the photocatalytic degradation, electron acceptors such as hydrogen peroxide were added to the dye solution. Hydrogen peroxide has been found to enhance the degradation of compounds due to a more efficient generation of hydroxyl radical and inhibition of electron/hole pair recombination. The degradation rates for the C.I Reactive Black 5 and C.I. Reactive Red 239 in presence of $UV/TiO_2/H_2O_2$ are showed in Figure 10, in order to find the optimal H_2O_2 concentration to be used. It was observed that the added hydrogen peroxide had a beneficial effect on the degradation of both azo dyes. The maximum reaction rate was observed with $0.3x10^{-2}molL^{-1}$ of H_2O_2 for both dyes (achieving a 96% degradation rate in 60 min). The two H_2O_2 concentrations below the later ($0.6x10^{-2}$ and $0.9x10^{-2}$ $molL^{-1}$) produced satisfactory and similar photocatalytic degradation rates (93

and 91%) for both dyes. At higher concentrations of H_2O_2 the degradation efficiency decreased significantly for C.I. Reactive Red 239, with only 25% of degradation being obtained with the highest concentration of H_2O_2 used. For C.I Reactive Black 5 respectively 89 and 82% of degradation were achieved with $1.2x10^{-2}molL^{-1}$and $3x10^{-2}molL^{-1}$ of H_2O_2, but the highest concentration of H_2O_2 used degraded just 29%.

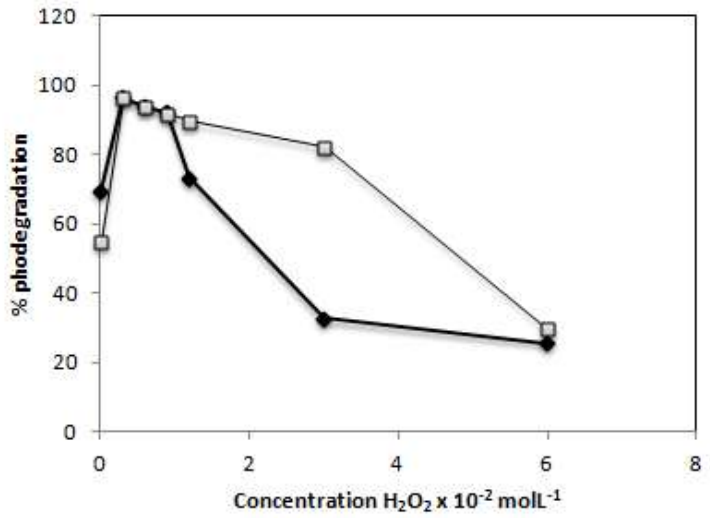

Figure 10. Effect of the presence of hydrogen peroxide on the photodegradation of C.I. Reactive Red 239 (—◆—) and C.I Reactive Black 5 (—□—) dyes after 60 minutes of irradiation with 0.1 gL^{-1} of TiO_2 and 2,60 mW/cm^2 of irradiation power by a 125W mercury lamp.

The electron/hole recombination is a problem in photocatalytic degradation in presence of the TiO_2, and then one strategy to inhibit electron-hole pair recombination is to add other electron acceptors to the reaction [43]. When present at a low concentration, hydrogen peroxide enhanced degradation rate, this fact could be attributed to a suitable trapping of electrons by hydrogen peroxide thereby preventing the recombination of e^- and h^+ pairs and thus increasing the chances of formation of hydroxyl radicals on the surface of catalyst [44, 45]. However, when increase the

concentration of H_2O_2, the electron acceptor reacts with hydroxyl radicals, and acts as scavenger of the photoproduced holes. In addition, H_2O_2 can modify TiO_2 surface. This fact probably decreases its photocatalytic efficiency [46].

3.3.7 Effect of the mixture of the two azo dyes

Since in real effluents from dye industries the presence of several dyes in the waters is frequent we decided to test the effect of the simultaneous presence in solution of both azo dyes under study in this work. The obtained results are present below in figures 11 and 12.

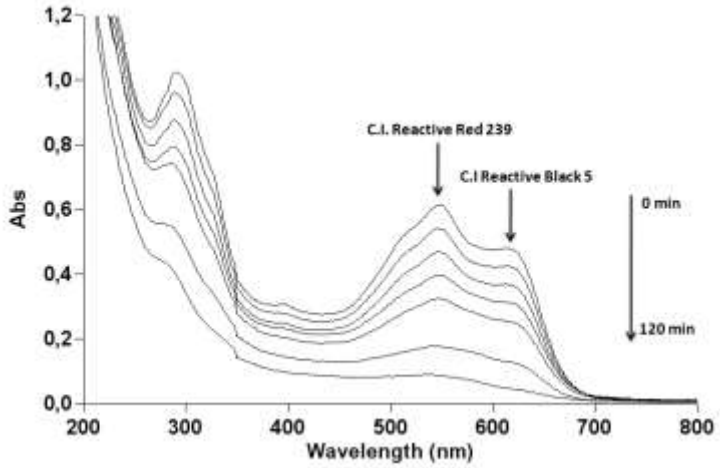

Figure 11. Photocatalytic degradation under 125W mercury-vapor lamp irradiation with 0.1gL^{-1} of TiO_2 followed by UV-Vis spectrophotometry from 200 to 900 nm for a 30 mgL^{-1} mixture of C.I Reactive Black 5 and C.I Reactive Red 239.

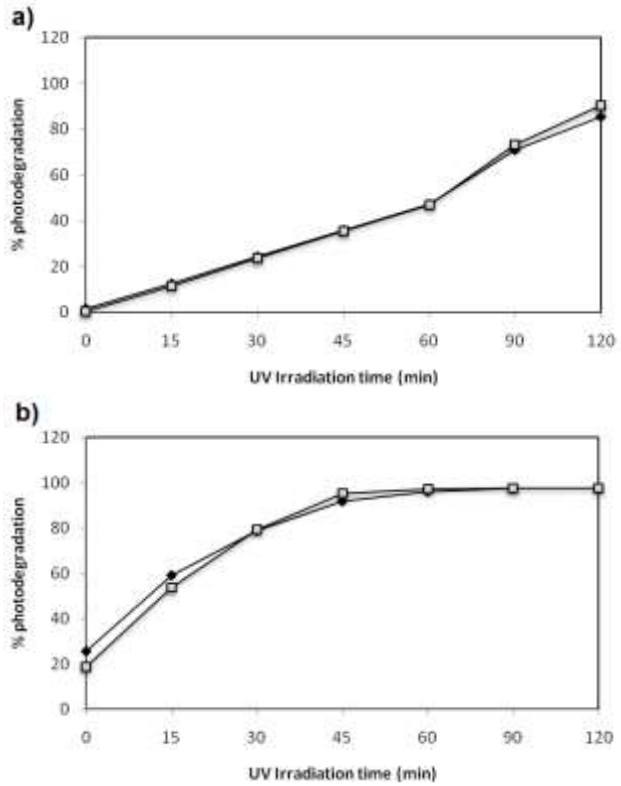

Figure 12. Effect of UV-Irradiation time on the degradation of a 30 mgL^{-1} mixture of the azo dyes C.I. Reactive Red 239 (—◆—) and C.I Reactive Black 5 (—□—) with (a) 0.1 gL^{-1} and (b) 1 gL^{-1} of TiO_2 and 2.60 mW/cm^2 of irradiation power by a 125W mercury lamp.

The photocatalytic degradation of the mixture of the two azo dyes was very satisfactory. C.I Reactive Red 239 degraded 96% with $1gL^{-1}$ of TiO_2 after 120 min of irradiation and when in presence of C.I Reactive Black 5 in solution; the same results (97% degraded) have been observed when the dye in solution was irradiated alone in the same conditions. When using $0.1gL^{-1}$ of TiO_2 the degradation observed is also similar after 120 min of irradiation either for monocomponent solutions or bi-component solutions. C.I Reactive Black 5 achieved a similar degradation for both concentrations of TiO_2 in monocomponent solutions and bi-component solutions. The simultaneous presence of the two azo dyes in solution did not disturb the photocatalytic degradation

of each of them. The degradation rates achieved in mono and bi-component system were identical. These results obtained for azo dyes suggest that TiO_2 can be efficiently used in complex systems containing more than one organic molecule to be degraded, because TiO_2 is a powerful oxidizing agent and enables a non specific attack to organic compounds as Bergamini et al. demonstrated [22].

3.4 Conclusions

The photocatalytic degradation of two commercial azo dyes mediated by TiO_2 was successfully achieved. Results indicated that the photocatalytic degradation of two dyes in water with powdered TiO_2 depended on the concentration of dye, amount of photocatalyst used, UV-irradiation time, solution pH and concentration of added hydrogen peroxide. It was found that the optimal content of catalyst to be used was 0.1 g L^{-1}. Concerning the initial dye concentration, it has been observed that the increase in the initial dye concentration leaded to the decrease in photodegradation. The photodegradation is favored in acidic solution. The optimal H_2O_2 concentration to be added was found to be $3x10^{-3}$ $molL^{-1}$. The recycling of TiO_2 can be performed with photocatalyst being able to be adequately used in other reactions. The TiO_2 have the same photocatalytic activity in reactions with monocomponent solutions and bi-component solutions.

Acknowledgements

Authors gratefully acknowledge Fundação para a Ciência e Tecnologia (FCT, Portugal) through projects PTDC|QUI|65510\2006 and PTDC|QUI|70153\2006 and DyStar Brazil for the gift of the azo dyes. E.M. Saggioro thanks Faperj and ENSP/FioCruz for Master grants.

3.5 References and Notes

1. Chen, C.; Wang, Z.; Ruan, S.; Zou, B.; Zhao, M.; Wu, F. Photocatalytic degradation of C.I. Acid Orange 52 in the presence of Zn-doped TiO_2 prepared by a stearic acid gel method. *Dyes Pigm.* **2008**, *77*, 204-209.
2. Vautier, M.; Guillard, C.; Herrmann, J. Photocatalytic Degradation of Dyes in Water: Case Study of Indigo and of Indigo Carmine. *J. Catal.* **2001**, *201*, 46-59.
3. Wang, C.; Lee, C.; Lyu, M.; Juang, L. Photocatalytic degradation of C.I. Basic Violet 10 using TiO_2 catalysts supported by Y zeolite: An investigation of the effects of operational parameters. *Dyes Pigm.* **2008**, *76*, 817-824.
4. Zainal, Z.; Hui, L.K.; Hussein, M.Z.; Taufiq-Yap, Y.H.; Abdullah, A.H.; Ramli, I. Removal of dyes using immobilized titanium dioxide illuminated by fluorescent lamps. *J. Hazard. Mater.* **2005**, *125*, 113-120.
5. Behnajady, M.A.; Modirshahla, N.; Daneshvar, N.; Rabbani, M. Photocatalytic degradation of an azo dye in a tubular continuous-flow photoreactor with immobilized TiO_2 on glass plates. *Chem. Eng. J.* **2007**, *127*, 167-176.

6. Robinson, T.; McMullan, G.; Marchant, R.; Nigam, P. Remediation of dyes in textile effluent: a critical review on current treatment technologies with a proposed alternative. *Bioresour. Technol.* **2001**, *77*, 247-255.

7. Habibi, M.H.; Hassanzadeh, A.; Mahdavi, S. The effect of operational parameters on the photocatalytic degradation of three textile azo dyes in aqueous TiO_2 suspensions. *J. Photochem. Photobiol. A: Chem.* **2005**, *172*, 89-96.

8. Bizani, E.; Fytianos, K.; Poulios, I.; Tsiridis, V. Photocatalytic decolorization and degradation of dye solutions and wastewaters in the presence of titanium dioxide. *J. Hazard. Mater*. **2006**, *136*, 85-94.

9. Chen, C.; Lu, C.; Chung, Y. Photocatalytic degradation of ethyl violet in aqueous solution mediated by TiO_2 suspensions. *J. Photochem. Photobiol. A: Chem.* **2006**, *181*, 120-125.

10. Oliveira, A.S.; Saggioro, E.M.; Barbosa, N.R.; Mazzei, A.; Ferreira, L.F.V.; Moreira, J.C. Surface Photocatalysis: A Study of the Thickness of TiO_2 Layers on the Photocatalytic Decomposition of Soluble Indigo Blue Dye. *Rev. Chim. (Bucharest, Rom.)* **2011**, *62*, 462-468.

11. Sojić, D.; Despotović, V.; Abramović, B.; Todorova, N.; Giannakopoulou, T.; Trapalis, C. Photocatalytic Degradation of Mecoprop and Clopyralid in Aqueous Suspensions of Nanostructured N-doped TiO_2. *Molecules* **2010**, *15*, 2994-3009.

12. Vasapollo, G.; Mele, G.; Del Sole, R.; Pio, Iolanda.; Li, J.; Mazzetto, S.E. Use of Novel Cardanol-Porphyrin Hybrids and Their TiO_2-Based Composites for the Photodegradation of 4-Nitrophenol in Water. *Molecules* **2011**, *16*, 5769-5784.

13. Gouvêa, C.A.K.; Wypych, F.; Moraes, S.G.; Durán, N.; Nagata, N.; Peralta-Zamora, P. Semiconductor-assisted Photocatalytic Degradation of Reactive Dyes in Aqueous Solution. *Chemosphere* **2000**, *40*, 433-440.

14. Gonçalves, M.S.T.; Campos, A.M.F.O.; Pinto, E.M.M.S.; Plasencia, P.M.S.; Queiroz, M.J.R.P. Photochemical treatment of solutions of azo dyes containing TiO_2. *Chemosphere* **1999**, *39*, 781-786.

15. Tariq, M.A.; Faisal, M.; Saquib, M.; Muneer, M. Heterogeneous photocatalytic degradation of an anthraquinone and a triphenylmethane dye derivative in aqueous suspensions of semiconductor. *Dyes Pigm.* **2008**, *76*, 358-365.

16. Saien, J.; Soleymani, A.R. Degradation and mineralization of Direct Blue 71 in a circulating upflow reactor by UV/TiO_2 process and employing a new method in kinetic study. *J. Hazard. Mater.* **2007**, *144*, 506-512.

17. Aarthi, T.; Narahari, P.; Madras, G. Photocatalytic degradation of Azure and Sudan dyes using nano TiO_2. *J. Hazard. Mater.* **2007**, *149*, 725-734.

18. Saquib, M.; Abu Tariq, M.; Haque, M.M.; Muneer, M. Photocatalytic degradation of disperse blue 1 using UV/TiO_2/H_2O_2 process. *J. Environ. Manage.* **2008**, *88*, 300-306.

19. Huang, M.; Xu, C.; Wu, Z.; Huang, Y.; Lin, J.; Wu, J. Photocatalytic discolorization of methyl orange solution by Pt modified TiO_2 loaded on natural zeolite. *Dyes Pigm.* **2008**, *77*, 327-334.

20. Andronic, L.; Duta, A. TiO_2 thin films for dyes photodegradation. *Thin Solid Films* **2007**, *515*, 6294-6297.

21. Liu, H.L.; Chiou, Y.R. Optimal decolorization efficiency of Reactive Red 239 by UV/TiO_2 photocatalytic process coupled with response surface methodology. *Chem. Eng. J*. **2005**, *112*, 173-179.

22. Bergamini, R.B.M.; Azevedo, E.B.; Araújo, L.R.R. Heterogeneous photocatalytic degradation of reactive dyes in aqueous TiO_2 suspensions: Decolorization kinetics. *Chem. Eng. J*. **2009**, *149*, 215-220.

23. Zielinska, B,; Grzechulska, J.; Grzmil, B.; Morawski, A.W. Photocatalytic degradation od Reactive Black 5 A comparison between TiO_2-Tytanpol A11 and TiO_2-Degussa P25 photocatalysts. *Appl. Catal.*, B **2001**, *35*, L1-L7.

24. Alaton, I.A.; Balcioglu, I.A. Photochemical and Heterogeneous photocatalytic degradation of waste vinylsulphone dyes: a case study with hydrolysed Reactive Black 5. *J. Photochem. Photobiol. A: Chem.* **2001**, *141*, 247-254.

25. Muruganandham, M.; Sobana, N.; Swaminathan, M. Solar assited photocatalytic and photochemical degradation of Reactive Black 5. *J. Hazard. Mater.* **2006**, *137*, 1371-1376.

26. Tang, C.; Chen, V. The photocatalytic degradation of reactive black 5 using TiO_2/UV in an annular photoreactor. *Water Res.* **2004**, *38*, 2775-2781.

27. Saquib, M.; Munner, M. Photocatalytic degradation of two selected textile dye derivates, Eosine Yellowish and ρ-Rosaniline, aqueous suspensions of titanium dioxide. *J. Environ. Sci. Health, Part A: Toxic/Hazard. Subst. Environ. Eng.* **2003**, *38*, 2581-2598.

28. Fox, M.A.; Dulay, M.T. Heterogeneous Photocatalysis. *Chem. Rev*. **1993**, *93*, 341-357.

29. Konstantinou, I.K.; Albanis, T.A. TiO_2-assisted photocatalytic degradation of azo dyes in aqueous solution: kinetic and mechanistic investigations: A review. *Appl. Catal., B* **2004**, *49*, 1-14.

30. Feng, W.; Nansheng, D.; Helin, H. Degradation mechanism of azo dye C.I. reactive red 2 by iron powder reduction and photooxidation in aqueous solutions. *Chemosphere* **2000**, *41*, 1233-1238.

31. Karkmaz, M.; Puzenat, E.; Guillard, C.; Herrmann, J.M. Photocatalytic degradation of the alimentary azo dye amaranth. Mineralization of the azo group to nitrogen. *Appl. Catal., B* **2004**, *51*, 183-194.

32. Mozia, S.; Tomaszewska, M.; Morawski, A.W. Photodegradation of azo dye Acid Red 18 in a quartz labyrinth flow reactor with immobilized TiO_2 bed. *Dyes Pigm.* **2007**, *75*, 60-66.

33. Al-Ekabi, H.; Serpone, N. Photocatalytic degradation of chlorinated phenols in aerated aqueous-solutions over TiO_2 supported on a glass matrix. *J. Phys. Chem.* **1988**, *92*, 5726-5731.

34. Wang, N.; Li, J.; Zhu, L.; Dong, Y.; Tang, H. Highly photocatalytic activity of metallic hydroxide/titanium dioxide nanoparticules prepared via a modified wet precipitation process. *J. Photochem. Photobiol. A: Chem.* **2008**, *198*, 282-287.

35. Dostanic J.M.; Loncarevic D.R.; Bankovic P.T.; Cvetkovik O.G.; Jovanovic D.M.; Mijin D.Z. Influence of process parameters on the photodegradation of synthesized azo pyridine dye in TiO_2 water suspension under simulated sunlight. *J. Environ. Sci. Health, Part A: Toxic/Hazard. Subst. Environ. Eng*. **2011,** *46,* 70-79.

36. Xie Y.; Yuan C. Transparent TiO_2 sol nanocrystallites mediated homogeneous-like photocatalytic reaction and hydrosol recycling process. *J. Mater. Sci.* **2005**, *40*, 6375-6383.

37. Han F.; Kambala V.S.R.; Srinivasan M. Tailored titanium dioxide photocatalysts for the degradation of organic dyes in wastewater treatment: A review. *Appl. Catal., A* **2009,** *359*, 25-40.

38. Muruganandham M.; Swaminathan M. Photocatalytic decolourisation and degradation of Reactive Orange 4 by TiO_2-UV process. *Dyes Pigm.* **2006**, *68*, 133-142.

39. Daneshvar N.; Salari D.; Khataee A.R. Photocatalytic degradation of azo dye acid red 14 in water: investigation of the effect of operational parameters. *J. Photochem. Photobiol. A: Chem.* **2003,** *157*, 111-116.

40. Grzechulska J.; Morawski A.W. Photocatalytic decomposition of azo-dye acid black 1 in water over modified titanium dioxide. *Appl. Catal., B* **2002,** *36*, 45-51.

41. Carter S.R.; Stefan M.I.; Bolton J.R.; Safarzadeh-Amiri A. UV/H_2O_2 Treatment of methyl tert-butyl ether in contaminated waters. *Environ. Sci. Technol.* **2000**, *34*, 659-662.

42. Malato S.; Blanco J.; Ritchter C.; Braun B.; Maldonado M.I.. Enhancement of the rate of solar photocatalytic mineralization of organic pollutants by inorganic oxidizing species. *Appl. Catal., B* **1998**, *17*, 347-356.

43. Mahmoodi N.M.; Arami M.; Limaee N.Y.; Gharanjig K.; Ardejani F.D. Decolorization and mineralization of textile dyes at solution bulk by heterogeneous nanophotocatalysis using immobilized nanoparticles of titanium dioxide. *Colloids Surf. A* **2006**, *290*, 125-131.

44. Prado A.G.S.; Bolzon L.B.; Pedroso C.P.; Moura A.O.; Costa L.L. Nb_2O_5 as efficient and recyclable photocatalyst for indigo carmine degradation. *Appl. Catal., A* **2008**, *82*, 219-224.

45. Aguedacha A.; Brosillonb S.; Morvanb J.; Lhadi E.K. Photocatalytic degradation of azo-dyes reactive black 5 and reactive yellow 145 in water over a newly deposited titanium dioxide. *Appl. Catal., B* **2005**, *57*, 55-62.

46. Zhu C.; Wang L.; Kong L.; Yang X.; Wang L.; Zheng S.; Chen F.; Maizhi F.; Zong H. Photocatalytic degradation of AZO dyes by supported TiO_2/UV in aqueous solution. *Chemosphere* **2000**, *41*, 303-309.

47. Hachem C.; Bocquillon F.; Zahraa O.; Bouchy M. Decolourization of textile industry wastewater by the photocatalytic degradation process. *Dyes Pigm*. **2001**, *49*, 117-125.

4. ARTIGO 2

REVISTA DE CHIMIE
ISSN 0034-7752
REV. CHIM. (Bucharest) ♦ 65 ♦ No. 2 ♦ 2014

Research
Article

Effect of activated carbon and titanium dioxide on the remediation of an indigoid dye in model waters

Enrico Mendes Saggioro[1]*, Anabela Sousa Oliveira[2,3], Thelma Pavesi[1], Josino Costa Moreira[1]

1 – CESTEH - Centro de Estudos da Saúde do Trabalhador e Ecologia Humana, Escola Nacional de Saúde Pública - Fundação Oswaldo Cruz, Av. Leopoldo Bulhões, 1480, Rio de Janeiro, RJ, Brasil, 21041-210.

2 – C3i - Centro Interdisciplinar de Investigação e Inovação, Escola Superior de Tecnologia e Gestão, Instituto Politécnico de Portalegre, Lugar da Abadessa Apartado 148 7301901 - Portalegre, Portugal.

3 – CQFM - Centro de Química-Física Molecular and IN - Instituto de Nanociencias e Nanotecnologia, Instituto Superior Técnico, Universidade Técnica de Lisboa, Av. Rovisco Pais 1049-001, Lisboa, Portugal.

Abstract

Indigo carmine (IC) is considered as a highly toxic indigoid dye. Most dyes are toxic and recalcitrant to biodegradation, causing a decrease in their treatment efficiency at the biological wastewater treatment plants. Once each treatment technique has its own advantages and drawbacks, thus the aim of the present study was to investigate the decolorization of a model water effluent containing indigo carmine dye under physical and chemical different treatments. Experiments on decolorization of the effluent containing indigo dye were performed using activated carbon in the dark and under irradiation. Furthermore the effect of activated carbon/TiO_2/UV was tested for the same systhem. The decolorization was followed by UV-Vis absorption spectroscopy. Results showed that the adsorption capacity of carbon black was of 28.5 mg Indigo Carmine per grame of carbon. In low concentrations, activated carbon was not able to remove the dye from the solution, even under irradiation. Only in high concentrations activated carbon was able to remove the dye from water. The TiO_2 activity decreased when in presence of activated carbon. The physical and chemical treatments together were be able to successfully remove indigo carmine dye from the simulated wastewater.

Keywords: indigo carmine, activated carbon, TiO_2, adsorption, photocatalysis, remediation

4.1 Introduction

Organic dyes are one of the largest groups of wastewaters pollutants. In general they are released into the environment by textile and some other industries [1]. Dyes are used in the processing of textile industries and are lost in significant quantities during dyeing steps. Wastewaters containing 5-15% of untreated dye can be released into the environment and are considered to pose serious problems [2, 3]. These dyes pose an environmental concern due to both their high visibility and their recalcitrant character. Moreover, many dyes and their degradation products have been associated with toxicity and/or mutagenicity [4].

Indigo blue dye's main component is indigotine which is extracted from the leaves of *Indigofera tinctoria* [5]. Indigo carmine is also one of the oldest dyes and still one of the most used in textile industry [6]. The basic color-producing structure of indigoid dyes is a cross-conjugated system or H-chromophore, consisting of a single -C=C- double bond substituted by two NH donor groups and two CO acceptor groups [7].

Indigo carmine (IC) is considered as a highly toxic indigoid dye. Contact with skin and eyes can cause permanent injury to cornea and conjunctiva and if consumed by oral via can cause disturbs in reproductive, developmental and neuronal systems, and may cause death [8, 9]. Most dyes are recalcitrant to biodegradation, causing decay in the efficiency of biological wastewater treatment plants; so these effluents are usually efficiently treated by traditional physic-chemical wastewater treatment methods such as flocculation or adsorption [2, 10].

The use of activated carbon (AC) is an efficient water and wastewater treatment; the treatment is based in the use of adsorbent substrates and have many applications on textile dye´s wastewater treatments [11-14]. Activated carbon is probably the most versatile adsorbent because of its large surface area, polymodal porous structure, high adsorption capacity and variable surface chemical composition [15]. Furthermore, what makes ACs attractive to (textile) wastewater treatment is the possibility of tailoring their physical and/or chemical properties in order to optimize their performance [16].

Among the new methods for wastewater treatment, AOPs based on the generation of very reactive species such as hydroxyl radicals have been proposed to oxidize quickly and non-selectively a large range or organic pollutants [17-21]. Titania is a well-know photocatalyst with many applications in photo reactions for wastewater treatment [22]. The use of TiO_2 has advantages such as ease of use, low cost, high photochemical reactivity and non specific oxidative attack ability. In this way, it can promote the degradation of different target organic compounds and industrial effluents with little change of operational parameters [23, 24]. Titanium dioxide mediated photooxidation is indeed used for environmental remediation, where toxic materials at low concentration are converted, in a series of chemical steps, to harmless oxidation products such CO_2 and H_2O [25].

Each technique has its own advantages and drawbacks, thus the aim of the present study was to investigate the decolorization of a model effluent containing indigo carmine dye using different physical and chemical treatments. This study compared the adsorption efficiency of activated carbon in the dark and under irradiation. Furthermore,

it was investigated the synergic effect of the presence of activated carbon together with TiO_2 in the photocatalysis.

4.2 Experimental

4.2.1 Reagents and Materials

Indigo carmine (IC) dye (3,3-dioxo-2,2-bis-indolyden-5,5-disulfonic acid disodium salt, $C_{16}H_8N_2S_2O_8Na_2$, M.W. = 466.36 g mol^{-1}) was obtained from Sigma Aldrich (85 % dye content) and used without further purification (fig. 1). The photocatalyst used in all experiments was titanium dioxide, Degussa P25, containing 75% anatase and 25% rutile, with a specific BET surface area of 50 m^2 g^{-1} and primary particle size of 20 nm. The activated carbon powder used was obtained from Vetec, Brazil. All dye solutions were prepared using Mili-Q water.

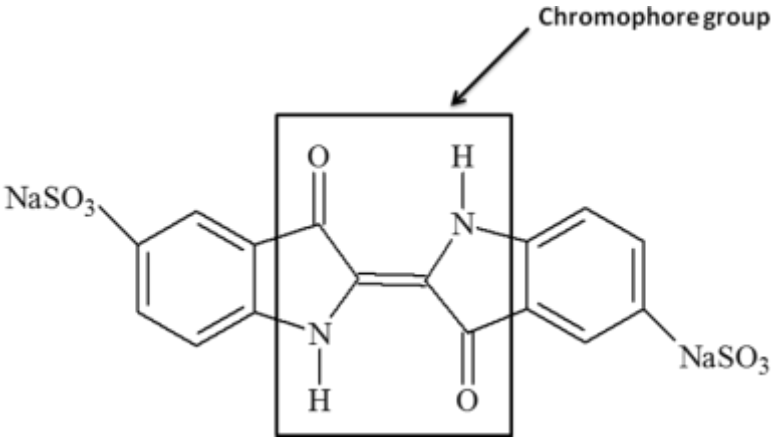

Fig. 1. Chemical structure of indigo carmine dye.

4.2.2 Experiments procedure

Aliquots of 100 ml of solution containing 30 mg L^{-1} of indigo carmine were treated with different concentrations of activated carbon (0, $1x10^{-3}$, $2.5x10^{-3}$, $5x10^{-3}$, $1x10^{-2}$, $1x10^{-1}$ and 1 g L^{-1}) that were kept in the dark while other set of samples were irradiated under stirring. This experiment allowed us to evaluate the ability of activated carbon to remove dye by adsorption (dark) and if it has photocatalytic activity under irradiation.

The effect of AC on the photocatalytic activity of the titanium dioxide was also tested. For that, a mixture of activated carbon (1.5 g) and titanium dioxide (1.5 g) was homogenized for 24h and added at different concentrations (0, $1x10^{-3}$, $2.5x10^{-3}$, $5x10^{-3}$, $1x10^{-2}$, $1x10^{-1}$ and 1 g L^{-1}) to 100 ml solutions containing 30 mg L^{-1} indigo carmine and irradiated. Also, TiO_2 only was tested on the photodegradation of indigo carmine dye under the same conditions of the experiments described above.

After treatment (with AC, AC+TiO_2 or TiO_2 only), each collected sample is centrifuged for 10 min at 1000 rpm, filtered with a 0.45μm Milipore® membrane and the post treatment indigo carmine concentration at different irradiation times is determined measuring its UV-visible absorption at dye's maximum absorption wavelength (ie, 610 nm). All experiments were repeated twice, so each result is the average of two experiments. The reactor used was a batch magnetically stirred reactor irradiated with a high-pressure 125 W mercury vapor lamp.

4.2.3 Decolorization kinetics of the activated carbon and titanium dioxide

The Langmuir–Hinshelwood model was used to describe kinetics of photocatalytic degradation (equation 1). Isotherms represent the relationship between the amount absorbed and the concentration at a constant temperature. They also provide useful information about the adsorption process and enabled determination of useful surface parameters such as surface area, pore size distribution and pore volume of the adsorbent.

$$r_o = dC/dt = krKC/(1 + KC) \quad (1)$$

Where r_o is the initial reaction rate of dye removal (mg L^{-1} min^{-1}), k_r is the limiting rate constant of the reaction at maximum coverage under the given experimental conditions (mg L^{-1} min^{-1}), and K is the adsorption coefficient of dye on TiO_2 particles (mg L^{-1}). When $KC<<1$, the Langmuir-Hinshelwood equation is simplified to a pseudo first-order expression (Equation 2):

$$-dC/dt = k_{app}C \quad (2)$$

After integration, the relation is expressed as in Equation 3:

$$\ln(C_0/C) = k_{app}t \quad (3)$$

Where C_0 is the equilibrium concentration (at zero irradiation). The slope of the linear relation is the apparent first-order rate constant, k_{app} (min^{-1}). The latter parameter was determined for each experiment and used as a measure of the photocatalytic efficiency.

4.2.4 Efficient Photon Flux Determination

The efficient photon flux was determinate measuring the radiant flux (in mW/cm^2) at the surface of the sample being treated. In each case stated above, the radiant flux was measured with a radiometer (Cole-Parmer Instrument Co.; model 9811-50), calibrated against a microcalorimeter, taking in account the spectral distribution of the lamp, the optical filter transmission and the absorbance spectrum of titanium dioxide (measurement at 366 nm).

4.2.5 Equipment

A double beam UV-Visible spectrophotometer (Shimadzu UV-1601PC) was used for spectrophotometric determination of molecular ultra-violet-visible absorption spectra of indigo carmine dye solutions, from 200 to 900 nm. Spectra of the dye in water were recorded using 1 cm quartz cuvettes.

4.3 Results and Discussion

4.3.1 Decolorization of indigo carmine dye using activated carbon

The activated carbon was used on two different situations. First, the AC in different concentrations was add in solution of indigo carmine dye and kept in the dark. Figure 2 shows these results. For 0 to 10 mgL^{-1} of AC in solution, the same concentration of the dye was observed for all time of stirring. The presence of AC on these concentrations is not able to adsorb the molecule of indigo carmine dye. The AC concentration of $1x10^2$ mg L^{-1} is able to remove 23% of dye in 5 hours under stirring. Therefore, only $1x10^3$ mgL^{-1} of AC promote 95% the decolorization in 15 minutes of stirring and this percentage was the same after 5 hours.

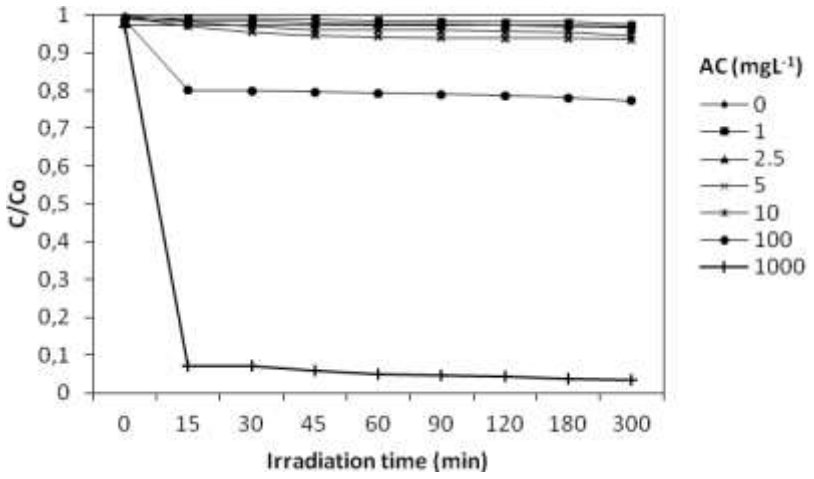

Fig. 2. Decolorization of indigo carmine by different concentrations of activated carbon (AC) at different time intervals in the dark.

Furthermore, AC was submitted to the same conditions of the first experiment but kept under artificial irradiation during the all-time of the experiment. Similar decolorization rates were obtained when comparing experiments with different amounts of activated carbon in the dark with those under irradiation, according to the results of Figure 3. Only in high concentrations activated carbon was able to remove the dye, but in this case the determinant removal mechanism was adsorption of the dye in activated carbon microporous structure. These results showed (Figure 4) that activated carbon was not able to produce strong photocatalytic activity, and had only adsorptive properties with an adsorption capacity of 28.5 mg Indigo Carmine per gram of carbon. Choy et al. [11] showed an adsorption capacity of 101.0 mg of Acid Red per gram of carbon, 100.9 mg of Acid Blue per gram of carbon and 128.8 mg of Acid Yellow per gram of carbon. Activated carbons, prepared from low-cost materials with Malik, [14] demonstrated similar results on AC absorbing capacity when activated carbons prepared from sawdust and rice husk for removal of Acid Yellow 36 were used. Indeed, it was identified that the rate limiting step for adsorption is the intraparticle diffusion of dye molecule within the carbon particle. Namasivayam and Kavitha, [13] performed the adsorption of Congo Red by coir pith carbon varying the parameters such as stirring time, dye concentration, adsorbent dose, pH and temperature. The adsorption capacity was found to be 6.7 mg dye per gram of the adsorbent. Kannan and Sundaram, [12] used the commercial activated carbon to remove methylene blue and observed that the extent of dye removal increased with decrease in the initial concentration of the dye and particle size of the adsorbent and also increased with the increase of the contact time, used amount of adsorbent and the initial pH of the solution. On the other hand, Santos et

al. [26] used on commercial activated carbon as catalyst and promoted wet oxidation of three dyes commonly found in textile wastewaters and the catalyst showed high catalytic activity in dye conversion and color removal.

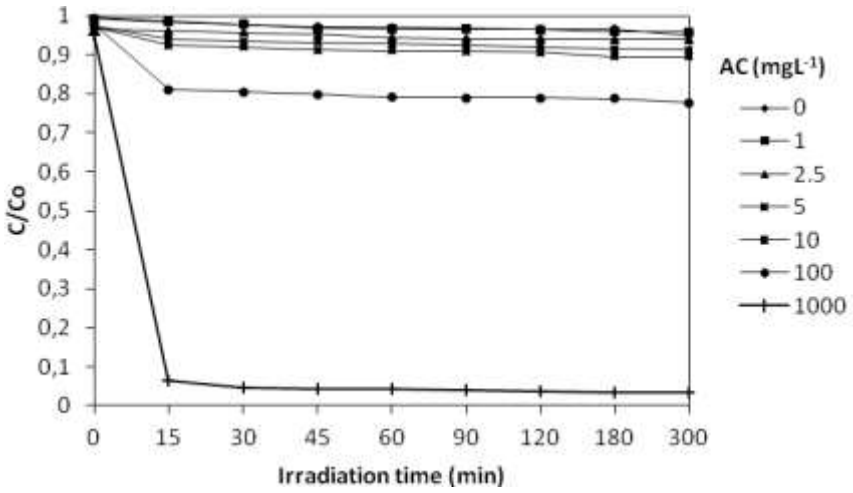

Fig. 3. Decolorization of indigo carmine by different concentrations of activated carbon (AC) at different time intervals under 125W mercury-vapor lamp irradiation and intensity of irradiation of 2,60 mW/cm^{-2}.

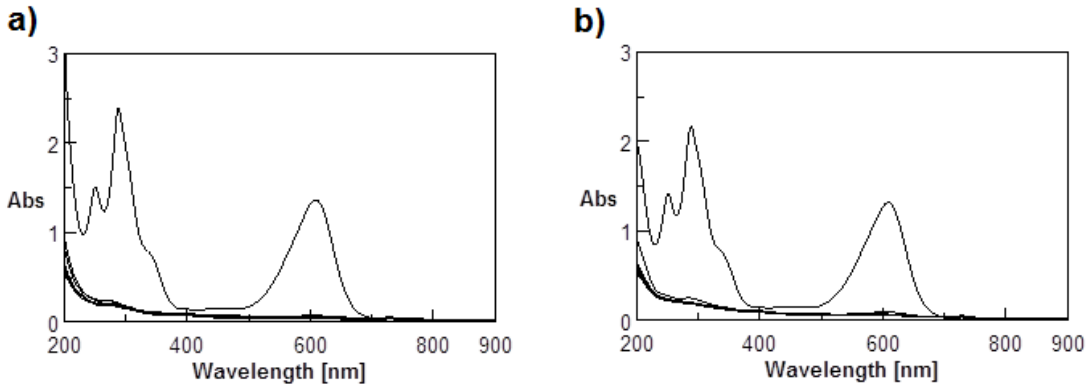

Fig. 4. Decolorization of indigo carmine with 1x10^3 mgL^{-1} of AC in different times (0, 15, 30, 45, 60, 90, 120, 180, 300 minutes) followed by UV-Vis spectrofotmetry 200-900 nm; **a)** AC in the dark, **b)** AC under intesive of irradiation of 2,60 mW/cm^{-2} with mercury vapor lamp 125 Watts.

4.3.2 Decolorization of indigo carmine dye with TiO_2/UV and activated carbon/TiO_2/UV

The photodegradation with TiO_2 was performed in two combinations. On the photodegradation with TiO_2 under 125 Watts mercury vapor lamp irradiation, the efficiency of the photocatalytic degradation of indigo carmine was directly related with the used amount of photocatalyst. For concentrations of $1x10^3$ mgL^{-1} and $1x10^2$ mgL^{-1} of TiO_2, photocatalysis had an efficiency of 96 and 65% in 30 minutes of irradiation, respectively and in 300 minutes around 99% of dye was photodegraded. Furthermore, for 5 and 2.5 mg L^{-1} photocatalysis had an efficiency of 87 and 55% in 180 minutes of irradiation and in 300 minutes each concentration degraded 99 and 88% (Figure 5). Under irradiation, only the molecules adsorbed on the surface of TiO_2 can be degraded. When the amount of catalyst used on the photocatalytic degradation is very high the turbidity of the suspension strongly inhibits further light penetration in the photoreactor [27, 28]. The decolorization of activated carbon/TiO_2/UV following the same profile of TiO_2/UV (Figure 6), but the constant K in TiO_2/UV was by itself more efficiency when compared to activated carbon/TiO_2/UV (Figure 7). TiO_2 activity decreased when in presence of activated carbon because activated carbon can absorb light – *i.e* by decreasing the light flux in the sample - but also because activated carbon can adsorb TiO_2, reducing the amount of photocatalyst available. Table 1 summarizes pseudo-first-order rate constants (K) and R^2 values with different treatments.

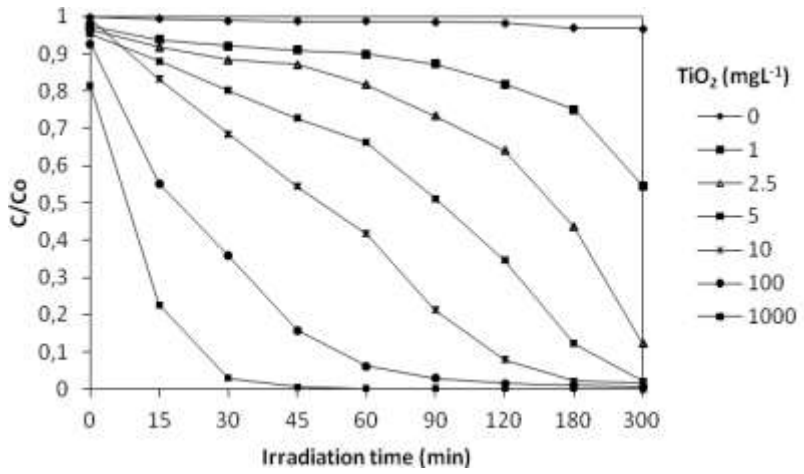

Fig. 5. Photocatalytic decolorization of indigo carmine dye at different time intervals of intesive irradiation of 2,60 mW/cm^{-2} mercury-vapor lamp 125 Watts and different concentrations of TiO_2.

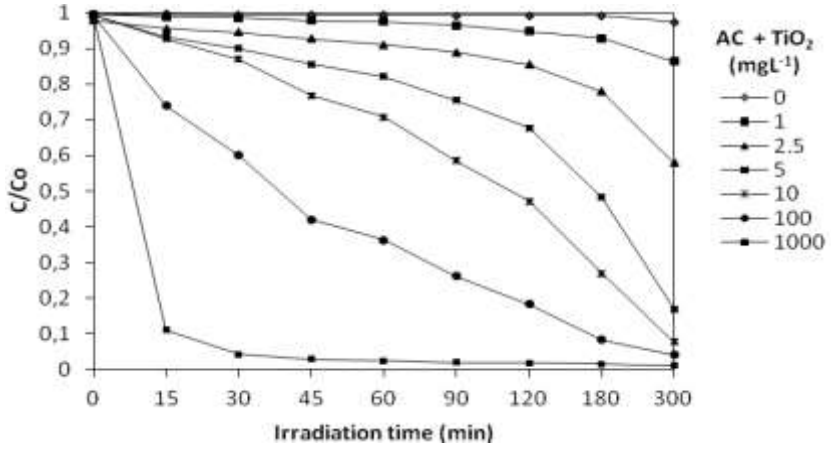

Fig. 6. Photocatalytic decolorization of indigo carmine dye at different time intervals of intesive irradiation of 2,60 mW/cm^{-2} mercury-vapor lamp 125 Watts and different concentrations a mixture of activated carbon (AC) and TiO_2.

Table 1. Pseudo-first-order rate constants (K) and R^2 values with different treatments, under mercury-vapor lamp 125W irradiation.

Concentrations gL^{-1}	Activated Carbon in the dark		Activated Carbon/UV		TiO_2/UV		Activated Carbon + TiO_2/UV	
	K (min^{-1})	R^2	K (min^{-1})	R^2	K (min^{-1})	R^2	K (min^{-1})	R^2
Control	0.0003	0.965	0.0047	0.905	0.0036	0.869	0.0003	0.968
$1x10^{-3}$	0.0017	0.966	0.0049	0.908	0.0318	0.878	0.0072	0.923
$2.5x10^{-3}$	0.0028	0.969	0.0035	0.915	0.063	0.908	0.0211	0.971
$5x10^{-3}$	0.0032	0.868	0.004	0.979	0.1542	0.892	0.0595	0.964
$1x10^{-2}$	0.0058	0.928	0.0045	0.948	0.5504	0.898	0.1202	0.949
$1x10^{-1}$	0.0046	0.943	0.0053	0.924	0.6502	0.988	0.2732	0.993
1	0.1159	0.979	0.0812	0.842	0.8307	0.865	0.2724	0.862

A combined treatment of TiO_2 and activated carbon had been tested. Zhang et al. [29] studied nano-TiO_2-supported activated carbon (TiO_2/AC) and it has been found the supported-TiO_2 on the surface of AC can be excited resulting in the production of •OH in the aqueous solution under irradiation, which significantly enhanced the performance of AC/microwave process for the degradation of Methyl Orange. Also, the TiO_2/AC system displayed higher catalytic activity than AC alone under microwave irradiation. Xu et al. [30] synthesized V-doped titania–activated carbon composite film was prepared by a modified sol–gel method and found that the photocatalytic activity was

enhanced due to expansion of absorption edge by vanadium doping, and the synergistic effect of activated carbon and titania.

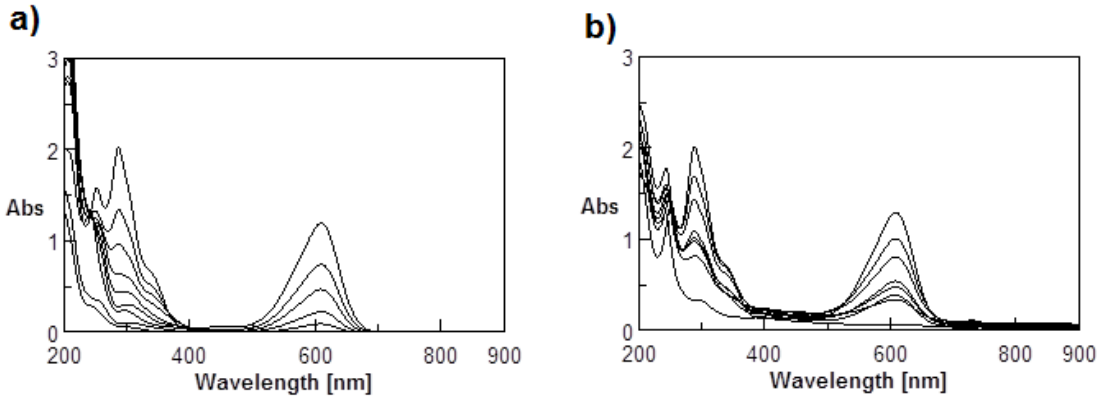

Fig. 7. Photocatalytic degradation of indigo carmine dye under mercury vapor lamp 125 Watts at intesive of irradiation 2,60 mW/cm^{-2} in different time intervals (0, 15, 30, 45, 60, 90, 120, 180, 300 minutes) following UV-Vis spectrofotmetry 200-900 nm; **a)** $1x10^2$ mgL^{-1} of TiO_2/UV, **b)** $1x10^2$ mgL^{-1} of AC/TiO_2/UV.

4.4 Conclusions

The physical and chemical treatments were able to successfully remove color from a simulated wastewater contain indigo carmine dye. Activated carbon in low concentrations was not able to remove the dye from the solution, even under irradiation. Only in high concentrations activated carbon was able to remove the dye, demonstrating to have an adsorption capacity of 28.5 mg of Indigo Carmine per gram of carbon. The decolorization of activated carbon/TiO_2/UV system was more efficient than activated carbon alone. The TiO_2 activity decreased when in presence of activated carbon.

Acknowledgements

The authors gratefully acknowledge Fundação para a Ciência e Tecnologia (FCT, Portugal) for project PTDC|QUI|70153/2006, ERA-MNT/0003/2009 and ERA-MNT/0004/2009. E.M. Saggioro thanks Faperj and ENSP/FIOCRUZ for scholarship. J.C. Moreira thanks Faperj and CNPq.

4.5 References

1. Barka, N., Assabbane, A., Nounah, A., Aîlchou, Y., J. Hazard. Mater., **152**, nr. 3, 2008, p. 1054.

2. Zainal, Z., Hui, L. K., Hussein, M. Z., Taufiq-Yap, Y. H., Abdullah, A. H., Ramli, I., J. Hazard. Mater., **125**, nr. 1-3, 2005, p. 113.

3. Wang, C., Lee, C., Lyu, M., Juang, L., Dyes Pigm., **76**, nr. 3, 2008, p. 817.

4. Chen, C., Wang, Z., Ruan, S., Zou, B., Zhao, M., Wu, F., Dyes Pigm., **77**, nr. 1, 2008, p. 204.

5. Andreotti, A., Bonaduce, L., Colombini, M. P., Ribechini, E., Rapid Commun. Mass Spectrom., **18**, nr. 11, 2004, p. 1213.

6. Oliveira, A. S., Saggioro, E. M., Barbosa, N. R., Mazzei, A., Ferreira, L. F. V., Moreira, J. C., Rev. Chim., **62**, nr. 4, 2011, p. 462.

7. Vautier, M., Guillard, C., Herrmann, J., J. Catal., **201**, nr. 1, 2001, p. 46.

8. Jenkins, C. L., Arch. Environ. Health, **40**, nr. 5, 1978, p. 7.

9. Saggioro, E. M., Oliveira, A. S., Moreira, J. C., Ferreira, L. F.V., Epidemiology., **22**, 2011, S249-S249.

10. Sanromán, M. A., Pazos, M., Ricart, M. T., Cameselle, C., Chemosphere, **57**, nr. 3, 2004, p. 233.

11. Choy, K. K. H., McKay, G., Porter, J.F., Resour. Conserv. Recy., **27**, nr. 1-2, 1999, p. 57.

12. Kannan, N., Sundaram, M.M., Dyes Pigm., **51**, nr. 1, 2001, p. 25.

13. Namasivayam, C., Kavitha, D., Dyes Pigm., **54**, nr. 1, 2002, p. 47.

14. Malik, P.K., Dyes Pigm., **56**, nr. 3, 2003, p. 239.

15. Mezohegyi, G., van der Zee, F. P., Font, J., Fortuny, A., Fabregat, A., J. Environ. Manage., 102, nr. 1, 2012, p. 148.

16. Marsh, H., Rodríguez-Reinoso, F., Activated Carbon, 1 ed., Elsevier : Oxford, 2006, p. 322-327.

17. Sano, T., Puzenat, E., Guillard, C., Geantet, C., Matsuzawa, S., J. Mol. Catal. A: Chem., **284**, 2008, 127.

18. Khataee, A. R., Vatanpour, V., Amani, A. R., J. Hazard. Mater., **161**, nr.2-3, 2009, 1225.

19. Oliveira, A. S., Saggioro, E. M., Pavesi, T., Moreira, J.C., Ferreira, L. F. V., Solar Photochemistry for Environmental Remediation - advanced oxidation processes for industrial wastewater treatment, Molecular Photochemistry- Various aspects, InTech in press, 2012, ISBN 979-953-307-364-3.

20. Xavier, L. F. W., Moreira, I. M. N. S., Higarashi, M. M., Moreira, J. C., Ferreira, L. F. V., Oliveira, A. S., Química Nova, **28**, 2005, 409-413.

21. Oliveria, A. S., Ferreira, L. F. V., Moreira, J. C., Rev. Roum. Chim., **53**, 2008, 893-902.

22. Fujishima, A., Rao, T.N., Tryk, D.A., J. Photochem. Photobiol. C: Photochemical. Rev., **1**, 2000, p. 1.

23. Saggioro E. M., Oliveira, A. S., Pavesi, T., Maia, C. G., Ferreira, L. F. V., Moreira, J. C., Molecules, **16**, nr. 12, 2011, p. 10370.

24. Guillard, C., Disdier, J., Monnet, C., Dussaud, J., Malato, S., Blanco, J., Maldonado, M. I., Herrmann, J., Appl. Catal. B, **46**, nr. 2, 2003, p. 319.

25. Hoffman, M. R., Martin, S. T., Choi, W. Y., Bahnemann, D. W., Chem. Rev., **95**, nr. 1, 1995, p. 69.

26. Santos, A., Yustos, P., Rodríguez, S., Garcia-Ochoa, F., de Gracia, M., Ind. Eng. Chem. Res., **46**, nr. 8, 2007, p. 2423.

27. Tang, C., Chen, V., Water Res., **38**, nr. 11, 2004, p. 2775.

28. Saquib, M., Munner, M., J. Environ. Sci. Health, Part A: Toxic/Hazard. Subst. Environ. Eng., **38**, 2003, p. 2581.

29. Zhang, Z., Xu, Y., Ma, X., Li, F., Liu, D., Chen, Z., Zhang, F., Dionysiou, D. D., J. Hazard. Mater., **209-210**, 2012, p. 271.

30. Xu, J., Ao, Y., Chen, M., Fu, D., Yuan, C., Thin Solid Films, **518**, 2010, p. 4170.

5. ARTIGO 3

Research Article

Photo-decolorization and ecotoxicological effects of solar CPC pilot plant and artificial light photocatalysis of indigo carmine dye

Enrico Mendes Saggioro[1]*, Anabela Sousa Oliveira[2,3], Daniel Forsin Buss[4], Danielly de Paiva Magalhães[4], Thelma Pavesi[1], Margarita Jimenéz[5], Manuel Ignacio Maldonado[5] Luis Filipe Vieira Ferreira[2], Josino Costa Moreira[1]

1 – CESTEH - Centro de Estudos da Saúde do Trabalhador e Ecologia Humana, Escola Nacional de Saúde Pública - Fundação Oswaldo Cruz, Av. Leopoldo Bulhões, 1480 21041-210, Rio de Janeiro, Brazil.

2 – CQFM - Centro de Química-Física Molecular and IN - Instituto de Nanociencias e Nanotecnologia, Instituto Superior Técnico, Universidade Técnica de Lisboa, Av. Rovisco Pais 1049-001, Lisboa, Portugal.

3 – C3i - Centro Interdisciplinar de Investigação e Inovação, Escola Superior de Tecnologia e Gestão, Instituto Politécnico de Portalegre, Lugar da Abadessa Apartado 148 7301901 - Portalegre, Portugal.

4 – LAPSA - Laboratório de Avaliação e Promoção da Saúde Ambiental, Instituto Oswaldo Cruz, Fundação Oswaldo Cruz. Av. Brasil 4362 21045-900, Rio de Janeiro, Brazil.

5- CIEMAT - Plataforma Solar de Almería, Ctra. De Senés, Km. 4 04200, Tabernas, Almería, Spain.

Abstract

The aim of this study was to analyze the photocatalytic degradation of indigo carmine dye under artificial and solar irradiation using TiO_2 (Titanium Dioxide) and to evaluate the ecotoxicity of the photodegradation products in organisms of two different food chain levels. To determine the efficiency of three different artificial photoreactors (Reactor 1 – batch magnetically stirred reactor with 125 watts mercury vapor lamp; Reactor 2 - batch magnetically stirred reactor with 4 lamps daylight 20 watts; Reactor 3 - glass tubular continuous-flow reactor, illuminated inside by one daylight 20W lamp), the ideal amount of TiO_2 and the necessary time period of UV-light irradiation was evaluated. Same parameters were evaluated for batch solar experiments. The optimized experiments were performed in a solar CPC pilot plant with different water matrices at Plataforma Solar de Almería. Photodegradation of the indigo dye was followed by UV-Vis spectroscopy, HPLC-DAD, TOC and ion chromatography. Among tested reactors the one equipped with the mercury vapour lamp was the most efficient. Solar photocatalysis was also very efficient, regardless of season (100% and 70% photodegradation efficiency for 30 minutes irradiation, during summer and winter, respectively). Solar CPC pilot plant photocatalysis was efficiency for different water matrices but the photodegradation was found to be somewhat slower to the more complex matrixes. Ecotoxicological evaluation with *Daphnia similis* and *Pseudokirchneriella subcapitata* (organisms of two different food chain levels) showed that photodegradation products were more toxic than untreated indigo carmine and that TiO_2 residues affected the two tested species and may have potentiated the toxic effects

of photoproducts. These later results show the importance of toxicity evaluation of photoproducts and stress the need of processes that warrantee the complete post-treatment removal of TiO_2.

Keywords: solar photocatalysis, indigo carmine, compound parabolic collector, *Daphnia similis*, *Pseudokirchneriella subcapitata*

5.1. Introduction

Organic dyes are one of the largest groups of wastewaters pollutants. In general they are released into the environment by textile and some other industries [1]. Dyes are used in the processing of textile industries and are lost in significant quantities during dyeing steps. Wastewaters containing 5-15% of untreated dye can be released into the environment [2]. Colored effluents are of great environmental concern because even small amounts of dye may produce strong visible effects in water, affecting oxygen and nitrogen cycles through photosynthesis and also may be toxicity for aquatic biota [2].

Around 100,000 dyes are currently in use by textile industry and 7 x 10^5 ton of dye-stuff is produced annually worldwide. Among these, indigoids are the largest class of commercial dyes used mostly for cotton cloth dying (blue jeans) [3, 4]. Indigo blue dye's main component is indigotine which is extracted from the leaves of *Indigofera tinctoria* [5]. Indigo carmine is also one of the oldest dyes and still one of the most used in textile industry [6]. The basic color-producing structure of indigoid dyes is a cross-conjugated system or H-chromophore, consisting of a single -C=C- double bond substituted by two NH donor groups and two CO acceptor groups [7].

Indigo carmine is considered as a highly toxic indigoid dye. Its contact with skin and eyes can cause permanent injury to cornea and conjunctiva and its oral intake can cause disturbs in reproductive, developmental and neuronal systems and may cause death [8]. Most toxic dyes are recalcitrant to biodegradation, causing decrease in the efficiency of biological wastewater treatment plants. Furthermore they show also low

treatment efficiency by traditional physical-chemical wastewater treatment methods such as flocculation or adsorption [2, 9].

Different types of advanced oxidative processes (AOPs) have been used as alternative treatment for wastewater containing dyes [10-18]. Fujishima and Honda [19] report on the heterogeneous photocatalytic oxidation of water in the presence of titanium dioxide (TiO_2) triggered the interest on its use for wastewater treatment. As a consequence, several studies have reported the use of titanium dioxide in photocatalytic degradation of all sort of persistent pollutants and their residues [20-25] including those from textile industries [26, 27]. The use of TiO_2 has advantages such as low cost, high photochemical reactivity and nonspecific oxidative attack ability [10, 11]. In this way it can promote the degradation of different target organic compounds and industrial effluents with little change on operational parameters [28, 29].

Although studies on the photodegradation of azo dyes are much more frequent in literature [3, 10, 12, 14, 16], several investigations have been conduced to verify the efficiency of using AOPs to promote indigo carmine's photodegradation under different experimental conditions. Vautier et al., [7] for instance, studied its degradation in aqueous heterogeneous suspensions submitted to continuous exposure to visible light; UV–visible ground state absorption, total organic carbon, HPLC/UV and CG/MS were used to follow its photocatalytic degradation and a degradation route was proposed. In a related study, Hachem et al., [30] showed that TiO_2 (Degussa P25) was efficient on the degradation of several dyes (including indigo carmine) and verified the influence of the presence of hydrogen peroxide and of the adsorption on the catalyst; studies of photodegradation kinetics were also performed. Guillard et al., [31] investigated the

degradation of chlorophenol, pesticides and indigo carmine promoted by Millennium PC500 anatase under sunlight and artificial light.

The aim of the present study is to investigate TiO_2 mediated photocatalytic degradation of indigo carmine in water (model textile effluent) using artificial irradiation and sunlight, to evaluate whether the photocatalytic treatment effectively reduced the post treatment toxicity (for that an ecotoxicological evaluation with organisms of two different food chain levels is undertaken). Different reactors geometries (batch and continuous) and artificial light sources (125 watts mercury vapor lamp and 20 watts day light lamps) were tested. Solar photocatalysis in a pilot plant equipped with a compound parabolic collector (CPC) was evaluated for different water matrices.

The ecotoxicological effects of the dye by itself were tested, that of the photodegradation products and finally that of the TiO_2 post-treatment residues remaining in treated wastewater using the Cladocera *Daphnia similis* and the algae *Pseudokirchneriella subcapitata*. It is important to ensure that after photocatalysis the toxicity of the treated water is effectively reduced [11]. Several authors report that, frequently, either resultant photoproducts or photocatalyst residues are more toxic to organisms than the parent compounds under treatment [7, 11, 32]. Brazilian legislation states that toxicity must be tested in organisms belonging to two different food chain levels, and so a productor (ie., *Pseudokirchneriella subcapitata*) and a primary consumer (ie., *Daphnia similis*) were selected for toxicological tests in the present work. The toxicity tests performed help to predict potential environmental impacts of these

treatment processes on riverine biota. Later information is vital for adequate water and wastewater management strategies.

5.2 Experimental

5.2.1 Reagents and Materials

Indigo carmine dye (3,3-dioxo-2,2-bis-indolyden-5,5-disulfonic acid disodium salt, $C_{16}H_8N_2S_2O_8Na_2$, M.W. = 466.36 g mol^{-1}) was obtained from Sigma Aldrich (85 % dye content) and used without further purification (Fig. 1). Photocatalyst used in all experiments was titanium dioxide, EVONIK P25, containing 75% anatase and 25% rutile, with a specific BET surface area of 50 m^2 g^{-1} and primary particle size of 20 nm. All dye solutions were prepared using Mili-Q water.

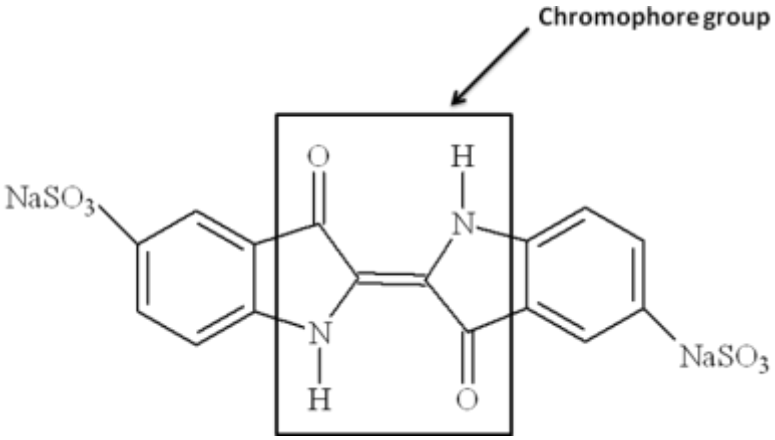

Fig. 1. Chemical structure of indigo carmine dye.

5.2.2 Photoreactors

5.2.2.1 Artificial irradiation

Three different photoreactor systems with artificial irradiation were used in this study. Reactor 1 was a batch magnetically stirred reactor, irradiated with a high-pressure 125 W mercury vapor lamp. Samples were irradiated in 100 mL beakers (Fig. 2(A)). Due to lamp geometry a single point of stirring was used, as can be seen in Fig. 2(A). Reactor 2 was also batch magnetically stirred with samples irradiated in 100 mL beakers (similarly to Reactor 1), but with irradiation being ensured by four parallel daylight 20W lamps (Fig. 2(B)); since light distribution is always identical below the lamps, multipoint stirring was used. In reactors 1 and 2 distance between UV lamp and irradiated solution is 25 cm, in order to avoid solution overheating and evaporation. Reactor 3 was a glass tubular continuous-flow reactor illuminated by one daylight 20W lamp, fitted inside the tubular reactor. Dye solution was pumped through this reactor, in between lamp and inside's reactor wall, circulating to/from a storage beaker (Fig. 2(C)). UV-irradiation time for Reactor 1 was 300 minutes; this time was set to be optimal to complete color removal from the dye solution. For Reactors 2 and 3 the irradiation time was extended up to 24h, because preliminary experiments has showed that, due to the weaker power of light source used in these two cases (four or one daylight lamps), 300 minutes of irradiation were insufficient for the complete photodegradation of the dye. Photon flux was measured, for each reactor and at each collection time, as explained at 5.2.3.3.

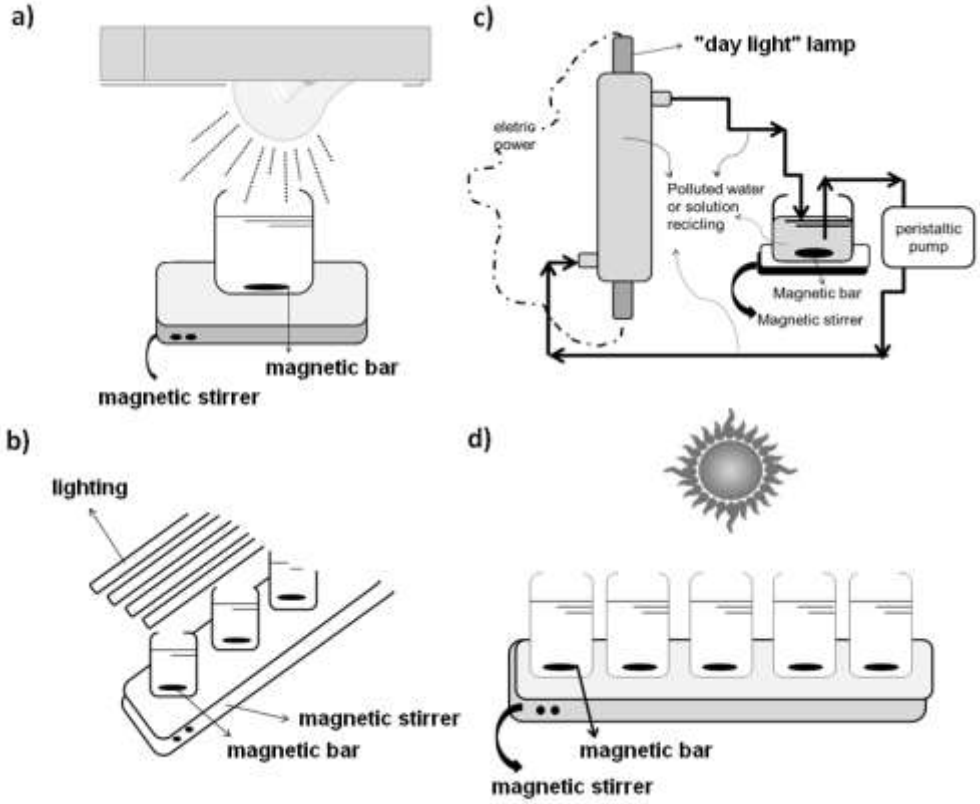

Fig. 2. Reactors used on photocatalytic degradation of indigo carmine dye in water. (A) Reactor 1 – batch magnetically stirred reactor irradiated by a high-pressure mercury vapor lamp of 125 W; (B) Reactor 2 – batch magnetically stirred reactor irradiated with four day light lamps of 20 W each; (C) Reactor 3 – tubular continuous-flow glass reactor with one day light lamp 20 W inside the tubular reactor; (D) batch static stirred reactor under solar irradiation.

5.2.2.2 Solar irradiation

Solar irradiated experiments were conducted in Rio de Janeiro, Brazil (location S22°52’37.3”; W43°15’0.9”), using the same batch magnetically stirred (multipoint) arrangement described above for Reactor 2 (Fig. 2(D)). Photodegradation experiments were conducted during summer (January/February) and winter (July/August) months. In

each of these four months, solar irradiated experiments were conducted from 10 a.m. to 3 p.m. and irradiated samples were collected at the same times used for Reactor 1. Each month, experiments were performed during two random days. During each experiment, efficient photon flux was determined every 60 minutes.

5.2.2.3 Efficient Photon Flux Determination

For each photoreactor (artificial or solar irradiation) the efficient photon flux was determined measuring the radiant flux (in mW/cm^2) at the surface of the sample being treated. In each case, the radiant flux was measured with a radiometer (Cole-Parmer Instrument Co.; model 9811-50), calibrated against a microcalorimeter, taking in account the spectral distribution of the lamp, the optical filter transmission and the absorbance spectrum of titanium dioxide (measurement at 366nm).

For Reactors 1 and 2 the radiometer's head was placed just above the solution surface. For Reactor 3 the radiant flux was measured placing the radiometer's head on the external side of the glass tubular continuous-flow reactor since for this reactor there is no way to fit the available radiometer's measurement head inside the continuous reactor. The measured radiant fluxes were 2.60, 0.032 and 0.071 mW/cm^2, respectively to Reactors 1 to 3.

During the all-time of indigo solar photodegradation experiment, solar irradiation was measured on ten random days, every 60 min from 10 a.m. to 4 p.m.. This was made every month, during all the twelve months of the year. Detailed results are present in section 3.2. These experiments enabled to observe that the photon flux

achieved with solar irradiation (in batch static stirred reactor) is of the same order of magnitude of that used with the 125 watts mercury vapor lamp, at Reactor 1.

5.2.3 Photodegradation Experiments

For Reactors 1 and 2 and solar irradiated experiments, a volume of 100 mL of indigo carmine solution (30 mg L^{-1}) was submitted to photodegradation using different concentrations of TiO_2. For Reactor 3, a volume of 200 mL of indigo carmine solution (30 mg L^{-1}) was used, circulating at a 20 mL/min flux and subjected to similar procedure. 30 mg L^{-1} is representative of indigoid dyes concentrations usually found in textile waters.

Before irradiation and after TiO_2 addition, samples were kept in the dark for 30 min, under stirring. During irradiation step, samples were continuously stirred (for batch reactor) or were kept under continuous pump driven movement (for continuous reactor). Control samples, without photocatalyst, were submitted to identical treatment. Optimal times for sample collection to accurately follow the photodegradation process were tested and optimized: aliquots of 3 ml were taken at 0, 15, 30, 45, 60, 90, 120, 180 and 300 min for Reactor 1 as well as for solar irradiated experiments. For Reactors 2 and 3, one last extra sample was collected after 24 hours of irradiation. Then, each collected sample is centrifuged for 10 min at 1000 rpm, filtered with 0.45μm membrane Milipore®. The final post treatment indigo carmine concentration, at the different irradiation times, is determined measuring its absorbance at the maximum absorption wavelength of the dye (ie, 610 nm) and comparing it with a calibration curve for indigo

carmine concentration (made with freshly prepared and non irradiated solutions of the dye; see section 2.5 for details).

Optimal amount of photocatalyst to be used was determined using Reactor 1, where solutions of indigo carmine in water (100 ml) containing 30 mg L^{-1} of the dye were treated with six different concentrations of TiO_2 (respectively, $1x10^{-3}$, $2.5x10^{-3}$, $5x10^{-3}$, $1x10^{-2}$, $1x10^{-1}$ and 1g L^{-1}), plus control sample without photocatalyst. All samples were equally submitted to complete treatment process. All experiments were repeated twice, so each result is the average of two experiments.

Adsorption efficiency of the dye by TiO_2 was determined before exposure to artificial or solar light. The dye removal is expressed as $(Co - C)/Co$, where *Co* is the initial dye concentration and *C* is dye concentration determined after treatment /irradiation time *t*, both given in mg L^{-1}. Photocatalytical kinetics was analyzed using the Langmuir-Hinshelwood model [33].

5.2.4 Photocatalytic experiments in a CPC solar pilot plant

Solar CPC photocatalytic experiments (30 mgL^{-1} of IC; 0.1 gL^{-1} of TiO_2) were carried out in a 32-L pilot plant (22 L illuminated volume, 3.08 m^2 total irradiated surface) installed at the Plataforma Solar de Almería (PSA, latitude 37ºN, longitude 2.4ºW). A schematic of the plant can be seen in a previous publication [34]. It consists of two compound parabolic collectors (CPCs), a continuously stirred tank, a centrifugal recirculation pump (20 L min^{-1}) and connecting tubing and valves. Each collector

consists of borosilicate glass tubes connected in series (inner diameter 30.0 mm, outer diameter 31.8 mm, length 1.41 m, 12 tubes) and mounted on a fixed platform tilted 37◦ (local latitude). At the beginning of the experiments, while collectors were kept covered, the chemicals were added to the tank and mixed by recirculating the water throughout the system until constant concentration was reached. Then the covers were removed from the collectors and samples were collected at predetermined times. The temperature inside the reactor was continuously recorded by Pt-100 temperature probe. A global UV radiometer (KIPP&ZONEN, model CUV 3, the Netherlands) also tilted 37º was used for measuring global solar UV radiation intensity (UV_G) in terms of incident Wuv/m^2. Once UV_G is known, the total UV energy received on a surface in the same position with regard to the sun per unit of volume of water inside the reactor during the interval Δt can be determined by applying Eq. (1). [35]:

$$Q_{UV,n} = Q_{UV,n-1} + \Delta t_n UV_{G,n} \frac{A_i}{V_T} \quad ; \quad \Delta t_n = t_n - t_{n-1} \tag{1}$$

Where t_n is the time corresponding to n water sample, V_T total reactor volume (32 L), A_i illuminated surface area (3.08 m^2) and $UV_{G;n}$ average solar ultraviolet radiation measured during the period Δ_{tn}.

The experiments in solar CPC pilot plant were spiked in different types of water: distilled water, synthetic moderately hard fresh water [36], synthetic secondary municipal wastewater treatment plant (MWWTP) effluent [37] and secondary effluent

from the MWWTP "El Bobar" (Almería, Spain). Table 1 shows some physical and chemical characteristics of the different types of water used in this work.

Table 1. Physical and chemical characteristics of the different types of water.

Type of water	Total Carbon (mgL^{-1})	Inor. Carbon (mgL^{-1})	TOC (mgL^{-1})	pH	Conduc. ($\mu s\ cm^{-1}$)	Ionic species (mM)							
						Na^{+}	Ca^{+2}	Mg^{+2}	K^{+}	NH^{+4}	PO_4^{-3}	Cl^{-}	SO_4^{-2}
Fresh water moderately hard	17.24	13.89	3.40	7.5	208	0.8	0.35	0.41	0.08	—	—	0.06	1.05
Synthetic MWWTP secondary effluent	22.74	9.98	17.76	7.7	301	1.3	0.37	0.45	0.13	0.11	0.02	0.06	1.4
Real MWWTP secondary effluent	75.86	44.74	31.1	7.4	1156	7.8	1.5	0.7	0.64	1.38	0.07	11.3	1.85

5.2.5 Ecotoxicity tests

Photocatalytical degradation may generate toxic photoproducts and so they must be assessed in order to determine if the effluent treatment strategy is leading or not to the desired result. Acting like that, one may prevent the contamination of receptor water bodies with toxic substances generated by decontamination treatment itself. In this work, the ecotoxicity of the indigo carmine - TiO_2 mixture and that of the photoproducts of its photocatalytic remediation treatment was tested in organisms of two trophic levels: a producer organism, the algae *Pseudokirchneriella subcapitata*, Chlorophycea and a primary consumer, the *Daphnia similis*, Cladocera. These species were chosen because they have standardized regulations and they are already commonly used for studies on toxicity of photoproducts of dye remediation [38, 39].

For both organisms, ecotoxicity tests were performed comparing the effects of solutions containing 30 mg L^{-1} of indigo carmine prior (*sample A*) and after (*sample B*) photocatalytic treatment with 0.1 g L^{-1} of TiO_2.

Since, after photocatalysis, pH was acid (around 4.0), pH was adjusted to 7 using NaOH 1M and the sample ecotoxicity tested once again (*sample C*) to measure the effect of photoproducts in the biota, without interference of low pH.

Experiments were carried out also using negative control solutions, ie, solutions with the dye and TiO_2, then filtered to remove the photocatalyst (time 0, kept in the dark, no degradation) (*sample D*).

Furthermore, a TiO_2 solution diluted in Mili-Q water was prepared and filtered next to remove titanium dioxide (*sample E*) was also tested to verify possible toxic effects of residues of the TiO_2.

For *Daphnia similis* further tests were performed for samples using 30 mg L^{-1} of the dye diluted in maintenance mineral water, instead of Mili-Q water (*sample F*) and TiO_2 diluted in maintenance mineral water followed by filtration (time 0, in the dark, no degradation) (*sample G*).

5.2.5.1. Chronic toxicity tests using Pseudokirchneriella subcapitata

Procedures for culture and tests using *Pseudokirchneriella subcapitata* were performed according the Brazilian regulations NBR 12648 (2005) [40]. Algae were cultivated in MBL medium and test solutions were prepared with 90% of the sample and 10% of the MBL medium with 200 µL of algal suspension [38]. Three replicates

were used for each sample (samples A, B, C, D and E). Replicates were stirred (100-175 rpm) under continuous light for 72h. Then, the *Potential Inhibition of Growth* (IG) was calculated using Eq. (2):

$$IG = [(C_c - C_t)/C_c] \times 100 \quad (2)$$

Where C_c is the average number of cells per milliliter of the three control replicates and C_f is the average number of cells per milliliter of the three exposition replicates (both counted on the microscope in a newbauer camera); equation is applied for each concentration to calculate the potential of inhibition or the potential of growth.

In chronic tests, toxicity was considered when *Potential Inhibition of Growth* of groups subjected to treatment were >20% than control groups. The increased growth (>20%) was considered a trophic effect.

5.2.5.2 Acute toxicity tests using Daphnia similis

Procedures for culture and tests using *Daphnia similis* followed Brazilian regulations NBR 12713 (2004) [41]. Static toxicity tests were performed using twenty daphnids for each concentration kept in the dark, at 23.5ºC constant temperature and exposed for 48h to the respective samples. Controls were exposed to mineral water only. Results were expressed as percentage of immobilization of daphnids after 48h exposition. In toxicity tests with Daphnia the term “immobilization” instead “mortality” is generally used because it is not possible to perceive if the organism is dead or just

immobilized. In acute toxicity tests, toxic effects were considered when immobilization in treatment groups was >10%. For the maintenance, cultures of the *Daphnia similis* were kept in mineral water, fed with algae *Ankistrodesmus falcatus* under 23.5ºC constant temperature and 12/12h photoperiod.

5.2.6 Analytical determinations

Absorbance measurements were performed in a double beam UV-Visible spectrophotometer (Shimadzu UV-1601PC) and HPLC-DAD (Agilent Technologies, series 1100) system provide with a C-18 column (LUNA 5 mm, 3 mm x 150 mm, from Phenomenex) and using an amonium acetate 10 mM : methanol (80:20) mixture a mobile phase (flow rate: 0.8 mL min^{-1}). Absorbance detection was made at 610 nm. Total organic carbon (TOC) was measured in filtered samples (Millipore- Miliex-GN Nylon 0.2 µm filters) with a Shimadzu-5050A TOC analyser. Anion concentrations were determined with a Metrohm 872 Extension Module 1 and 2 ion chromatograph (IC) system configured for gradient analysis. Cation concentrations were determined with a Metrohm 850 Professional IC configured for isocratic analysis.

5.3 Results and Discussion

5.3.1. Degradation of indigo carmine with artificial irradiation

Figure 3 compares the effect of TiO_2 amount on the photodegradation rate of 30 mg L^{-1} of indigo carmine under artificial irradiation for the 3 reactors used. In all cases, the efficiency of photocatalytical degradation of indigo carmine was directly related with the amount of photocatalyst. Optimum concentration of TiO_2 (i.e. the minimum photocatalyst concentration enabling the highest photodegradation rate, ie., if possible 100% photodegradation in the maximum time of 300 minutes) depended on the geometry of the photoreactor, that should enable all photocatalyst particles to be fully illuminated [42]. Reactor 1, equipped with a 125 W mercury vapor lamp, had the best results on photocatalytical degradation for indigo carmine. For concentrations of 1 g L^{-1} and 1 x 10^{-1} g L^{-1} of TiO_2, photocatalysis had efficiencies of 96 and 92% in 30 minutes of irradiation, respectively. Furthermore, for $5x10^{-3}$ and $2.5x10^{-3}$ g L^{-1} photocatalysis had efficiencies of 87 and 55% in 180 minutes of irradiation (Fig. 3(A)). Reactor 2 and Reactor 3 also reached percentages of degradation close to 100% for 1 g L^{-1} and 1 x 10^{-1} g L^{-1} of TiO_2, although in these two cases 1440 minutes of irradiation were necessary. Obviously the stronger irradiation power delivered by the 125 W mercury vapor lamp determined the higher efficiency observed to Reactor 1 (2.60 $mWcm^{-2}$). When comparing Reactor 2 and 3, that used both 20W day light lamps, the highest photodegradation efficiencies were also related with the higher irradiation power. For the geometries used at Reactor 2 and 3, the highest irradiation power was not delivered

by the four day light lamps of Reactor 2 (0.031 $mWcm^{-2}$) but to the single lamp of Reactor 3 (0.071 $mWcm^{-2}$), due to its proximity to the solution to be treated.

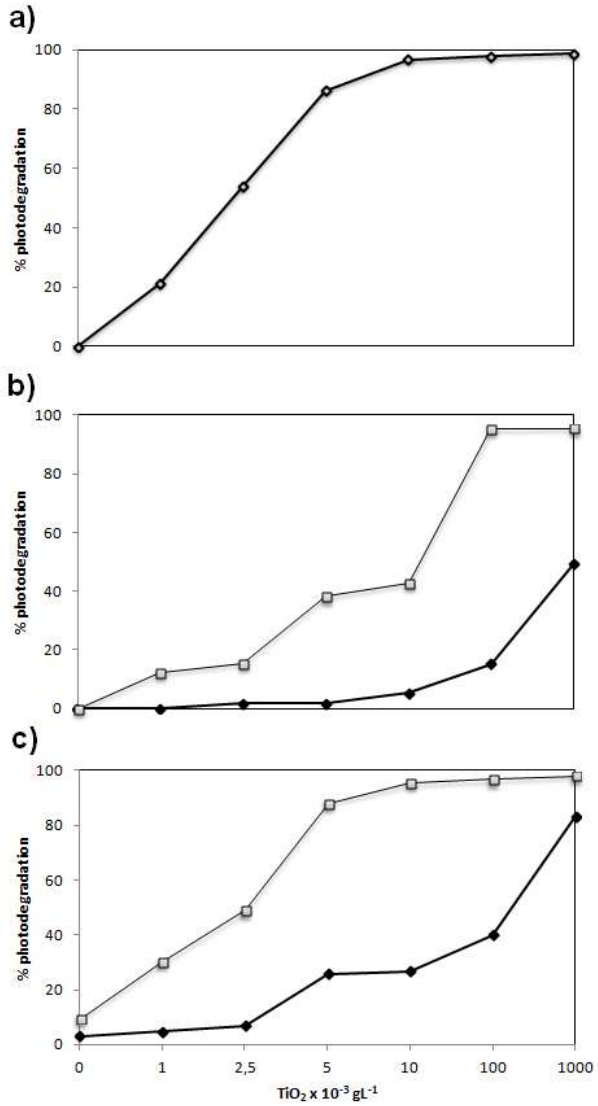

Fig. 3. Effect of TiO_2 amount on the rate of degradation of 30 mg L^{-1} of indigo carmine dye. (A) 180 min of irradiation using Reactor 1 with a 125W mercury vapor lamp and 2.60 $mWcm^{-2}$ of irradiation power; (B) 180 min (—◆—) and 1,440 min (—□—) of irradiation using Reactor 2 with four 20W day light lamps and 0.031 $mWcm^{-2}$ of irradiation power; (C) 180 min (—◆—) and 1,440 min (—□—) of irradiation using Reactor 3 with one 20 W day light lamp and 0.071 $mWcm^{-2}$ of irradiation power.

Figure 4 compares the effect of UV-Irradiation time on the degradation of 30 mg L^{-1} of indigo carmine dye with $1x10^{-1}$ g L^{-1} of TiO_2 under sunlight irradiation (in the summer and winter) and artificial irradiation on the three above mentioned reactors.

As can be seen from Figure 4, results for Reactor 1 were very similar to the ones obtained under sunlight irradiation during summer, because the photon flux used in both processes was similar (see photon fluxes for solar irradiation on Table 2; same data for artificial irradiation is indicated above in the text and in the legend of Figure 3). This result confirms that it is possible to replace the use of an artificial light source by natural solar light irradiation, without losing efficiency. Furthermore reasonably good efficiencies can be attained with solar irradiation also during winter months.

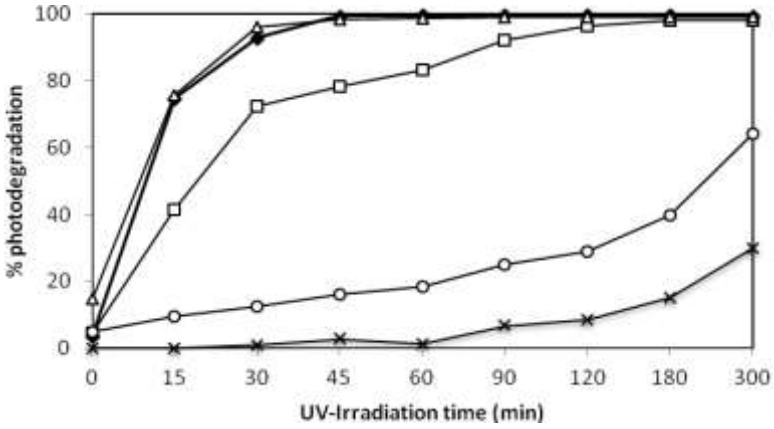

Fig. 4. Effect of UV-Irradiation time on the degradation of 30 mg L^{-1} of indigo carmine dye under sunlight in the summer (—●—) and winter (—□—) and artificial irradiation on Reactor 1 (—△—) with a 125W mercury vapor lamp and 2.60 $mWcm^{-2}$ of irradiation power, Reactor 2 (—×—) with four 20W day light lamps and 0.031 $mWcm^{-2}$ of irradiation power and Reactor 3 (—○—) with one 20 W day light lamp and 0.071 $mWcm^{-2}$ of irradiation power. All experiments performed with $1x10^{-1}$ g L^{-1} of TiO_2.

Comparing the efficiency of the reactors using artificial light, the rate of degradation was Reactor 1> Reactor 3> Reactor 2. The efficiency of indigo degradation, expressed in percentage (%), observed to Reactor 2 (using four day light 20 W lamps) were, respectively, 62, 30, 8, 6, and 2% for 1, $1x10^{-1}$, $1x10^{-2}$, $5x10^{-3}$ and $2.5x10^{-3}$ g L^{-1} of TiO_2 for an irradiation time of 300 minutes. For Reactor 3, the tubular continuous-flow with full length internal illumination of a 20 W day light lamp, these values varied from 91, 64, 40, 39 and 15%, respectively, for the same TiO_2 amounts. These results were expected since Reactor 3 allows recirculation of the dye solution containing suspended TiO_2, keeping this suspension in frequent and close contact with light. This may increase the electron/hole pair generation, thus increasing the chance of formation of hydroxyl radicals on the surface of the catalyst [43]. Moreover photon flux is higher for the later reactor.

It was possible to achieve higher degradation rates for reactors 2 and 3 increasing the UV irradiation time up to 24h (see results on Fig. 3(B) and 3(C)). The minimum concentration of TiO_2 needed to achieve 95% of photocatalytical degradation in reactors 2 and 3 was $1x10^{-1}$ and $1x10^{-2}$ g L^{-1}, respectively. Therefore, for each system to be remediated using different reactors geometries and light intensities, the optimum amount of TiO_2 must be determined beforehand to avoid excessive use of catalyst.

5.3.2 Degradation of indigo carmine under sunlight using TiO_2

Indigo carmine photodegradation under sunlight irradiation in presence and in absence of TiO_2 was investigated (Table 2). Indigo carmine is highly stable under sunlight: little or no photolysis of this dye was observed.

In summer and in the presence of TiO_2, the photocatalytical degradation after 300 minutes of irradiation reached around 99% for most TiO_2 concentrations used. For instance, $1x10^{-1}$ and 1 g L^{-1} of TiO_2 degraded 92 and 99% of the dye in 30 minutes.

Table 2. Percentage degradation of indigo carmine dye during summer and winter seasons and using different concentrations of TiO_2 (initial concentration of dye: 30 mg L^{-1}; time of irradiation: 120 min).

Concentration of TiO_2	Summer				Winter			
	January		February		July		August	
Accumulated Energy (Q_{uv}, k JL^{-1})	day 1 (18.46)	day 2 (26.59)	day 1 (15.48)	day 2 (15.37)	day 1 (16.93)	day 2 (3.37)	day 1 (13.55)	day 2 (16.82)
Control	0	9.27	3.66	2.32	1.94	0	1.81	0.90
$1x10^{-3}$ gL^{-1}	45.86	61.54	45.44	26.04	42.67	22.83	20.90	42.79
$2.5x10^{-3}$ gL^{-1}	89	91.07	83.57	64.28	72.92	31.30	66.56	86.72
$5x10^{-3}$ gL^{-1}	97.51	98.92	95.70	93.67	95.95	57.57	59.60	89.84
$1x10^{-2}$ gL^{-1}	99.52	99.30	95.93	96.97	96.55	81.66	95.88	92.29
$1x10^{-1}$ gL^{-1}	99.60	99.46	99.77	99.13	97.24	96.56	97.59	97.83
1 gL^{-1}	99.67	99.61	99.17	99.45	97.32	97.56	97.97	98.01

In winter, even with lower sunlight intensity, photodegradation was also significant: for all TiO_2 concentrations tested, except $1x10^{-3}$ and $2.5x10^{-3}$ g L^{-1}, photocatalytical degradation was always between 90 and 100% after 300 minutes of irradiation. For $1x10^{-1}$ and 1 g L^{-1} of TiO_2, degradation in 30 min reached 91 and 97%, respectively. As the system efficiency depends of the amount of added TiO_2 and also of the UV irradiation time, it is important to determine the lowest concentration of TiO_2 that can be used that still keeps treatment efficient [44]. Song et al., [45] reported 100% degradation of the azo dye Direct Blue 78 under sunlight after 16h. Augugliaro et al., [46] also studying degradation of azo dyes using sunlight observed complete decolorization in few hours. In our study, either in summer or winter and irrespective lower winter photon fluxes, good rates of TiO_2 photodegradation were always achieved. This can be concluded from the analysis of the solar photodegradation data presented in Table 2 and of the average solar ligth intensity measured for each month presented in Figure 5. These results indicate the feasibility of using solar photocatalysis with TiO_2 to remediate indigo carmine effluents from textile industry, especially in countries with abundant sunlight throughout the year. In addition, the capacity of titanium dioxide to be activated by sunlight is compatible with green chemistry key principles [47].

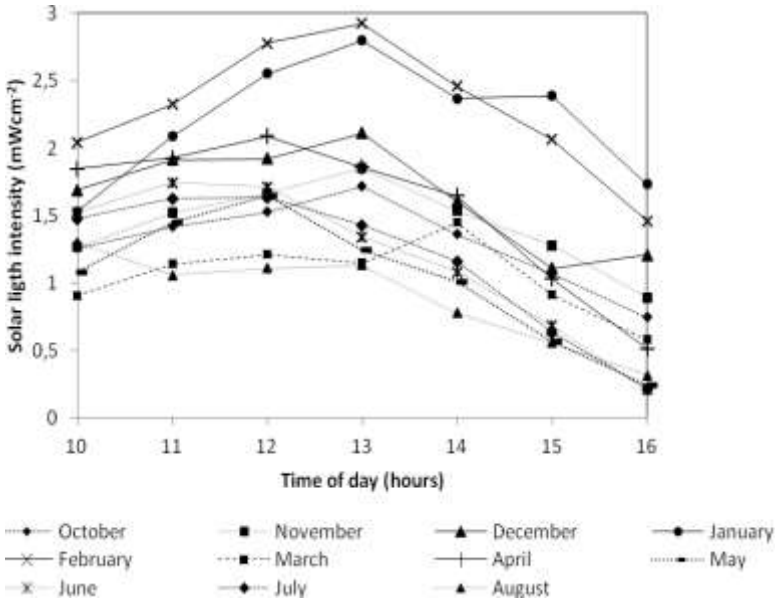

Fig. 5. Average solar ligth intensity in location S22°52'37.3" W43°15'0.9" measured hourly in random days for each month from 10 a.m to 4 p.m.

5.3.3 Effect of irradiation time on the degradation of indigo carmine

Photocatalytic degradation rates observed in Reactor 1, using both mercury vapor lamp or sunlight irradiation in the summer reached 80% in 15 minutes and 100% at 30 minutes of irradiation). In the winter, photocatalytical degradation rates decreased to 40% in 15 minutes and to 70% after 30 minutes. It is important to notice that in cloudy days, 300 minutes of solar irradiation were necessary to photodegrade 100% of the dye. Reactors 2 and 3 equipped with daylight lamps showed a poorer photodegradation percentage when compared with Reactor 1. An efficiency of 60% photodegradation in 300 minutes was observed for Reactor 3 and 30% for Reactor 2. The higher efficiency of Reactor 3 compared to Reactor 2 was due to the closer distance

between solution and irradiation source, which allowed higher photon flux efficiency (0.071mW/cm^2 at the exterior of the glass wall for Reactor 3 against only 0.031mW/cm^2 for Reactor 2). Decolorization and photodegradation increases with increasing irradiation time and/or photon flux efficiency. Thus, due to the lower photon flux efficiencies of reactors 2 and 3, the time of irradiation had to be extended up to 24 hours, in order to have 95% of the dye solutions degraded.

Solar irradiation varies with the season and other environmental conditions. Thus, this information must be taken into account to calculate the concentration of titanium dioxide to be used in order to maintain the systems with high efficiency. For the photocatalytic degradation in summer days, it was observed that the concentration of $1x10^{-3}$ g L^{-1} of TiO_2 is able to degraded 98% of indigo carmine by the end of 300 minutes. Similar results were observed when using the Reactor 1 with the 125 W mercury vapor lamp. Comparison is possible because photon fluxes are of the same order of magnitude for both Reactor 1 and sunlight irradiation during summertime (photon fluxes of 2.60 mWcm^{-2} for Reactor 1 and between 1.464 and 2.834 mWcm^{-2} for summertime sunlight irradiation, respectively; for values of photon fluxes under solar irradiation refer to Figure 5 and Table 2). For degradation in winter days, to obtain the same efficiency, the minimum concentration of TiO_2 to be used was $1x10^{-2}$ g L^{-1} in order to degrade 100% of the dye in 300 minutes.

Figure 6 show the effect of time of UV-light irradiation on the photocatalytical degradation of indigo carmine dye with artificial light and $1x10^{-2}$g L^{-1} of TiO_2, at different irradiation times (similar results were obtained for solar irradiation in same conditions; data not shown). The absorption spectrum of the dye was characterized by a

band in visible region with its maximum at 610 nm. The absorbance of the dye at 610 nm decreased gradually with prolonged light exposure due to the increase of decolorization and light induced degradation. The decrease in color of indigo carmine solutions is associated with the cleavage of the carbon to carbon double bonds (-C=C-), characteristic of indigoid dyes molecule's [48]. Before irradiation, indigo carmine dye exhibits peaks at 610, 286 and 250 nm. Absorption in the UV region can be assigned to the aromatic rings [49]. Fig. 6 showed the fast decolorization for 610 nm and also the changes of the spectra in the UV region. These changes can indicate that a series of intermediates may have been formed. After remediation for 90 min, very low absorption was observed all over the analyzed spectral region (ie., ultra-violet bands disappeared also). This means that most intermediates formed have already been oxidized to lower molecular weight organic compounds and carbon dioxide [47], as proved by total organic carbon (TOC) analysis (see Figure 8).

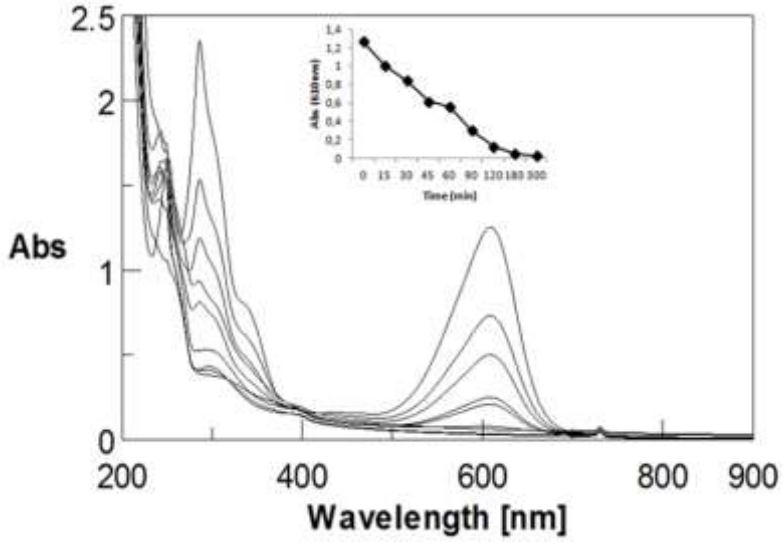

Fig. 6. Time dependent UV visible spectrum of indigo carmine. Initial concentration of indigo carmine: 30 mg L^{-1}; dosage of TiO_2: $1x10^{-2}$ g L^{-1}. Spectra from top to bottom correspond to irradiation times of 0, 15, 30, 45, 60, 90, 120, 180, 300 min, respectively. Experiments performed with Reactor 1.

5.3.4 Solar photocatalytic degradation a CPC pilot plant

The indigo carmine dye of 30 mgL^{-1} was degraded by photocatalysis in a CPC pilot plant with 0.1 gL^{-1} of TiO_2 suspensions in different matrices of water. The evolution of the remaining normalized concentration of dye is shown in Figure 7. The photolysis of the dye was negligible in CPC reactor like for the experiments in batch reactors. On the other hand, in distilled water its degradation was observed to be complete for an accumulated UV energy of 15 kJL^{-1}, correspondingly ~ 12 min of irradiation time. However, for complex matrices of water like freshwater and simulated MWWTP secondary effluent, the degradation was slower. The required accumulated energy for complete photodegradation for both waters was ~ 25 kJL^{-1}. When the

photocatalytic degradation proceeded in real MWWTP secondary effluent it was necessary even more accumulated energy, around 33 kJL^{-1}, for the complete photodegradation of the IC dye. As the matrix became more complex, the degradation rate of the dye was slower because of the presence of compounds in the matrix that acted as scavengers of the reactive species generated. As it can be seen in Table 1, in case of carbonate (inorganic carbon), which is typically found in wastewater in high concentration [50] and could have been an $HO^{\bullet}$ scavenger. The design of solar detoxification reactors is a multi-step task, which involves several technical, chemical and local considerations. Sometimes the lab-scale experiments can be helpful to evaluate geometrical parameters and/or operative conditions for large-scale propose. In our case, in order to evaluate the correspondence between the different reactors with artificial irradiation, solar irradiation in batch reactors and solar CPC pilot plant photodegradation of indigo carmine dye, the solar irradiation batch lab experiments were helpful to found the better conditions of different geometrics and light source for the photodegradation for this compound.

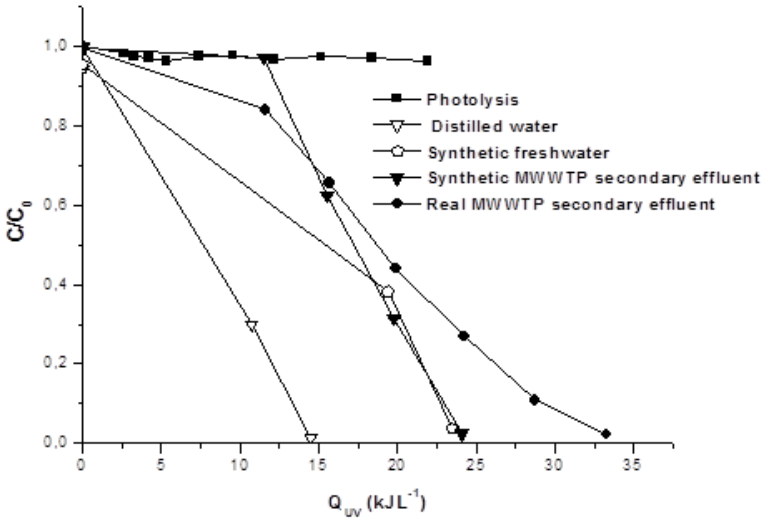

Fig. 7. Solar CPC photodegradation of 30 mgL^{-1} indigo carmine for different type of water mediated by 0.1 gL^{-1} of TiO_2 suspensions.

5.3.5 Mineralization

The total degradation organic dyes lead to the conversion of organic carbon into gaseous CO_2, whereas nitrogen and sulfur heteroatoms are converted into inorganic ions, such as nitrate or ammonium, and sulfate ions, respectively. The mineralization of indigo carmine dye was studied by TOC, SO_4^{-2}, NH_4^+ and NO_3^- evolution, and formation of carboxylic acids. The evaluation of TOC analysis in different water matrices can be seen in Figure 8. The mineralization of the dye in distilled water was completely for UV accumulated energy 90 kJL^{-1}. However, for other water matrices to the mineralization was not completed but considering the theoretic TOC of the dye (12 mgL^{-1}) and initial TOC of the matrices (see Table 1) the indigo carmine was totally mineralized. The ions and carboxylic acids concentrations formed during solar CPC

photodegradation of indigo carmine in synthetic MWWTP secondary effluent can be seen in Figure 9. For all matrices the ions and carboxylic acids were evaluated but only for synthetic MWWTP secondary effluent was possible to effectively monitor ions and identify the carboxylic acids, them this matrix was chosen. The quantity of sulfate ions is lower than that expected from stoichiometry, which can be explained by adsorption of SO_4^{-2} at the surface of titania [51]. The ammonium ions formed are slowly oxidized into nitrate ions, corresponding to the stable maximum oxidation state of nitrogen. The formic and oxalic acids remain for UV accumulated energy of 80 kJL^{-1}, with this being probably the cause of the observed results from ecotoxicity tests for *Daphnia similis* as further discuss in section 5.3.6.

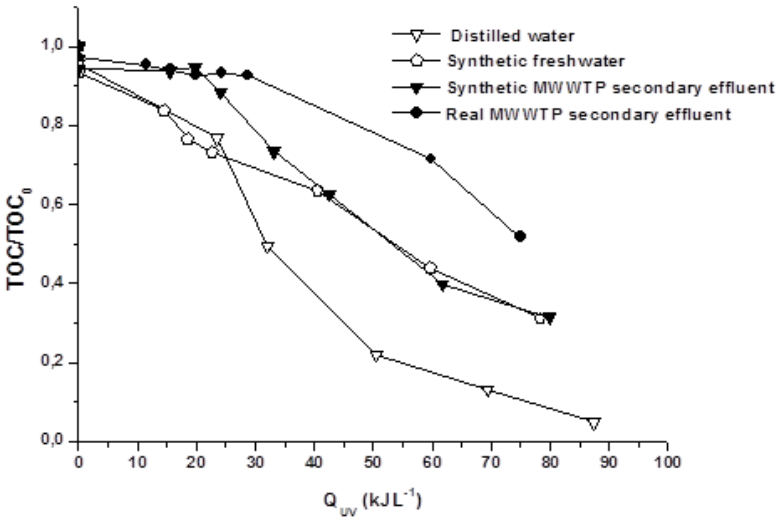

Fig. 8. Evolution of TOC concentrations of solar CPC photodegradation of 30 mgL^{-1} indigo carmine for different type of water mediated by 0.1 gL^{-1} of TiO_2 suspensions.

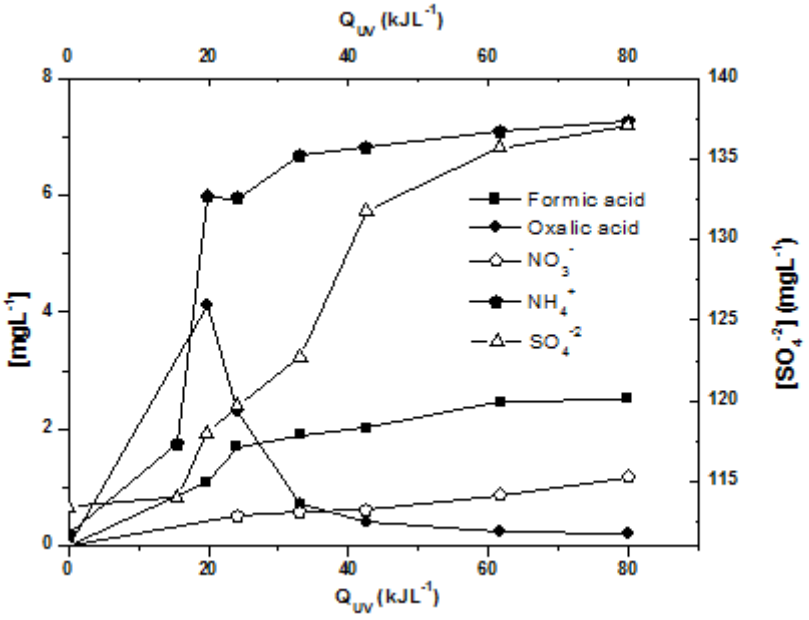

Fig. 9. Ions and carboxylic acids concentrations formed during solar CPC photodegradation of 30 mgL^{-1} indigo carmine with 0.1 gL^{-1} of TiO_2 P25 suspensions in synthetic MWWTP secondary effluent.

5.3.6 Ecotoxicity tests

The chronic and acute ecotoxicological effects of indigo carmine dye, of TiO_2 residues after TiO_2 removal, and that of photoproducts generated from degradation by the most efficient treatment system (100 mL of indigo carmine solution containing 30 mg L^{-1} with 0.1 g L^{-1} TiO_2 irradiated on Reactor 1 for 300 minutes), were studied for *Pseudokirchneriella subcapitata* and *Daphnia similis*, respectively.

The chronic toxicity tests with *Pseudokirchneriella subcapitata* indicated no significant toxic effect for these algae for all tested samples, as presented in Table 3. Sample identification can be found in section 5.2.4 and Table 3. Samples B and D were within the normal variation expected in such tests (<20% variation of growth). Samples

A, C and E strongly stimulated algae growth indicating nutritional effects (trophic, not toxic, effects).

Acute toxicity tests performed with *Daphnia Similis* showed that the photoproducts generated by the performed treatment where highly toxic. In fact samples B and C exhibited both mortalities of 100%. Still for *Daphnia similis,* samples D and G had no toxic effect, while samples A, E and F had low toxicity (also in Table 3) showing that both the dye or the photocatalyst, by themselves or together have low or no toxicity.

For aquatic organisms, no previous studies on the ecotoxicity of indigo carmine or its photoproducts after TiO_2 photocatalysis were found in literature. In the present study, it was found that the presence of either the dye or its photoproducts of photocatalysis has increased the number of cells of *Pseudokirchneriella subcapitata* (see Table 3). Thus, the release of indigo carmine dye or its photoproducts into aquatic ecosystems may be expected to cause algal growth. On the other hand, acute toxicity tests with *Daphnia similis* indicated that photoproducts from indigo carmine were highly toxic. In fact, 100% of immobilization for both samples B and C (pH=4.0 and after correction to pH=7). In solutions containing only the dye, this value was of 15% (Table 3). According to Vautier et al., [7] photocatalysis of indigo carmine produces different photoproducts along the process. The main aromatic metabolites for indigo carmine were 2-nitrobenzaldehyde and anthranilic. Carboxylic acids fragments were identify like fumaric acid which by oxidation generates malic and tartaric acids. Up to now, it is unclear which photoproduct is responsible for the toxic effects on *Daphnia similis* and even if the observed toxicity could be reduced if degradation time is

increased – *e.g.* by increasing mineralization – as suggested by Rizzo et al., [52] for diclofenac potassium. Further studies are necessary to identify all photoproducts generated along the degradation process and to access their individual toxicity.

Some authors have described that in the presence of TiO_2, absorption of some toxicants by living organisms can be increased. Zhang et al., [53] showed that fish (carp) exposed to cadmium in water (97 μg L^{-1}) with 10 mg L^{-1} photocatalytical nano-TiO_2 accumulated more Cd than fish exposed to Cd only. After 25 days of exposure, Cd concentration in the fish was 9.07 μg g^{-1} in the Cd-only group and 22.3 μg g^{-1} in the Cd with nano-TiO_2 group, a 146% increase in Cd bioconcentration in the presence of nano-TiO_2, affecting particularly internal organs rather than gills, muscle, skin and scales [54].

Considering the potential of nano-TiO_2 in facilitating transport of some toxicants into the organism it is of paramount importance to ensure its complete removal after releasing treated effluents into the environment.

Although it was possible to detect residuals of TiO_2 after filtration, *Pseudokirchneriella subcapitata* showed a trophic effect (227% growth; Table 3) when exposed to sample E. Several studies reported that nano-TiO_2 formed aggregates or agglomerates in water, and that these aggregates/agglomerates could not be separated into primary particles by ultrasound or chemical dispersants [55, 56]. It was reported that membrane filtration with a pore size of 0.45 μm, performed after sedimentation, removed nano-TiO_2 aggregates larger than 500 nm, leaving 1-8% of the initial TiO_2 in the treated water [57]. Taking this literature result in account it is likely that filtration removed only a part of TiO_2. Unfiltered nano-TiO_2 suspension with

aggregates/agglomerates has been reported to be less toxic than a filtered nano-TiO_2 suspension that mostly contained primary particles. Lovern and Klaper [58] reported that unfiltered nano-TiO_2 samples (with clumps ranging from 100 to 500 nm in diameter) produced immobilization in *Daphnia* never exceeding 11% at up to a concentration of 500 mg L^{-1}, but filtered nano-TiO_2 samples (average particle size of 30 nm after going through a 0.22 µm Nylaflo filter) produced a 48h-LC_{50} (media lethal concentration) of 5.5 mg L^{-1}.

Also, toxicological effects of TiO_2 alone are well studied, further stressing the importance of preventing its contamination in aquatic ecosystems. Algae *Scenedesmus* sp. and *Chlorella* sp. tolerated up to 0.8 and 1.2 mg L^{-1} of nano-titania and 1.4 and 1.6 mg L^{-1} of micron-titania, respectively [59], and a IC_{25} (inhibition concentration) value of 1–2 mg L^{-1} was registered for *Pseudokirchneriella subcapitata* [60]. Previous studies indicated a 48h-EC_{50} (effect concentration) >100 mg L^{-1} for cladocerans [60, 61] and *Ceriodaphnia dubia* and *Daphnia pulex* had LC_{50} 7.6 and 9.2 mg L^{-1}, respectively [60].

In sample D (dye + TiO_2 filtered, without photocatalysis), it is likely that filtration for removal of TiO_2 may have removed part of the dye which was adsorbed to it, reducing the effects of dye exposition for both *Pseudokirchneriella subcapitata* (in comparison to sample A dye + Mili-Q water; 164% growth) and *Daphnia similis* (in comparison to sample F; dye + Mineral water; 15% mortality). Similar results were obtained by Gharbani et al., [62] where nano-TiO_2 was an effective adsorbent for the removal of chloroform from aqueous solution. In that case, adsorption was highly dependent on adsorbent dose, contact time, pH and initial contaminant concentrations, and whist the percentage adsorption increased with increasing stirring time, the removal

started after the first minutes of contact. Many other studies reported the adsorption potential of nanoparticles of TiO_2 due to its high surface [63, 64].

Table 3. Number of *Pseudokirchneriella subcapitata* cells per ml after 72h exposition, observed response in relation to control samples, percent immobilization of *Daphnia similis* after 48h exposition, pH and dissolved oxygen (DO mg L^{-1}) measured at the end of the acute toxicity tests. See text for detailed description of samples and reasoning.

Samples	*P. subcapitata* chronic test		*D. similis* acute test		
	Mean ± SD (#cells ml^{-1})	Observed Response	%mortality	pH	DO
Control	119±5	--	0	7.84	5.6
(A) Indigo carmine dye + Mili-Q water	315±99	164% growth	20	7.10	5.5
(B) By-products of photocatalysis (pH 4)	113±20	5% inhibition	100	4.29	5.7
(C) By-products of photocatalysis (pH 7)	395±48	231% growth	100	7.03	5.0
(D) Indigo carmine dye + TiO_2 (filtered, in dark, time 0)	135±15	13% growth	0	7.18	4.4
(E) TiO_2 + Mili-Q water	389±37	227% growth	20	7.22	5.4
(F) Indigo carmine dye + Mineral water	--	--	15	7.96	5.4
(G) TiO_2 + Mineral water	--	--	0	7.92	5.6

5.4 Conclusions

Photodegradation of indigo carmine by TiO_2 was successful to remove colour from water. Among the tested reactors, the one equipped with a 125 W mercury vapour lamp (Reactor 1) was the most efficient. Solar photocatalysis was also very efficient regardless of season (summer or winter). Solar CPC pilot plant photocatalysis is thus an attractive alternative, because the degradation of the dye was very fast and simulated the real situations of environmental remediation, consequently reducing the duration and costs of the treatment. Evaluation of the degradation at different water matrices is necessary due to the presence of different ions that acted as scavengers of the reactive

species generated and consequently slow down the efficiency of the photodegradation process.

Ecotoxicological evaluation with *Pseudokirchneriella subcapitata* and *Daphnia similis* showed that photoproducts of photodegradation while promoted algae growth revealed to be more toxic than untreated indigo carmine for *Daphnias*, leading their mortality to 100%. Also, it was found that TiO_2 residues, after traditional filtration processes, affected the tested species and may have potentiated the toxic effects of the photoproducts. These results show the importance of photoproducts toxicity evaluation and the need of a complete removal process for TiO_2.

Acknowledgements

The authors gratefully acknowledge Fundação para a Ciência e Tecnologia (FCT, Portugal) for project ERA-MNT/0003/2009 and ERA-MNT/0004/2009. E.M. Saggioro thanks Faperj and ENSP/FIOCRUZ for scholarship and Ciencia sem Fronteiras program for grant for visiting Plataforma Solar de Almería, Spain. J.C. Moreira thanks Faperj and CNPq. D.F. Buss, D.P. Magalhães and L.G.C. Vidal acknowledges CNPq for research grant (Edital CNPq/PROEP 400107/2011-2).

5.5 References

[1] N. Barka, A. Assabbane, A. Nounah, Y. Aîlchou, Photocatalytical degradation of índigo carmine in aqueous solution by TiO_2-coated non-woven fibres, *J. Hazard. Mater.* 2008, *152 (3)*, 1054-1059.

[2] Z. Zainal, L. K. Hui, M. Z. Hussein, Y. H. Taufiq-Yap, A. H. Abdullah, I. Ramli, Removal of dyes using immobilized titanium dioxide illuminated by fluorescent lamps, *J. Hazard. Mater.* 2005, *125 (1-3)*, 113-120.

[3] M. A. Behnajaday, N. Modirhahla, N. Daneshvar, M. Rabban, Photocatalytical degradation of an azo dye in a tubular continuous-flow photoreactor with immobilized TiO_2 on glass plates, *Chem. Eng. J.* 2007, *127 (1-3)*, 167-176.

[4] T. Robinson, G. McMullan, R. Marchant, P. Nigam, Remediation of dyes in textile effluent: a critical review on current treatment technologies with a proposed alternative, *Bioresour. Technol.* 2001, *77 (3)*, 247-255.

[5] A. Andreotti, L. Bonaduce, M. P. Colombini, E. Ribechini, Characterisation of natural indigo and shellfish purple by mass spectrometric techniques, *Rapid Commun. Mass Spectrom.* 2004, *18 (11)*, 1213-1220.

[6] A. S. Oliveira, E. M. Saggioro, N. R. Barbosa, A. Mazzei, L. F. V. Ferreira, J. C. Moreira, Surface Photocatalysis: A Study of the Thickness of TiO_2 Layers on the Photocatalytical Decomposition of Soluble Indigo Blue Dye, *Rev. Chim.* 2011, *62 (4)*, 462-468.

[7] M. Vautier, C. Guillard, J. Herrmann, Photocatalytical Degradation of Dyes in Water: Case Study of Indigo Carmine, *J. Catal.* 2001, *201 (1)*, 46-59.

[8] C. L. Jenkins, Textile dyes are potential hazards, *Arch. Environ. Health* 1978, *40 (5)*, 7-12.

[9] M. A. Sanromán, M. Pazos, M. T. Ricart, C. Cameselle, Electrochemical decolourisation of structurally different dyes, *Chemosphere* 2004, *57 (3)*, 233-239.

[10] M. R. Hoffman, S. T. Martin, W. Choi, D. W. Bahnemenn, Photocatalytical degradation of Reactive Black 5: A comparison between TiO_2-Tytanpol A11 and TiO_2-Degussa P25 photocatalysts, *Chem. Rev.* 1995, *95 (49)*, 69-96.

[11] A. S Oliveira, E. M Saggioro, T. Pavesi, J. C Moreira, L. F. Vieira Ferreira, *in Solar Photochemistry for Environmental Remediation - Advanced Oxidation Processes for Industrial Wastewater Treatment* (Eds.: S. Saha), InTech, 2012, ch. 9, p. 195-222.

[12] S. K. Sharma, H. Bhunia, P. K. Bajpai, Photocatalytical Decolorization Kinetics and Mineralization of Reactive Black 5 Aqueous Solution by UV/TiO_2 Nanoparticles, *Clean – Soil Air Water* 2012, *40 (11)*, 1290-1296.

[13] N. Sridewi, L. T. Tan, K. Sudesh, Solar Photocatalytical Decolorization of Industrial Batik Dye Wastewater Using P(3HB)-TiO_2 Nanocomposite Films, *Clean – Soil Air Water* 2011, *39 (3)*, 265-273.

[14] Z. Eren, Degradation of an Azo Dye with Homogeneous and Heteregeneous Catalysts by Sonophotolysis, *Clean – Soil Air Water* 2012, *40 (11)*, 1284-1289.

[15] N. Modirshahla, M. A. Behnajady, R. Rahbarfam, A. Hassani, Effects of Operational Parameters on Decolorization of C. I. Acid Red 88 by UV/H_2O_2 Process: Evaluation of Electrical Energy Consumption, *Clean – Soil Air Water* 2012, *40 (3)*, 298-302.

[16] A. O. Yildirim, S. Gul, O. Eren, E. Kusvuran, A Comparative Study of Ozonation, Homogeneous Catalytic Ozonation and Photocatalytical Ozonation for CI Reactive Red 194 Azo Dye Degradation, *Clean – Soil Air Water* 2011, *39 (8)*, 795-805.

[17] Q. F. Zeng, J. Fu, Y. Zhou, Y. T. Shi, H. L. Zhu, Photooxidation Degradation of Reactive Brilliant Red K-2BP in Aqueous Solution by Ultraviolet Radiation/Sodium Hypochlorite, *Clean – Soil Air Water* 2009, *37 (7)*, 574-580.

[18] E. M. Saggioro, A. S. Oliveira, T. Pavesi, J. C. Moreira, Effect of activated carbon and titanium dioxide on the remediation of an indigoid dye in model waters, *Rev. Chim.* 2013, accepted for publication.

[19] A. Fujishima, K. Honda, Electrochemical Photolysis of Water at a Semiconductor Electrode, *Nature* 1972, *238 (5358)*, 37-38.

[20] K. Mao, Y. Li, H. Zhang, W. Zhang, W. Yan, Photocatalytical Degradation of 17-Ethinylestradiol and Inactivation of Escherichia coli Using Ag-Modified TiO_2 Nanotube Arrays, *Clean – Soil Air Water* 2013, *41 (5)*, 455-462.

[21] J. P. Ghosh, G. Achari, C. P. Langford, Reductive Dechlorination of PCBs Using Photocatalyzed UV Light, *Clean – Soil Air Water* 2012, *40 (5)*, 455-460.

[22] F. Beduk, M. E. Aydin, S. Ozcan, Degradation of Malathion and Parathion by Ozonation, Photolytic Ozonation and Heterogeneous Catalytic Ozonation Processes, *Clean – Soil Air Water* 2012, *40 (2)*, 179-187.

[23] A. F. Martins, F. Mayer, E. C. Confortin, C. S. Frank, A Study of Photocatalytical Processes Involving the Degradation of the Organic Load and Amoxicillin in Hospital Wastewater, *Clean – Soil Air Water* 2009, *37 (4-5)*, 365-371.

[24] L. T. Kist, C. Albrecht, E. L. Machado, Hospital laundry wastewater disinfection with catalytic photoozonation, *Clean – Soil Air Water* 2008, *36 (9)*, 775-780.

[25] A. S. Oliveira, C. G. Maia, P. Brito, R. Boscencu, R, Socoteanu, M. Ilie, L. F. V. Ferreira, Photodegradation of photodynamic therapy agents in aqueous TiO_2 suspensions, *Sustainable Develop. Plan. VI* 2013, *173 (1)*, 359-369.

[26] M. H. Habibi, A. Hassanzadeh, S. Mahdavi, The effect of operational parameters on the photocatalytical degradation of three textile azo dyes in aqueous TiO_2 suspensions, *J. Photochem. Photobiol. A Chem.* 2005, *172 (1)*, 89-96.

[27] M. Neamatu, I. Simiriceanu, A. Yediler, A. Kettrup, Kinetics of decolorization and mineralization of reactive azo dyes in aqueous solution by the UV/H_2O_2 oxidation, *Dyes Pigm.* 2002, *53 (2)*, 93-99.

[28] C. Chen, Z. Wang, S. Ruan, B. Zou, M. Zhao, F. Wu, Photocatalytical degradation of C.I. Acid Orange 52 in the presence of Zn-doped TiO_2 prepared by a stearic acid gel method, *Dyes Pigm.* 2008, *77 (1)*, 204-209.

[29] C. Wang, C. Lee, M. Lyu, L. Juang, Photocatalytical degradation of C.I. Basic Violet 10 using TiO_2 catalysts supported by Y zeolite: An investigation of the effects of operational parameters, *Dyes Pigm.* 2008, *76 (3)*, 817-24.

[30] C. Hachem, F. Bocquillon, O. Zahraa, M. Bouchy, Decolourization of textile industry wastewater by the photocatalytical degradation process, *Dyes Pigm.* 2001, *49 (2)*, 117-125.

[31] C. Guillard, J. Disdier, C. Monnet, J. Dussaud, S. Malato, J. Blanco, M. I. Maldonado, J. Herrmann, Solar efficiency of a new deposited titania photocatalyst: chlorophenol, pesticide and dye removal applications, *Appl. Catal. B* 2003, *46 (2)*, 319-332.

[32] C. Flux, S. Ammar, C. Arias, E. Brillas, A. V. Vargas-Zavala, R. Abdelhedi, Electron-Fenton and photoelectron-fenton degradation of indigo carmine in acidic aquous medium, *Appl. Catal. C* 2006, *67 (1-2)*, 93-104.

[33] M. S. T. Gonçalves, A. M. F. O. Campos, E. M. M. S. Pinto, P. M. S. Plasência, M. J. R. P. Queiroz, Photochemical treatment of solutions of azo dyes containing TiO_2, *Chemosphere* 1999, *39 (5)*, 781-786.

[34] M. S. Lucas, R. Mosteo, M. I. Maldonado, S. Malato, J. A. Peres, Solar Photochemical Treatment of Winery Wastewater in a CPC reactor, *J. Agric. Food Chem. 2009, 57,* 11242–11248.

[35] E. M. Rodríguez, G. Fernández, N. Klamerth, M. I. Maldonado, P. M. Álvarez, S. Malato, Efficiency of different solar advanced oxidation processes on the oxidation of bisphenol A in water, *Appl. Catal. B: Environ 2010, 95*, 228-237.

[36] L. S Clesceriv, A. E Greenberg, A. D Eaton, Standard Methods for the Examination of Water and Wastewater, *American Public Health Association 1998,* Washington, DC.

[37] R. Zhang, S. Vigneswaran, H. Ngo, H. Nguyen, A submerged membrane hybrid system coupled with magnetic ion exchange (MIEX®) and flocculation in wastewater treatment, *Desalination 2007, 216,* 325-333.

[38] E. Franciscon, A. Zille, F. G. Dias, C. R. Menezes, L. R. Durrant, A. Cavaco-Paulo, Biodegradation of textile azo dyes by a facultative *Staphylococcus arlettae* strain VN-11 using a sequential microaerophilic/aerobic process, *Int. Biodeterior. Biodegrad.* 2009, *63 (3),* 280–288.

[39] L. R. Bergsten-Torralba, M. M. Nishikawa, D. F. Baptista, D. P. Magalhães, M. da Silva, Decolorization of different textile dyes by *Penicillium simplicissimum* and toxicity evaluation after fungal treatment, *Braz. J. Microbiol.* ***2009,*** *40 (4)****,*** 808-817.

[40] Brazilian regulations NBR 12648, (2005). Aquatic Ecotoxicology - Chronic toxicity - test method with algae (*Chlorophyceae*). Rio de Janeiro.

[41] Brazilian regulations NBR 12713, (2004). Aquatic Ecotoxicology. Acute toxicity. Test method with *Daphnia spp* (Cladocera, Crustacea). Rio de Janeiro.

[42] J. M. Dostanic, D. R. Loncarevic, P. T. Bankovic, O. G. Cvetkovic, D. M. Jovanovic, D. Z. Mijin, Influence of process parameters on the photodegradation of synthesized azo pyridone dye in TiO_2 water suspensions under simulated sunlight, *J. Environ. Sci. Health A Tox. Hazard. Subst. Environ. Eng.* 2011, *46 (1)*, 70-79.

[43] E. M. Saggioro, A. S. Oliveira, T. Pavesi, C. G. Maia, L. F. V. Ferreira, J. C. Moreira, Use of Titanium Dioxide Photocatalysis on the Remediation of Model Textile Wastewaters Containing Azo Dyes, *Molecules* 2011, *16 (12)*, 10370-10386.

[44] J. Xu, Y. Ao, D. Fu, C. Yuan, Study on photocatalytical performance and degradation kinetics of X-3B with lanthanide-modified titanium dioxide under solar and UV illumination, *J. Hazard. Mater.* 2009, *164 (2-3)*, 762-768.

[45] Y. Song, J. Li, B. Bai, TiO_2-Assisted Photodegradation of Direct Blue 78 in Aqueous Solution in Sunlight, *Water Air Soil Pollut.* 2010, *213 (1-4)*, 311-317.

[46] V. Augugliaro, C. Baiocchi, A. B. Prevot, E. Garcáa-Lopéz, V. Loddo, S. Malato, G. Marcí, L. Palmisano, M. Pazzi, E. Pramauro, Azo-dyes photocatalytical degradation in aqueous suspension of TiO_2 under solar irradiation, *Chemosphere* 2002, *49 (10)*, 1223-1230.

[47] R. Velmurugan, M. Swaminathan, An efficient nanostructured ZnO for dye sensitized degradation of Reactive Red 120 dye under solar light, *Sol. Energ. Mat. Sol. C.* 2011, *95 (3)*, 942-950.

[48] A. H. Gemeay, I. A. Mansour, R. G. El-Sharkawy, A. B. Zaki, Kinetics and mechanism of the heterogeneous catalyzed oxidative degradation of indigo carmine, *J. Mol. Catal. A Chem.* 2003, *193 (1-2)*, 109-120.

[49] H. Al-Ekabi, N. Serpone, Photocatalytical degradation of chlorinated phenols in aerated aqueous solutions over TiO_2 supported on a glass matrix, *J. Phys. Chem.* 1998, *92 (20)*, 5726-5731.

[50] X. Guohong, L. Guoguang, S. Dezhi, Z. Liqing, Kinetics of Acetamiprid Photolysis in Solution, *Bull. Environ. Contam. Toxicol. 2009, 82,* 129-132.

[51] J. M. Herrmann, C. Guillard, M. Arguello, A Agüera, A. Tejedor, L. Piedra, A Fernandez-Alba, Photocatalytic degradation of pesticide pirimiphos-methyl – determination of the reaction pathway and identification of intermediate products by various analytical methods, *Catal. Today 1999, 54,* 353.

[52] L. Rizzo, S. Meric, D. Kassinos, M. Guida, F. Russo, V. Belgiorno, Degradation of diclofenac by TiO_2 photocatalysis: UV absorbance kinetics and process evaluation through a set of toxicity bioassays, *Water Res.* 2009, *43 (4)*, 979-988.

[53] X. Zhang, H. Sun, Z. Zhang, Q. Niu, Y. Chen, J. C. Crittenden, Enhanced bioaccumulation of cadmium in carp in the presence of titanium nanoparticles, *Chemosphere* 2007, *67 (1)*, 160-166.

[54] R. J. Griffitt, J. Luo, J. Gao, J. C. Bonzongo, D. S. Barber, Effects of particle composition and species on toxicity of metallic nanomaterials in aquatic organisms, *Environ. Toxicol. Chem.* 2008, *27 (9)*, 1972-1978.

[55] Y. Zhang, Y. Chen, P. Westerhoff, K. Hristovski, J. C. Crittenden, Stability of commercial metal oxide nanoparticles in water, *Water Res.* 2008, *42 (8-9)*, 2204-2212.

[56] K. Hund-Rinke, M. Simon, Ecotoxicity Effect of Photocatalytical Active Nanoparticles (TiO_2) on Algae and Daphnids, *Environ. Sci. Pollut. Res.* 2006, *13 (4)*, 225-232.

[57] Z. Zainal, C. Y. Lee, M. Z. Hussein, A. Kassim, N. A. Yusof, Electrochemical-assisted photodegradation of mixed dye and textile effluents using TiO_2 thin films, *J. Hazard. Mater.* 2007, *146 (1-2)*, 73-80.

[58] S. B. Lovern, R. Klaper, *Daphnia magna* mortality when exposed to titanium dioxide and fullerene (C60) nanoparticles, *Environ. Toxicol. Chem.* 2006, *25 (4)*, 1132-1137.

[59] I. M. Sadiq, S. Dalai, N. Chandrasekaran, A. Mukherjee, Ecotoxicity study of titania (TiO_2) NPs on two microalgae species: *Scenedesmus sp*. and *Chlorella sp*., *Ecotoxicol. Environ. Saf.* 2011, *74 (5)*, 1180-1187.

[60] S. Hall, T. Bradley, J. T. Moore, T. Kuykindall, L. Minella, Acute and chronic toxicity of nano-scale TiO_2 particles to freshwater fish, cladocerans, and green algae and effects of organic and inorganic substrate on TiO_2 toxicity, *Nanotoxicol.* 2009, *3 (2)*, 91-97.

[61] I. Velzeboer, A. J. Hendriks, A. M. Ragas, D. van de Meent, Aquatic ecotoxicity tests of some nanomaterials, *Environ. Toxicol. Chem.* 2008, *27 (9)*, 1942-1947.

[62] P. Gharbani, S. M. Tabatabaei, S. Dastmalchi, S. Ataie, A. Mosenharzandi, A. Mehrizad, Adsorption of chloroform from aqueous solution by nano -TiO_2, *Int. J. Nano. Dim.* 2011, *1 (4)*, 287-296.

[63] K. Hristovski, A. Baumgardner, P. Westerhoff, Selecting metal oxide nanomaterials for arsenic removal in fixed bed columns: From nanopowders to aggregated nanoparticle media, *J. Hazard. Mater.* 2007, *147 (1-2)*, 265-274.

[64] P. K. Dutta, A. K. Ray, V. K. Sharma, F. J. Millero, Adsorption of arsenate and arsenite on titanium dioxide suspensions, *J. Colloid Interface Sci.* 2004, *278 (2)*, 270-275.

6. ARTIGO 4

Research Article

Solar CPC pilot plant photocatalytic degradation of Indigo Carmine dye in waters and wastewaters using supported-TiO_2. Influence of photodegradation parameters.

Enrico Mendes Saggioro[1]*, Anabela Sousa Oliveira[2,3], Thelma Pavesi[1], Margarita Jiménez Tototzintle[4], Manuel Ignacio Maldonado[4], Fábio Verissimo Correia[5], Josino Costa Moreira[1]

1 – CESTEH - Centro de Estudos da Saúde do Trabalhador e Ecologia Humana, Escola Nacional de Saúde Pública - Fundação Oswaldo Cruz, Av. Leopoldo Bulhões, 1480, 21041-210, Rio de Janeiro, Brazil.

2 – CQFM - Centro de Química-Física Molecular and IN - Instituto de Nanociencias e Nanotecnologia, Instituto Superior Técnico, Universidade Técnica de Lisboa, Av. Rovisco Pais 1049-001, Lisbon, Portugal.

3 – C3i - Centro Interdisciplinar de Investigação e Inovação and Escola Superior de Tecnologia e Gestão, Instituto Politécnico de Portalegre, Lugar da Abadessa, Apartado 148, 7301-901 - Portalegre, Portugal.

4- CIEMAT – Centro de Investigaciones Energéticas, Medioambientales y Tecnológicas, Plataforma Solar de Almería, Carretera Sénes, km 4, 04200 Tabernas (Almería), Spain.

5- UNIRIO - Universidade Federal do Estado do Rio de Janeiro, Av. Pasteur, 296 22290-240, Rio de Janeiro, Brazil.

Abstract

Photocatalytic degradation of indigo carmine (IC) dye in the presence of titanium dioxide was performed under different conditions. The effects of parameters in the IC degradation were evaluated under artificial irradiation with a 125 W mercury vapor lamp. The effects of the amount of TiO_2, pH of the solution, initial concentration of the dye, presence of inorganic anions, temperature and addition of different concentrations of hydrogen peroxide were investigated. A TiO_2 catalyst supported on glass beads was prepared (sol-gel method) and used a CPC solar pilot plant for the photodegradation of dye. IC was spiked in several types of water such as distilled water, synthetic moderately hard freshwater, synthetic and real secondary municipal wastewater treatment plant (MWWTP). Total organic carbon (TOC), carboxylic acids and SO_4^{2-} and NH_4^+ were determined to evaluate the IC mineralization. Formate, acetate and oxalate were detected during degradation in real MWWTP secondary effluent. *Eisenia andrei* earthworms were used to evaluate biological effects. No significant difference ($p > 0.05$) of reduction in mean weight earthworms was observed from the different concentrations of IC and its photoproducts. The photocatalytic degradation of IC on TiO_2 supported on glass beads suffered strong influence of the water matrix, nevertheless the method has the enormous advantage that it eliminates the need of catalyst removal step therefore reducing the cost of treatment.

Keywords: Compound parabolic collector, *Eisenia andrei* earthworms, Indigo carmine, TiO_2 supported, Real wastewater.

6.1 Introduction

Organic dyes are one of the largest groups of pollutants of wastewaters. In general, they are released into the environment by textile and some other industries (Barka et al. 2008). Dyes are used in the processing of textile industries and significant quantities are lost during dyeing steps. Wastewaters containing 5-15% of untreated dye can be released into the environment and are considered to pose serious problems, because they have considerable environmental effects on the water and are visually unpleasant (Zainal et al. 2005). Moreover, environmental pollution by organic dyes also sets a severe ecological problem, which is increased by the fact that most of them are often toxic to microorganisms and a have long degradation time in the environment (Wang et al. 2008).

Around 100,000 dyes are currently in use by textile industry and 7 x 10^5 ton of dyestuff is produced annually worldwide. Among these, the indigoids are the largest class of commercial dyes, used mostly for cotton cloth dying (blue jeans) (Robinson et al. 2001; Behnajaday et al. 2005). Indigo blue dye's main component is indigotine, which is extracted from the leaves of *Indigofera tinctoria* (Andreotti et al. 2004). Indigo carmine (3,3-dioxo-2,2-bis-indolyden-5,5-disulfonic acid disodium salt) is also one of the oldest dyes and still one of the most used in textile industry (Oliveira et al. 2011). The basic color-producing structure of indigoid dyes is a cross-conjugated system or H-chromophore, consisting of a single -C=C- double bond substituted by two NH donor groups and two CO acceptor groups (Vautier et al. 2001).

Indigo carmine (IC) is considered as a highly toxic indigoid dye. Contact with skin and eyes can cause permanent injury to cornea and conjunctiva and if consumed by oral via can cause disturbs in reproductive, developmental and neuronal systems, and may cause death (Jenkins 1978). Most toxic dyes are recalcitrant to biodegradation, causing decay in the efficiency of biological wastewater treatment plants and having low treatment efficiency by traditional physic-chemical wastewater treatment methods such as flocculation or adsorption (Sanromán et al. 2004; Zainal et al. 2005).

Among the new methods of wastewater treatment, Advanced Oxidative Processes (AOPs) based on the generation of very reactive species such as hydroxyl radicals have been proposed to oxidize quickly and non-selectively range or organic pollutants (Sano et al. 2008; Khataee et al. 2009). Among AOPs, heterogeneous photocatalysis has been attracting a lot of attention for its efficiency and promising economy (Zhao et al. 1998; Liu et al. 1999; Konstantinou and Albanis 2003). Titanium dioxide is a well-know photocatalyst with many applications in photoreactions for treatment pollutant wastewater (Fujishima et al. 2000). The use of TiO_2 has advantages such as ease of use, low cost, high photochemical reactivity and non-specific oxidative attack ability. In this way, it can promote the degradation of different target organic compounds and industrial effluents with little change of operational parameters (Chen et al. 2008; Wang et al. 2008). Titanium dioxide mediated photooxidation is indeed used for environmental remediation, where toxic materials at low concentration are converted, in a series of chemical steps, to harmless oxidation products such CO_2 and H_2O (Hoffmann et al. 1995). Additionally, it can be used as antibacterial agent because of strong oxidation activity and hydrophilicity (Fujishima et al. 2006).

Nowadays, TiO_2 is one of the most suitable semiconductors for photocatalysis and has been applied into various photocatalytic reactions (Aarthi et al. 2007; Saien and Soleymani 2007; Andronic and Duta 2008; Huang et al. 2008; Saquib et al. 2008). However, in the large-scale applications, the use of suspensions require the separation and recycling of TiO_2 particles of nanometric dimension from treatment wastewater prior to the discharge in water bodies and this can limit process development once it is a time-consuming expensive process. Alternatively, the catalyst may be immobilized onto a suitable solid inert material, which eliminates the catalyst removal step (Barka et al. 2008; Mahmoodi et al. 2006), and permits the reuse of the photocatalyst several times.

The aim of the present work is to investigate the photocatalytic oxidation of indigo carmine (IC) dissolved in different water matrices mediate by TiO_2 supported on glass beads and sunlight. The latter is focused on a photoreaction system composed by compound parabolic collectors (CPC) installed at the "Plataforma Solar de Almería" (PSA, Spain) that already demonstrated to have capacities to remove several other organic pollutants in large quantity from different water matrixes (Guillard et al. 2003). The dependence of dye photooxidation on the various parameters: TiO_2 amount, initial dye concentration, temperature, H_2O_2 addition, initial pH and some inorganic ions usually present in real wastewater produced by textile industry were investigated under artificial irradiation in presence of TiO_2 suspensions. The repeatability of photocatalytic activity of the photocatalyst was also tested.

Furthermore, ecotoxicological testes with *Eisenia andrei* earthworms were performed. The earthworms are affected by a variety of organic and inorganic

compounds, which may cause bioaccumulation and theirs preliminary results serve as a rapid indicator on the toxicity compounds of the compound under text and can be used as complementary test for risk assessment of polluted areas (Paoletti 1999). *Eisenia andrei* has been chosen as test specie because it reproduces easily in the laboratory, it was approved by the European Union and OECD for use in toxicity tests and has been used by the U.S. Environmental Protection Agency (EPA) as a wide test for contaminant residues in several polluted sites (Correia and Moreira 2010).

6.2 Experimental

6.2.1 Reagents and Materials

Indigo carmine (IC) dye, 85 % ($C_{16}H_8N_2S_2O_8Na_2$, M.W. = 466.36 $gmol^{-1}$) was obtained from Sigma Aldrich (USA) and used without further purification. Photocatalyst used in all experiments was titanium dioxide, EVONIK-P25, containing 75% anatase and 25% rutile, with a specific BET surface area of 50 $m^2 g^{-1}$ and primary particle size of 20 nm. The other materials such as NaOH, HCl, H_2O_2, $NaHCO_3$, NaCl, Na_2SO_4 and KH_2PO_4 were obtained from Merck.

6.2.2 Photocatalytic experiments with artificial irradiation

A volume of 100 ml of indigo carmine solution (30 mgL^{-1}) was submitted to photodegradation using batch static stirred reactor with a high-pressure 125 W mercury vapor lamp to investigate the influence of various parameters on the photocatalytic

degradation by TiO_2 suspensions. Before irradiation, samples were kept in the dark for 30 min, also under stirring. During irradiation step, samples were continuously stirred. Control samples were submitted to identical treatment. Samples were taken at different time and analyzed. The efficient photon flux was determinate measuring the radiant flux (in mW/cm^2) at the surface of the sample being treated. In each case stated above, the radiant flux was measured with a radiometer (Cole-Parmer Instrument Co.; model 9811-50). All experiments were performed in duplicated as described elsewhere (Saggioro et al. 2011).

6.2.3 Photocatalytic experiments in a CPC solar pilot plant

Solar TiO_2 photocatalytic experiments were carried out in a pilot plant reactor with CPC optics installed at the Plataforma Solar de Almería (PSA, latitude 37ºN, longitude 2.4ºW). A schematic of the plant can be seen in a previous publication (Lapertot et al. 2006). The reactor, which has sixteen DURAN^{TM} glass tubes (28.45 mm inner diameter) and was mounted on a fixed platform tilted 37º (local latitude), was modified to work with only two of the glass tubes. These two glass tubes were uniformly packed with the glass spheres (~ 4600 spheres per tube). The pump flow was 2.5 L min^{-1} and the tank (containing the effluent to be treated) continuously stirred. At the beginning of the experiments, while collectors were kept covered, the chemicals were added to the tank and mixed by recirculating the water throughout the system in order to reach a constant concentration. Then the covers were removed from the CPC and samples were collected at predetermined times. A global UV radiometer

(KIPP&ZONEN, model CUV 3, the Netherlands) also tilted 37º was used for measuring global solar UV radiation intensity (UV_G) in terms of incident Wuv/m^2.

To start run the experiments, the pilot plant, still with the collectors covered, was filled with 8 L of a 30 mg L^{-1} indigo carmine dye water solution. The chemicals for each experiment were added and the solution was homogenized for 30 min pior to sun irradiation. After sun irradiation started samples were taken at different times and analyzed.

The supported-TiO_2 photocatalyst was prepared by sol-gel technique (Jimenez et al. 2014). Enough amount of distilled water was acidified with 13 mL of nitric acid and titanium isopropoxide, $(Ti(iOPr)_4$, (TIOP) was added to the solution and the suspensions was stirred for 24 h, until complete peptization. A solution of 20 mgL^{-1} of polyethylene glycol in isopropanol was prepared separately and added to the TIOP sol under continuous magnetic stirring. The acid sol was dialyzed until a final pH of 2.4-2.5. Finally, 10 gL^{-1} of EVONIK P-25 TiO_2 were incorporated under continuous stirring. The glass spheres were coated with TiO_2 sol by dip coating. Then the glass beads were dried at 110ºC for 90 min and calcinated at 400ºC for 5 h (Miranda-García et al. 2010).

The experiments in solar CPC pilot plant were spiked with IC in different types of water: distilled water, synthetic moderately hard freshwater (Clesceriv et al. 1998), synthetic secondary municipal wastewater treatment plant (MWWTP) effluent (Zhang et al. 2007) and secondary effluent from the MWWTP "El Bobar" (Almería, Spain). Table 1 shows some physical and chemical characteristics of the different types of water used in this work. All experiments were performed in duplicated.

Table 1. Physical and chemical characteristics of the different types of water.

Type of water	Inorg. Carbon (mgL^{-1})	TOC (mgL^{-1})	COD (mgL^{-1})	pH	Conduc. ($\mu s\ cm^{-1}$)	Ionic species (mM)							
						Na^{+}	Ca^{+2}	Mg^{+2}	K^{+}	NH^{+4}	PO_4^{-3}	Cl^{-}	SO_4^{-2}
Fresh water moderately hard	13.89	3.40	11.6	7.4	206	0.76	0.36	0.44	0.1	—	—	0.09	0.04
Synthetic MWWTP secondary effluent	9.98	17.76	57.59	8.0	261	1.27	0.36	0.45	0.17	0.35	0.01	0.04	0.93
Real MWWTP secondary effluent	69.92	26.9	81.2	8.3	1504	8.2	1.5	1.3	0.63	2.96	0.05	9.94	1.02

6.2.4 Evaluation of IC degradation and solar UV radiation

In those cases where IC degradation was observed, IC concentration followed first-order kinetics according to Eq. (1):

$$\ln\left(\frac{[IC]}{[IC]_0}\right) = -kt \qquad (1)$$

where k ($time^{-1}$) is the pseudo-first-order rate constant. However, to compare the efficiency of the batch static stirred reactor and solar CPC pilot plant, it is necessary to consider that the reaction time needed to degrade IC also depends on the intensity of the incident UV radiation. So, IC degradation is expressed as a function of the accumulated UV energy in the reactor, $Q_{UV,n}$:

$$\ln\left(\frac{[IC]}{[IC]_0}\right) = -k'Q_{UV,n} \qquad (2)$$

where k_0 is the pseudo-first-order rate constant (L kJ^{-1}) and $Q_{UV,n}$ (kJ L^{-1}) the amount of accumulated UV energy received on any surface in the same position with regard to the sun, per unit of volume of water inside the reactor in the interval Δt. $Q_{UV,n}$ can be found by applying Eq. (3) (Rodríguez et al. 2010):

$$Q_{UV,n} = Q_{UV,n-1} + \Delta t_n UV_{G,n} \frac{A_i}{V_T} \quad ; \quad \Delta t_n = t_n - t_{n-1} \tag{3}$$

where t_n is the time corresponding to n water sample, V_T is the total reactor volume (8 L), A_i is the illuminated surface area (0.25 m^2) and $UV_{G,n}$ is the average solar ultraviolet radiation measured during the period Δ_{tn}. With this equation, the combination of the data from experiments of several different days and their comparison with other photocatalytic experiments is possible (Fernández et al. 2005).

6.2.5 Analytical determinations

The Indigo Carmine (IC) degradation was determined by UV-Visible spectrophotometry (Shimadzu UV-1601PC) acquired from 200-900 nm and HPLC-DAD (Agilent Technologies, series 1100) system equiped with a C-18 column (LUNA 5 mm, 3 mm x 150 mm, from Phenomenex) and using an amonium acetate 10 mM : methanol (80:20) mixture as mobile phase (flow rate: 0.8 mL min^{-1}). Absorbance detection was made at 610 nm. Total organic carbon (TOC) was measured in filtered samples (Millipore- Miliex-GN Nylon 0.2 µm filters) with a Shimadzu-5050A TOC

analyser. Anion concentrations were determined with a Metrohm 872 Extension Module 1 and 2 ion chromatograph (IC) system configured for gradient analysis. Cation concentrations were determined with a Metrohm 850 Professional IC configured for isocratic analysis.

6.2.6 Ecotoxicologycal tests

Photocatalytic degradation may generate toxic photoproducts and so they must be assessed in order to determine if the effluent treatment strategy is leading or not to the the desired toxicity reduction result. Acting like that, we may prevent the contamination of receptor water bodies with toxic substances generated by decontamination treatment itself. In this work, the ecotoxicity of the indigo carmine and its photoproducts at different times were tested with *Eisenia andrei* earthworms.

Organisms *Eisenia andrei* used in the tests were created in the Ecotoxicology sector, Laboratory of Toxicology in Center of Occupational Health and Human Ecology Studies (CESTEH), Oswaldo Cruz Foundation (Fiocruz). Prior to the experiments the earthworms were acclimated for at least 24h in the environment to be tested. To the test adult worms were selected (under 2 months of age and well-developed clitellum) with individual weight around 300-600 mg (ISO 11268-1 2012). The masses of earthworms survivors had their means were compared by ANOVA (analysis of variance) with Bonferroni correction (alpha bilateral 0.05), using BioEstat 2.0.

6.2.6.1 Acute toxicity test – contact test

Studies for acute toxicity (US EPA 1996; OECD 1984) were made with 15 replicates each concentration by contacting of each earthworm in a vial with filter paper (60 cm^2) soaked with different concentrations (0.17; 1.67; 16.67 and 166.67 $\mu g.cm^{-2}$) of indigo solutions. As a control, 15 replicates on filter paper moistened with only 1 mL of water were also prepared.

After preparation of vessels, an earthworm was added to each of them and the containers were sealed with perforated paraffin film, to enable oxygenation. After 24h of incubation, the containers were opened, survivor and dead earthworms were counted, and weight was verified. Earthworms were classified as dead when they did not respond to a gentle mechanical stimulus. The same experiment were performed with products of the indigo carmine (80 mgL^{-1}) dye in different degradation times (60, 120, 180 and 300 min) of indigo photocatalysis mediated TiO_2 (0.1 gL^{-1}) suspensions.

6.3 Results and Discussion

6.3.1 Effect of catalyst amount

The effect of TiO_2 amount on the photocatalytic degradation of indigo carmine dye was studied at optimized conditions for all others experimental parameters and results are shown in Fig. 1. The significance of catalyst adsorption in the dark was also evaluated. The indigo carmine adsorption on TiO_2 was observed to be around 10% after 90 min and adsorption/desorption equilibrium time (30 min in the dark). The

photocatalytic degradation efficiency of indigo carmine dye was increased by increasing the amount of photocatalyst. It was concluded that most of the tested concentrations of TiO_2 were able to photodegraded the dye for accumulated energies between Q_{uv} 10-30 kJL^{-1}. This can be rationalized in terms of availability of actives sites on TiO_2 surface and on the light penetration for activation of TiO_2 suspensions (Habib et al. 2005). The fact is that in solutions with 1 gL^{-1} of TiO_2 in suspension the light penetration depth is considerably smaller than in those containing only 0.1 gL^{-1} of TiO_2, although the availability of actives sites is much higher. The agglomeration and sedimentation of TiO_2 particles for highest concentrations of TiO_2 have also been reported (Saggioro, 2011). In this way, for each system to be remediated thought this method, the optimum amount of TiO_2 has to be determined in order to avoid the unnecessary use of catalyst in excess. In this study, the amount of 0.1 gL^{-1} of TiO_2 was considered optimum for all subsequent experiments.

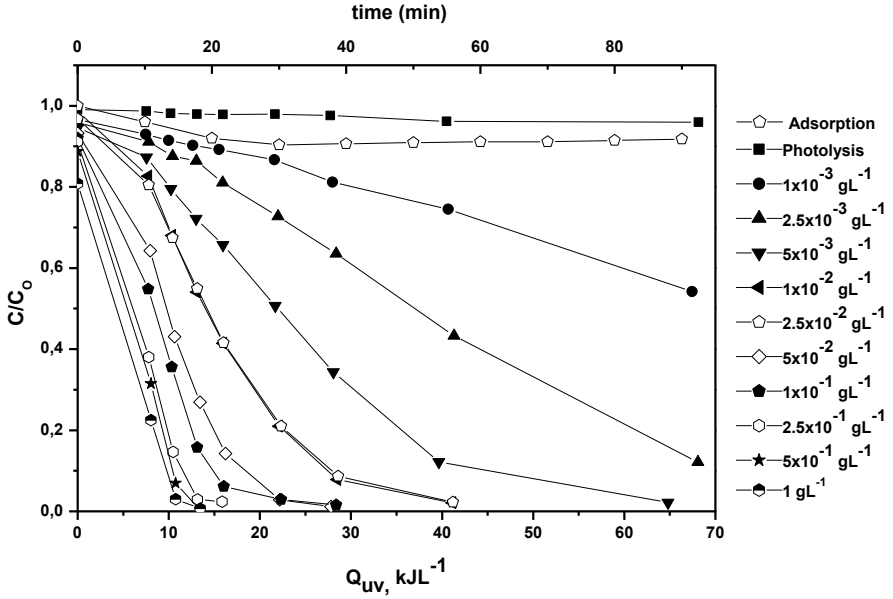

Fig. 1. Effect of TiO_2 suspension concentrationon the photocatalytic degradation of 30 mgL^{-1} of indigo carmine dye.

6.3.2 Effect of initial dye concentration

The effect of the initial dye concentration on photodegradation efficiency is shown in Fig. 2. The photocatalytic degradation of the dye decreased with increase in the initial dye concentration. An accumulated energy, $Q_{uv,}$ of 30 kJL^{-1} degraded dye concentrations of 30 and 50 mgL^{-1} whereas for 100 mgL^{-1} was needed an energy of 65 kJL^{-1} to degrade the dye. However, for initial dye concentrations of 120 and 150 mgL^{-1} remained non-degraded until accumulated energy reach ~ 70 kJL^{-1}. The strong decrease of the observed photodegradation rate constant was probably due to adsorption of more dye molecules on the surface of the catalyst, and to the consequent reduction on generation of OH• radicals since the actives sites were already occupied by cations of the dye (Wang et al. 2008). Moreover, as the concentration of dye increased, this also caused a significant absorption of light, consequently the photon flow reaching the catalyst surface particles decreased and so, photodegradation efficiency decreased either (Augugliaro et al. 2003).

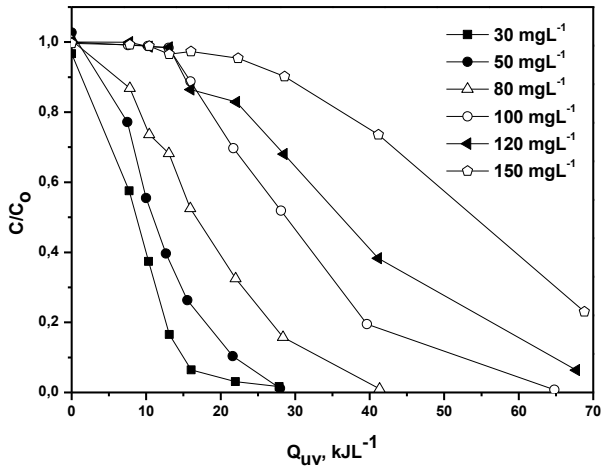

Fig. 2. Effect of initial concentration of Indigo Carmine dye on the photocatalytic degradation with 0.1 gL^{-1} of TiO_2 suspensions.

6.3.3 Effect of inorganic anions

For the investigation on the photocatalytic degradation of IC it is important to determine how various anions affect the chemical yield of the process. The effects of various anions that are common in dye-containing industrial wastewater like NaCl, $NaHCO_3$, Na_2SO_4 and KH_2PO_4 (2.5 mM) were tested in TiO_2 suspensions (0.1 gL^{-1}) in the presence of IC (30 mgL^{-1}) and are shown in Fig. 3. The occurrence of dissolved inorganic ions may compete for the active sites on the TiO_2 surface or deactivate the photocatalyst and, subsequently, decrease the degradation rate of the dye (Konstatinou et al. 2004). In this case, it was observed inhibition of IC decolorization for all anions in the following order:

$HCO_3^- < Cl^- < HPO_4^{-2} < SO_4^{-2}$

Inhibition effect of anions can be explained as the reaction of positive holes (h_{vb}^+) with anions and resulting from the high reactivity and non-selectivity of hydroxyl radicals towards non-target compounds present in the water matrix (Mahmoodi et al. 2006).

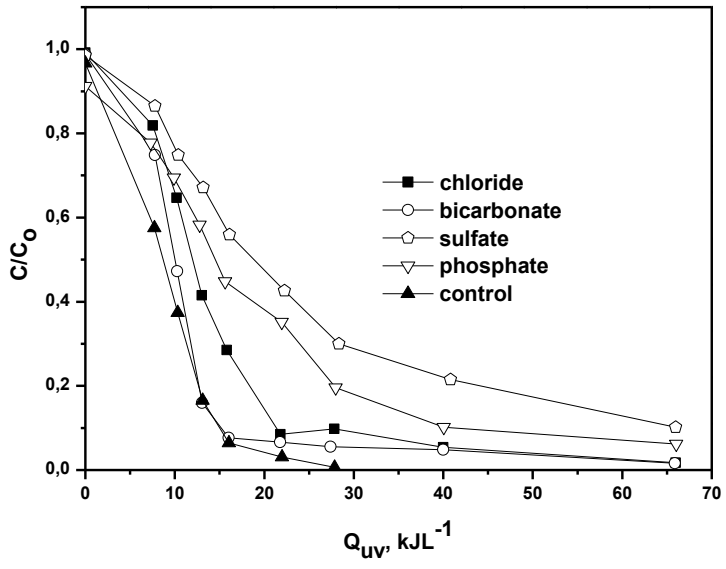

Fig. 3. Effect of inorganic anions (2.5 mM) on decolorization of Indigo Carmine (30 mgL^{-1}) with 0.1 gL^{-1} TiO_2 suspensions.

6.3.4 Effect of temperature

Fig. 4 shows the effect of the temperature of the solution on the complete degradation of indigo carmine dye. Experiments have been made at different working temperature in the range of 25-60^oC, the results indicates that, the rate of the photodegradation is temperature dependent and is disfavored with the raise of solution temperature. It is known that an increase in temperature can affect the efficiency of e^-/h^+ recombination and adsorption/desorption processes of dyes molecules on the TiO_2 photocatalyst surface (Danhesevar et al. 2004). Some of the most important surface phenomena are dye molecule aggregation, tautomerization and geometric (*cis-trans*) isomerization and all those processes can be affected by temperature variation. The increase on solution temperature causes disaggregation of the dye molecules (Habib et al. 2005). Habib et al. (2005), considered molecular weight and anion site (sulfate and

carboxylic group) of three azo dyes, which can interact with molecules by ion-dipole interactions. According this author the dye (C.I Reactive Yellow 2), having the lowest molecular weight (M.W. = 872.5 $gmol^{-1}$) and less anionic sites (three sulfate groups) has significant variation of hydration compared the other dyes, consequently, solution temperature has significant effect on the effective collisions between this dye and TiO_2 photocatalyst. In our case, the indigo carmine is also a comparatively low molecular weight dye (M.W. = 466.36 $gmol^{-1}$) and have two anion site (sulfate groups), consequently the variation of the temperature has also significant effect on photodegradation for this molecule.

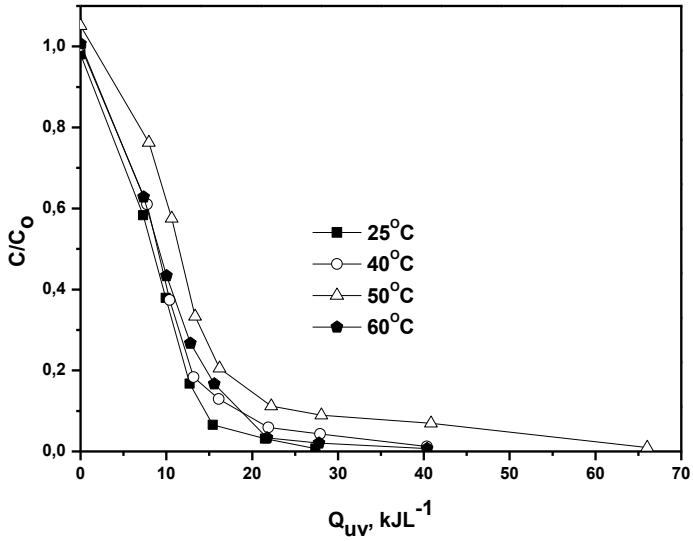

Fig. 4. Effect of temperature on decolorization of Indigo Carmine (30 mgL^{-1}) with 0.1 gL^{-1} TiO_2 suspensions.

6.3.5 Effect of hydrogen peroxide addition

In this work, the effect of H_2O_2 on the photocatalytic degradation of indigo carmine dye was examined, in order to find the optimal H_2O_2 concentration. As

illustrated in Fig. 5, as the hydrogen peroxide concentration increases, the photodegradation first increases, showing its highest value for H_2O_2 concentration equal to 0,022 M. When the H_2O_2 concentration is further increased, this has a strong inhibiting effect on the photocatacalytic degradation. The H_2O_2, present at low concentration, acts mainly as a source of hydroxyl radicals and as an electron scavenger, consequently inhibiting electron-hole recombination. However, at higher concentrations, H_2O_2 reacts with hydroxyl radicals, and acts itself as a scavenger of the photoproduced holes, thus resultsing in decrease of the photocatalytic efficiency (Dostanic et al. 2011), in accordance with results shown in Fig. 5. Gemeay et al. (2003) found similar results, observing that the rate of reaction has a first-order dependence on H_2O_2 at lower concentration, while at higher H_2O_2 the reaction order has decreased, reaching almost zero on kinetic heterogeneous phocatalysis experiments with indigo carmine dye.

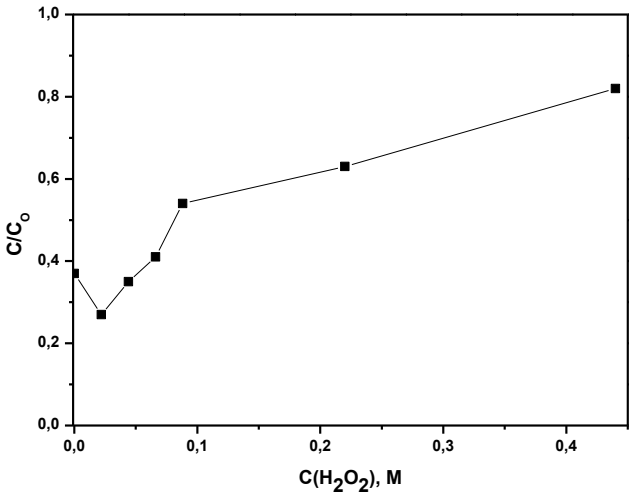

Fig. 5. Effect of concentration of Hydrogen Peroxide on the photocatalytic degradation of Indigo Carmine (30 mgL^{-1}) with 0.1 gL^{-1} of TiO_2 on the accumulated energy, Q_{uv} of 13 kJL^{-1}.

6.3.6 Effect of initial pH

The effect of pH values on the photodegradation was also studied, as shown in Fig. 6. The degradation of indigo carmine was higher in acids solution (i.e. pH range from 2 to 5). Up to a neutral and basic solution, the dye degradation was slow, but in the end of accumulated energy around Q_{uv} 70 kJL^{-1} all solutions were degraded. The interpretation of different photodegradation rates under different pH conditions can be explained by the surface charge density of TiO_2. The point of zero charge (pzc) of TiO_2 is at pH= 6.8. Thus, the TiO_2 surface is fully protonated in acidic medium solution and negatively charged under alkaline conditions, to the following reactions (Santiago et al. 2013):

$$TiOH + H^+ \Leftrightarrow TiOH_2^+ \quad (4)$$

$$TiOH + OH^- \Leftrightarrow TiO^- + H_2O \quad (5)$$

Considering the indigo carmine structure, in low pH solutions the positive charge in the photocatalyst surface promote a strong interaction with SO_3^- groups of the dye consequently promoting the photocatalytic degradation. On the order hand, the basic solutions support the repulsions between surface of catalyst and dye molecules, disadvantaging further photocatalytic degradation.

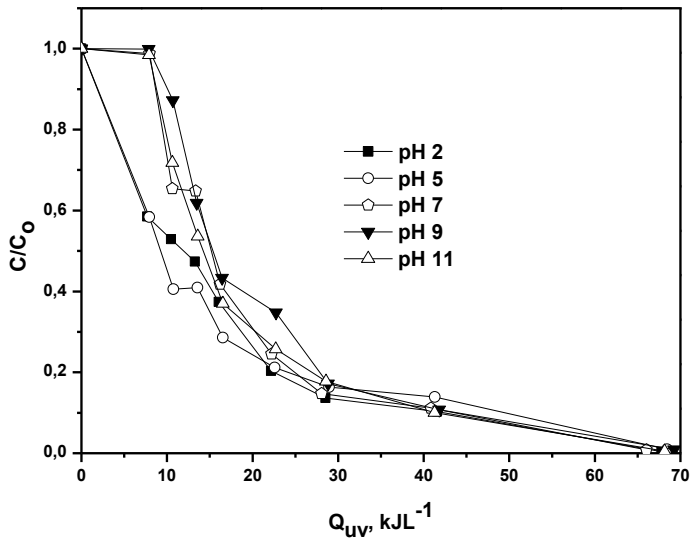

Fig. 6. Photodegradation of indigo carmine dye (30 mgL^{-1}) by TiO_2 (0.1 gL^{-1}) at different pH values.

6.3.7 Recycling of TiO_2

One of today`s main industrial wastewater treatment strategies is focused on the development of green technologies and management practices for environmental benefit. The recycling of the photocatalyst was performed and can be shown in Fig. 7. The TiO_2 catalyst was used and recycled for consecutive reuse on the indigo carmine dye. The process was repeated up to 8 times. The TiO_2 recycling studies were performed with 1 gL^{-1} of the catalyst and the efficiency of the photodegradation process was evaluated and compared between the reuse cycles. These studies reveled that first cycle degraded 98% and until the fifth cycle 80% of the dye was photodegraded. Subsequently, the efficiency markedly decreased, and from the sixth until the eight cycles the degradation was around 50%. However, the rate of degradation kept

significant after eight cycles of TiO_2 reuse. Agglomeration and sedimentation of the indigo carmine around TiO_2 particles after each cycle of photocatalytic degradation is a possible cause of the observed decrease on the degradation rate.

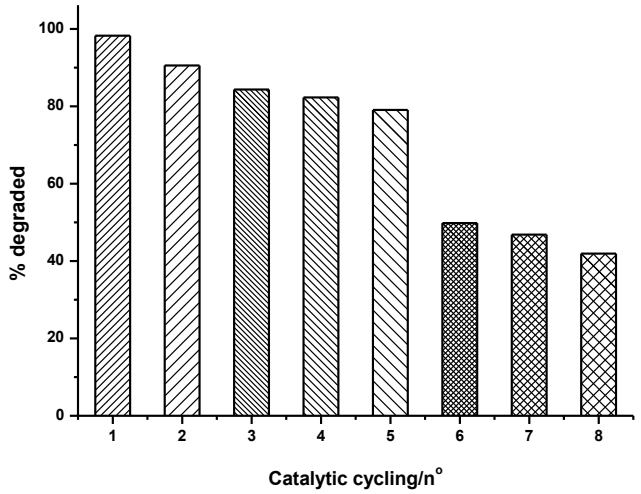

Fig. 7. Recycling and reuse of 1 gL^{-1} of TiO_2 on the photocatalytic degradation of 30 mgL^{-1} of indigo carmine dye for an accumulated energy, Q_{uv}, of 15 kJL^{-1}.

6.3.8 Solar CPC photocatalytic degradation using TiO_2 supported on glass spheres

Solar CPC reactor using TiO_2 supported on glass beads degraded 30 mgL^{-1} of indigo carmine dye in different water matrices. Previously, other study (Jiménez et al. 2014) used the same method for supported TiO_2, and demonstrated its photocatalytic stability and activity towards acetaminophen. Approximately, 0.6 mg of TiO_2 was supported on the surface of each glass bead. The color disappearance of the solution was associated with cleavage of indigoid linkage in dye molecule. Indigoids dyes are characterized by carbon to carbon double bonds (-C=C-) that are usually attached to two electrons groups donors (NH) and receptors (CO). The color of indigoids dyes is

determined by carbon double bonds and their associated chromophores and auxochromes groups (Vautier et al. 2001). IC can be oxidized by positive hole or hydroxyl radical or reduced by electrons in the conduction band all processes leading to the decrease of the color of water.

The solar CPC pilot plant photocatalytic activity of supported TiO_2 in different water matrices in the degradation of indigo carmine dye is shown in Fig. 8. These results demonstrated strong influence of the matrix on photocatalytic degradation of dye. Thus, in distilled water indigo carmine was completely degraded after Q_{uv} of 11 kJL^{-1}, on the order hand for synthetic freshwater the energy needed it was observed to be slightly longer (~ 17 kJL^{-1}) for total degradation; probably this is due to synthetic freshwater composition, and to the fact that some of the ions present in it have a negative effect on the photocatalytic degradation of indigo carmine. When an even more complex water matrix was used, the system efficacy on indigo carmine degradation clearly decreases. After a Q_{uv} of 17 kJL^{-1}, 32% and 37% of the contaminant remain in solution when the synthetic and real MWWTP secondary effluents were used, respectively. For total degradation of the dye was necessary, respectively, Q_{uv} of 36 and 42 kJL^{-1} for both matrices. This fact can be explained due to the presence of different substances in the water matrix (see Table 1), like carbonate, CO_3^{-2}, which is generally found in wastewater in high concentrations (Guohong et al. 2009), then they can be absorbed onto the catalyst surface (blocking and/or competing for the reaction) and/or $OH^{\bullet}$ scavenger.

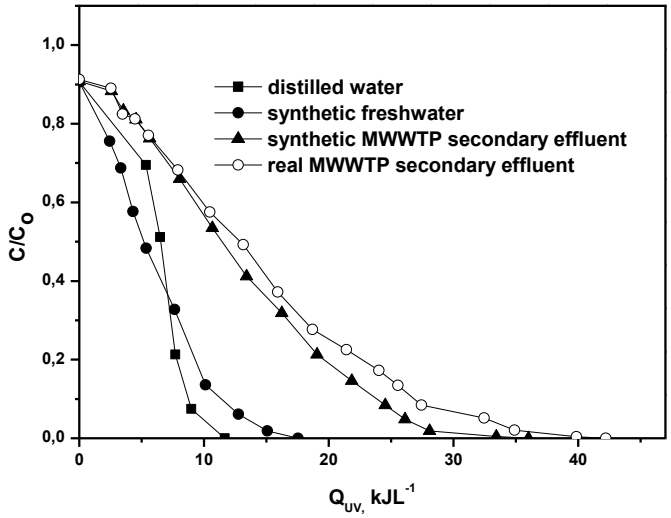

Fig. 8. Solar CPC photodegradation of 30 mgL^{-1} of Indigo Carmine for different matrices of water mediated TiO_2 supported on glass beads.

In our results (not show) a solar CPC photocatalytic degradation of the indigo carmine dye using TiO_2 slurry for treatment of real MWWTP secondary effluent demonstrated that the system was very efficiency when compared to the same conditions with supported TiO_2. This would indicate that the catalyst coated on the glass beads is not correctly illuminated, with large amounts of TiO_2 particles inside the CPC tube and/or probably a considerable amount of TiO_2 supported on glass beads having some sites not activated for photocatalysis. However, supported TiO_2 has the enormous advantage of eliminating the catalyst removal step and thus considerably reducing the costs of treatment.

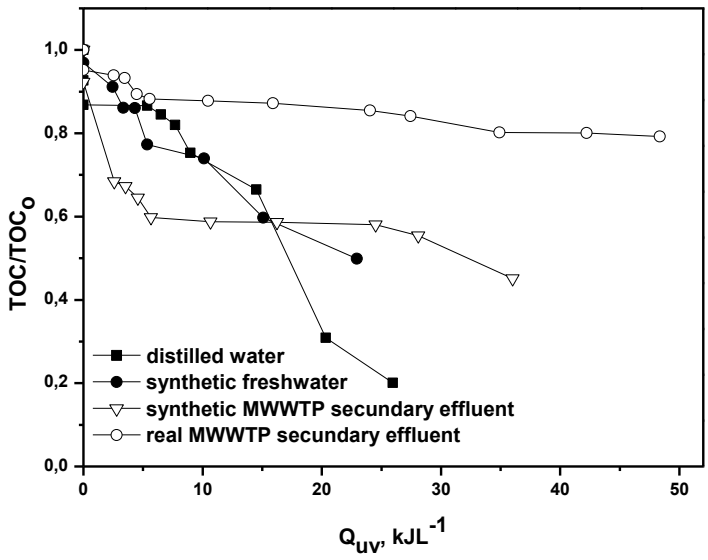

Fig. 9. Evolution of TOC concentration during solar CPC photodegradation of 30 mgL^{-1} indigo carmine mediated TiO_2 supported on glass beads for different water matrixes.

It should be emphasized that the decolorization of the solution does not provide the complete data on the indigo carmine dye degradation. Therefore, other parameters such as TOC, ions, carboxylic acids, conductivity and pH should be monitored. Fig. 9 presents the effectiveness of mineralization of indigo carmine determined on the basis of changes of TOC concentration. The significant TOC decrease was observed only in distilled water; for other complexes matrices the mineralization was not so effective: For matrixes such as real MWWTP secondary effluent (initial TOC 26.9 mgL^{-1}) mineralized only got down to ~ 6 mgL^{-1} of correspondent TOC concentration of the dye. This water contained high concentrations of inorganic carbons (69.92 mgL^{-1}) which promoted the decrease of the activity of $OH^{\bullet}$ radicals. This result on TOC decrease could suggest that during the irradiation of indigo carmine solution in the presence of supported TiO_2 a significant number of lower molecular weight compounds

are formed. Further hydroxylation of aromatic reaction products leads to cleavage of the aromatic ring, resulting in the formation of oxygen-containing aliphatic compounds (Al-Ekabi et al. 1998; Velmurugan et al. 2011). On the other hand, after decolorization stage and breakdown of carbon-to-carbon double bond of indigo carmine dye, inorganic ions are formed. The intermediates (organic acids) and SO_4^{2-} and NH_4^+ ions generated during the degradation process were analyzed by ion chromatography and results are shown in Fig. 10. Formate, acetate and oxalate were detected during degradation in real MWWTP secondary effluent of indigo carmine dye, as shown in Fig. 10a. The evolution of SO_4^{-2} and NH_4^+ ions is presented in Fig. 10b. The structure of indigo carmine dye has two sulfonic groups attached into two aromatic rings and this result indicates that SO_4^{-2} ions form after decolorization stage and breakdown of carbon-to-carbon double bond of dye. It is observed that the concentration of SO_4^{-2} ions continuously increases. The evolution of NH_4^+ mineralization during the photocatalytic degradation of indigo carmine dye shows that it is the main N-containing mineralization product and the fact that it is not observed a delay time, like it was for SO_4^{-2}, indicates that these ions are initial products, directly resulting from the initial attack on the carbon-to-carbon double bond of indigo carmine dye.

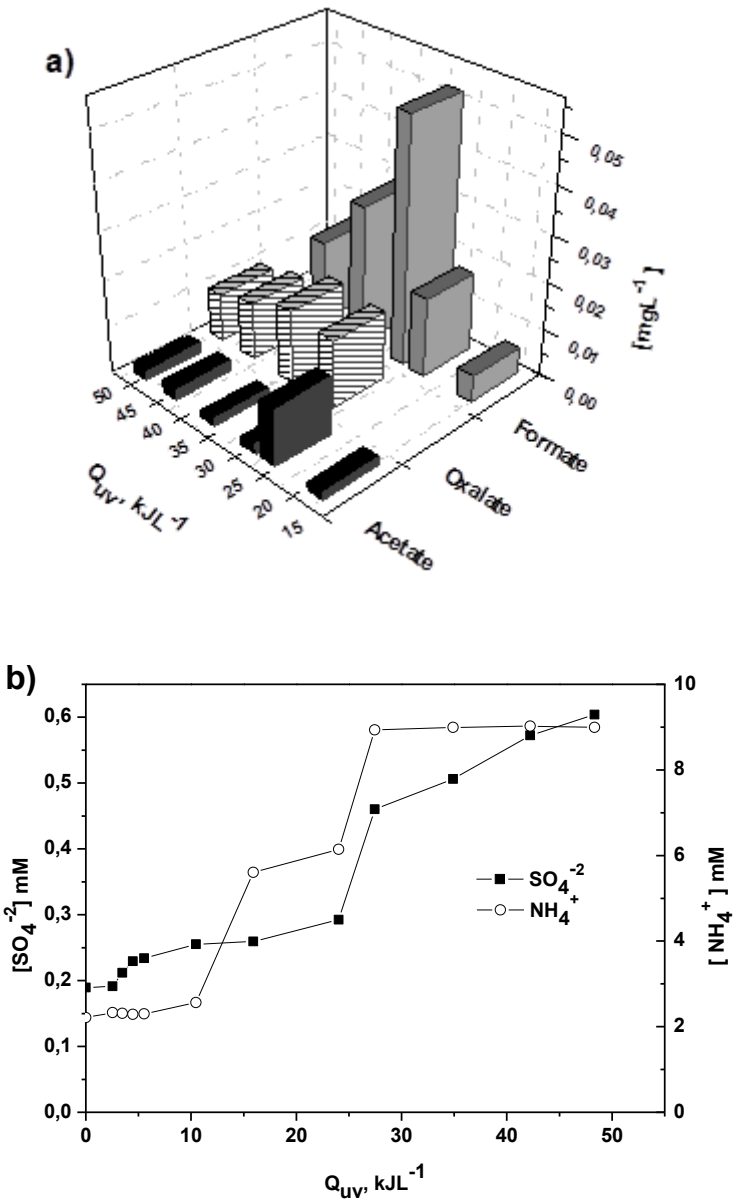

Fig. 10. Evaluation of the concentrations of (a) carboxylic acids; (b) SO_4^{-2} and NH_4^+ ions, followed by ion chromatography; formed during solar CPC photodegradation of 30 mgL^{-1} indigo carmine with supported TiO_2 in real MWWTP secondary effluent.

6.3.9 Ecotoxicity test with Eisenia andrei earthworms

Effect of different IC concentrations and its photoproducts on the biomass gains and mortality of the earthworms were studied. The mortality in all IC concentrations was found to be 0% as no death was observed. The biomass loss effect was observed at all concentrations when compared to control (see Fig. 11a). However, no significant difference ($p > 0.05$) of reduction in mean weight earthworms was observed from the paper treated with different concentrations of IC. Toxicity tests with earthworms were also carried out for the photodegradation products of IC, no mortality was observed after 24h exposure for different treatments. The effect on the reduction of weight can be shown in Fig. 11b. The difference of masses observed between initial time (t=0 min) and 24h of exposure, did not show significant difference according to ANOVA analysis ($p > 0.05$), for control and all photodegradation times (60, 120, 180, 300 min). These results suggest that the presence of IC and its photoproducts no demonstrated effect on the earthworms for acute contact test (24h). However, more tests must be performed for better available the IC toxicity for *Eisenia andrei*.

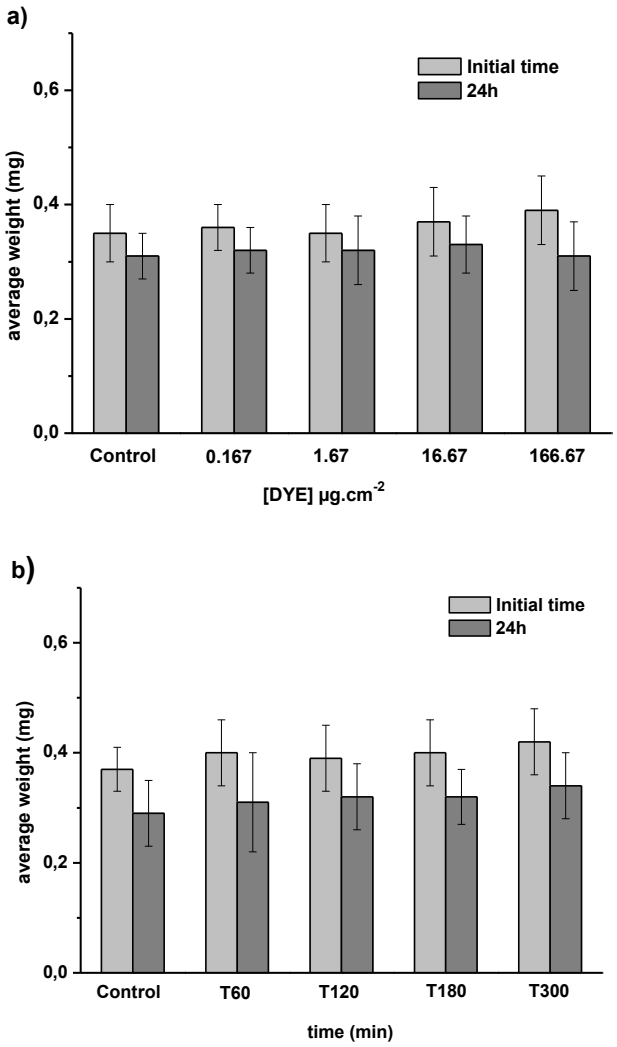

Fig. 11. Acute ecotoxicology test by *Eisenia andrei* earthworms; a) different initial IC concentrations; b) IC (80 mgL^{-1}) photoproducts at different times.

6.4 Conclusions

Photocatalytic degradation of indigo carmine dye in the presence of titanium dioxide was performed under different conditions. Results indicated that the photocatalytic degradation of IC in water with powdered TiO_2 depend of various parameters, as concentration of dye, amount of photocatalyst, presence of inorganic

anions, solution pH, temperature and hydrogen peroxide. It was found, that the optimal amount of catalyst to be used was 0.1 gL^{-1}. Concerning the different initial dye concentration, caused a significant absorption of light leaded to a decrease in photodegradation. Several inorganic anions were tested competing for the active sites on the TiO_2 surface. The temperature demonstrated to be dependent disfavoring IC remove. The photodegradation is favored in acidic solution. The recycling of TiO_2 can be performed with the photocatalyst being able to be adequately used in other reactions. A TiO_2 catalyst supported on glass beads demonstrated to have high efficiency to remove IC in different water matrices. However, it was also demonstrated the strong influence of the water matrix on IC photocatalytic degradation. Oxalate, acetate, formate acids were detected during photocatalysis of IC. The IC acute toxicity test (24h) and its photoproducts no demonstrated effect on the earthworms.

Acknowledgments: E.M. Saggioro thanks ENSP/FIOCRUZ and Ciência sem Fronteiras for scholarship and Plataforma Solar de Almería. J.C. Moreira thanks Faperj and CNPq. The authors thank P.C.G. Pereira for the assistance with ecotoxicological tests.

6.5 References

Aarthi T, Narahari P, Madras G, Photocatalytic degradation of Azure and Sudan dyes using nano TiO_2, *J. Hazard. Mater. 2007, 149,* 725-734.

Al-Ekabi H, Serpone N, Photocatalytical degradation of chlorinated phenols in aerated aqueous solutions over TiO_2 supported on a glass matrix, *J. Phys. Chem. 1998, 92 (20),* 5726-5731.

Andreotti A, Bonaduce L, Colombini M.P, Ribechini E, Characterisation of natural indigo and shellfish purple by mass spectrometric techniques, *Rapid Commun. Mass Spectrom. 2004, 18 (11),* 1213-1220.

Andronic L, Duta A, TiO_2 thin films for dyes photodegradation, *Thin Solid Films 2007, 515,* 6294-6297.

Augugliaro V, Baiocchi C, Prevot A.B, García-López, Loddo V, Malato S, Marcí G, Palmisano L, Pazzi M, Pramauro E, Azo-dyes photocatalytic degrdation in aqueous suspension of TiO_2 under solar irradiation, *Chemosphere 2003, 49 (10),* 1223-1230.

Barka N, Assabbane A, Nounah A, Aîlchou Y, Photocatalytic degradation of índigo carmine in aqueous solution by TiO_2-coated non-woven fibres, *J. Hazard. Mater. 2008, 152 (3),* 1054-1059.

Behnajaday M.A, Modirhahla N, Daneshvar N, Rabban M, Photocatalytic degradation of an azo dye in a tubular continuous-flow photoreactor with immobilized TiO_2 on glass plates, *Chem. Eng. J. 2007, 127 (1-3),* 167-176.

Clesceriv L.S, Greenberg A.E, Eaton AD, Standard Methods for the Examination of Water and Wastewater. American Public Health Association, 1998, Washington, DC.

Chen C, Wang Z, Ruan S, Zou B, Zhao M, Wu F, Photocatalytic degradation of C.I. Acid Orange 52 in the presence of Zn-doped TiO_2 prepared by a stearic acid gel method, *Dyes Pigm. 2008, 77,* 204-209.

Correia F.V, Moreira J.C, Effects of Glyphosate and 2,4-D on Earthworms (*Eisenia foetida*) in Laboratory Tests. *Bull. Environ. Contam. Toxicol. 2010, 85,* 264-268.

Daneshvar N, Rabbani M, Modirshahla N, Behnajady M.A, Kinetic modeling of photocatalytic degradation of Acid Red 27 in UV/TiO_2 process, *J. Photoch. Photobio. A: chemistry 2004, 198,* 39-45.

Dostanic J.M, Loncarevic D.R, Bankovic P.T, Cvetkovic O.G, Jovanovic D.M, Mijin D.Z, Influence of process parameters on the photodegradation of synthesized azo pyridine dye in TiO_2 water suspensions under simulated sunlight, *J. Environ. Sci. Health 2011, 46 (1),* 70-79.

Fernádez P, Blanco J, Sichel C, Malato S, Water disinfection by solar photocatalysis using compound parabolic collectors, *Catal. Today, 2005, 101,* 345-352.

Fujishima X, Zhang CR, Titanium dioxide photocatalysis: Present situation and future approaches, *Chimie 2006, 9 (5),* 750-760.

Fujishima A, Rao T.N, Tryk D.A, Titanium dioxide photocatalysis, *J. Photochem. Photobiol. C: Photochemical. Rev. 2000, 1 (1)* 1-21.

Gemeay A.H, Mansour L.A, El-Sharkawry R.G, Zaki A.B, Kinetics and mechanism of the heterogeneous catalysed oxidative degradation of indigo carmine, *J. Mol. Catal. A: Chem. 2003, 193,* 109:120.

Guillard C, Disdier J, Monnet C, Dussaud J, Malato S, Blanco J, Maldonado M.I, Herrmam J.M, Solar efficiency of a new deposited titania photocatalyst: chlorophenol, pesticide and dye removal applications, *Appl. Catal. B-Environ. 2003, 46,* 319-332.

Guohong X, Guoguang L, Dezhi S, Liqing Z, Kinetics of Acetamiprid Photolysis in Solution, *Bull. Environ. Contam. Toxicol. 2009, 82,* 129-132.

Habibi M.H, Hassanzadeh A, Mahdavi S, The effect of operational parameters on the photocatalytic degradation of three textile azo dyes in aqueous TiO_2 suspensions, *J. Photoch. Photobio. A. 2005, 172,* 89-96.

Hoffman M.R, Martin S.T, Choi W.Y, Bahnemann D.W, Environmental applications of semiconductor photocatalysis, *Chem. Rev. 1995, 95 (1),* 69-96.

Huang M, Xu C, Wu Z, Huang Y, Lin J, Wu J, Photocatalytic discolorization of methyl orange solution by Pt modified TiO_2 loaded on natural zeolite, *Dyes Pigm. 2008, 77,* 327-334.

ISO 11268-1 (2007) Soil quality - Effects of pollutants on earthworms - Part 1: Determination of acute toxicity to Eisenia fetida/Eisenia Andrei.

Jenkins C.L, Textile dyes are potential hazards, *Arch. Environ. Health 1978, 40 (5),* 7-12.

Jiménez M, Maldonado M.I, Rodríguez E.M, Hernández-Ramírez A, Saggioro E, Carra I, Sánchez-Pérez J, A supported TiO_2 solar photocatalysis at semi-pilot scale: degradation of pesticides found in citrus processing industry wastewater, reactivity and influence of photogenerated species, *J. Chem. Technol. Biot. 2014*, In press.

Konstantinou I.K, Albanis, T.A, TiO_2-assisted photocatalytic degradation of azo dyes in aqueous solution: Kinetic and mechanistic investigations. A review, *Appl. Catal. B Environ. 2004, 49 (1),* 1-14.

Khataee A.R, Vatanpour V, Amani A.R, Decolorization of C.I. Acid Blue 9 solution by UV/Nano-TiO2, Fenton, Fenton-like, electro-Fenton and electrocoagulation processes: A comparative study, *J. Hazard. Mater. 2009, 161 (2-3),* 1225-1233.

Lapertot M, Pulgarin C, Fernández-Ibánez P, Maldonado M.I, Pérez-Estrada L, Oller I, Gernjak W, Malato S, Enhancing biodegradability of priority substances (pesticides) by solar photo-Fenton, *Water Res. 2006, 40,* 1086–1094.

Liu G, Wu T, Zhao J, Hidaka H, Serpone N, Irreversible degradation of Alizarin Red under visible light radiation in air-equilibrated aqueous TiO_2 dispersions, *Environmental Science & Technology 1999, 33 (12),* 2081-2087.

Mahmoodi N.M, Arami M, Limaee N.Y, Gharanjig K, Ardejani F.D, Decolorization and mineralization of textile dyes at solution bulk by heterogeneous nanophotocatalysis using immobilized nanoparticles of titanium dioxide, *Colloid Surface A. 2006, 290,* 125-131.

Miranda-García N, Suárez S, Sánchez B, Coronado J.M, Malato S, Maldonado M.I, Photocatalytic degradation of emerging contaminants in municipal wastewater treatment plant effluents using immobilized TiO_2 in solar pilot plant, *Appl Catal B: Environ 2011, 103,* 294-301.

Oliveira A.S, Saggioro E.M, Barbosa N.R, Mazzei A, Ferreira L.F.V, Moreira J.C, Surface Photocatalysis: A Study of the Thickness of TiO_2 Layers on the Photocatalytic Decomposition of Soluble Indigo Blue Dye, *Rev. Chim. 2011, 62 (4),* 462-468.

OECD (1984) Earthworm, Acute Toxicity Tests (207). Guideline for testing of chemicals. Adopted: 04.04.1984

Paoletti M.G, The role of earthworms for assessment of sustainability and as bioindicators, *Agr. Ecosyst. Environ. 1999, 74,* 137-155.

Robinson T, McMullan G, Marchant R, Nigam P, Remediation of dyes in textile effluent: a critical review on current treatment technologies with a proposed alternative, *Bioresour. Technol. 2001, 77 (3),* 247-255.

Rodríguez E.M, Fernández G, Klamerth N, Maldonado M.I, Álvarez P.M, Malato S, Efficiency of different solar advanced oxidation processes on the oxidation of bisphenol A in water, *Appl. Catal. B: Environ. 2010, 95,* 228-237.

Saggioro E.M, Oliveira A.S, Pavesi T, Maia C.G, Ferreira L.F.V, Moreira J.C, Use of Titanium Dioxide Photocatalysis on the Remediation of Model Textile Wastewaters Containing Azo Dyes, *Molecules 2011, 16 (12),* 10370-10386.

Saien J, Soleymani A.R, Degradation and mineralization of Direct Blue 71 in a circulating upflow reactor by UV/TiO_2 process and employing a new method in kinetic study, *J. Hazard. Mater. 2007, 144,* 506-512.

Sano T, Puzenat E, Guillard C, Geantet C, Matsuzawa S, Degradation of C_2H_2 with modified-TiO_2 photocatalysts under visible light irradiation, *J. Mol. Catal. A: Chem. 2008, 284,* 127-133.

Sanromán M.A, Pazos M, Ricart M.T, Cameselle C, Electrochemical decolourisation of structurally different dyes, *Chemosphere 2004, 57 (3),* 233-239.

Santiago D.E, Dona-Rodríguez J.M, Arana J, Fernández-Rodríguez C, González-Díaz O, Pérez-Pena J, Silva A.M.T, Optimization of the degradation of imazalil by photocatalysis: Comparison between comercial and lab-made photocatalysts, *J. Appl. Catal. B: Environ. 2013, 138-139,* 391-400.

Saquib M, Abu Tariq M, Haque M.M, Muneer M, Photocatalytic degradation of disperse blue 1 using UV/TiO_2/H_2O_2 process, *J. Environ. Manage. 2008, 88,* 300-306.

US EPA (1996) Ecological effects test guidelines - Earthworm Subchronic Toxicity Test. United States Environmental Protection Agency Federal Register, 96, 167.

Vautier M, Guillard C, Herrmann J, Photocatalytic Degradation of Dyes in Water: Case Study of Indigo Carmine, *J. Catal. 2001, 201 (1),* 46-59.

Velmurugan R, Swaminathan M, An efficient nanostructured ZnO for dye sensitized degradation of Reactive Red 120 dye under solar light, *Sol. Energ. Mat. Sol. C. 2011, 95 (3),* 942-950.

Wang C, Lee C, Lyu M, Juang L, Photocatalytic degradation of C.I. Basic Violet 10 using TiO_2 catalysts supported by Y zeolite: An investigation of the effects of operational parameters, *Dyes Pigm. 2008, 76,* 817-824.

Zainal Z, Hui L.K, Hussein M.Z, Taufiq-Yap Y.H, Abdullah A.H, Ramli I, Removal of dyes using immobilized titanium dioxide illuminated by fluorescent lamps, *J. Hazard. Mater. 2005, 125 (1-3),* 113-120.

Zhang R, Vigneswaran S, Ngo H, Nguyen H, A submerged membrane hybrid system coupled with magnetic ion exchange (MIEX®) and flocculation in wastewater treatment, *Desalination 2007, 216,* 325-333.

Zhao J, Wu T, Wu K, Oikawa K, Hidaka H, Serpone N, Photoassisted degradation of dye pollutants. 3. Degradation of the cationic dye rhodamine B in aqueous anionic surfactant/TiO_2 dispersions under visible light irradiation: evidence for the need of substrate adsorption on TiO_2 particles, *Environ. Sci. Technol. 1998, 32,* 2394-2400.

7. ARTIGO 5

Research Article

In press, aceito para publicação em 28/02/2014

Environmental Science and Pollution Research

ISSN: 0944-1344 (print version)

ISSN: 1614-7499 (electronic version)

Solar CPC pilot plant photocatalytic degradation of Bisphenol A in waters and wastewaters using suspended and supported-TiO_2. Influence of photogenerated species

Enrico Mendes Saggioro[1]*, Anabela Sousa Oliveira[2,3], Thelma Pavesi[1], Margarita Jiménez Tototzintle[4], Manuel Ignacio Maldonado[4], Fábio Verissimo Correia[5], Josino Costa Moreira[1]

1 – CESTEH - Centro de Estudos da Saúde do Trabalhador e Ecologia Humana, Escola Nacional de Saúde Pública - Fundação Oswaldo Cruz, Av. Leopoldo Bulhões, 1480, 21041-210, Rio de Janeiro, Brazil.

2 – CQFM - Centro de Química-Física Molecular e IN - Instituto de Nanociencias e Nanotecnologia, Instituto Superior Técnico, Universidade Técnica de Lisboa, Av. Rovisco Pais 1049-001, Lisbon, Portugal.

3 – C3i - Centro Interdisciplinar de Investigação e Inovação - Escola Superior de Tecnologia e Gestão, Instituto Politécnico de Portalegre, Lugar da Abadessa, Apartado 148, 7301-901 - Portalegre, Portugal.

4- CIEMAT – Centro de Investigaciones Energéticas, Medioambientales y Tecnológicas, Plataforma Solar de Almería, Carretera Sénes, km 4, 04200 Tabernas (Almería), Spain.

5- UNIRIO - Universidade Federal do Estado do Rio de Janeiro, Av. Pasteur, 296 22290-240, Rio de Janeiro, Brazil.

Abstract

Photocatalytic degradation of Bisphenol A (BPA) in waters and wastewaters in the presence of titanium dioxide (TiO_2) was performed under different conditions. Suspensions of the TiO_2 were used to compare the degradation efficiency of BPA (20 mgL^{-1}) in batch and CPC reactors. A TiO_2 catalyst supported on glass spheres beads was prepared (sol-gel method) and used in a CPC solar pilot plant for the photodegradation of BPA (100 μgL^{-1}). The influence of $OH^{\bullet}$, $O_2^{\bullet-}$, h^+ on the BPA degradation were evaluated. The radicals $OH^{\bullet}$ and $O_2^{\bullet-}$ were proved to be the main species involved on BPA photodegradation. Total organic carbon (TOC) and carboxylic acids were determined to evaluate the BPA mineralization during the photodegradation process. Some toxicological effects of BPA and its photoproducts on *Eisenia andrei* earthworms were evaluated. The results show that the optimal concentration of suspended TiO_2 to degrade BPA in batch or CPC reactors was 0.1 gL^{-1}. According to biological tests the BPA LC_{50} in 24h for *Eisenia andrei* was of $1.7x10^{-2}$ $mg.cm^{-2}$. The photocatalytic degradation of BPA mediated by TiO_2 supported on glass spheres suffered strong influence of the water matrix. On real MWWTP secondary effluent, 30% of BPA remains in solution; nevertheless the method has the enormous advantage since it eliminates the need of catalyst removal step, reducing the cost of treatment.

Keywords: Bisphenol A, *Eisenia andrei* earthworms, Immobilized TiO_2, Real wastewater, Solar pilot plant, Wastewater reuse.

7.1 Introduction

The environmental pollution caused by residues of endocrine disrupting chemicals mainly in water sources and factory effluents has aroused the public concern in recent years (Miranda-García et al. 2010; Oliveira et al. 2012). Bisphenol A (4,4'-dihydroxy-2,2-diphenylpropane) is included in the list of chemicals with endocrine disrupting character (estrogenic activity), and therefore has received wider attention (Tsai 2006). Several dairy products such as plastic packing, baby bottles, drinking water bottles, water pipes, lining of food cans, dental sealant, and plastic orthodontic brackets contain BPA (Cooper et al. 2011). It has been reported that the most important routes for environmental contamination (specially the aquatic system) by BPA include, effluents from municipal wastewater treatment plants (MWWTP), waste landfill sites and migration from BPA-based product. The BPA concentration found in water bodies is generally in the 0.1-20.0 μgL^{-1} concentration range concentration (Kang et al. 2007; Staples et al.1998). As expected, BPA environmental contamination is highly widespread (Ptak et al. 2011) and it is able to induce hormone-related effects including altered peripubertal mammary gland development in mice, early puberty in females, and feminization in males (Yamagushi et al. 2005). Additionally, it was reported that BPA metabolites have shown *in vivo* xenoestrogenic toxicity when administrated to Japanese medaka fish (Nah et al. 2011). The scientific response has been the development of efficient removal methods of endocrine disrupting chemicals from wastewater effluents. Thus, efforts have been devoted to develop suitable treatment methods that can remove or destroy these bio-recalcitrant organic contaminants in water by biological processes

(Zhao et al. 2008), chemical oxidation (Nakada et al. 2007) and advanced oxidation process (AOPs) (Gueltekin and Ince 2007). Biological treatments are inefficient for complete removal of endocrine disruptors during wastewater treatments reason why they are ubiquitous in MWWTP effluents at low concentrations (Miranda-García, et al. 2011).

Methods of wastewater treatment based on the generation of reactive species for destructive oxidation of organic pollutants are being considered as promising techniques for removing endocrine disruptors from effluents originated from biological treatment plants and/or surface waters. In particular, the use of titanium dioxide (TiO_2) a well-know photocatalyst with many applications in photoreactions for treatment of pollutants in wastewater (Fujishima et al. 2000). The use of TiO_2 has attracted attention as an efficient method for degrading the recalcitrant contaminants in water, because it can promote the degradation of different target organic compounds from industrial effluents with little change of operational parameters and nearly mineralize them using radiation with energy in the near-UV range (Chen et al. 2008; Wang et al. 2008). On the other hand, titanium dioxide has advantages such as low cost, high activity, insolubility, resistance to corrosion and non-specific oxidative attack ability (Tsai et al. 2009).

With regard to degradation process of BPA by photocatalysis mediated by TiO_2, few studies reported available in the literature involve concentrations in the range of μgL^{-1} of BPA, influence of the matrix on photodegradation efficiency, evaluation of the toxicity of its photoproducts by ecotoxicological tests. Additionally, very few studies were performed in large-scale applications with TiO_2 immobilized onto a suitable solid inert material, which eliminates the catalyst removal step as required when using TiO_2

suspensions. This step limits process development because it needs a time-consuming expensive (Mahmoodi et al. 2006).

Tsai et al. (2009) investigated the photodegradation efficiency of BPA under controlled process parameters in a batch TiO_2 suspension reactor. They found optimal conditions for the photoreaction process with at initial BPA concentration of 20 mgL^{-1}, a TiO_2 amount of 0.5 gL^{-1}, an initial pH=7.0 and temperature of 25°C. Rodríguez et al. (2010) investigated the efficiency of different solar oxidation processes on the degradation of BPA using a CPC (compound parabolic collector) reactor and studied the evolution of toxicity by measuring the luminescence inhibition of the marine bacterium *V. fischeri*. They found that, at pH 3, Fenton and photo-Fenton systems were the most effective in BPA degradation, but at the same pH the highest mineralization was achieved by photo-Fenton and TiO_2/Fe(III) systems. However, at pH 6.5, the highest BPA degradation was found for Fe(III)/oxalic acid and TiO_2/UV system. Additionally, the results indicated that some of the phenolic intermediates formed could be more toxic than BPA. Wang et al. (2009) searched for the optimum parameters for BPA degradation in a horizontal circulating bed photocatalytic reactor (HCBPR) with TiO_2 immobilized on the surface of polyurethane foam cubes via microwave-assisted liquid phase deposition. The results demonstrated that under optimum conditions, 95% removal of total organic carbon (TOC) and 97% removal of BPA after 6 h of UV irradiation. Daskalaki et al. (2011) investigated the degradation of BPA under artificial solar light over immobilized TiO_2/Ti-film by sol-gel method or deposition from Degussa-P25 slurry. They found that process performance is affected by several factors and that the stability of the immobilized catalysts is dependent on the preparation

method, and demonstrated that the catalyst prepared by sol-gel method was highly stable. To clarify the relationship between the variations in estrogenic activity of the intermediates and the BPA degradation pathways, Nomiyama et al. (2007) decomposed BPA by TiO_2 oxidation and analyzed photoproducts by gas chromatography (CG) mass spectrometry (MS) and liquid chromatography coupled to mass spectrometry (LC-MS). Estrogenic activities of the photodegradation products were assessed by using hybrid assay system for human and fish estrogen receptor. They observed hydroxylated-BPA, carboxylic and phenolic intermediates produced by cleavage of a benzene ring. On the other hand, the estrogenic activity was reduced to less than 20% of initial activity of BPA after 240 min of UV irradiation. However, estrogenic activity of BPA for fish receptors increased by 110% at 60 min of UV irradiation, evidencing that the photoproducts of BPA oxidation can behave as xenoestrogen to the aquatic wildlife in the environmental.

On the basis of the above discussion and data, the main focus of this work was to study the photocatalytic degradation of BPA under different operation conditions. For this purpose, the photocatalytic treatment was carried out both in batch and compound parabolic collectors (CPC) reactors mediated TiO_2 in suspensions and supported on glass spheres. The photocatalytic oxidation with TiO_2 supported was performed for different water matrices in solar CPC pilot plant in order to evaluated the main photoreactive species ($OH^{\bullet}$, $O_2^{\bullet -}$, h^+) involved in the BPA degradation.

The release of BPA into the environment can also occur through the application of biosolids to agricultural land. This compound is considered relatively hydrophobic, with a log K_{ow} of 3.32; therefore, it is likely to have a high affinity to the solid phase in

soils and biosolids (Langdon et al. 2013). Biosolids may contain a broad range of organic contaminants that can be unintentionally applied to agricultural land when biosolids are used as a replacement or supplement for inorganic fertilisers. BPA have been detected in biosolids in a concentration range up to 4.6 mg kg^{-1} (Langdon et al. 2011). For this reason, ecotoxicological testes with *Eisenia andrei* earthworms were performed. The earthworms are affected by a variety of organic and inorganic compounds, which may suffer bioaccumulation. Its preliminary results serve as a rapid indicator of the presence of toxic compounds and can be used as complementary test for risk assessment of polluted areas (Paoletti 1999). Additionally, *Eisenia andrei* has been chosen as a monitoring species, because it easily reproduces in laboratory, it was approved by the European Union, Organization for Economic Co-operation and Development (OECD) for use in toxicity tests and has been used by the U.S. Environmental Protection Agency (EPA) as a wide test for contaminant residues in several polluted sites (Correia and Moreira 2010).

7.2 Experimental

7.2.1 Products, experimental set-up and procedure

All chemicals were analytical grade and used as received. Bisphenol A (99% analytical grade) was supplied by Sigma-Aldrich. Powdered P25 TiO_2 (surface area 51-55 m^2 g^{-1}) was supplied by EVONIK (former Degussa), Nanopowder Anatase 99.7% (surface area 45-55 m^2 g^{-1}, size <25nm) and Rutile 99.99% (size < 100nm) were

supplied by Sigma-Aldrich. 2-propanol (C_3H_8O), potassium iodide (M.W. = 166 $gmol^{-1}$) and Tiron (4,5-Dihydroxy-1,3-benzenedisulfonic acid disodium salt) were supplied by Sigma-Aldrich.

BPA was spiked in different types of water: distilled water, synthetic moderately-hard freshwater (Clesceriv et al. 1998), synthetic secondary municipal wastewater treatment plant (MWWTP) effluent (Zhang et al. 2007), and a real secondary biological treatment from the "El Bobar" MWWTP (Almería, Spain) and used the following day to collection.

Artificially irradiated photocatalytic experiments were carried out in batch magnetically stirred reactor irradiated with a high-pressure 125 W mercury vapor lamp. These experiments were performed using different amounts of TiO_2 P25 and 0.1 gL^{-1} of anatase and rutile nanopower. Furthermore, in order to determine the main species involved in the photocatalysis degradation of BPA, scavengers were add in the solution. The efficient photon flux was determined measuring the radiant flux (in Wcm^{-2}) at the surface of the sample being treated with a radiometer (Cole-Parmer Instrument Co.; model 9811-50).

Solar photocatalytic experiments were carried out in two steps using a pilot plant reactor with CPC optics installed at Plataforma Solar de Almería (PSA, latitude 37ºN, longitude 2.4ºW). The first step was performed (20 mgL^{-1} of BPA added; different concentrations of TiO_2 suspensions) in a 32-L pilot plant (22 L illuminated volume, 3.08 m^2 total irradiated surface). The pilot plant consists of two compound parabolic collectors (CPCs), a continuously stirred tank, a centrifugal recirculation pump (20 L

min^{-1}) and connecting tubing and valves. Each collector consists of borosilicate glass tubes connected in series (inner diameter 30.0 mm, outer diameter 31.8 mm, length 1.41 m, 12 tubes) and mounted on a fixed platform tilted 37ºN (local latitude) (Lucas et al. 2009)

Since the concentrations of BPA in environment are relatively low, the second step was performed using 100 μgL^{-1} of BPA added at different water matrices as described above. TiO_2 catalyst was supported on glass spheres. The CPC reactor, which had sixteen DURAN^{TM} glass tubes (28.45 mm inner diameter), was modified to work with only two of the glass tubes (8 L total volume and 0.250 m^2 total irradiated surface). These two glass tubes were uniformly packed with the glass spheres (~ 4600 spheres per tube, ~ 0.6 mg of TiO_2 on the surface of each glass spheres). The pump flow was 2.5 L min^{-1} and the tank continuously stirred (Jiménez et al. 2014).

At the beginning of the experiments, while collectors were kept covered, the chemicals were added to the tank and mixed by recirculating the water to reach constant concentration throughout the system. Then the covers were removed from the collectors and samples were collected at predetermined times of solar irradiation. The temperature inside the reactor was continuously recorded by a Pt-100 temperature probe. A global UV radiometer (KIPP&ZONEN, model CUV 3, the Netherlands), also tilted 37º, was used for measuring global solar UV radiation intensity (UV_G) in terms of incident $Wuv.m^{-2}$. Once UV_G is known, the total UV energy received on a surface in the same position with regard to the sun per unit of volume of water inside the reactor during the interval Δt can be determined by applying Eq. (1) (Rodríguez et al. 2010):

$$Q_{UV,n} = Q_{UV,n-1} + \Delta t_n UV_{G,n} \frac{A_i}{V_T} \quad ; \quad \Delta t_n = t_n - t_{n-1} \qquad (1)$$

Where t_n is the time corresponding to n water sample, V_T is the total reactor volume, A_i is the illuminated surface area and $UV_{G;n}$ is the average solar ultraviolet radiation measured during the period Δt_n. All experiments were performed in duplicate.

Supported-TiO_2 photocatalyst was prepared by sol-gel technique (Sirisuk et al. 1999). Enough amount of distilled water was acidified with 13 mL of nitric acid and then titanium isopropoxide ($Ti(iOPr)_4$, TIOP) was added to the solution and the suspension was stirred for 24 h until complete peptization. The solution of 20 mgL^{-1} of polyethylene glycol was prepared in isopropanol and added to the TIOP sol under continuous magnetic stirring. The acid sol was dialyzed until a final pH of 2.4-2.5. Finally, 10 gL^{-1} of EVONIK P-25 TiO_2 were incorporated under continuous stirring. The glass spheres (Ø= 6 mm) were coated with TiO_2 sol by dip coating. Then the glass spheres were dried at 110ºC for 90 min and calcinated at 400ºC for 5 h (Miranda-García et al. 2010).

7.2.2 Analytical determinations

Bisphenol A (BPA) degradation was followed by UPLC-DAD (Agilent Technologies, series 1200) system in a reverse-phase C-18 analytical column (Agilent, XDB-C18, 1.8 µm, 4.6 x 50 mm). A mixture of ultrapure water and acetonitrile (60:40) was used as mobile phase (flow rate: 0.7 mL min^{-1}; injection volume: 100 µL).

Absorbance detection was made at 227 nm. In all cases, before UPLC analyse, 6 mL of sample were filtered (0.45 μm) and the filter was then washed with 4 mL of acetonitrile (ACN) for final volume of 10 mL (ratio 6:4 sample:ACN). TOC was measured in filtered samples (Millipore-PVDF 0.45 μm filters) with a Shimadzu-TOC-V SCN analyzer. Anion concentrations were determined with a Metrohm 872 Extension Module 1 and 2 ion chromatograph (IC) system configured for gradient analysis. Cation concentrations were determined with a Metrohm 850 Professional IC configured for isocratic analysis.

Photocatalytic degradation may generate toxic photoproducts and so they must be assessed in order to determine if the effluent treatment strategy is leading or not to the desired result. The ecotoxicity of the BPA and its photoproducts in different times was tested with *Eisenia andrei* earthworms. Organisms *Eisenia andrei* used in the tests were created in bovine manure, by the Ecotoxicology sector, of the Laboratory of Toxicology at the Center of Human Ecology and Occupational Health Studies (CESTEH), Oswaldo Cruz Foundation (Fiocruz). Prior to the experiments the earthworms were acclimated for at least 24h in environment testing, 22°C±1. The tests were performed with selected adult worms (less than 2 months of age and well-developed clitellum) and individual weight around 300-600 mg (ISO 11268-1 2012). The mean masses of earthworms survivors were compared by ANOVA (analysis of variance) with Bonferroni correction (alpha bilateral 0.05), using BioEstat 2.0.

Studies of acute toxicity (US EPA 1996; OECD 1984) were made using 15 replicates for each concentration by contacting each earthworm in a vial with filter

paper (60 cm^2) soaked with BPA solutions of different concentrations ($1x10^{-3}$, $1x10^{-2}$, 0.1 and 1 $mg.cm^{-2}$). The BPA solutions were prepared in 1 ml of methanol soaked on filter paper. Then methanol was evaporated for 24 hours and the paper was moistened with 1 ml of water. Identical procedure was used for the controls. The contaminated paper was transferred into a glass vessel and an earthworm was introduced into it. The vessels were sealed with perforated parafilm to enable oxygenation. After 24h of incubation, the containers were opened, survivor's earthworms were counted and weighted. Earthworms were classified as dead when they did not respond to a gentle mechanical stimulus. Identical experiments were performed using a BPA/$Ti0_2$ suspensions irradiated at different times (60, 90, 120, 180 and 300 min).

7.3 Results and Discussion

7.3.1 Photocatalytic degradation of BPA with TiO_2 suspensions

In order to compare the efficiency of TiO_2 suspensions of different concentrations in batch and CPC reactors, the effect of photocatalyst concentrations on the degradation of a constant concentration of Bisphenol A (20 mgL^{-1}) in water was investigated. The results are shown in Fig. 1. The rate of photocatalysis (increase in the efficiency) seems to be due to the increase in the total surface area, the number of photons absorbed by the catalyst to produce more e^-, h^+ and $OH^\bullet$ for both reactors. However, when TiO_2 was present in very high concentrations it may cause light

scattering and screening effects causing decrease of light penetration and consequently reducing the specific activity of the catalyst. Additionally, high concentration of the catalyst promoted agglomeration (particle-particle interaction) which may also reduce the catalyst activity (Jia et al. 2012; Kaneco et al. 2004). In this study, the optimum amount of catalyst for both reactors was found to be 0.1 gL^{-1}. This amount allowed evaluating the treatments in laboratorial model effluents of BPA and demonstrated to be a reliably estimated concentration with larger volumes of effluent in CPC reactor. The results demonstrated that CPC systems were more efficiency than batch reactor. For the same concentration of TiO_2 (0.1 gL^{-1}) the CPC reactor degraded 100% of BPA for an accumulated energy of 39 kJL^{-1}, whereas batch reactor needed 68.95 kJL^{-1} for removing only 85% of BPA. This result comes from CPC being a reactor that has the capacity of treatment several organic pollutants from large quantities of water because it has an optics design (concentration factor of 1) that allows to use both direct and diffuse radiation, this advantages improves the CPC optical efficiency (Rodríguez et al. 2010).

Additionally, the BPA photocatalytic degradation under main crystalline phases of TiO_2 alone was performed and results are also shown in Fig. 1. Both crystalline phases yield results of low photocatalytic efficiency for BPA. Nanopowder anatase (99.7%) and rutile (99.99%) crystalline phase removed only 28% and 10% of BPA for an accumulated energy of 64.65 and 66.39 kJL^{-1}, respectively. The TiO_2 photocatalytic activity depends on its intrinsic properties, such as band-gaps. Mitsionis and Vaimakis (2013) investigated the synthesis of TiO_2 under different conditions; variation of temperature and type of solvent. They found that, at 600°C, the mixture of both crystalline phases (61% anatase and 39% rutile) was formed whereas at 450°C only

anatase phase was produced. For them the resultant band-gap energies were 2.92 and 3.10 eV, respectively. These results agree with the low BPA photodegradation observed for experiments with only pure crystalline phases (anatase or rutile only), which have both higher energy band-gaps, thus lower photocatalytic activities. Moreover, recently some researchers proposed that it is the combination of both rutile stability and appropriated lifetime of anatase active species that enhances their photocatalytic activity (Sun and Smirniotis 2003).

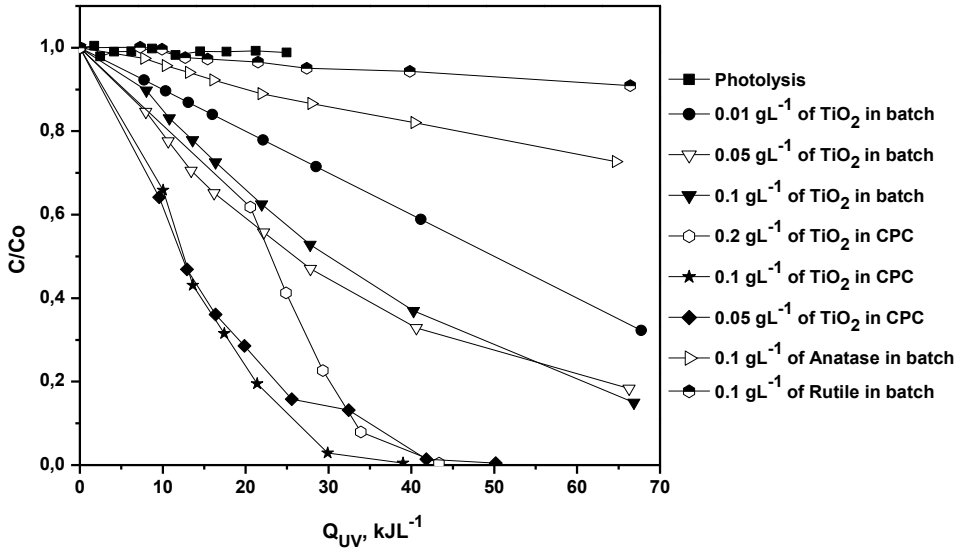

Fig. 1 Photocatalytic degradation of BPA (initial concentration: 20 mgL^{-1}) in batch and CPC reactors with anatase, rutile and P25 TiO_2 suspensions.

7.3.2 Solar CPC photocatalytic degradation using TiO_2 supported on glass spheres

Solar photodegradation at CPC pilot plant scale using TiO_2 supported on glass spheres was carried out of for BPA (100 µgL^{-1}) in all water matrices above described. The endocrine disruptor's concentrations in MWWTP effluents are in the low range

then the 100 μgL^{-1} of BPA was chosen between the minimum concentration required for UPLC analysis sensitivity for kinetics concentration and the need of using a concentration simulating real conditions in MWWTP effluents. Previously, others studies (Miranda-García et al. 2010, 2011) used the same method to produce TiO_2 supported on glass spheres, and characterized it by X-ray diffraction (XRD), thermogravimetric analysis (TGA), surface area determination (BET) and scanning electronic microscopy (SEM) analysis. It was also demonstrated its durability, repeatability and photoactivity for 15 emerging contaminants (five "cycles" or run of treatment).

The photocatalytic activity using supported TiO_2 and tested in solar CPC pilot plant for different water matrices with BPA is shown in Fig. 2. Approximately, 0.6 mg of TiO_2 was supported on the surface of each glass spheres. These results demonstrated strong influence of the water matrix on photocatalytic degradation of BPA. Thus, in distilled water BPA was completely degraded after on accumulated energy of 3.3 kJL^{-1} and for synthetic freshwater that was observed to be slightly longer (~ 9 kJL^{-1}) for total degradation, probably due to freshwater composition where some of the ions presents act having a negative effect on the photocatalytic degradation of BPA. When a more complex water matrix was used efficacy on BPA photodegradation clearly decreased. After an accumulated energy of 23.97 kJL^{-1} (corresponding to 240 min of solar irradiation), BPA remains still at concentration of 6.89 μgL^{-1} on synthetic MWWTP secondary effluent. When real MWWTP secondary effluent was tested the system showed to be inefficient to remove a significant amount of compound, with 28% of BPA remaining in water for an accumulated energy of 24.7 kJL^{-1}. This fact can be

explained due of the presence of different substances in the matrix (organics, carbonates, sulphate, chloride, etc. see Table 1). For example, carbonate (CO_3^{-2}) is commonly found in high concentrations in secondary biological treatment (Guohong et al. 2009) and it can behave as hydroxyl radical scavenger and/or became absorbed onto the catalyst surface (reducing available surface for degradation as thus reducing photoactivity) consequentially, the photodegradation rate of BPA decreases significantly. However, from all the tested waters it is evident that supported-TiO_2 use has enormous advantages once it eliminates the catalyst removal step and thus highly reduces the costs of treatment.

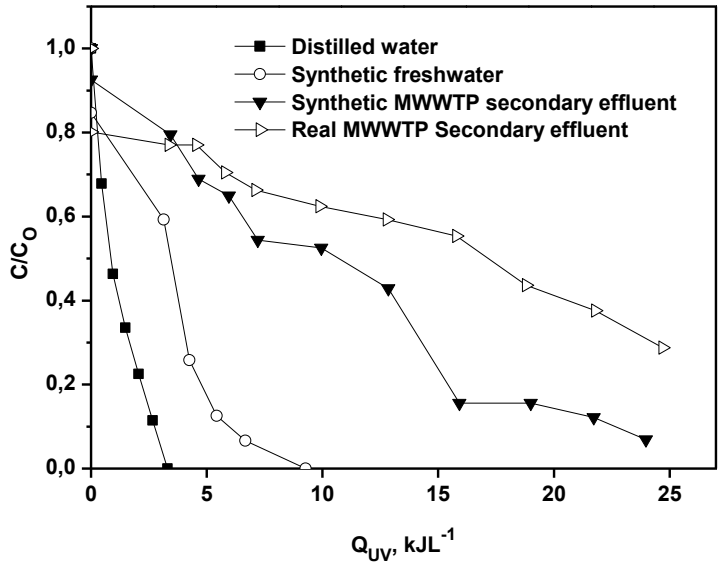

Fig. 2 Influence of the water matrix on Solar CPC photodegradation of BPA (initial concentration: 100 μgL^{-1}) mediated by TiO_2 supported on glass sphere.

Table 1 Physical and chemical characteristics of the different types of water used.

Type of water	Total Carbon (mgL^{-1})	Inorganic Carbon (mgL^{-1})	TOC (mgL^{-1})	pH	Conductivity ($\mu s\ cm^{-1}$)	Ionic species (mM)							
						Na^{+}	Ca^{+2}	Mg^{+2}	K^{+}	NH^{+4}	PO_4^{-3}	Cl^{-}	SO_4^{-2}
Fresh water moderately hard	17.24	13.89	3.4	7.58	241	1.09	0.34	0.44	0.07	—	—	0.06	1.18
Synthetic MWWTP secondary effluent	22.74	9.98	17.7	7.75	301	1.23	0.34	0.45	0.17	0.32	0.03		1.38
Real MWWTP secondary effluent	94.53	70.5	24.0	8.46	564	22.3	65.6	4.82	0.68	1.38	12.92	13.0	1.85

7.3.3 Species involved in TiO_2 photocatalytic degradation of BPA

According to solar activation mechanism semiconductor's different reactive species can be generated on BPA photodegradation, them the contribution each of these oxidative species was assessed using different scavengers. The participation of hydroxyl radicals ($OH^{\bullet}$) on the photocatalytic process was assesses with 2-propanol, 0.14 M (Zhao et al. 2013). Other oxidative specie is h^{+}, when adding potassium iodide (KI), 1.2 x 10^{-3} M, the iodide anions can be adsorbed on the TiO_2 surface and I^{-} oxidized to I_2 by reaction with h^{+} (Palominos et al. 2008). Beside this reactive species generated on photo-oxidation system, the participation of $O_2^{\bullet -}$ can be evaluated adding 3 x 10^{-5} M of Tiron ($C_6H_4Na_2O_8S_2$), which reacts with superoxide radical anions (Greenstock and Miller 1975). The $OH^{\bullet}$ radicals can oxidize KI and Tiron compounds, them both experiments were carried out also with 2-propanol, 0.14 M. Table 2 summarize the strategy to determine the participation of these oxidative species on BPA degradation. The experiments were performed in distilled water using TiO_2 (0.1 gL^{-1}) suspensions in the reactor irradiated with a high-pressure 125 W mercury vapor lamp.

Table 2 Strategy to determine the main reactive specie involved in BPA photocatalysis mediated by TiO_2 (Jimenéz et al. 2014).

Inhibited reactive species	Added Scavenger	Evaluation Mechanism
$OH^{\bullet}$	2-propanol (0.14 M)	Degradation occurs, participation of (e^-, $O_2^{\bullet-}$, H_2O_2, h^+)
h^+ and $OH^{\bullet}$	KI (1.2×10^{-3} M) and 2-propanol (0.14 M)	Degradation occurs, participation of (e^-, $O_2^{\bullet-}$, H_2O_2)
$O_2^{\bullet-}$ and $OH^{\bullet}$	Tiron (3×10^{-5} M) and 2-propanol (0.14 M)	Degradation occurs, participation of (e^-, H_2O_2, h^+)

The results of evaluation of reactive species in BPA (20 mgL^{-1}) photodegradation are shown in Fig. 3. As observed, both the adsorption of BPA on the catalyst surface as well as its UV photolysis was negligible. The BPA degradation with 0.1 gL^{-1} of TiO_2 revealed total removal of compound in Q_{uv} of 74.08 kJL^{-1}. However, the simultaneous presence of catalyst and 2-propanol drastically affects the degradation (70% of reaction was inhibited), therefore confirming that $OH^{\bullet}$ radicals play an important role on BPA photodegradation, nevertheless other species would contribute to the elimination of the pollutant. When tested the reaction in presence of 2-propanol and KI, the result of the photocatalytic experiments were similar to that conducted in presence of 2-propanol, indicating that probably, under these experimental conditions, the contribution of h^+ to the degradation of BPA is negligible. On the order hand, for the reaction conducted with 2-propanol and Tiron the elimination of BPA was more affected than the one just with 2-propanol indicating that most likely $O_2^{\bullet-}$ radicals also participated on elimination of BPA.

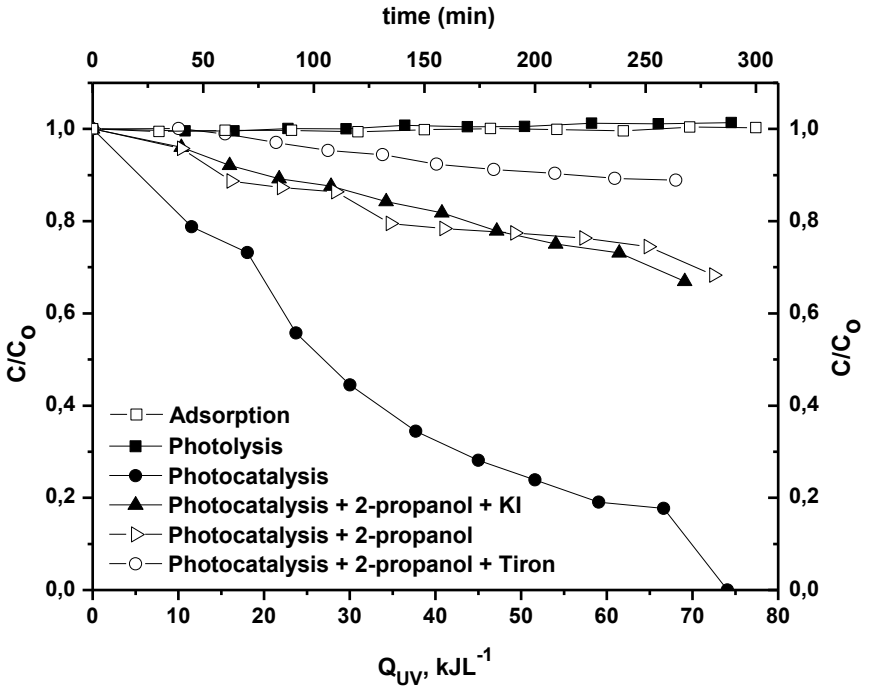

Fig. 3 Evaluation of reactive species involved in photodegradation of BPA (20 mgL^{-1}). Influence of the presence/absence of scavengers.

7.3.4 Mineralization of BPA

A solar CPC pilot plant BPA photocatalytic mineralization was monitored by measuring TOC and carboxylic acids for the different water matrices. The evaluation of TOC concentrations during photocatalytic decomposition is illustrated in Fig. 4a. It shows that TOC evolution is strongly dependent on water matrices. TOC for distilled water was totally removed in Q_{uv} of 13.39 kJL^{-1}. However, for other water matrices, respectively, 0.39, 0.53, and 0.58 % of TOC initial values remained for freshwater, synthetic and real MWWTP secondary effluent, at Q_{uv} ~ 24 kJL^{-1}. For the latter, the BPA was not entirely transformed into carbon dioxide and water, which implies the

formation of some organic intermediates. Thus, the UPLC chromatograms of the BPA samples under treatment, took from the photocatalytic reactor at different treatment times during the photocatalytic process, are illustrated in Fig. 5. The results show the disappearance of BPA and formation of its photodegradation products's peaks. The products have retention times shorter than BPA, which indicates that they are more polar than BPA. According to other authors (Tsai et al. 2009; Watanabe et al. 2003) the possible mechanisms for the photodegradation of BPA in water, involves an first step of initial photo-oxidation by reactive species ($OH^{\bullet}$ and $O_2^{\bullet-}$ as demonstrated in section 3.3) that promotes cleavage of electron-rich carbons in the phenyl groups of BPA, forming phenol radical ($^{\bullet}C_6H_4OH$) and isopropylphenol radical ($^{\bullet}C(CH_3)_2C_6H_4OH$). After, the phenol radical is converted to *p*-hydroquinone and at the same time, isopropylphenol radical is converted to 4-hydroxyphenyl intermediates. Furthermore, these single-aromatic intermediates were subsequently oxidized through ring-opening reactions into aliphatic acids. These results were demonstrated by ion chromatography, which evaluated the formation of carboxylic acids in photodegradation of BPA, as shown in Fig. 4b. Oxalate, acetate, formate, glycolate and maleate acids were detected during BPA photocatalysis. It can be seen that as photodegradation reaction proceeds successively smaller carboxylic acids are formed.

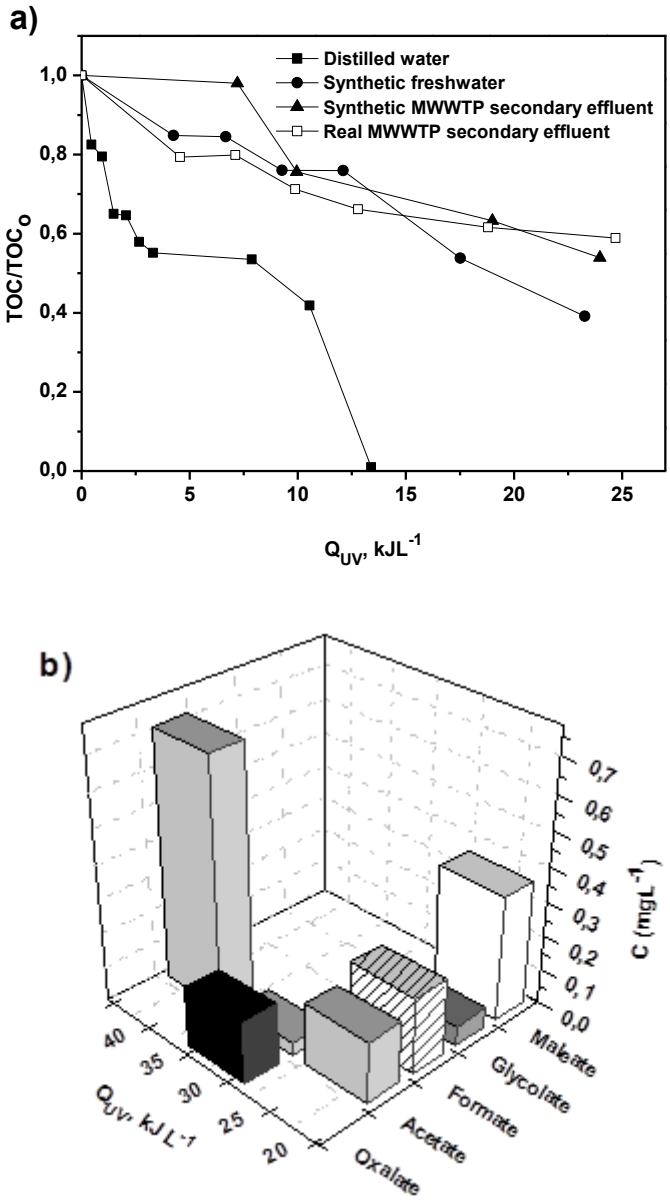

Fig. 4 Monitoring of BPA mineralization; (a) TOC evolution on different water matrices; (b) carboxylic acids formed, during solar CPC photodegradation.

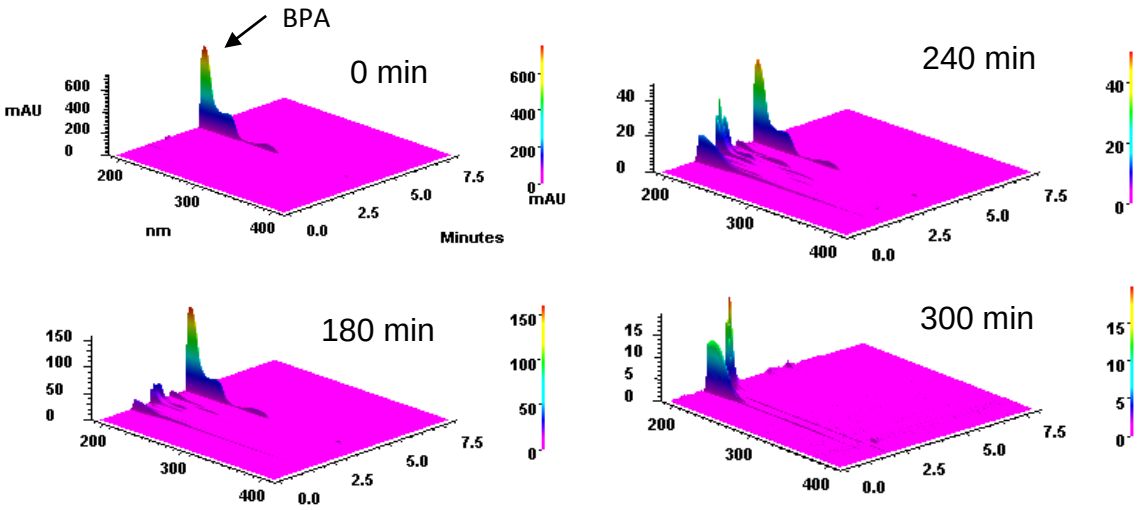

Fig. 5 UPLC chromatograms of BPA and its photodegradation products obtained from the photoreaction conditions of [TiO_2] = 0.1 gL^{-1}, C_o = 20 mgL^{-1}.

7.3.5 Ecotoxicological tests

Under laboratorial conditions, some effects were observed in earthworms put in contact with substrates containing BPA residues. In the acute toxicity test, earthworms put in contact with filter papers previously treated with different concentrations of BPA showed a reduction in mean weight and increase in mortality. These effects were more pronounced in higher concentrations of BPA as shown in Fig 6a. In all experiments a control test was simultaneously performed. The percentage of weight loss after 24h exposition was 18, 25, and 42% for control, $1x10^{-3}$ and $1x10^{-2}$ $mg.cm^{-2}$ of BPA, respectively. On the order hand, for higher concentrations of BPA (0.1 and 1 $mg.cm^{-2}$) 100% mortality was observed at the end of the experiment. The BPA acute toxicity test (24h) suggested a significant toxic effect for *Eisenia andrei* earthworms, since dermal absorption is the most important intake route in pollutants absorption by earthworms (Correia and Moreira, 2010). These results allowed estimate by Spearman-Karber

method a LC_{50} of $1.7x10^{-2}$ $mg.cm^{-2}$ for BPA. Toxicity tests with earthworms were also carried out during the photodegradation of BPA, no mortality was observed after 24h exposure for different treatments. The effect on the reduction of weight was time-dependent and can be shown in Fig. 6b. The difference of masses observed between initial time (t=0 min) and 24h of exposure, did not show significant difference according to ANOVA analysis ($p > 0.05$), for control and photodegradation time of 60 min. The exposure of earthworms to photodegradation products collected at different irradiation times (120, 180 and 300 min) demonstrated a significant reduction ($p < 0.05$) in weight loss after 24h exposure. These results suggest the increase of the weight effects by BPA photoproducts. However, more tests must be performed for better available the BPA toxicity for *Eisenia andrei*.

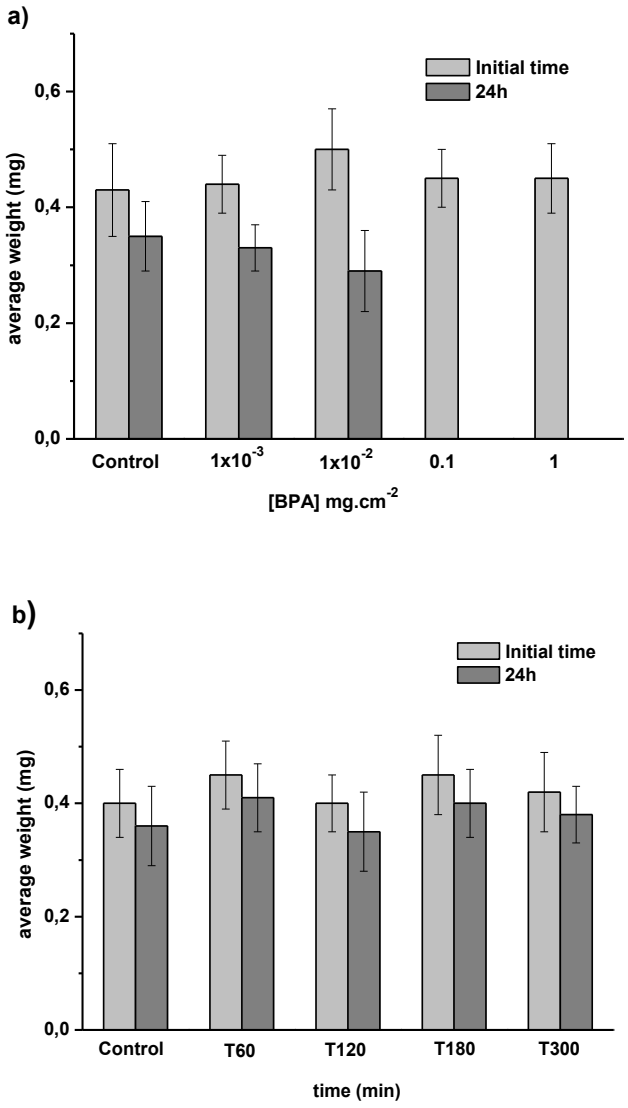

Fig. 6 Acute ecotoxicology test by *Eisenia andrei* earthworms; a) different initial BPA concentrations; b) BPA (20 mgL^{-1}) photoproducts at different times.

7.4 Conclusions

Photocatalytic degradation of Bisphenol A in the presence of titanium dioxide was performed under different conditions. 0.1 gL^{-1} suspended-TiO_2 was an optimal concentration to remove BPA (20 mgL^{-1}) for batch and CPC reactors. The main

crystalline phases of TiO_2 showed low photocatalytic activity for BPA, suggesting that the combination of both rutile stability and anatase active species lifetime together effectively enhances their photocatalytic activity. A TiO_2 catalyst supported on glass spheres demonstrated to have high efficiency to remove BPA (100 μgL^{-1}) in different water matrices. However, it was also demonstrated the strong influence of the water matrix on BPA's photocatalytic degradation, especially in real MWWTP secondary effluent. The $OH^{\bullet}$ and $O_2^{\bullet-}$ radicals were the main species involved on photodegradation of BPA. Oxalate, acetate, formate, glycolate and maleate acids were detected during photocatalysis of BPA. The BPA acute toxicity test (24h) demonstrated significant toxic effect for *Eisenia andrei* earthworms with LC_{50} of $1.7x10^{-2}$ $mg.cm^{-2}$. The effect on the reduction of weight for the photodegradation products was time-dependent. In conclusion, the photocatalytic degradation of BPA in the presence of TiO_2 process proves to be an efficient method for quickly lower the concentration of this endocrine disrupting compound in waters, moreover when supported-TiO_2 is used, which has the advantage of eliminating the catalyst removal step and reduce the costs of treatment.

Acknowledgments: E.M. Saggioro thanks ENSP/FIOCRUZ and Ciência sem Fronteiras for scholarship and Plataforma Solar de Almería. J.C. Moreira thanks Faperj and CNPq. The author thanks E.S Gonçalves for chromatography method development. The authors thank P.C.G. Pereira for the assistance with ecotoxicological tests.

7.5 References

Chen C, Wang Z, Ruan S, Zou B, Zhao M, Wu F (2008) Photocatalytic degradation of C.I. Acid Orange 52 in the presence of Zn-doped TiO_2 prepared by a stearic acid gel method. Dyes Pigm 77:204-209. doi: 10.1016/j.dyepig.2007.05.003

Clesceriv LS, Greenberg AE, Eaton AD (1998) Standard Methods for the Examination of Water and Wastewater. American Public Health Association, Washington, DC.

Cooper JE, Kendig EL, Belcher SM (2011) Assessment of bisphenol A released from reusable plastic, aluminium and stainless steel water bottles. Chemosphere 85:943–947. doi: 10.1016/j.chemosphere.2011.06.060

Correia FV, Moreira JC (2010) Effects of Glyphosate and 2,4-D on Earthworms (*Eisenia foetida*) in Laboratory Tests. Bull Environ Contam Toxicol 85:264-268. doi: 10.1007/s00128-010-00897

Daskalaki VM, Frontistis Z, Mantzavios D, Katsaounis A (2011) Solar light-induced degradation of bisphenol-A with TiO_2 immobilized on Ti. Catal Today 161:110-114. doi: 10.1016/j.cattod.2010.09.018

Fujishima A, Rao TN, Tryk DA (2000) Titanium dioxide photocatalysis. J Photoch Photobio C 1:1-21. doi: 10.1016/S1389-5567(00)00002-2

Greenstock CL, Miller RW (1975) The oxidation of tiron by superoxide anion. Kinetics of the reaction in aqueous solution and in chloroplasts. BBA - Bioenergetic 396:11-16. doi: 10.1016/0005-2728(75)90184-X

Gueltekin I, Ince NH (2007) Synthetic endocrine disruptors in the environment and water remediation by advanced oxidation processes J Environ Manage 85:816–832. doi: 10.1016/j.jenvman.2007.07.020

Guohong X, Guoguang L, Dezhi S, Liqing Z (2009) Kinetics of Acetamiprid Photolysis in Solution. Bull Environ Contam Toxicol 82:129-132. doi: 10.1007/s00128-008-9520-8

ISO 11268-1 (2007) Soil quality - Effects of pollutants on earthworms - Part 1: Determination of acute toxicity to Eisenia fetida/Eisenia Andrei

Jia C, Wang Y, Zhang C, Qin Q, Kong S, Yao S (2012) Photocatalytic Degradation of Bisphenol A in Aqueous Suspensions of Titanium Dioxide. Environ Eng Sci 29:630-637. doi: 10.1089/ees.2011.0132

Jiménez M, Maldonado MI, Rodríguez EM, Hernández-Ramírez A, Saggioro E, Carra I, Sánchez-Pérez J (2014) A supported TiO_2 solar photocatalysis at semi-pilot scale: degradation of pesticides found in citrus processing industry wastewater, reactivity and influence of photogenerated species. J Chem Technol Biot In press.

Kaneco S, Rahman MA, Suzuki T, Katsumata H, Ohta K (2004) Optimization of solar photocatalytic degradation conditions of bisphenol A in water using titanium dioxide. J Photochem Photobio B 163:419-424. doi: 10.1016/j.jphotochem.2004.01.012

Kang JH, Aasi D, Katayama Y (2007) Bisphenol-A in aquatic environment and its endocrine-disruptive effects on aquatic organisms. Crit Rev Toxicol 37:607–625. doi: 10.1080/10408440701493103

Langdon KA, Warne MJ, Smernik RJ, Shareef A, Kookana RS (2013) Comparison of degradation between indigenous and spiked bisphenol A and triclosan in a biosolids amended soil. Sci Total Environ 447:56-43. doi: 10.1016/j.scitotenv.2012.12.064

Langdon KA, Warne MJ, Smernik RJ, Shareef A, Kookana RS (2011) Degradation of 4-nonylphenol, 4-t-octylphenol, bisphenol A and triclosan following biosolids addition to soil under laboratory conditions. Chemosphere 84:1556-1562. doi: 10.1016/j.chemosphere.2011.05.053

Lucas MS, Mosteo R, Maldonado M I, Malato S, Peres JA (2009) Solar Photochemical Treatment of Winery Wastewater in a CPC reactor. J Agric Food Chem 57:11242–11248. doi: 10.1021/jf902581b

Mahmoodi NM, Arami M, Limaee NY, Gharanjig K, Ardejani FD (2006) Decolorization and mineralization of textile dyes at solution bulk by heterogeneous nanophotocatalysis using immobilized nanoparticles of titanium dioxide. Colloid Surface A 290:125-131. doi: 10.1016/j.colsurfa.2006.05.012

Miranda-García N, Maldonado MI, Coronado JM, Malato S (2010) Degradation study of 15 emerging contaminants at low concentration by immobilized TiO_2 in pilot plant. Catal Today 151:107-113. doi: 10.1016/j.cattod.2010.02.044

Miranda-García N, Suárez S, Sánchez B, Coronado JM, Malato S, Maldonado MI (2011) Photocatalytic degradation of emerging contaminants in municipal wastewater treatment plant effluents using immobilized TiO_2 in solar pilot plant. Appl Catal B: Environ 103:294-301. doi: 10.1016/j.apcatb.2011.01.030

Mitsionis AI, Vaimakis TC (2013) The effect of thermal treatment in TiO_2 photocatalytic activity. J Term Anal Calorim 112:621-628. doi: 10.1007/s10973-012-2631-9

Nah WH, Park MJ, Gye MC (2011) Effects of early prepubertal exposure to bisphenol A on the onset of puberty, ovarian weights, and estrous cycle in female mice. Clin Exp Reprod Med 38:75-81. doi: 10.5653/cerm.2011.38.2.75

Nakada N, Shinohara H, Murata A, Kiri K, Managaki S, Sato N, Takada H (2007) Removal of selected pharmaceuticals and personal care products (PPCPs) and endocrine-disrupting chemicals (EDCs) during sand filtration and ozonation at a municipal sewage treatment plant. Water Res 41:4373-4382. doi: 10.1016/j.watres.2007.06.038

Nomiyama K, Tanizaki T, Koga T, Arizono K, Shinohara R (2007) Oxidative Degradation of BPA Using TiO_2 in Water, and Transition of Estrogenic Activity in the Degradation Pathways. Arch Environ Contam Toxicol 52:8-15. doi: 10.1007/s00244-005-0204-7

OECD (1984) Earthworm, Acute Toxicity Tests (207). Guideline for testing of chemicals. Adopted: 04.04.1984

Oliveira AS, Saggioro EM, Pavesi T, Moreira JC, Vieira Ferreira LF (2012) Molecular Photochemistry - Various Aspects. In: Saha S (ed) Solar Photochemistry for Environmental Remediation - Advanced Oxidation Processes for Industrial Wastewater Treatment, InTech, pp 195-222.

Palominos R, Freer J, Mondaca MA, Mansilla HD (2008) Evidence for hole participation during the photocatalytic oxidation of the antibiotic flumequine. J Photochem Photobio A 193:139-145. doi: 10.1016/j.jphotochem.2007.06.017.

Paoletti MG (1999) The role of earthworms for assessment of sustainability and as bioindicators. Agr Ecosyst Environ 74:137-155. doi: 10.1016/S0167-8809(99)00034-1

Ptak A, Wrobel A, Gregoraszczuk EL (2011) Effect of bisphenol-A on the expression of selected genes involved in cell cycle and apoptosis in the OVCAR-3 cell line. Toxicol Lett 202:30-35. doi: 10.1016/j.toxlet.2011.01.015

Rodríguez EM, Fernández G, Klamerth N, Maldonado MI, Álvarez PM, Malato S (2010) Efficiency of different solar advanced oxidation processes on the oxidation of bisphenol A in water. Appl Catal B: Environ 95:228-237. doi: 10.1016/j.apcatb.2009.12.027

Sirisuk A, Hill CG, Anderson MA (1999) Photocatalytic degradation of ethylene over thin films of titania supported on glass rings. Catal Today 54:159-164. doi: 10.1016/S0920-5861(99)00177-7

Staples CA, Dorn PB, Klecka GM, O'Block ST, Harris LR (1998) A Review of the environmental fate, effects, and exposures of bisphenol-A. Chemosphere 36:2149–2173. doi**:** 10.1016/S0045-6535(97)10133-3

Sun B, Smirniotis PG (2003) Interaction of anatase and rutile TiO_2 particles in aqueous photooxidation. Catal Today 88:49–56. doi**:** 10.1016/j.cattod.2003.08.006

Tsai WT, (2006) Human health risk on environmental exposure to bisphenol-A: a review, J Environ Sci Health C 24:225–255. doi: 10.1080/10590500600936482

Tsai W, Lee M, Su T, Chang Y (2009) Photodegradation of bisphenol-A in batch TiO_2 suspension reactor. J Hazard Mater 168:269-275. doi: 10.1016/j.jhazmat.2009.02.034

US EPA (1996) Ecological effects test guidelines - Earthworm Subchronic Toxicity Test. United States Environmental Protection Agency Federal Register, 96, 167

Wang C, Lee C, Lyu M, Juang L (2008) Photocatalytic degradation of C.I. Basic Violet 10 using TiO_2 catalysts supported by Y zeolite: An investigation of the effects of operational parameters. Dyes Pigm 76:817-824. doi: 10.1016/j.dyepig.2007.02.004

Wang R, Ren D, Xia S, Zhang Y, Zhao J (2009) Photocatalytic degradation of Bisphenol A (BPA) using immobilized TiO_2 and UV illumination in a horizontal circulating bed photocatalytic reactor (HCBPR). J Hazard Mater 169: 926-932. doi: 10.1016/j.jhazmat.2009.04.036

Watanabe N, Horikoshi S, Kawabe H, Sugie Y, Zhao J, Hidaka H (2003) Photodegradation mechanism for bisphenol A at the TiO_2/H_2O interfaces. Chemosphere 52:851-859. doi: 10.1016/S0045-6535(02)00837-8

Yamaguchi A, Ishibashi H, Kohra S, Arizono K, Tominaga N (2005) Short-term effects of endocrine-disrupting chemicals on the expression of estrogen-responsive genes in male medaka (Oryzias latipes). Aquat Toxicol 30:239–249. doi: 10.1016/j.aquatox.2004.12.011

Zhang R, Vigneswaran S, Ngo H, Nguyen H (2007) A submerged membrane hybrid system coupled with magnetic ion exchange (MIEX®) and flocculation in wastewater treatment. Desalination 216:325-333. doi: 10.1016/j.desal.2006.11.025

Zhao C, Pelaez M, Duan X, Deng H, O`Shea K, Kassinos DF, Dionysiou DD (2013) Role of pH on photolytic and photocatalytic degradation of antibiotic oxytetracycline in aqueous solution under visible/solar light: Kinetics and mechanism studies. Appl Catal B: Environ 134:83-92. doi: 10.1016/j.apcatb.2013.01.003

Zhao J, Li Y, Zhang C, Zeng Q, Zhou Q (2008) Sorption and degradation of bisphenol A by aerobic activated sludge. J Hazard Mater 155:305–311. doi**:** 10.1016/j.jhazmat.2007.11.075

8. CONCLUSÕES E PERSPECTIVAS FUTURAS

A degradação fotocatalítica dos dois azos corantes medida pelo TiO_2 em suspensão foi satisfatória. Diversos parâmetros foram avaliados na degradação do C.I Reactive Black 5 e C.I Reactive Red 239, e concluímos que a concentração de 0.1 gL^{-1} TiO_2 foi a mais favorável, assim como quanto maior a concentração inicial de corante menor é a eficiência fotocatalítica. O meio ácido favoreceu o processo fotocatalítico e foi determinada a concentração de $3x10^{-3}$ mol L^{-1} de H_2O_2 como sendo ótima. Ainda para os azo corantes, o TiO_2 demonstrou o mesmo perfil de degradação, tanto em um sistema monocompartimental como para um bicompartimental. Concluímos com este trabalho a importância de se avaliar em laboratório os diversos parâmetros físicos-químicos que venham a influenciar um processo de degradação fotocatalítica mediado por TiO_2.

O trabalho com o corante índigo carmine (IC) se caracterizou como um extenso estudo de avaliação de parâmetros reacionais, aplicação de diferentes fontes luminosas e reatores, uso dióxido de titânio em suspensão e suportado, remoção por processo físico, assim como diversos testes ecotoxicológicos. Incialmente concluímos que diversos fatores influem na degradação do IC, e a concentração de TiO_2 considerada ótima encontrada foi de 0,1 gL^{-1}, o aumento da concentração inicial de IC causou significante absorção de luz diminuindo consideravelmente a fotodegradação. Diversos ânions foram testados, demonstrando competir com os sítios ativos na superfície do TiO_2. Além do mais, diferentes temperaturas foram desfavoráveis para a remoção do IC. A degradação do IC mostrou-se favorecida em meio ácido e o TiO_2 foi reutilizado em diversos outros ciclos mantendo a mesma eficiência das reações iniciais. Diversos reatores em escala laboratorial foram testados, e dentre eles o reator do tipo batch equipado com lâmpada de vapor de mercúrio 125W foi o mais eficiente. A degradação

solar em duas diferentes estações do ano foi avaliada, e concluímos que apesar do verão ter uma maior radiação incidente, o inverno obteve resultados de degradação muito similares ao próprio, demonstrando que no local avaliado a variação sazonal não altera o processo solar fotocatalítico.

O reator solar piloto CPC demonstrou ser uma alternativa atrativa para degradação do IC tanto com TiO_2 em suspensão como suportado, uma vez que a degradação foi mais rápida e pode simular situações reais de remediação ambiental. Quando suportado foi necessário uma energia acumulada maior em comparação com o TiO_2 em suspensão, porém foi capaz de degradar totalmente o IC mesmo em matrizes mais complexas, revelando reduzir a duração e os gastos com o tratamento.

Diferentes organismos foram utilizados para avaliar a toxicidade do IC e seus fotoprodutos de degradação. A avaliação ecotoxicológica dos fotoprodutos do IC com a alga *Pseudokirchneriella subcapitata* promoveu o crescimento destas, enquanto que os fotoprodutos produziram 100% de mortalidade para *Daphnia similis*. Também foi encontrado que os resíduos do TiO_2, após tradicional processos de filtração, afetou as espécies estudadas e podem ter efeitos potencialmente tóxicos juntamente com os fotoprodutos. Esses resultados revelaram a importância de avaliar a toxicidade dos fotoprodutos e a completa remoção do TiO_2.

A degradação fotocatalítica do Bisfenol A na presença do TiO_2 foi realizada sob diferentes condições. A concentração 0,1 gL^{-1} de TiO_2 foi considerada ótima para remover o BPA (20mgL^{-1}) tanto em reator batch como em CPC. As fases cristalinas anatase e rutile mostraram-se com baixa eficiência fotocatalítica, sugerindo que a combinação de ambas as espécies aumenta o poder fotocatalítico. O TiO_2 suportado em esferas de vidro removeu o BPA (100 μgL^{-1}) eficientemente em diferentes matrizes de água, no entanto forte influência da matriz foi observado. Os radicais $OH^{\bullet}$ e $O_2^{\bullet -}$ foram

as principais espécies envolvidas na fotodegradação do BPA. O BPA revelou significante toxicidade aguda para as minhocas *Eisenia andrei* com LC_{50} de $1.7x10^{-2}$ $mg.cm^{-2}$ e os fotoprodutos de degradação foram tempo dependentes para redução de peso das minhocas.

Em linhas gerais, podemos concluir que o presente trabalho revelou a importância de se avaliar e conhecer os parâmetros que influenciam o processo fotocatalítico, a necessidade de se trabalhar com matrizes mais complexas, que em sua composição possuem sequestradores das espécies reativas, estudar a cinética e a eficiência do processo em escala piloto, assim como utilizar organismos de diferentes níveis tróficos para avaliar a toxicidade dos produtos de degradação, e por fim não menos importante às vantagens de se trabalhar com o catalisador suportado, na qual elimina a etapa de remoção e reduz os custos do tratamento.

A contaminação das águas de abastecimento é um grave problema conhecido de Saúde Pública que acomete muitos países em desenvolvimento, principalmente a contaminação por interferentes endócrinos que mesmo em baixas concentrações causam danos graves a saúde em longo prazo, como propensão para o desenvolvimento de diferentes tipos de câncer e danos no sistema reprodutor tanto masculino como feminino. Desta forma, o desenvolvimento e pesquisa de diferentes tratamentos das águas residuárias mais eficientes, torna-se uma necessidade para a melhoria da qualidade da água que chega até a população.

As perspectivas para futuros estudos de degradação de substâncias persistentes no ambiente, de forma geral, podem focar em simular o mais próximo possível a que acontece no ambiente real. Inserido neste contexto, os futuros estudos devem considerar concentrações de contaminantes mais próximas daquelas encontradas no ambiente, no caso dos poluentes emergentes trabalhar na ordem de μgL^{-1} de concentração. Outro

fator a ser considerado é a matriz a ser trabalhada, muitos estudos encontrados na literatura utilizam água destilada ou MilliQ, distanciando os resultados quando comparados a uma matriz real, onde muitos outros fatores devem ser considerados, como exemplo a carga orgânica presente em água reais, a qual afeta consideravelmente cinética de degradação dos compostos. Quando a escolha de tratamento com POAs objetivar um estudo com dióxido de titânio, a preferência será para um estudo com o semicondutor suportado em um sólido, evitando assim futuras etapas de separação. Outra grande vertente de estudos com TiO_2 é a sua síntese e dopagem com diferentes metais, com o objetivo de aumentar seu "band dap", ou seja, melhorar o aproveitamento do espectro solar. O volume de efluente a ser tratado é um grande fator diferencial entre os estudos encontrados na literatura, uma vez que normalmente os reatores utilizados são em escala laboratorial, dentro deste cenário os reatores CPC, capazes de tratar até 300 litros de efluente, tornam-se um atrativo campo a ser explorado. As ferramentas analíticas que existem para avaliar a qualidade do efluente tratado são diversas, mas não menos importantes estão os testes ecotoxicológicos, estes permitem avaliar os efeitos do produto final e/ou seus intermediários em diferentes organismos, uma vez que diferentes espécies respondem de maneiras variadas frente ao mesmo composto.

Sabemos que os POAs sozinhos não são a solução dos problemas, uma vez que promovem a degradação de diversas substâncias, mas por outro lado não têm a capacidade de depuração de águas residuárias, assim estudos podem dedicar-se a promover tratamentos acoplados, como exemplo, tratamentos biológicos com lodo ativado e POAs, para avaliar a eficiência do processo em conjunto.

9. REFERÊNCIAS BIBLIOGRÁFICAS

Aguinaco A, Beltrán FJ, Sagasti JJP, Gimeno O. *In situ* generation of hydrogen peroxide from pharmaceuticals single ozonation: A comparative study of its application on Fenton like systems. Chem. Eng. J., 2014; 235: 46-51.

Agência Estadual de Meio Ambiente (CPRH). Available from: www.cprh.pe.gov.br

Albers PH. Birds and polycyclic aromatic hydrocarbons. Avian. Poult. Biol. Rev., 2006; 17:125–140.

Alfano OM, Bahnemann D, Cassano AE, Dillert D, Goslich R. Photocatalysis in water environments using artificial and solar light. Catal. Today., 2000; 58:199-230.

Al-Hayek N, Dor´e M. Oxidation of organic compounds by Fenton's reagent: possibilities and limits. Environ. Technol. Lett., 1985; 6:37–50.

Allen E, Doisy EA. An ovarian hormone preliminary report on its localization, extraction and partial purification, and action in test animals**.** J. Am. Med. Inform. Assn., 1923; 81(10).

Alshamsi FA, Albadwawi AS, Alnuaimi MM, Rauf MA, Ashraf SS. Comparative efficiencies of the degradation of Crystal Violet using UV/hydrogen peroxide and Fento`s reagent. Dyes Pigments., 2006; 72(2):647-52.

Baird C. Environmental Chemistry. 2ª Edição. New York: Freeman and Company, 1999, p.557.

Bahnemann D. Photocatalytic detoxification of polluted waters. In: The Handbook of Environmental Chemistry. Springer-Verlag. Berlin, Germany. 1999.

Balan DSL. Biodegrabilidade e Toxicidade de Efluentes Têxteis. Rev. Bras. Quím. Têxtil. 1999; 56:5-14.

Barka N, Assabbane A, Nounah A, Ait Ichou Y. Photocatalytic degradation of indigo carmine in aqueous solution by TiO_2 – coated non - woven fibers. J. Hazard. Mater., 2007; 152:1054-59.

Bautista P, Mohedano AF, Casas JA, Zazo JA, Rodriguez JJ. An overview of the application of Fenton oxidation to industrial wastewaters treatment. J. Chem. Technol. Biotechnol., 2008; 83: 1323-38.

Behnajady MA, Modirshahla N, Daneshvar N, Rabbani M. Photo catalytic degradation of an azo dye in a tubular continuous-flow photoreactor with immobilized TiO_2 on glass plates. Chem. Eng. J., 2007; 127:167-76.

Billa DM, Dezotti M. Desreguladores endócrinos no meio ambiente: efeitos e consequências. Quim. Nova., 2007; 30(3):651-66.

Birkett JW, Lester JN. Endocrine Disrupters in Wastewater and Sludge Treatment Process, 1°Edição. Lewis Publishers. 2003.

Bisphenol-a-europe.org *[Internet]*. PlasticsEurope, *Bisphenol-A BPA and Low Dose [accessed 2012 Aug 6]*. Available from: http://www.bisphenol-a-europe.org/index.php?page=low-dose.

Bizani E, Fytianos K, Poulios I, Tsiridis V. Photocatalytic decolorization and degradation of dye solutions and wastewaters in the presence of titanium dioxide. J. Hazard. Mater., 2006; 136:85-94.

Blanco J, Malato S, in: D. Ollis, H. Al-Ekabi (Eds.), Photocatalytic Purification and Treatment of Water and Air. Elsevier. Amsterdam. 1993. p.639.

Bonancêa CE. Estudo dos mecanismos de fotodegradação de corantes sobre dióxido de titânio atrvés de técnicas de espectroscopia Raman intensificadas [dissertação]. Química: Universidade de São Paulo; 2005.

Braúna CHC. Efeito do nitrato na descoloração redutiva de corante azo por lodo anaeróbio mesofílico [dissertação]. Saneamento Ambiental: Universidade Federal do Ceará; 2007.

Braham RJ, Harris AT. Review of Major Desing and Scale-up Considerations for Solar Photocatalytic Reactors.Ind. Eng. Chem. Res., 2009; 48:8890-8905.

Burkhardt-holm P. Endocrine Disruptors and Water Quality: A State of the Art Review. Int. J. Water Res. Develop., 2010; 26:477-93.

Caliman F, Gavrilescu M. Pharmaceuticals, personal care products and edocrine disrupting agents in the environment – a Review. Clean., 2009; 37:277-303.

Cisneros RL, Espinoza AG, Litter MI. Photodegradation of an azo dye of the textile industry. Chemosphere, 2002; 48:393-9.

Carlsen E, Giwercman A, Keiding N, Skakkebaek NE. Evidence for decreasing quality of semen during past 50 years. BMJ, 1992; 305: 609-13.

Chapin RE, Adams J, Boekelheide K, Jr. Gray LE, Hayward SW, Lees PSJ, et al. Birth Defects Res. (Part B), 2008; 83:157-395.

Chirila L, Sandu I, Butnaru R, Crivoi F. Study of some new Ni(II) and Zn(II) premetallised complexes derived from orto-aminoazo dyes. Rev. Chim., 2011; 62(9): 867-71.

Cirja M, Ivashechkin P, Schäffer A, Corvini PFX. Factors affecting the removal oforganic micropollutants from wastewater in conventional treatment plants (CTP) andmembrane bioreactors (MBR). Rev. Environ. Sci. Biotechnol., 2008; 7(1):61–78.

Clarke BO, Smith SR. Review of 'emerging' organic contaminants in biosolids and assessment of international research priorities for the agricultural use of biosolids. Environ. Int., 2011; 37:226-47.

Colborn T, Vom Sall FS, Soto AM. Developmental effects of endocrine-disrupting chemicals in wildlife and humans. Environ. Health Perspect.,1993; 101:378.

Curcó D, Malato S, Blanco J, Giménez J, Marco P. Photocatalytic degradation of phenol: Comparison between pilot-plant-scale and laboratory results. Sol. Energy, 1996; 56(5): 387-400.

Daneshvar N, Rabbani M, Modirshahla N, Behnajady MA. Kinetic modeling of photocatalytic degradation of Acid Red 27 in UV/TiO2 process. J. Photoch. Photobio., 2004; 168(1-2):39-45.

Davis ML, Cornwell DA. Introduction to Environmental Engineering. 3ª edição. New York: McGraw Hill, 1998. p.320.

Eckenfelder Jr WW. Industrial water pollution control. 3ª edição. New York: McGraw Hill, 2000. p.528.

European Union Risk Assessment Report: 4,4'-isopropylidenediphenol (bisphenol-A), Risk Assessment, Complete risk assessment in one document, Part II – Human Health, Office for Official Publications of the European Communities. 2010:244–71.

European Union Risk assessment report: 4,4'-isopropylidenediphenol (Bisphenol A). Risk Assessment, Complete risk assessment in one document, Part II – Human Health, Office for Official Publications of the European Communities 2003:1–302.

Fernández-Ibáñez P, Malato S, De Las Nieves FJ. Relationship between TiO2 particle size and reactor diameter in solar photoreactors efficiency. Catal. Today., 1999; 54(2-3):195-204.

Ferreira IVL, Daniel LA. Fotocatálise heterogênea com TiO_2 aplicada ao tratamento de esgoto sanitário secundário. Eng. San. Amb., 2004; 9(4):335-42.

Figueiredo SA, Loureiro JM, Boaventura RA. Natural waste material containing chitin as adsorbents for textile dyestuffs: Bach and contínuous studies. Water Res., 2005; 39:4242-52.

Fujishima A, Honda K. Electrochemical Photolysis of Water at a Semiconductor Electrode.Nature. 1972; 238(5358): 37-8.

Fujishima A, Rao TN, Tryk DA. Titanium dioxide photocatalysis. J. Photoch. Photobio. C: Photoch. Rev., 2000: 1-21.

Gibson R, Durán-Álvarez JC, Estrada KL, Chávez A, Cisneros BJ. Accumulation and leaching potential of some pharmaceuticals and potential endocrine disruptors in soils irrigated with wastewater in the Tula Valley, Mexico. Chemosphere, 2010; 81:1437-45.

Glaze WH, Kang JW, Chapin DH. The chemistry of water treatment processes involving ozone, hydrogen peroxide and ultraviolet radiation. Ozone-Sci. Eng, 1987; 9:335–52.

Gogate PR, Pandit AB. A review of imperative technologies for wastewater treatment II: hybrid methods. Adv. Environ. Res., 2004; 8:553-97.

Gonçalves ES. Ocorrência e distribuição de fármacos, cafeína e bisfenol-A em alguns corpos hídricos no Estado do Rio de Janeiro [tese de doutorado]. Geoquímica Ambiental: Universidade Federal Fluminense; 2012.

Goswami DY, Sharma SK, Mathur GD, Jotshi CK. Techno-Economic Analysis of Solar Detoxification Systems. Sol. Energy Eng., 1997; 119(2):108-13.

Grcic I, Papic S, Mesec D, Koprivanac N, Vujevic D. The kinetics and efficiency of UV assisted advanced oxidation of various types of commercial organic dyes in water. J. Photoch. Photobio. A., 2014; 273:49-58.

Guaratini CCI, Zanoni MVB. Corantes Têxteis. Quim. Nova, 2000; 23(1):71-8.

Guillette LJJ, Pickford DB, Crain DA, Rooney AA, Percival HF. Environmental influences on fertility: can we learn lessons from studies of wildlife? Gen. Comp. Endocrinol. 1996;101:32.

Habibi MH, Hassanzadeh A, Mahdavi S. The effect of operational parameters on the photocatalytic degradation of three textile azo dyes in aqueous TiO_2 suspensions. J. Photoch. Photobio. A., 2005; 172:89-96.

Haighton LA, Hlywka JJ, Doull J, Kroes R, Lynch BS, Munro IC. An evaluation of the possible carcinogenicity of bisphenol A to humans. Regul. Toxicol. Pharmacol., 2002; 35:238–54.

Haimi H, Mulas M, Corona F, Vahala R. Data-derived soft-sensors for biological wastewater treatment plants: An overview. Environ. Modell. Softw., 2013; 47:88-107.

Hassemer ME. Oxidação fotoquímica – UV/H_2O_2 – para degradação de poluentes em efluentes da indústria têxtil [tese de doutorado]. Engenharia Ambiental: Universidade Federal de Santa Catarina; 2006.

Hassemer MEN, Dalsano RL, SENS ML. Processo físico-químico para Indústria têxtil. Rev. San. Amb., 2001; 81:28-34.

Heimeier RA, Shi YB. Amphibian metamorphosis as a model for studying endocrine disruption on vertebrate development: effect of bisphenol A on thyroid hormone action. Gen. Comp. Endocrinol., 2010; 168:181–9.

Huang CP, Dong C, Tang Z. Advanced chemical oxidation; its present role and potencial future in hazardous waste treatment. Wastew. Maneg., 1993; 1(5-7):361-77.
Instituto de Estudos e Marketing Industrial (IEMI). Perfil e Dimenção do Setor Têxtil no Brasil. 2002.

Jefferson B, Laine AL, Stephenson T, S.J. Judd SJ. Advanced biological unit processes for domestic water recycling. Water Sci. Technol., 2001; 43(10):211–18.

Jobling S, Nolan M, Tyler CR, Brighty G, Sumpter JP. Widespread sexual disruption in wild fish. Environ Sci Technol. 1998; 32:2498–506.

Karkmaz M, Puzenat E, Guillard C, Herrmann JM. Photocatalytic degradation of the alimentary azo dye amaranth Mineralization of the azo group to nitrogen. Appl. Catal. B-environ., 2004; 51:183-94.

Khan SJ, Reed RH, Rasul MG. Thin-fim fixed-bed reactor (TFFBR) for solar photocatalytic inactivation of aquaculture pathogen *Aeromonas hydrophila*. BMC Micro., 2012; 12:5.

Kim E, Choi J. Synthesis of cationized anthraquinone dyes and their dyeing properties for *meta*- aramid fiber. Fiber Pol., 2013; 14(12): 2054-60.

Kudlich M, et al. Localization of the enzyme system involved in anaerobic reduction of azo dyes by *Sphingomonas* sp. Strain BN6 and effect of artificial redox mediators on the rate of azo dye reduction. Appl. Environ. Microbiol., 1997; 63(9): 3691-4.

Kunz A, Zamora PP, Moraes SG, Durán N. Novas tendências no tratamento de efluentes têxteis. Quim. Nova., 2002; 25(1):78-82.

Kwon M, Kim S, Yoon Y, Jung Y, Hwang T, Kang J. Prediction of the removal efficiency of pharmaceuticals by a rapid spectrophotometric method using Rhodamine B in the UV/H_2O_2 process. Chem. Eng. J., 2014; 236: 438-47.

Lee MB, Kim SH, Han SH, Kang SW, Koh KN. A self-assembled squarylium dye monolayer for the detection of metal ions by surface plasmon resonances. Dyes Pigments.,1999; 44:55-61.

Legrini O, Oliveros E, Braun A. Photochemical Processes for Water Treatment. Chem. Rev.,1993; 93:671-98.

Liao H, Stenman D, Jonsson M. Study of Indigo carmine as radical probe in photocatalysis. J. Photoch. Photobio. A., 2009; 202: 86-91.

Malato S, Blanco J, Richter C, Curcó D, Giménez J. Low-concentrating CPC collectors for photocatalytic water detoxification: comparison with a medium concentrating solar collector. Water Sci. Technol., 1997; 35(4): 157-64.

Malato S, Blanco J, Vidal A, Richter C. Photocatalysis with solar energy at pilot-plan: an overview. Appl. Environ. Microbiol., 2002; 37(1):1-15.

Manahan SE. Fundamentals of Environmental Chemistry. 2ª edição. Flórida: Lewis Publishers, 2001. p.811.

Matsuda Y, Fujisawa T, Fujikawa S, et al. Oxidation of cyanide ion in aqueous alkaline-solution by ozone. Nippon Kagaku Kaishi, 1975; 4: 602-6.

Mboula VM, Héquet V, Andrès Y, Pastrana-Martínez LM, Doña-Rodríguez JM, Silva AMT, Falaras P. Photocatalytic degradation of endocrine disruptor compounds under simulated solar light. Water Res., 2013; 47: 3997-4005.

Medellin-Castillo NA, Ocampo-Pérez R, Levya-Ramos R, Sanchez-Polo M, Rivera Utrilla J, Méndez-Diaz JD. Removal of diethyl phthalate from water solution by adsorption, photo-oxidation, ozonation and advanced oxidation process (UV/H_2O_2, O_3/H_2O_2 and O_3/ activated carbon). Sci. Total. Environ., 2013; 442: 26-35.

Mercea P. Physicochemical Processes Involved in Migration of Bisphenol A from Polycarbonate. J. Appl. Polym. Sci., 2009; 112(2):579–93.

Metcalf & Eddy. Wastewater Engineering – Treatment and Reuse. 4ª edição. McGrawHill, 2003. p.1334.

Mitsionis AI, Vaimakis TC. The effect of thermal treatment in TiO_2 photocatalytic activity. J. Therm. Anal. Calorim., 2013; 112: 621-8.

Montagner C, Jardim W. Spatial and seasonal variations of pharmaceuticals and endocrine disruptors in the Atibaia River, São Paulo State (Brazil). J. Braz. Chem. Soc., 2011; 22(8):1452-62.

Morais JL, Sirtori C, Zamora PGP. Tratamento de chorume de aterro sanitário por fotocatálise heterogênea integrada ao processo biológico convencional. Quim. Nova., 2006; 29(1): 20-3.

Moreira JC, Higarashi MM, Ferreira LFV, Oliveira AS, Xavier LFW, Moreira IMNS. Fotodegradação de hidrocarbonetos aromáticos em placas de sílica impregnadas com dióxido de titânio. Quim. Nova, 2005; 28(3): 409-13.

Moriyama K, Tagami T, Akamizu T, Usui T, Saijo M, Kanamoto N, et al. Thyroid hormone action is disrupted by bisphenol A as an antagonist. J. Clin. Endocrinol. Metab., 2002; 87:5185–90.

Muthukumar M, Sargunamani D, Selvakumar N. Statistical analysis of the effect of aromatic, azo and sulphonic acid groups on decolouration of acid dye effluents using advanced oxidation processes. Dyes Pigments, 2005; 65: 151-8.

Nevers N. Air Polution Control Engineering. 2ª edição. Boston: McGrawHill, 2000. p.586.

Nogueira RFP, Jardim WF. A fotocatálise heterogênea e sua aplicação ambiental. Quim. Nova., 1998; 21(1): 69-72.

Oliveira S, Saggioro EM, Pavesi T, Moreira JC, Vieira Ferreira LF. Solar Photochemistry for Environmental Remediation - Advanced Oxidation Processes for Industrial Wastewater Treatment. In: Molecular Photochemistry - Various aspects. Saha S, editors. InTech, 2012, p. 195.

Olsson G. State of the Art in Sewage Treatment Control. In: American Inst. Of Chemical Engineers, Symp Series 159, 1977, p. 52-76.

Othman I, Mohamend RM, Ibrahem FM. Study of photocatalytic oxidation of indigo carmine dye on Mn-supported TiO_2. J. Photoch. Photobio., 2007; 189: 80-5.

Paschoal FM, Tremiliosi-Filho G. Aplicação da tecnologia de eletrofloculação na recuperação do corante Índigo Blue a partir de efluentes industriais. Quim. Nova., 2005; 28(5): 766-72.

Péres M, Torrades F, Hortal JAG, Domenech X, Peral J. Removal of organic contaminants in paper pulp treatment effluents under Fenton and photo-Fenton conditions. Appl. Catal. B-environ., 2002; 36: 63-74.

Peterson EW, Davis RK, Orndorff HA. 17β-Estradiol as an indicator of animal water contamination in mantled karst aquifers. J. Environ. Qual., 2000; 29: 826.

Pinheiro HM, Touraud E, Thomas O. Aromatic amines from azo dye reduction: status review with amphasis on direct UV spectrophotometric detection in textile industry wastewaters. Dyes Pigments., 2004; 61(2): 121-39.

Ramstedt M, Norgren C, Shchukarev A, Sjöberg S, Persson P. Coadsorption of cadmium(II) and glyphosate at the water–manganite (c-MnOOH) interface. J. Colloid Interf. Sci., 2005; 285: 493–501.

Relatório Setorial da Indústria Têxtil Brasileira 2006-2011. IEMI. 11º edição. Brasil, 2011.

Robinson T, Mcmullan G, Marchant R, Nigam P. Remediation of dyes in textile effluent: a critical review on current treatment technologies with a proposed alternative. Bioresource Technol., 2000; 77: 247-55.

Rubin BS. Bisphenol A: An endocrine disruptor with widespread exposure and multiple effects. J. Steroid. Biochem., 2011; 127:27-34.

Santos EO. Caracterização, biodegradabilidade e tratabilidade do efluente de uma lavanderia industrial [dissertação]. Engenharia Civil: Universidade Federal de Pernambuco; 2006.

Secula MS, Cretescu I, Petrescu S. Na experimental study of índigo carmine removal from aqueous solution by electrocoagulation. Desalination, 2011; 277:227-35.

Sillanpää MET, Kurniawan TA, Lo W. Degradation of chelating agents in aqueous solution using advanced oxidation process (AOP). Chemosphere, 2011; 83: 1443-60.

Silva TCF. Processos oxidativos avançados para tratamento de efluentes de indústria de celulose kraft branqueada [dissertação]. Agroquímica: Universidade Federal de Viçosa; 2007.

Sipma J, Osuna B, Collado N, Monclús H, Ferrero G, Comas J, Rodriguez-Roda I. Comparison of removal of pharmaceuticals in MBR and activated sludge systems. Desalination, 2010; 250: 653-9.

Staples CA, Dorn PB, Klecka GM, O'Block ST, Harris LR. A review of the environmental fate, effects, and exposures of bisphenol A. Chemosphere, 1998; 36(10): 2149-73.

Stokstad E. Species conservation. Can the bald eagle still soar after it is delisted? Science, 2007; 316:1689–90.

Teixeira CP, Jardim WF. Processos Oxidativos Avançados. Cad. Temático, 2004: 6.
Tochobanoglous G, Theisen H, Vigil SA. Integrated Solid Waste Management. International editions: McGraw Hill, 1993. p.978.

Teixeira SCG, Canela MC. Degradação do pesticide PADRON* por processos fotoquímicos utilizando luz artificial e solar. Quim. Nova., 2007; 30(8): 1830-4.

The ecological and toxicological association of dyes and organic pigments manufactures (ETAD). Available from: http://www.etad.com/

Umar M, Roddick F, Fan L, Aziz HA. Application of ozone for the removal of bisphenol A from water and wastewater- A review. Chemosphere, 2013; 90:2197-2207.

United State Environmental Protection Agency (USEPA). Available from: http://www.epa.gov/endo/

U.S. Environmental Protection Agency (EPA). Special Report on Environmental Endocrine Disruption: An Effects Assessment and Analisys. Report No. EPA/630/R-96/012, Washington D. C, 1997.

Vandenberg LN, Hauser R, Marcus M, Olea N, Welshons WV. Human exposure to bisphenol A (BPA). Reprod. Toxicol., 2007; 24:139- 77.

Vandenberg LN, Maffini MV, Sonnenschein C, Rubin BS, Soto AM. Bisphenol-A and the great divide: a review of controversies in the field of endocrine disruption. Endocr. Rev., 2009; 30:75–95.

Vandevivere PC, Bianchi R, Verstraete W. Treatment and reuse of wastewater from the textile wet-processing industry: Review of emerging technologies. J. Chem. Techol. Biot.,1998; 72(4): 289-302.

van Well M, Dillert R, Bahnemann D, Benz V, Mueler M. A novel nonconcentrating reactor for solar water detoxification. J. Solar Energy Eng., 1997; 119: 114–119.

Vautier M, Guillard C, Hermann J. Photocatalytic Degradation of Dyes in Water: Case Study of Indigo of Indigo Carmine. J. Catal., 2001; 201: 46-59.

vom Saal F, Welshons W. Large Effects from Small Exposures. II. The Importance of Positive Controls in Low-Dose Research on Bisphenol A. Environ. Res., 2006; 100(1):50-76.

Wilkins FW, Blake DM. Use Solar Energy to Drive Chemical Processes. Chem. Eng. Prog. 1994; 90:41-49.

Will IBS, Moraes JEF, Teixeira ACSC, Guardani R, Nascimento CAO. Photo-Fenton degradation of wastewater containing organic compounds in solar reactors. Sep. Purif. Technol., 2004; 34: 51-7.

Wols BA, Hofman-Caris CHM. Review of photochemical reaction constants of organic micropollutants required for UV advanced oxidation processes in water. Water Res., 2012; 46: 2815-27.

Wu CH. Decolorization of C.I. Reactive Red 2 in O_3, Fenton-like and O_3/Fenton-like hybrid systems. Dyes Pigments., 2007; 77: 24-30.

Yonar T, Kestioglu K, Azbar N. Treatability studies on domestic wastewater using UV/H_2O_2 process. Appl. Catal. B-environ., 2006; 67(3-4): 223-8.

Zahraa O, Maire S, Evenou F, Hachem C, Pons MN, Alinsafi A, Bouchy M. Treatment of wastewater dyeing agent by photocatalytic process in solar reactor. Int. J. Photoen., 2006; 2(2): 59-66.

Zainal Z, Hui LK, Hussein MZ, Taufiq-Yap YH, Abdullah AH, Ramali I. Removal of dyes using immobilized titanium dioxide illuminated by fluorescent lamps. J. Hazard. Mater., 2005; 125: 113-20.

Zamora P, Kunz AP, Moraes SG, Duran N. Novas tendências no tratamento de efluentes têxteis. Quím. Nova., 2002; 25: 78 – 82.

Zanoni MVB, Carneiro PA. Corantes têxteis e o meio ambiente. Cienc. Hoje., 2001; 29(174): 61-4.

Ziolli RL, Jardim WF. Mecanismo de compostos orgânicos catalisada por TiO_2. Quim. Nova., 1998; 21(3).